THE Fe-Ti MINERALS OF ICELANDIC BASIC ROCKS AND THEIR SIGNIFICANCE IN ROCK MAGNETISM

by

STEPHEN E. HAGGERTY

A Thesis Submitted for the Degree
of Doctor of Philosophy in the
Faculty of Science
University of London

Department of Geology
Imperial College of Science and Technology
London

May 1968

CONTENT

VOLUME I

Page

Chapter 5 ILMENITE

ABSTRACT

Spontaneous reversal of magnetization in rocks and its apparent dependence on the oxidation state of the Fe-Ti oxide minerals is highly significant in view of the overwhelming evidence that exists in support of field reversal.

An attempt has been made in this study to classify these "states" of oxidation in terms of characteristic mineral assemblages. The series which has evolved is a texturally progressive series of high temperature origin. The series is supported by known thermal equilibria, by whole rock chemical analysis, and by experimental oxidation of titanomagnetite, ilmenite and olivine.

The magnetic and associated mineralogy is discussed in detail and a correlation study with some magnetic properties has been made in controlled sampling of traverses across fourteen single lavas from Iceland. These results show that the degree of oxidation is highly variable throughout a lava and that the maximum degree of oxidation is towards the central part of a lava. Several factors suggest that oxidation takes place deuterically at the time of cooling. The magnetic and petrological implications of this zonation is discussed. In spite of the fact that mixed magnetic polarities and a self reversal mechanism are absent, within single units, a strong

positive correlation is nevertheless demonstrated between samples which are highly oxidized and samples which are reversely magnetized. The correlation is well defined but is not fully understood.

ACKNOWLEDGEMENTS

The laboratory work described in this thesis was carried out in the Department of Geology, Imperial College, London, under the supervision of Dr. A.P. Millman. I would like to express my sincere thanks to Dr. Millman for his assistance, interest and advice throughout the course of the work. I would also like to thank my colleagues Dr. R.L. Wilson and Dr. N.D. Watkins for their continued encouragement and help and also for their contribution in determining the magnetic properties of the rocks used in this study.

I would like to thank members of the College staff and fellow students for their advice. I am particularly endebted to Mr. M. Frost for his help in computer processing the unit cell parameter data and the electron microprobe data.

I am grateful to Mrs. E.J. Hill and Mrs. E. Irving for their tolerance and patience in preparing many hundreds of polished sections.

A three year research grant from the N.E.R.C. is also gratefully acknowledged.

Finally I would like to thank Mrs. P. Panaino for the careful and efficient typing of this manuscript.

CHAPTER 1

INTRODUCTION

The study of palaeomagnetism is based on the essential fact that most rocks contain a small proportion of magnetic material which imparts to a rock specimen the complete properties of a magnet, and in particular the vector properties of a magnetic moment. This moment is usually acquired by the rock at the time of its formation and is termed the Natural Remanent Magnetization (NRM).

A rock may acquire a magnetic moment or remanence in a number of ways but the most important are Thermal Remanence (TRM), Chemical Remanence (CRM) and Depositional Remanence (DRM). An ingeous rock which cools in the earth's field from above the Curie temperature of the magnetic material in it, will acquire a thermal remanence. Other rocks in the neighbourhood of an igneous body may be heated above their Curie points and also acquire a TRM. Depositional or detritial remanence is acquired when small ferromagnetic particles are deposited under water in an external field; and CRM is produced when some types of chemical or phase change take place in a magnetic material, again in the presence of an external magnetic field. In each case, the presence of a preferred field is necessary

to produce a preferred direction of the magnetic moment in the rock. In the absence of such a field, the fundamental units of the magnetic material become randomly oriented so that no moment results. There is no definite correlation between the type of NRM and the type of rock producing it; but in general, igneous rocks and rocks baked by igneous rocks possess a TRM and unbaked sediments possess a DRM or a CRM. In the case of sedimentary rocks it is often difficult to differentiate between the two latter types of remanence.

A fourth type of remanence, isothermal remanent magnetization, also referred to as viscous magnetization, is a secondary form of magnetization and is acquired by all rocks by virtue of their presence in the earth's magnetic field at ordinary temperature, over very long periods of time. This time-dependant magnetization may be superimposed on the primary magnetization or it may have the effect of completely remagnetizing the rock.

Considerable effort has been devoted to the determination of the earth's main magnetic field at various localities and on rocks dating back to the Pre-Cambrian by measuring the directions of the NRM's in rocks of various types. The fundamental assumptions are (i) that the moment

measured in the rock is that acquired at the time the rock was laid down or at some known point in its history, and (ii) that this moment faithfully represents the direction of the ambient field during the magnetization process. Laboratory experiments and observation on recently extruded lavas support the validity of these assumptions.

Two important results have emerged from these studies; one which confirms the hypothesis of continental drift and permits quantitative estimates to be made of the movement of land masses; and the other, which was completely unexpected, is the fact that approximately 50% of all rocks which have been measured magnetically show a direction of magnetization which is anti-parallel to the direction of the earth's present main magnetic field.

There are two possible explanations for this reversed magnetism: the rock was formed and was magnetized at a time when the earth's magnetic field was reversed relative to its present polarity (field-reversal); or alternatively, a physiochemical mechanism existed in the rock which permitted a spontaneous "self-reversal" of the magnetic direction. The weight of evidence is in favour of field reversal although a few isolated examples of self-reversal, such as the now famous Mt. Haruna dacite are known.

The following are the three main lines of evidence for field reversal:

(a) World wide simultaneous zones of one polarity have been established in the upper Carboniferous (IRVING 1966) and radiometric dating of discrete Pleistocene lavas has given rise to a well defined polarity-time scale (DOELL et.al. 1966); the latter is amply supported by recent investigations on deep sea cores (OPDYKE et.al. 1966; WATKINS and GOODELL, 1967). The sedimentary cores preserve a more continuous record of the earth's magnetic field but both the continental and the oceanic investigations agree that the earth has reversed its polarity at least 11 times in the past 3.5 million years.

(b) Time-ordered sequences of lavas have been found in which the earth's magnetic field has been caught in the act of reversing its polarity. In vertical sequences of lavas, and once again in the deep sea cores, transitional directions of magnetization occur which are continuous between normal and reversed, or visa-versa.

(c) Strong evidence for reversals of the magnetic field arises from a comparison of the magnetic polarity of an igneous body, with the polarity of the associated rock which it has baked upon contact. The baking and the

baked rock often have a totally different mineralogy but since both cool contemporaneously in the same magnetic field they record essentially the same magnetic field direction, regardless of the polarity away from the baked contact. If self-reversing mechanisms operate, then only 50% of igneous-baked pairs should agree in polarity since a statistical analysis of all rocks indicate an equal proportion of normal and reversed polarity. But in a recent survey by WILSON (1966) a 97% polarity agreement is shown between igneous rocks and their baked contacts, which firmly supports the field reversal hypothesis.

Many deliberate attempts have been made to find evidence which would upset the well substantiated field-reversal theory. The only other suggested interpretation to account for reversely magnetised rocks is that about 50% of all rocks possess an intrinsic self-reversing property which enables the rock to acquire a polarity opposed to the applied magnetic field.

There are two methods by which self-reversing properties may be tested. The first and obvious method is to produce self-reversal in natural and synthetic material; and the second is to examine statistically large numbers of normal and reversed rocks in an attempt to find some chemical

or physical differences between them.

NEEL (1951) has proposed several mechanisms by which self-reversal of magnetisation could occur and others have been suggested since (VERHOOGEN 1962). When natural rocks are subjected to simple thermal and demagnetization tests in the laboratory very few in fact show self-reversal properties. This does not discount the possibility of self-reversal, however, since the process involved might require many millions of years. The only reported case of a rock which shows repeatable self-reversal in the laboratory is the Haruna dacite discovered by NAGATA et.al. (1952). On cooling a sample from above its Curie point in fields of the order of 1 oersted, this rock acquires a reversed TRM. The explanation of this behaviour has been a problem for many years as the mechanism of reversal is not fully understood.

Full self-reversal has not been convincingly and repeatedly demonstrated in magnetite or members of the magnetite-ulvospinel solid solution series, which are the chief magnetic minerals in most rocks. Partial self reversal has, however, been demonstrated in members of the ilmenite-hematite series (UYEDA, 1958 and CARMICHAEL 1961). The mechanism once again is obscure but CARMICHAEL suggests

that it may concern the exchange of electrons between Fe^{+2} and Fe^{+3} ions on the oppositely directed magnetic sub-lattices of the solid solution. EVERITT (1962) and BHIMASANKARAM (1964) have demonstrated self-reversal behaviour in natural and synthetic pyrrhotite.

Recently ADE-HALL (1964) and WILSON (1964) have found correlations between the petrology, and the polorization of basalts from **Mull**. The normal specimens contained homogeneous titanomagnetite grains, while the reversed samples contained "exsolution" lamellae of ilmenite. The same samples showed no magnetic differences even under very varied and perservering tests. The authors were unable to give any final explanation of their results but it must be accepted, nevertheless, that systematic mineralogical differences were found to occur for normal and reversely magnetised lavas within the same sequence of flows.

The presence of ilmenite lamellae in titanomagnetite has now been conclusively proved to result from a process of oxidation (LINDSLEY 1962-63). Other polarity-oxidation correlations, similar to those described by ADE-HALL and WILSON, have been found and it is interesting to note that some research workers did not believe their own results to be significant. The known correlations that have been

reported in the literature will be discussed in Chapter 20.

It was on the basis of these findings that the present study was undertaken.

1.2. Aim and Scope of the present study

The aim of the study may be summerised by asking the following questions.

1. Can any link be established between petrology and magnetic polarity? How do changes in the ferromagnetic mineralogy affect the magnetic properties of the rock?

2. What are the primary magnetic minerals in igneous rocks? What are the derived secondary products and what quantitative data can be presented in support of their identification?

3. On the basis of reflected light microscopy can the mineralogy be classified into progressive states of alteration and what experimental evidence exists, or can be presented, in support of this classification?

4. What are the chief processes affecting the mineralogy of igneous rocks and what criteria can be

used to estimate the time and conditions under which alteration takes place?

5. Accepting the oxidation-polarity correlation in regional surveys what is the expected background or "noise level", magnetically and mineralogically, within single units?

The general field of study was originally suggested by PROFESSOR P.M.S. BLACKETT and DR. R.L. WILSON.

Samples for the study were collected from a long sequence of lavas in Iceland. The magnetic properties were measured by the geophysics group at Liverpool University (DR. WILSON) and by DR. N.D. WATKINS at Florida State University who suggested the single unit study. Mineralogically the samples have been studied by reflection microscopy in polished section; X-ray techniques and the electron probe microanalyser have also been used. Wet chemical analyses for Fe and Ti on whole rock samples have been determined on some selected specimens.

The samples fall into two groups of material. In the first, the regional study, the mineralogy has been investigated in a general way and in the second, the single unit study, samples have been observed in much greater

detail. As the optical work progressed the complexity of the mineralogy gradually became apparent and enormous variations, not only between units but also within the same unit, were found to occur. In view of these variations the field of polarity-petrology correlation has been restricted to the single unit material. It is emphasised, however, that much valuable data has emerged from the regional study and that the mineralogy will be treated from both collections as though it were one suite.

Additional material for comparative study has been obtained through the kind co-operation of many co-workers but the magnetic properties on this material have not been determined.

CHAPTER 2

GEOLOGY AND SAMPLE COLLECTION

2.1 Regional Geology

Iceland, an oceanic island, lies on the northern extension of the Mid-Atlantic Ridge and forms part of the Brito-Arctic Tertiary volcanic province.

The Tertiary basalt plateau of Iceland is separated into two main areas by a graben-like zone of subsidence running NE-SW across the country (Figure 2.1a). The zone widens towards the south and is infilled by younger Quaternary lavas. Lavas to the east and west of the graben are predominently Tertiary in age; the regional dip ($\sim 10^{\circ}$) of both sequences of lavas is towards the central intervening trough.

One of the most striking features of Iceland is the great thickness of basalt lavas which are exposed. The total stratigraphic thickness measured at sea level in eastern Iceland, for example, is at least 10 km. and measurements by WALKER (1959) suggest that some 10,000 km^3 of material has been extruded since early Tertiary.

Approximately 80% of the total volume of material consists of basalt lavas and subordinate basaltic tuffs; of the remainder, most consists of rhyolite lavas and pyroclastic rocks, with subordinate basaltic-andesite lavas.

The plateau basalts have originated from fissure-type eruptions, whereas the acid and intermediate rocks are derived from Tertiary volcanic centres which are recognisable as central-type strato-volcanoes (WALKER 1963). The acid tuff beds are also derived from these emanating centres and extend for long distances into the flood basalts.

The basalt lavas were mostly erupted on dry land and form different petrographic types which are sufficiently distinctive to be recognised and mapped in the field. Individual basalt groups can be mapped along strike sometimes for distances of up to 60 km. Stratigraphic mapping of this type (particularly in eastern and south-eastern Iceland by G.P.L. WALKER) has revealed the basic simplicity of the structure which in addition has shown that large scale faults, those with vertical displacements of more than 100 m. or so, are rare.

2.2 Sample Material

The samples collected for the present study, from eastern Iceland may be divided into (a) the regional collection (b) the single unit collection. Additional material for comparative study has been obtained from Teneriefe (BORLEY, RIDLEY, ABBOTT), St. Helena (BAKER), United Arab Republic (MILLMAN), Somalia (SKIBA) and Western Australi

(TRAVIS).

2.3. Regional Collection

The regional collection forms part of an extensive palaeomagnetic survey of eastern Iceland directed by DR. R.L. WILSON, University of Liverpool. Cores were collected from twenty-one overlapping profiles (Figure 2-1b) so that the chronological sequence, not only within profiles but also between profiles, is known by superposition. The cores were from a predominantly basaltic succession and range from lower Tertiary to Quaternary in age.

The profiles A to V comprise a total thickness of 11.0 km. of volcanic rocks; they are mostly lava flows and flow units, some 1,140 of which were sampled. Some lava flows are made up of two or more flow units, all of which are probably the products of the same volcanic eruption; the units are separated by intervals of time ranging from several hours to several years. Non-exposure accounts for some 4.5% of the total thickness making allowances for repetition of overlap of one profile on another this represents a succession of 8.8 km. thick, comprising some 900 separate lava units.

At least two cores were obtained from each unit and where possible the underlying baked, sedimentary or

tuffaceous, beds were also sampled.

2.4. Single Unit Study

With four exceptions the single unit study forms part of the same coastal succession of lavas as the regional survey. Fourteen lavas, two profiles from one lava, and six dykes were sampled of which one was a composite dyke. Details of the location, thickness and number of samples obtained from each unit are given in Table 2.1. The units were carefully chosen in that only "fresh" lavas and dykes were selected for detailed profiling. Their field relationships were closely examined to ensure that only single and not multiple units were sampled. This is not a difficult task in Iceland. Most of the valleys are of glacial origin and the lava pile is extremely well exposed with little or no soil cover on the steep faces. All the units have well defined and clear-cut contacts; joint surfaces, particularly columnar jointing was avoided. In the case of the dykes the glassy margins were easily sampled but the tops and bottoms of lavas tend, at times, to be somewhat frothy so that adequate sampling of these highly vesicular regions is made somewhat more difficult. If it were not for the use of a motorised drill, good sampling of unaltered material would, on occasion, have been impossible. The lavas

were sampled in as near a vertical traverse as was possible, no problem arose in the case of horizontal sampling across the dykes. Underlying baked red beds were sampled where these occured and horizontal sampling of the dykes was extended into the adjacent lavas for distances of 4-5 meters. The drill cores are 2.5 cms. in diameter and 10-15 cms. in length. Distances between samples varied in accordance with the thickness of the unit but was of the order of 50 cms. The magnetic and mineralogical properties were determined on the same core.

TABLE 2.1

Lava No.	Lava Location			Thickness (meters)	No.of aamples	Strati-graphic position
	Area	Longtitude (W)	Latitude (N)			
AS	Asbergi	16° 31'	66° 02'	2.5	16	1
BS	Asbergi	16° 31'	66° 02'	5.2	13	3
CS	Asbergi	16° 31'	66° 02'	4.3	13	2
DS	Dettifoss	16° 23'	65° 51'	3.6	14	4
ES	Neskaupstadir	13° 39'	65° 09'	2.6	12	8
FS	Neskaupstadir	13° 39'	65° 09'	8.7	19	7
GS	Neskaupstadir	13° 40'	65° 09'	16.0	38	6
HS	Berufjordur	14° 28'	64° 45'	16.3	30	9
IS	Hamersfjordur	14° 27'	64° 41'	11.5	36	11
JS	Hamersfjordur	14° 27'	64° 41'	14.0	29	10
KS	Hamersfjordur	14° 34'	64° 38'	14.8	28	14
LS	Hamersfjordur	14° 34'	64° 38'	14.2	33	13
* S	Hamersfjordur	14° 27'	64° 41'	11.0	35	12
* MS	Hamersfjordur	14° 27'	64° 41'	11.8	61	12
XS	Egilstadir	14° 30'	65° 16'	11.1	34	5

* Two profiles from the same flow

Composite Dyke

Dyke No.					
AD	Streilishorn	13° 58'	64° 44'	27.4	83
BD	Berufjordur	14° 19'	64° 40'	2.8	16
CD	Berufjordur	14° 18'	64° 39'	4.8	22
DD	Hamersfjordur	14° 20'	64° 39'	5.3	27
ED	Hamersfjordur	14° 21'	64° 39'	3.8	27
FD	Streitishorn	13° 58'	64° 44'	16.5	28

Location, thickness and the number of samples obtained and used in the single unit study.

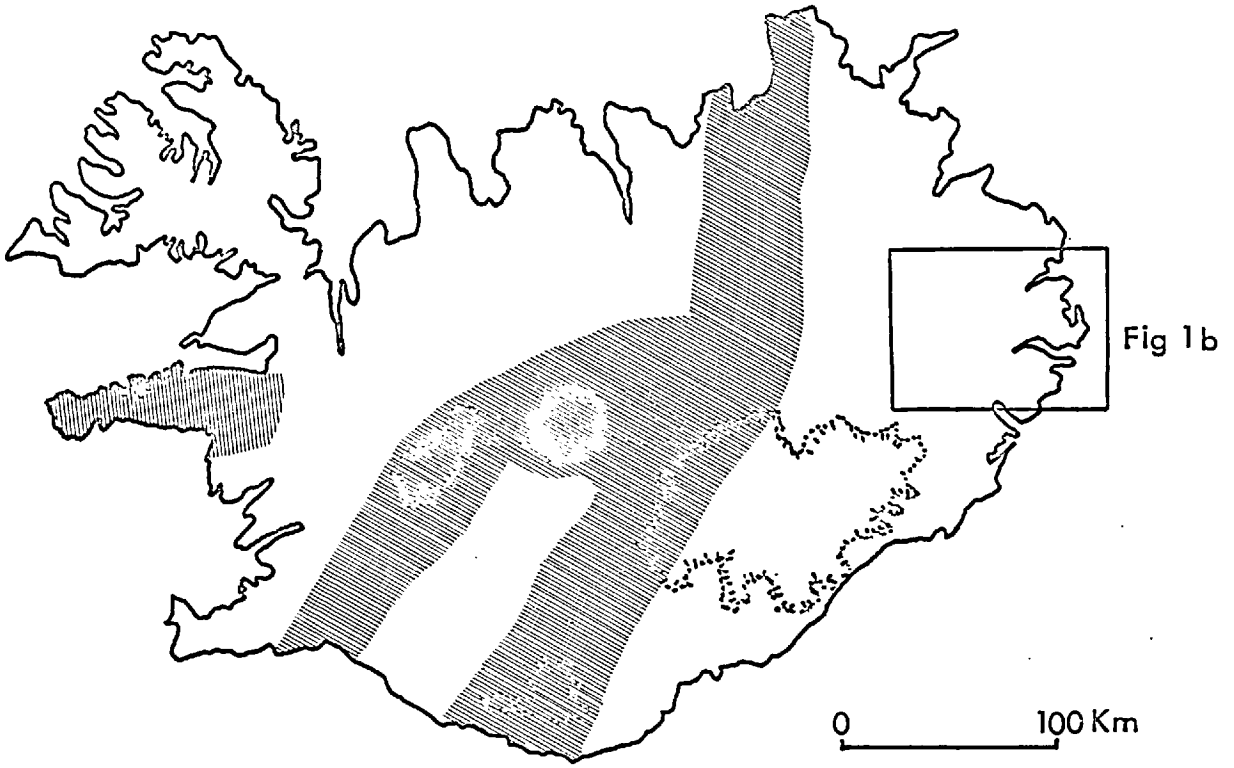

ICELAND NEO–VOLCANIC ZONE Fig 2.1a

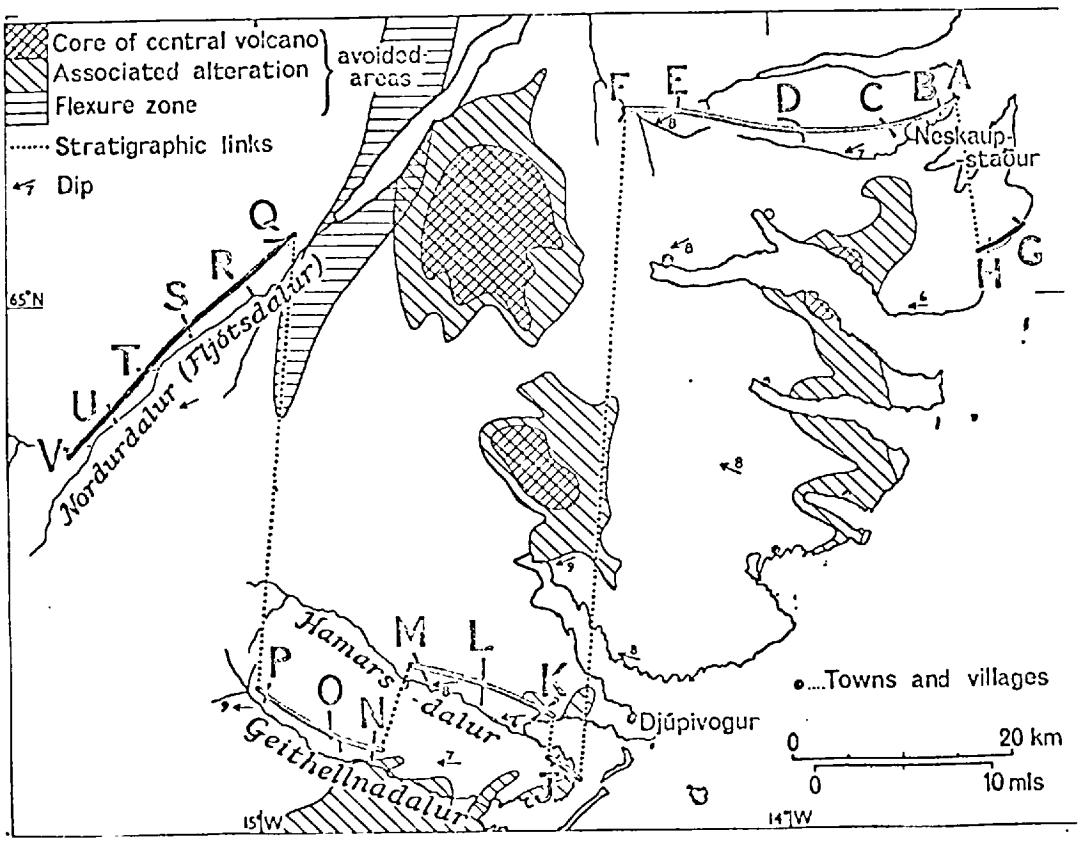

REGIONAL SAMPLING PROFILES Fig 2.1b

CHAPTER 3

MAGNETIC MINERALOGY

3.1. Introduction

A thorough knowledge of the iron-titanium oxide minerals is necessary as a background for the study and interpretation of the phenomena of rock magnetism.

Magnetically, minerals may be divided into those which are ferromagnetic, paramagnetic or diamagnetic in character. The minerals responsible for the magnetic properties of rocks are the oxides of iron and titanium. Natural magnetic minerals are always ferrimagnetic with iron as the main magnetic carrier. The common silicate minerals quartz and feldspar are diamagnetic whereas olivine, pyroxene and biotite are paramagnetic.

Natural ferrimagnetic minerals may be further classified into two groups, the oxides and the sulphides. The oxides are generally more abundant than sulphides, and in consequence, have a greater influence on the magnetic properties of the rocks containing them. Frequently in discussions of rock magnetism the possible presence of sulphides is ignored although the ferrimagnetic sulphide, pyrrhotite, may be more widespread, especially in intrusive rocks, than is generally supposed.

Magnetite is the chief primary magnetic mineral in igneous rocks. It is known to vary compositionally and a number of investigators have shown that the magnetic properties may vary in accordance with any change in composition. To a considerable degree, the intensity of saturation magnetization and Curie point depend on the chemical composition of the mineral but certain other magnetic properties depend also on the size (magnetic stability) and shape (magnetic anisotropy) of mineral grains.

How far the magnetic behaviour of the rock will be influenced by the occurrence of the ferrimagnetics in intergrowths, such as exsolution or by-products of oxidation, depends on the conditions under which the intergrowths formed and the way in which the component minerals acquired their magnetization. It is necessary, therefore, to consider the probable origin of any intergrowths present in any mineralogical study which accompanies an investigation into the magnetization of rocks.

3.2. Experimental Systems

A considerable amount of previous data has been published on the system Fe-Ti-O. The binary system Fe-O has been extensively studied, and the description of this system given by DARKEN and GURRY (1945-46) being generally accepted.

The system Ti-O has also been extensively studied but has, as yet, not been as well defined (DE VRIES and ROY, 1954; WAHLBECK and GILLES, 1966).

The experimental system of direct interest to rock magnetism is the FeO-Fe_2O_3-TiO_2 field which forms a sub-system to the ternary phase diagram Fe-Ti-O. The relationship of these systems is shown in Figure 3.1.

The system has been investigated by MoCHESNEY and MUAN (1959) in air from 1400°C to above the liquidus and by KARKHANAVALA and MOMIN (1959) from 620°-1200°C. The phases stable in air at 1200°C were reported to be hematite, rutile and pseudobrookite. A study of the system has also been made by SCHMAHL and MEYER (1959) at 1100°C using gas mixtures to control the oxygen partial pressure, as did WEBSTER and BRIGHT (1961) at 1200°C. Approximate liquidus temperatures in the system have also been determined by TAYLOR (1963).

Three main solid solution series have been reported in the system and these are as follows:

1. Magnetite (Fe_3O_4) - Ulvospinel (Fe_2TiO_4) series
2. Hematite (αFe_2O_3) - Ilmenite ($FeTiO_3$) series

3. Pseudobrookite series (Fe_2TiO_5 - $FeTi_2O_5$).

For convenience, the solid solution series are often referred to in the literature as the α or rhombohedral series for the ilmenite-hematite series; the β or cubic series for magnetite-ulvospinel; and the δ or orthorhombic series for pseudobrookite-ferropseudobrookite. Maghemite (titanomaghemite) although not strictly a solid solution series, but rather an oxidation series, is referred to as the γ series, derived from γFe_2O_3.

The solid solution joins are represented in Figure 3.1 and Figure 3.2. A feature of this ternary system is that if simple oxidation takes place and the bulk cation concentration remains unchanged, the trend in oxidation may be indicated by a series of lines of constant Fe:Ti ratio. Such lines are shown in Figure 3.1 (dotted), where the trend is from the base of the triangle (Fe-Ti) towards the oxygen apex. In Figure 3.2 the ternary diagram of the sub-system is shown in the convential orientation and a single oxidation reaction line is plotted from ulvospinel to pseudobrookite; this line may also be seen in Figure 3.1. The join is obvious when one considers the formulae of the respective end members, Fe_2TiO_4 (ulvospinel) and Fe_2TiO_5 (pseudobrookite). Further, it is evident from these

diagrams that ilmenite solid solutions form as intermediate products of oxidation of primary magnetite-ulvospinel solid solutions.

3.3. Properties of the solid solution series

3.3.1. Magnetite-Ulvospinel

Both magnetite (Fe_3O_4) and ulvospinel (Fe_2TiO_4) have cubic spinel structures. The spinel unit cell contains 32 oxygen ions and 24 cations. Of the cations 8 are in 4-fold co-ordination, and 16 are in 6-fold co-ordination.

There are two types of spinel structure, normal and inverse which may be represented thus:

	4-fold	6-fold		
	X_8	X_{16}	O_{32}	Normal
	Y_8	$(X + Y)_8$	O_{32}	Inverse

Where X is Fe^{+2}

Y is Fe^{+3}

Magnetite and ulvospinel are inverse spinel structures and their formulae may be written as follows:

Magnetite	$Fe^{+3}(Fe^{+2}\ Fe^{+3})\ O_4$
Ulvospinel	$Fe^{+2}(Fe^{+2}\ Ti^{+4})\ O_4$

Magnetite is typically ferrimagnetic and ulvospinel

is antiferromagnetic. Ulvospinel would therefore not be expected to have a spontaneous magnetization, and at room temperature it is known to be paramagnetic.

Physical Constants (NAGATA 1962)

Parameter	Magnetite	Ulvospinel
a. Unit cell (Å)	a = 8.396 (systematic increase)	a = 8.534
b. Density (Gm/cc)	5.20	4.84
c. Saturation Magnetization (emu/gm)	92	
d. Direction of easiest magnetization	[111]	
e. Melting point (°C)	1591	1470

A complete solid solution series is reported to occur above 600°C (VINCENT et.al. 1957). The pure ulvospinel end member has been synthesised but has, as yet, not been found as a single homogeneous phase in nature. It commonly occurs as an exsolution product in titanomagnetite and forms under conditions of slow cooling and low oxygen partial pressure. The degree of ulvospinel substitution in the magnetite structure is delicately controlled by the oxygen partial pressure of the melt, and the temperature of formation; the higher the partial pressure the lower is the titanium content (LINDSLEY 1963). Oxidation of the series may form

cation deficient spinels of the titanomaghemite series, or alternatively oxidation may induce the formation of members of the ilmenite-hematite solid solution series.

Magnetite and ulvospinel are optically isotropic. Magnetite may vary from pale grey to tan brown in colour; ulvospinel, on the other hand, is light brown, it is darker and browner in colour and has a slightly lower reflectivity than magnetite, especially in oil. The reflectivity in air at 589 nm. of magnetite is R_n = 17-18% (MILLMAN and D'OREY, pers. comm. 1967).

3.3.2. Ilmenite-Hematite

Ilmenite is a ferrous titanate of iron ($Fe^{+2}Ti^{+4}O_3$). It is rhombohedral with cell dimensions a_r = 5.543 Å, α = 54° .51′; or in the hexagonal notation, a_h = 5.089 Å, c_h = 14.163 Å.

Studies on synthetic ilmenite has shown that it is anti-ferromagnetic below -200° C and paramagnetic above this temperature.

Hematite (αFe_2O_3) is also rhombohedral with cell dimensions a_r = 5.427 = 55° 18 or expressed in terms of hexagonal symmetry a = 5.034 Å c = 13.479 Å. The cell parameters increase systematically from hematite to ilmenite.

Hematite is weakly magnetic and the origin of its magnetic moment is not fully understood. Regarding it as ferrimagnetic, it's Curie point is 675 °C and its saturation moment is of the order of 0.5 emu/gm at room temperature.

A complete solid solution series exists between ilmenite and hematite above 1000 °C, but at lower temperatures stable solid solution is restricted to small regions at each end of the series (CARMICHAEL 1961). Slow cooling of intermediate members of the series will produce exsolution intergrowths of ferri-ilmenite in titanohematite or visa versa, depending on the dominant end-member.

The magnetic properties of the series are rather complex. If the series is expressed as $x(FeTiO_3).1\text{-}x(Fe_2O_3)$, then the magnetic properties may be classified as follows:

(i) $x = 1$ (Ilmenite); antiferromagnetic

(ii) $1 > x > 0.45$; ferrimagnetic

(iii) $0.45 > x > 0$; weakly magnetic

The last of these three is considered to be superimposed ferromagnetism on antiferromagnetism (NAGATA 1961). In addition, for $x = 0.5$ the magnetic properties are extremely variable and are dependent on heat treatment and method of synthesis.

Ilmenite forms a major component of the opaque assemblage in igneous rocks. It occurs as a primary crystalline phase and also as a product of sub-solidus oxidation from magnetite-ulvospinel solid solutions. Ilmenite occurs extensively in some metamorphic rocks, in deep seated magmatic differentiates and as a detrital product in black sands. Its common alteration products are titanohematite, rutile and pseudobrookite.

Hematite is rare as a primary mineral in igneous rocks but is widely distributed as a secondary product after magnetite and ilmenite. Hematite is widespread in sediments either as thin ochreous veneers in red sandstones or in sizable deposits of economic proportion in metamorphic terraines.

In reflected light ilmenite is a pinkish-brown colour and is strongly anisotropic. Hematite is also strongly anisotropic but in shades of grey; its colour varies from grey to whitish yellow. The reflectivities of hematite at 589 nm. in air are R_g = 24% and R_p = 29%, and of ilmenite R_g = 17% and R_p = 21% (MILLMAN AND D'OREY, pers. comm.1967). Ilmenite and hematite commonly show lamellar twinning. An additional and distinguishing feature of hematite is that it frequently shows deep red internal reflections, especially

in oil.

3.1.3. Pseudobrookite series

The end-members of the series are pseudobrookite (Fe_2TiO_5) and ferropseudobrookite ($FeTi_2O_5$). The series is orthorhombic with the following cell parameters.

Fe_2TiO_5	$FeTi_2O_5$
a = 9.767 Å	a = 9.798 Å
b = 9.947 Å	b = 10.041 Å
c = 3.717 Å	c = 3.741 Å
V = 361.1 Å^3	V = 368.0 Å^3

Very little is known about the magnetic properties of the series except that it is paramagnetic at room temperature and is considered to be antiferromagnetic at very low temperatures.

The series is complete above 1150° C (AKIMOTO et.al. 1957). Recent work by LINDSLEY (1966) has shown that ferropseudobrookite decomposes at 1140° C to ilmenite + rutile and that pseudobrookite members breakdown at about 600° C to hematite + rutile.

Primary pseudobrookite is rare in nature (SMITH, 1966; OTTAMAN and FRENZEL, 1966) and as far as is known ferropseudobrookite has, as yet, not been identified as a naturally

occuring product. Pseudobrookite occurs more extensively than is generally supposed as a high temperature oxidation product of ilmenite and titanomagnetite.

In reflected light members of the series may range in colour from steel-grey to dark bluish-grey. The series is weakly anisotropic but this is variable; it shows reddish internal reflections and the reflectivity is lower than hematite, magnetite or ilmenite.

It is evident from this summary that only members of the magnetite-ulvospinel solid solution series contribute significantly to the overall magnetic properies of the rock. Members of the ilmenite-hematite series are ferromagnetic over a very narrow range of solidsolubility and towards the Fe_2O_3 end, members are only weakly magnetic. Pseudobrookite members are paramagnetic and the polymorphs of TiO_2 (rutile, anatase and brookite) which are likely to form as oxidation products, are also paramagnetic with weak magnetic susceptability values in the region of 0.050×10^{-6} emu/gm (PANKEY and SENFTLE 1959).

The only series which has not been considered and which is known to be magnetic within the system, is maghemite (γFe_2O_3). It has a basic spinel structure and forms at

ordinary temperatures as an oxidation product of magnetite. The structural formula is written as

$$Fe^{+3}\ (Fe^{+3}_{\frac{5}{3}}\ \square^{o})\ O_4$$

where $\square$ represent a vacant cation site. These cation-deficient spinels are matastable and are reported to invert to stable αFe_2O_3 between 200 and 500 ^{o}C. The cell size is not accurately known but is generally quoted as 8.35 $\mathring{A}$ (BASTA 1959). The saturation magnetization at room temperature is about 83 emu/gm (c.f. magnetite = 92 emu/gm).

Since titanomaghemite forms as an oxidation product of titanomagnetite (members of the magnetite-ulvospinel solid solution series) and since it has a spinel structure of hematite composition its field of stability, relative to the ternary diagram, must lie between the α and β solid solution joins and towards Fe_2O_3; this is partly supported by chemical analysis.

In reflected light maghemite is white or distinctly pale blue in colour. It is isotropic and its reflectivity value is slightly higher than magnetite but lower than hematite. It is distinguished from magnetite on the basis of colour and from hematite by its isotropism.

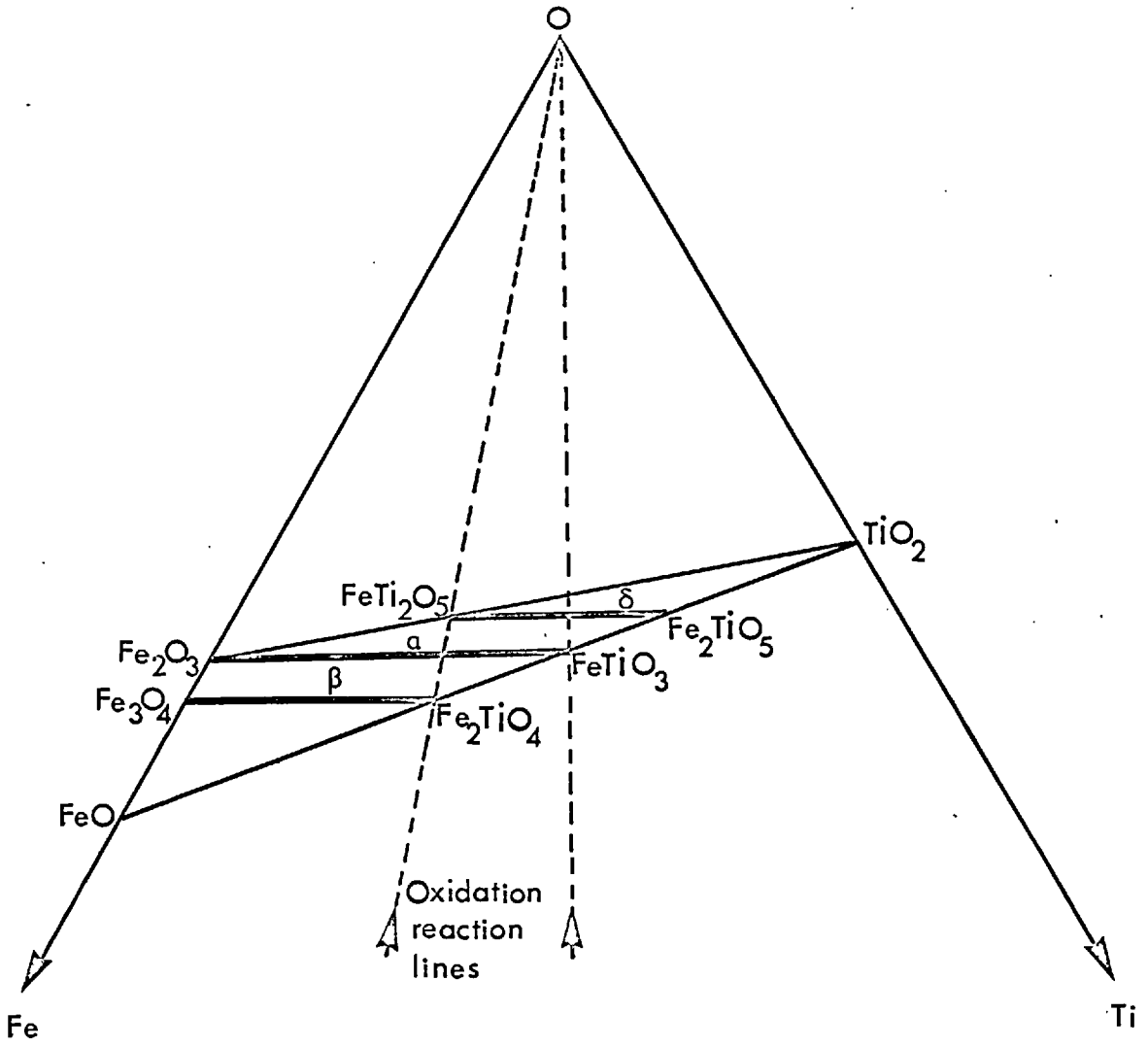

System Fe–Ti–O showing the sub-system $FeO-Fe_2O_3-TiO_2$; solid solution joins (α, β, δ) and oxidation reaction lines.

Fig 3.1

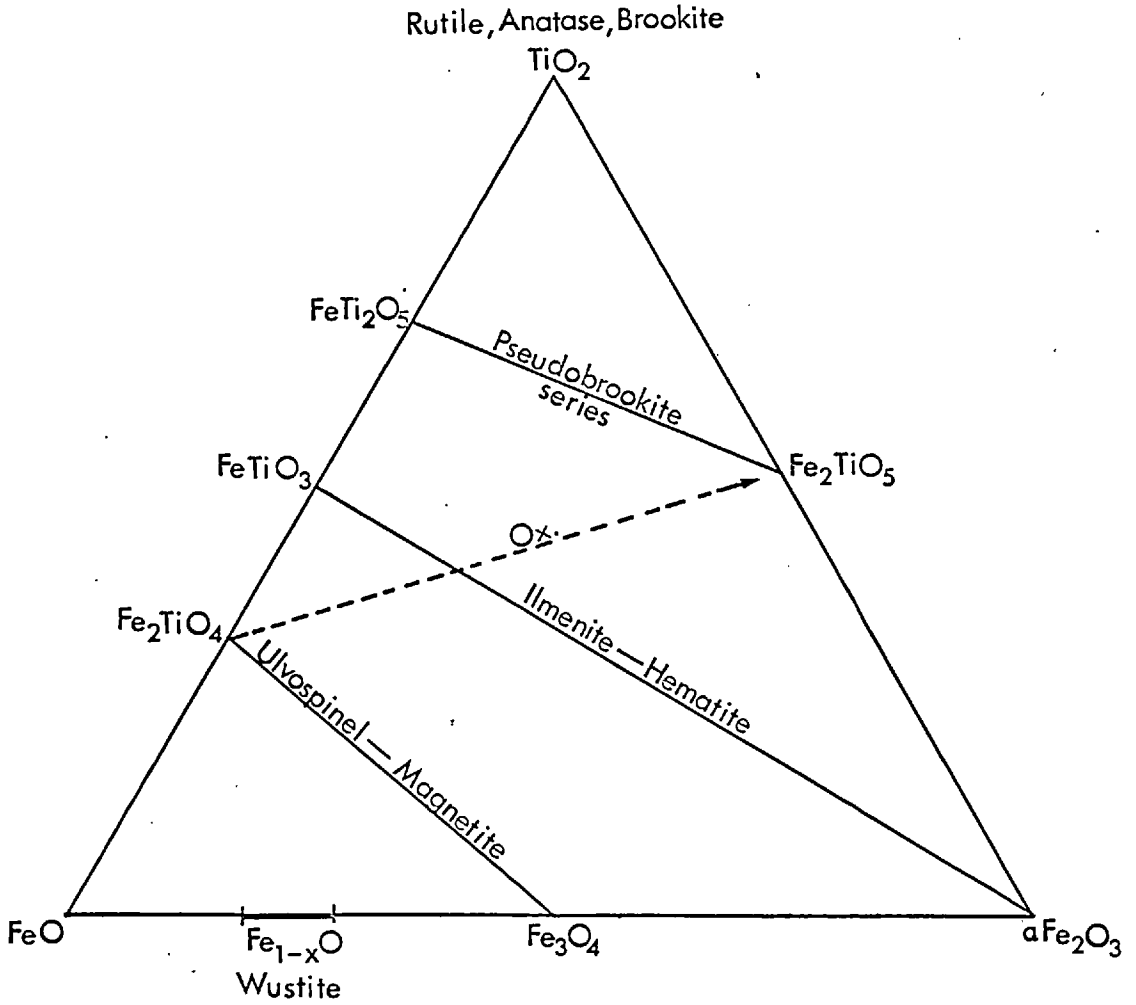

$FeO-Fe_2O_3-TiO_2$ ternary diagram showing solid solution relationships between :

$Fe_3O_4-Fe_2TiO_4$: cubic : β series

$Fe_2O_3-FeTiO_3$: rhomb. : α series

$Fe_2TiO_5-FeTi_2O_5$: ortho. : δ series

Fig 3·2

CHAPTER 4

SYSTEMATIC OPAQUE MINERALOGY OF ICELANDIC ROCKS

4.1. Introduction

One sample from each lava of the regional collection and all samples from the single unit collection have been polished and observed under the ore microscope.

The primary mineralogy is simple. This consists of homogeneous titanomagnetite and homogeneous ilmenite, accessary minerals are chrome-spinels, native copper, iron and copper-iron sulphides. On average the total opaque content is rarely more than 10% by volume and is usually of the order of 5% or less. The ratio of titanomagnetite to discrete ilmenite is usually close to 1 but wide variations around this norm are common.

The oxides of iron and titanium are modified to various degrees depending on the state of oxidation. It is this degree of oxidation that has been used in a system of classification which was found suitable to describe and directly compare specimens from the same lava as well as specimens from different lavas.

Lamellar ilmenite is produced in the primary stage of titanomagnetite oxidation. These textural intergrowths

are on a very fine scale and subsequent oxidation trends are often difficult to follow in detail. It is an advantage therefore to examine and understand the behaviour of discrete ilmenite under conditions of oxidation, the textures and identification of the phases which form and the progressive nature in which these phases form, before any consideration is given to the more complex assemblage ilmenite + titanomagnetite. For this reason ilmenite and titanomagnetite are treated separately and in this order.

The oxidation trends have been further classified on the basis of the temperature at which the minerals formed. Evidence supporting this division and oxidation heating experiments are described where appropriate.

The accessory minerals are described and the high temperature alteration of olivine is discussed in detail because the alteration products contribute significantly to the magnetic properties.

The optical classification is supported throughout by illustrating the progressive oxidation stages in great detail through the medium of optical photomicrography. Phase identifications are supported by X-ray and electron probe microanalyses.

CHAPTER 5

ILMENITE

5.1. Ilmenite Morphology

The shape of ilmenite grains is highly variable, but the relative perfection of crystal form attained by ilmenite is always far greater than that attained by titanomagnetite. One possible explanation for this feature is that in the normal crystallisation sequence of basalt, ilmenite crystallises before titanomagnetite and hence its crystal form is less restricted by interfering ground mass silicates. In the Icelandic basalts there are pseudo-skeletal crystals, euhedral plates parallel to (0001), graphic intergrowths, globular forms and somewhat irregular but generally more or less equidimensional grains.

Ilmenite plates, in particular, have a widespread distribution. They are frequently terminated by rhombohedral faces (Plate 5.1a) and are very thin. Large numbers of ilmenite crystals frequently clump together into narrow zones. These may have a parallel fabric (Plate 5.2b) or are often connected at right angles to longer central plates of ilmenite (Plate 5.2c). Agglomeration of ilmenite in this manner is particularly characteristic of the dykes. In many cases the enclosed silicates also show a preferred and

parallel orientation but often there is no relationship at all. It is interesting that although a textural fabric exists within the areas of high ilmenite content, as those illustrated in the photomicrographs, a preferential orientation of all the ilmenite throughout any one sample does not occur; the directional trends between clusters is random.

Initial precipitation produces a simple plate which may or may not be well terminated. The maximum rate of growth is normal to the c-axis and the laths extend by successive overgrowths. Thickening of the laths, parallel to the basal plane, takes place by the development of smaller plates (1-5u) which are connected to the main crystal by slender bridges (Plate 5.2a). These T-shaped bodies are frequently terminated by rhombohedral-like faces. Their form, however, is often difficult to determine accurately as these extensions are near the optical limit of the microscope. As these T-shaped bodies extend, they finally coalesce and substantial protuberances develop (Plate 5.2c). If the process of crystal growth stops at this stage the ilmenite is likely to be peppered with trapped particles of silicate material.

Plate 5.2b, which shows a selection of twelve ilmenite crystals in the same field of view, is an excellent example

of the stages and crystal growth pattern which ilmenite undergoes. The transitional process from pseudo-skeletal forms to euhedral plates is relatively smooth and contrasts strongly with that of titanomagnetite.

The large and well developed plates of ilmenite may act as nuclei for late stage Fe-Ti oxide precipitates. Later generations of ilmenite (Plate 5.1b) and titanomagnetite (Plate 5.3), form along the basal faces of the large primary crystals. Ilmenite overgrowths take the form of T-shaped structures. Titanomagnetite overgrowths frequently show extended, euhedral, cubic arms (Plate 5.3a) and trains of rounded, silicate inclusions parallel to the (0001) faces of the ilmenite. The titanomagnetite does not only develop along the outer edges of the plate but may also crystallise around silicate inclusions within the plate.

Graphic and subgraphic intergrowths of ilmenite occur in pyroxene, and in close association with interstitial silicates (Plate 5.4c). The latter intergrowths are fine grained and are invariably oxidised. The oxidation is probably the result of late stage crystallization in an environment of high volatile activity. The larger graphic intergrowths, with pyroxene, are unoxidized and probably formed by co-precipitation at a relatively early stage in

the crystallization sequence. Grains of titanomagnetite may nucleate on these graphic ilmenite intergrowths to form composite opaques (Plate 5.4d).

Large globular phenocrysts of unusually pale ilmenite occur in a few lavas (Plate 5.5). The pale colour of the ilmenite is exceptional and suggests that the ilmenite has a greater proportion of the hematite molecule in solid solution than normal ilmenite in the same lava. These ilmenite bodies are characterised by concentric rims and attached crystals of euhedral titanomagnetite. Euhedral crystals of normal discrete ilmenite in these lavas do not show similar titanomagnetite overgrowths.

Single or multiple, lobate inclusions of silicate material often form long, parallelcores to the ilmenite crystals, but small spherical drop-like inclusions may also occur in very large numbers (Plate 5.4b). It is characteristic of the silicate globules that they are not single phases, but are of two or more different silicates. In some cases, although very rare, some sulphides are also present. The globules are considered to be droplets of magma, which were captured and included in the ilmenite during its growth, and later crystallised into the separate mineral phases. Although many of the inclusions are lobe-

shaped some do show good polygonal outlines.

The comparative lack of silicate inclusions in ilmenite and the general abundance of inclusions in titanomagnetite is taken as evidence that $FeTiO_3$ formed at an early stage. Titanomagnetite overgrowths on ilmenite further support this observation and those of SATO and WRIGHT (1966), who report that during normal magmatic crystallisation ilmenite is followed by titanomagnetite. This is an important factor which will be considered more fully at a later stage. It is sufficient at this point to say that irregular composite inclusions of ilmenite in titanomagnetite are considered to be due to exsolution by many authors but are undoubtedly due to primary seeds of ilmenite around which titanomagnetite has nucleated. It is difficult to see, for example, that the ilmenite in the graphic and external composite grain illustrated in Plate 5.4d, could possibly have resulted by "exsolution" from an original cubic phase.

5.2. The Oxidation of Ilmenite

A large number of studies have been made on titaniferous beach sands in which ilmenite has been shown to alter in several successive stages. The secondary, hydrated products of ilmenite, resulting from supergene weathering, are

either cryptocrystalline or amorphous, and as a result of this the terminology and precise nature of the mineral phases involved in these alteration trends, has led to a considerable degree of uncertainty in the identification of the phases present, by optical and X-ray methods.

By contrast, a well defined, and hitherto undescribed continuous high temperature oxidation sequence has been traced in a study of the Icelandic lavas. The well developed crystalline phases are optically distinguishablein reflected light and have been chemically and structurally confirmed by electron probe microanalysis and by X-ray powder photography.

The high temperature nature of the oxidation trend and the intermediate phases involved, have been confirmed and duplicated in a series of heating experiments on samples of basalt and on an ilmenite concentrate.

An examination has also been made of an Egyptian black sand and a collection of Kimberlitic ilmenites. The alteration trends in these ilmenites are the result of supergene weathering and compare favourable with those described in the literature, but the trends are quite distinct from the basaltic high temperature trends.

RAMDOHR (1956), and BUDDINGTON and LINDSLEY (1964) have suggested that the oxidation of ilmenite may take place according to the following chemical reaction:-

$$4FeTiO_3 + O_2 = 4TiO_2 + 2Fe_2O_3 \quad \ldots\ldots\ldots (1)$$

It follows from (1) that

$$2TiO_2 + Fe_2O_3 = Fe_2Ti_5O_2 + TiO_2 \quad \ldots\ldots\ldots (2)$$

An alternative reaction to equation (1) has been proposed by BUDDINGTON and LINDSLEY who suggest further that ilmenite may break down directly to pseudobrookite plus rutile as in:-

$$4FeTiO_3 + O_2 = 2Fe_2Ti_5O_2 + 2TiO_2 \quad \ldots\ldots\ldots (3)$$

All three trends have been observed in the Icelandic basalts. The products of equation (1) generally form an intermediate or sub-stage assemblage in the oxidation trend, and invariably a polished section containing predominant rutile plus titanohematite will also show signs of incipient pseudobrookite. The equations are ideal in as much as solid solution series are involved and only apply therefore in general terms to the oxidation of ilmenite in nature. End members defined by these equations, were found to be rare, and further, the presence of titanohematite, which is

ideally excluded from equations (2) and (3), is ubiquitious.

The breakdown of ilmenite, on oxidation, at high temperatures, is not a simple inversion process, but is one in which a gradual partitioning and redistribution of iron and titanium takes place within the crystal. This results in the formation of a series of Fe-Ti oxide assemblages in which the Fe:Ti ratio, of the partitioned phases varies as oxidation proceeds. The effect of this titanium diffusion is to enrich the host phase in ferric iron. This initial segregation of Ti results in a phase, referred to in this study as ferri-rutile. The diffusion of titanium increases as oxidation progresses, until rutile is formed; the host phase is titanohematite. Subsequent or continued oxidation of this rutile-titanohematite intergrowth produces pseudobrookite. (Equations (1) and (2)).

The growth rate, of the segregated titanium-rich bodies within the ilmenite, from wisp-like lamellae to coarse lenses depends on the rate of diffusion, which may be controlled by temperature of formation and/or activity of available oxygen.

It is generally agreed (TEMPLE 1966) that a selective, chemical leaching of iron takes place during the supergene

alteration of ilmenite as in titaniferous beach sands. This results in a residual product, having a composition essentially TiO_2. But in the basaltic high temperature trend the oxidation process results in a chemical pseudomorphic effect (without the removal of material) in which the Fe:Ti ratio remains constant.

5.3. Reflection Microscopy

Particular attention has been directed towards the identification and the composition of the phases involved in the progressive oxidation of ilmenite, for the following reasons: Firstly, ilmenite is intimately associated with the oxidation of titanomagnetite. The intergrowths in highly oxidized titanomagnetite are on a very fine scale and hence good chemical analyses of individual phases are extremely difficult to obtain. Secondly, it is desirable to compare the high temperature deuteric oxidation trends in basaltic ilmenite, and the phases involved, with the number of "distinct" low temperature Fe-Ti oxide phases that have been described as intermediate mineral species in the natural (weathering) alteration of ilmenite to rutile.

The progressive stages in the oxidation of ilmenite has been traced in; (a) single lavas which show variable but systematic oxidation trends in vertical traverses

across the lava: (b) in single samples of basalt showing considerable oxidation variations over small distances (100-200u for example), and (c) in single crystals of ilmenite which show a steep oxidation gradient from one end of the crystal to the other.

It has been pointed out above that there are two main oxidation trends, one having a rutile-titanohematite assemblage as an intermediate stage to pseudobrookite (plus titanohematite and rutile), and the other in which pseudobrookite forms directly from ilmenite. The former trend will be referred to as the indirect trend; the latter, the direct trend. Generally one trend or the other predominates in any single lava but it is not always possible to decide which trend has been followed, as the end products are almost identical.

5.4. The Indirect Trend of Ilmenite Oxidation

(Plates 5.5. - 5.10)

The preferential migration of the titanium oxide phase into oriented intergrowths in the ilmenite is a continuous diffusion process in which the composition and ratio of iron and titanium varies as alteration progresses.

The indirect trend may be divided into the following stages:-

Stage 1. Homogeneous ilmenite (Plate 5.6a).

Stage 2. The first signs of alteration are indicated by the development of fine oriented filaments of a pale titanium-rich phase, ferri-rutile, along basal and rhombohedral parting planes (Plate 5.6b). The term ferri-rutile is used throughout to describe this primary segregation; it varies in composition from a titanium-rich ilmenite to a phase approaching TiO_2, and has a rutile structure.

Stage 3. As oxidation increases the pale filaments develop into thicker and darker sygmoidal, lens-shaped bodies which become strongly pleochroic and anisotropic (plate 5.6c-d). At the same time the ilmenitic zones adjacent to these lenses become lighter in colour. The lenses are sharply defined and are in optical continuity within any one structural plane. Lenses which develop along the (0001) planes of the oxidized ilmenite tend to be coarser than those which develop along subordinate parting planes. The fine stringers of pale ferri-rutile which develop in great abundance between the larger blades are probably the result of diffusion at lower temperatures. (Plate 5 7b). A synerisis distribution of the smaller bodies in relationship to the larger ones does not exist, as is common in exsolution intergrowths of titanohematite

and ferri-ilmenite.

Stage 4. The coarse segregated areas increase in anisotropy, and at this stage a large percentage of the bodies approach the optical properies of rutile. Texturally the grains are usually complex, consisting of an assemblage of large rutile (intermediate rutile) bodies interlaced with brighter segments of incipient titanohematite, finer wedges of ferri-rutile and areas of original ilmenite (Plate 5.7d).

Stage 5. The process which follows from the previous stage is one in which rutile develops extensively (Plate 5.8 a-d). This results in a simultaneous enrichment of ferric iron in the host phase. The rutile bodies are usually well oriented and sharply defined. Relic ilmenite and ferri-rutile appear as fine mottled phases in the host, but these disappear as the Fe-Ti diffusion limit is reached. The titanohematite host gradually increases in reflectivity and becomes lighter in colour, as the relic phases invert. In general terms this titanohemite-rutile assemblage is the end point of the trend postulated by equation (1) above.

Stage 6. The rutile-titanohematite assemblage now gives rise to a dominant pseudobrookitic phase which develops along cracks and grain boundaries (Plate5.9 a-d).

The pseudobrookite is associated with rutile according to equation (2) but invariable also contains fine undigested areas of titanohematite. It is significant that pseudobrookite is not crystallographically controlled. In fact as it develops from the grain boundaries it has a tendency to disrupt the well oriented lensoid structure of the rutile, causing it to be redistributed in a sub-graphic form.

Stage 7. The pseudobrookitic front gradually advances on the rutile-titanohematite intergrowth (Plate 5.10 a-c) until the entire grain is completely pseudomorphed (Plate 5.10d). Fine drop-like inclusions of rutile and titanohematite are always present: The ratio of pseudobrookite to rutile tends to be far greater than that demanded by reaction (2). On the basis of LINDSLEY'S (1965) work it is still uncertain whether this formation of pseudobrookite from rutile plus titanohemite, in a lava, is the result of an increase in the partial pressure of oxygen or an increase in the temperature of formation. The former suggestion is the most likely and is supported by the results of a series of heating experiments on ilmenite, which will be described in the latter part of this section.

5.5. The Direct Trend of Ilmenite Oxidation

(Plates 5.11 - 5.12)

In this trend pseudobrookite develops directly from ilmenite on oxidation. The pseudobrookitic phase is not structurally controlled within the ilmenite grain; the shape of the alteration product is therefore very irregular. Although the alteration generally starts at the edge of a grain, it is not necessarily confined to the grain boundaries. Crystals of ilmenite, which are partly replaced by pseudobrookite, frequently contain ferri-rutile, rutile, or rutile-titanohematite intergrowths in the unaltered areas of the grain, and hence reflect a tendency towards the indirect trend. The only clear distinction between ilmenite grains which have followed the rutile-titanohemite trend, and ilmenite grains which have followed the direct trend is that in the latter case pseudobrookite often contains fewer sub-graphic Fe-Ti oxide inclusions.

5.6 Electron Probe Analysis

The purpose of this study was to determine the distribution of Fe and Ti between the host and the segregated phases which form at different stages in the oxidation process, and further to support the optical evidence for the two continuous ilmenite oxidation trends. A total of 30

analyses were obtained on ilmenite grains from three lava samples. Two of the lavas showed the indirect ilmenite oxidation trend and the third the direct oxidation trend.

In order to eliminate the effects of primary compositional variations in the ilmenites, and in order to allow a direct comparison to be made of the phases involved in the ilmenite trends, as a function of oxidation, it was necessary to select single polished sections of basalt which showed a complete range of assemblages, from homogeneous ilmenite to pseudomorphous pseudobrookite after ilmenite.

Suitable grains were carefully selected under the ore microscope, examined at high magnification (x 1200) to ensure homogeneity, photographed or sketched, marked, and then analysed on the electron probe. Since the intergrowths are on a relatively fine scale great care was exercised during the analytical procedure to ensure that only single phases were being analysed.

Ilmenite, ferri-rutile, rutile, and pseudobrookite were analysed in the following types of single grain assemblages:

a. Homogeneous ilmenite (Stage 1 - Plate 5.6a)
b. Ilmenite + ferri-rutile (Stage 3 - Plate 5.6d)

c. Intermediate rutile in "meta-ilmenite" (Stage 4 - Plate 5.7d)

d. Rutile + titanohematite (Stage 5 - Plate 5.8a)

e. Pseudobrookite pseudomorph (Stage 7 - Plate 5.10d)

The stage numbers refer to the assemblages which have previously been discussed in the reflection microscopy section, and the plate numbers refer to typical examples.

No significant compositional differences were found between corresponding phases in either the direct or the indirect oxidation trends, so that all the analyses may conveniently be discussed as one group.

Electron probe data for the phases analysed are given in Table 5.1 and Figure 5.1. Only iron and titanium have been determined quantitatively.

Iron is plotted as a function of titanium in Figure 5.1. The straight line is drawn through the points which represent ideal stoichiometric values for the metallic iron contents of hematite, pseudobrookite and rutile.

	Wt.% Fe	Wt.% Ti
Hematite	69.90	-
Pseudobrookite	46.62	19.99
Rutile	-	59.95

It is emphasised that in the high temperature alteration of ilmenite the bulk Fe:Ti ratio remains constant. The following, therefore, are the most significant features of the plot:

1. The general trend of the probe determinations is coincident with the stoichiometric curve.

2. The values, although spaced along the trend, fall into distinct groups with little or no overlap.

3. A consideration of individual phases shows that the values for unaltered ilmenite and pseudobrookite are tightly grouped, whereas values for the rutile series and titanohematite are widely spaced.

4. The iron content of the rutile series varies between 1.49 and 29.25%. The values for iron between 9.87 and 16.60% are values for "rutile" from the complex Stage 4 meta-ilmenite grains (Plate 5.7d). Two of these values fall below the phase join but are nevertheless neatly situated between the rutile and the ferri-rutile fields. It has been demonstrated on textural evidence that the Stage 4 assemblage develops as an intermediate assemblage between (ferri-ilmenite + ferri-rutile) and (rutile + titanohematite). The Stage 4 iron-rich TiO_2 phase therefore is termed intermediate-rutile.

5.6.1. Ilmenite

Several homogenous grains of unaltered ilmenite were analysed. The average values for Fe (36.7%) and Ti (30.6%) indicate that the compositions are close to pure stoichiometric $FeTiO_3$. The range in composition within samples and between samples is small. Since the starting material does not vary in its primary composition, the data for the derived oxidation products may therefore be directly compared.

5.6.2. Titanohematite.

It has already been noted that titanohematite varies in colour, degree of anisotropy, and reflectivity at different stages of oxidation of ilmenite. All the probe analyses on titanohematite were determined in grains associated with rutile (e.g. Plate 5.8a). The areas which were chosen optically were carefully scanned with the electron beam and the point giving the maximum peak for iron, since the phase has been identified optically and by X-rays as (titanohematite), was the point chosen for the analysis. Within a reasonably confined area these counts did not vary drastically but because of the density of the rutile lamellae (Plate 5.8d) only large 10-15u homogeneous areas were selected which means that the analyses may have a compositional bias, since the purity of any phase in this type of

oxidation assemblage depends on the degree of Fe and Ti diffusion. At the very most, therefore, the four analyses which are presented in Table 5.1 are only reasonable guides to the possible range in titanohematite composition. A consideration of the ratio Fe:Fe + Ti, however, does give some idea of the dependability of the results. The ratio of the hematite-ilmenite solid solution series varies as follows:

$$Fe_2O_3 = 1.00 \qquad FeTiO_3 = 0.54$$

The range in the probe-determined compositions vary between 0.7 and 0.9, which indicates that the values are not only within the limits of the solid solution series but are also towards the hematite end member.

5.6.3. Pseudobrookite

Certain difficulties were encountered in selecting suitable grains for pseudobrookite analyses. Pseudobrookite may vary considerably in colour, and hence presumably in composition, within the same grain. Since the alteration of ilmenite to pseudobrookite is not a simple inversion process but involves the production of other phases such as rutile and titanohematite, it is not surprising that its composition varies. The chief concern however has been to select material which appears optically homogenous under the

ore microscope. Large, segregated areas of rutile and titanohematite are apparent in the photomicrographs, but at very high magnifications (x 2100), myriads of minute exsolution-like rods may be seen within the pseudobrookite phase. X-ray scanning images and element distribution profiles across these types of grains could not resolve the included phases, even at the highest magnification of the electron probe. The obvious difficulty is that the metallic ions in the rods are the same metallic ions in the host; it is only the ratio that varies.

Counts were found to vary considerably from point to point in the same selected pseudobrookite area so that only those analyses where reproduceable count rates were obtained are presented in Table 5.1 and Figure 5.1. The analyses show a relatively tight grouping and the ratio Fe:Fe + Ti varies between 0.59 and 0.63; the corresponding values for the end members of the pseudobrookite series are as follows:

$$FeTi_2O_5 = 0.37 \qquad Fe_2TiO_5 = 0.70$$

The probe-determined compositions are therefore within the limits of the pseudobrookite solid solution series and although no accurate assessment can be made of the position of the analyses on the ternary diagram one can say that the compositions do fall in the $FeTi_2O_5$ - TiO_2 - Fe_2TiO_5

triangular field.

According to ERNST (1943) there is a marked solubility of TiO_2 in pseudobrookite at high temperature (greater than 1500 °C). At lower temperatures the solubility is much reduced and highly titaniferous pseudobrookite would therefore appear to be uncommon in nature. The inclusions in pseudobrookite, referred to above, may reflect the expulsion of excess titania at lower temperatures or alternatively these inclusions may indicate the initial stages of breakdown to $Fe_2O_3 + TiO_2$.

Once again, only iron and titanium have been determined quantitatively; Mn, Mg and Al were all present in small quantities. Electron probe analyses for pseudobrookite from a wide variety of rock types, have been determined by OTTAMAN and FRENZEL (1966). Their results indicate that pseudobrookite may contain up to 3.0% MnO and 9.9% MgO. No mineralogical distinction has been made by these workers between primary pseudobrookite and secondary pseudobrookite derived from either altered ilmenite or altered ilmenite-titanomagnetite intergrowths. A chemical analysis for primary pseudobrookite determined by SMITH (1965) in an aluminous-rich emery rock contained 7.22% Al_2O_3 and 0.95% MgO; electron probe analyses on four other samples from the

same suite contained MgO values which ranged from 0.96% to 8.31% and Al_2O_3 values with a range from 5.18% to 7.88%. SMITH shows that these pseudobrookites may be recalculated in terms of Fe_2TiO_5, $FeTi_2O_5$, $MgTi_2O_5$ and Al_2TiO_5, and points out that the mineral cannot have formed simply by the oxidation of ilmenite, but that the latter must have entered into reaction with its highly aluminous, ferromagnesian environment.

It has been emphasised that strict mineralogical control needs to be exercised on the choice of sample material for analytical determinations. This point is strongly supported by SMITH'S criticism of VON KNORRING and COX (1961) in the naming of intermediate members of the pseudobrookite solid solution series. The new mineral "Kennedyite" ($Fe_2MgTi_3O_{10}$) was named on the basis of chemical analysis in spite of the fact that, "An examination of polished sections showed the new mineral in well defined laths. In some grains marginal patches of secondary hematite were observed and with "high" magnification (x500) lamellar intergrowths were seen. The lamellae are believed to be exsolved rutile".

5.6.4. Rutile

The rutile series shows a wide compositional spread which confirms the optical grouping of the series into rutile,

intermediate-rutile, and ferri-rutile. Although this division is made, it is not proposed that these terms should be rigidly used to indicate distinct mineral species. The usefulness of the terms is in describing the level of iron and titanium diffusion within altered ilmenite. This defines the optically determined assemblage and hence the state of oxidation of the grain.

The initial and preferential migration of titanium, which has been suggested on microscopic evidence, into ferri-rutile and subsequently into rutile has been confirmed by electron probe microanalysis. In view of the intermediate mineral phases (arizonite, proarizonite, pseudorutile) that have been reported to occur between ilmenite and rutile, this particular feature of titanium diffusion becomes highly significant and is demonstrated by a series of X-ray scanning photomicrographs in Plates 5.13 and 5.14. The electron images (EI) clearly define the bladed form of the rutile and the ferri-rutile phases. Rutile and ferri-rutile are respectively in titanohematite, and ferri-ilmenite hosts. Unfortunately, the reproduced photomicrographs do not show the same degree of contrast as the originals, but nevertheless an impoverishment in iron and an enrichment in titanium may be discerned in the lamellae. Even in the early stages of diffusion the ferri-rutile phase is optically well

defined but the Fe:Ti ratio is not significantly different from the ilmenitic host. This feature is well illustrated in the qualitative X-ray scanning images in Plate 5.13. With increasing diffusion the lamellae become enriched in titanium and the host in ferric iron. Plate 5.14 shows the pre-pseudobrookite assemblage rutile + titanohematite. A comparison of these photomicrographs with the previous Plate will demonstate that the lamellae have increased their resolution, from an element distribution point of view, and also that the mineral contacts are distinctly more definitive.

X-ray scanning profiles across lamellae of rutile and ferri-rutile show that the diffusion gradients for Fe and Ti are steeper in the former case than in the latter. With reference only to the rutile-titanohematite assemblage the diffusion profile for Fe is steeper than the diffusion profile for Ti. The reason being that the host titanohematite contains appreciable amounts of iron and titanium whereas the lamellae are distinctly titanium-enriched.

Analysis of rutile in the literature show that it contains, apart from a few exceptions, a variable quantity of iron. Iron-rich rutile has at times even received special names such as nigerine and iserine, where the former is considered to be an Fe^{+3} rich rutile and the latter an Fe^{+2}

rich variety (HENRIQUES 1963). Many examples of minerals considered to be iron-rich rutiles, on the basis of chemical analysis, have been shown by ore microscopy or by X-ray techniques to be rutile in close association with ilmenite, hematite or pseudobrookite (RAMDOHR 1939).

The only direct attempt that has been made to determine the solid solubility of iron in rutile is the study by WITTKE (1967) but the problem has also been considered by a number of other workers with varying results. The results, which are presented below, are expressed in terms of cation % iron (i.e. $\frac{Fe}{Fe + Ti}$ %), which has the advantage that no direct indication is given of the oxygen contents of the condensed phases.

(a) KARKHANAVALA and MOMIN (1959)

In a study of the series Fe_2O_3-TiO_2 it was found that the lowest determined iron-cation fraction of 6.25% was not completely soluble in TiO_2 at 1000 °C.

(b) McCHESNEY and MUAN (1961)

These authors determined the phase diagram for the system FeO - TiO_2 at 1 atm.air. Their investigation in the titanium rich region, although it did not define an upper solubility limit, showed that the

solubility of iron in rutile lies between 13.5 and 15.0 cation % iron at 1515°C.

(c) WEBSTER and BRIGHT (1961)

The study by these authors did not delineate the titania-rich portion of the system. But in studying the behaviour of the Fe-Ti-O system at 1200°C as a function of oxygen pressure they were able to show that the solubility of iron in rutile decreases with decreasing oxygen pressure, and is essentially constant at 10^{-3} to 1 atm. oxygen.

(d) WITTKE (1967)

An upper limit to the solubility of iron in rutile was determined in the temperature range 800°-1350°C. The results indicate somewhat lower solubilities than those inferred by previous measurements; the solubility ranges from 3 cation % iron at 1350°C to 1% at 800°C.

The range in values for Fe and Ti determined in the present probe study and the ratio $\left(\frac{Fe}{Fe + Ti}\%\right)$ for each member of the rutile series are as follows:

	Rutile	Intermediate Rutile	Ferri-Rutile
% Fe	1.5-8.8	9.9-16.6	21.5 -29.2
% Ti	56.4-62.2	43.2-55.2	34.4 -47.4
$(\frac{Fe}{Fe + Ti}\%)$	2 - 13	16 - 28	33 - 46

These values, and in particular the values for intermediate and ferri-rutile, contrast strongly with the synthetic data but it should be noted that in the synthetic studies no chemical analyses were determined on the final products. Charges of known composition were equilibrated and the products were identified by X-ray techniques. The solubility limit of iron in rutile is judged therefore on whether a single phase is formed (undersaturated) or whether rutile plus an iron-rich phase is formed (oversaturated).

In the study by KARKHANAVALA and MOMIN initial charges having a compositional range of cation % iron of 6.25-57.13 produced rutile + pseudobrookite; the 66.65% charge (stoichiometric Fe_2TiO_5) produced only pseudobrookite at 1000°C. It is a common feature to all the studies quoted above that the iron-rich phase which forms in association with rutile, in the oversaturated runs, is pseudobrookite. This assemblage contrasts with the natural products, where the iron-rich phases are either ferri-ilmenite or titanohematite. Since

the natural process which produces the alteration products in ilmenite is an oxidation process, it is possible that it is also a metastable process. The fact that the assemblage rutile + titanohematite gives rise to a pseudobrookitic phase is some evidence that the initial assemblage is metastable. HENRIQUES (1963), in a study of natural rutile, states that the iron content of stable ferriferous rutile is low, while that of unstable rutile may be fairly high.

The metallic ion plot in Figure 5.1 embraces all the electron probe data and shows a general compositional spread in the rutile series. This plot does not demonstrate the distribution of the rutile phases, however, in relation to the known solid solution series that exist within the Fe-Ti oxide system.

The compositions of unaltered ilmenite and the compositions of the rutile series are plotted therefore on the ternary diagram in Fiture 5.4. There are two main types of ternary diagram in use. The conventional type is shown in Figure 3.2, and the other type, the GORTER (1957) diagram, is shown in Figure 5.2.

The three basic components are TiO_2, FeO and $\frac{1}{2} Fe_2O_3$. The reason for using $\frac{1}{2} Fe_2O_3$ rather than Fe_2O_3 is that all

the compositions in the triangle may then be referred to one metal ion. The molecular fraction of each component in a given compound is proportional to the perpendicular distance from the side of the triangle opposite to the appropriate vertex. For example, any point on the base of the triangle represents a compound with no TiO_2, and any point on the horizontal line bisecting the two sloping sides possesses a molecular fraction of TiO_2 of one half.

The reference to one metal ion of any composition imparts to the Gorter diagram certain simple properties which facilitate its use. Firstly, the molecular proportion factor for each of the series, which varies between 0 and I, is linear along the length of the solid solution join; and secondly, lines of oxidation, defined as lines of constant Fe:Ti ratio, are parallel to the base of the triangle.

Certain difficulties arise when probe analyses are plotted on the Fe-Ti oxide phase diagram; these are outlined below.

One of the most serious drawbacks of the electron-probe is the lack of ability to investigate oxygen. It is possible in principle however to calculate the percentage

of oxygen present by subtracting the total percentage of metallic ions from 100%, but the procedure is not sound as there is no guarantee that all the metallic elements present have been detected. In addition to Fe and Ti only Al, Mg, Mn and Cr were sought and although these elements only appeared in small quantities other elements may nevertheless be present, to produce errors of the order of 1-2%. Such a small percentage error would not be important if it were not for the fact that the total metallic ion content for the end members of the ilmenite-hematite solid solution series is respectively 68.4% and 69.9%; and that of the $FeTi_2O_5$ - Fe_2TiO_5, pseudobrookite series is 65.6% and 66.6% respectively. The difference between one series and the other therefore has a range from 2.8% to 3.3%. The metallic ion content for stoichiometric rutile is 59.9%, but the average metal ion content for the rutile series which has been obtained in this study is 64.2%.

It is apparent from these figures that it is unrealistic to plot any probe-determined analysis of oxidized ilmenite as a single point on the ternary diagram; the error in the measured value of the metallic ion is itself of the order of the difference between the series.

With reference to Figure 5.2, since no distinction may be made between Fe^{+2} and Fe^{+3} all the iron has been calculated in terms of FeO which imparts a minimum state of oxidation to the phases and has the effect of concentrating the plot towards the FeO-TiO_2 join. It is emphasised, in view of the limitations referred to above, that the compositions are not intended to be represented by single points. Any probe-determined value may occur anywhere along a line which is parallel to the base of the triangle; an advantage in using the Gorter diagram. These oxidation lines are lines of constant Fe:Ti ratio and are indicated by heavy arrows in Figure 5.2. In essence, any oxidation of Fe^{+2} to Fe^{+3} will transfer the point along an oxidation line towards the TiO_2-Fe_2O_3 join.

The compositional trend is from ilemenite to rutile which infers an increase in the ratio of Ti:Fe. The analyses group in accordance with the metallic ion plot in Figure 5.1 which is in harmony with the optical classification. All but two of minimum oxidation points fall within the triangular field $FeTi_2O_5$ - TiO_2 - Fe_2TiO_5, and yet the associated host phases are either ferri-ilmenite or titanohematite. The oxidation heating experiments on ilmenite indicate that the mechanism of transgressing the pseudobrookite series

join, without necessarily producing a member of the series, is related to the partial pressure of oxygen. This problem will be fully dealt with in due course.

5.7 X-ray Results

The purpose of the X-ray study was firstly, to verify the optical phase classification for products of oxidized ilmenite; and secondly, to determine the validity of the intermediate mineral phases that have been reported to occur between ilmenite and rutile.

A total of 13 successfully uncontaminated samples were tested by extracting small amounts of material from the surfaces of polished sections using the microsampling technique. The phases were selected to cover the complete range of oxidation assemblages at each distinct stage of ilmenite alteration, and were examined in the following tyes of assemblages:

(a) Homogeneous ilmenite (Plate 5.6a)

(b) Ilmenite + ferri-rutile (Plate 5.6d)

(c) Rutile + titanohematite (Plate 5.8d)

(d) Pseudomorphous pseudobrookite after ilmenite (Plate 5.10d)

Because of the small quantity of sample used it was necessary to expose the X-ray films for at least 12 hours.

Iron filtered cobalt radiation was used in most of the runs but Mn. filtered Cu. radiation was also used in the rutile-rich assemblages.

Sample contamination is a serious problem when small quantities of material are drilled out, but fortunately it is easily recognised on the film. Contaminated films were rejected because of the confusion that is likely to arise in analysing complex multi-mineral assemblages, particularly as accurate cell parameters were being determined. Analysis is made even more difficult by the fact that the likely contaminants, chiefly silicates, cannot readily be identified in polished section.

Compositions, for the ilmenite-hematite series and for the pseudobrookite series, have been estimated using the determinative curves (Figure 5.3) of LINDSLEY (1964-65) and AKIMOTO et.al. (1967) respectively. In both cases the volume of the unit cell is the critical parameter. The difficulty that arises in using these curves is the assumption which needs to be made for an accurate determination; the assumption is that the phase is stoichiometric in composition and hence falls precisely on the solid solution join. The determined compositions are therefore only compositional guides to the possible range in values.

5.7.1 Homogeneous Ilmenite

Only one value has been determined for homogeneous, unaltered ilmenite and the following cell parameters were obtained:

$$a = 5.086 \text{ Å}$$
$$c = 14.071 \text{ Å}$$
$$V = 315.170 \text{ Å}^3$$

The volume of the unit cell is plotted on LINDSLEY'S determinative curve in Figure 5.3a which gives an approximate value of 98 mol.% $FeTiO_3$. This value agrees very well with the electron probe data which shows that the compositions form a tight cluster in the region of the $FeTiO_3$ end member (Figure 5.2).

It is known that considerable substitution of Fe^{+2} by Mg and Mn may take place in ilmenite to form the minerals $MgTiO_3$ (Geikielite) and $MnTiO_3$ (Pyrophanite). The cell parameters (PALACHE et.al. 1946) of these end members are as follows:-

$FeTiO_3$	$MgTiO_3$	$MnTiO_3$
$a = 5.083$ Å	$a = 5.086$ Å	$a = 5.126$ Å
$c = 14.040$ Å	$c = 14.093$ Å	$c = 14.333$ Å

It is evident from these figures that substitution by Mg (0.66 Å) for Fe^{+2} (0.74 Å) will have the effect of

decreasing the unit cell whereas substitution by Mn^{+2} ($0.80\ \mathring{A}$) will increase the unit cell. The electron probe has shown that both substitutional elements are present in quantities amounting to less than 1%, so the effect on the unit cell may be regarded as being negligible.

5.7.2 Ilmenite + Ferri-rutile

The following cell parameters were obtained for two grains containing (i) ilmenite + ferri-rutile and (ii) ferri-ilmenite + ferri-rutile.

	Assemblage (i)		Assemblage (ii)
Ilmenite	a = 5.086 c = 14.035 V = 314.419 = 92 mol.% $FeTiO_3$	Ferri-Ilmenite	a = 5.084 c = 13.701 V = 306.647 = 43 mol.% $FeTiO_3$
Ferri-rutile	a = 4.611 c = 2.939 V = 62.503	Ferri-rutile	a = 4.593 b = 2.947 V = 62.162

Typical examples of assemblage (i) and (ii) may be seen in Plate 5.6d and Plate 5.7d, respectively.

The values for ilmenite indicate that oxidation of Fe^{+2} has taken place and in accordance with LINDSLEY'S curve the compositions move towards the Fe_2O_3 end member. The host ferri-ilmenite phase in assemblage (ii) was markedly whitened and was at a more advanced stage of oxidation than

assemblage (i). The type (i) assemblage gave a well defined X-ray powder pattern and separation of the reflections was a relatively easy matter. In the case of assemblage (ii), prior examination of the phases was extremely helpful as the reflections normally attributable to ilmenite were found to have d- values slightly lower than the d- values for $FeTiO_3$. The trial cell parameters which were used in the computer programme to determine the intermediate composition were those of ilmenite.

The electron probe data, in support of the optical evidence, has shown that a continuous (rutile) oxidation series exists between ilmenite and rutile. It has come as a complete surprise therefore to find that the cell parameters of the high-iron rutile phases are comparable to the cell parameters of pure TiO_2. WITTKE (1967) in determining the solubility of iron in rutile found no systematic change in the cell parameters of rutile with up to 3 cation % iron in solid substitution. Even the rutile phases which were found to co-exist with pseudobrookite had cell parameters in the region of TiO_2.

The detailed nature of all the defects arising in the rutile lattice when iron is introduced is not known (WITTKE 1967), but it is considered that iron enters the

lattice as substitutional Fe^{+3}.

The small variations in the ionic radii of Fe^{+3} (0.64 Å) and Ti^{+4} (0.68 Å) probably accounts for the lack of variation in unit cell parameters of the rutile series.

5.7.3 Rutile + Titanohematite

	Titanohematite	Rutile		Titanohematite	Rutile
Grain 1	a = 5.045	a = 4.584	Grain 4	a = 5.050	a = 4.595
	c = 13.762	c = 2.971		c = 13.765	c = 2.961
	V = 303.397	V = 62.441		V = 304.065	V = 62.523
Grain 2	a = 4.999	a = 4.579	Grain 5	a = 5.039	a = 4.586
	c = 13.886	c = 2.974		c = 13.794	c = 2.965
	V = 300.574	V = 62.116		V = 303.312	V = 62.372
Grain 3	a = 5.047	a = 4.606	Grain 6	a = 5.040	a = 4.583
	c = 13.740	c = 2.974		c = 13.790	c = 2.944
	V = 303.085	V = 63.093		V = 303.354	V = 61.846

The volume of the unit cell for titanohematite varies between 304.065 $Å^3$ and 300.574 $Å^3$; these values correspond respectively to approximately 78 and 98 mol.% Fe_2O_3. These results are within the range of the electron probe data and are plotted on LINDSLEY'S determinative composition curve in Figure 5.3a.

The average unit cell volume obtained for the six rutile values is 62.398 $Å^3$. The cell parameters for pure

TiO_2 are as follows:

$$a = 4.590\ \text{Å}$$
$$c = 2.960\ \text{Å}$$
$$V = 62.360\ \text{Å}^3$$

The ratio c/a for pure TiO_2 is 0.645; the corresponding ratio for rutile, derived from oxidized ilmenite in this study, shows a spread from 0.642 to 0.646. These values do not differ significantly from the ferri-rutile values and so the points which have been made in the previous section also apply here.

The problem of the products of oxidation of ilmenite, and in particular the existence of discrete intermediate mineral phases, has long been in dispute. Phases which have hitherto been described as intermediate products (arizonite, proarizonite, pseudorutile) have <u>not</u> been directly observed under the microscope but have been inferred from chemical and/or X-ray analysis. The intermediate products have all been derived from ilmenite beach sand concentrates which have undergone extensive low temperature alteration and one result of this is that the phases are either cryptocrystalline or amorphous (see Chapter 14 for a detailed discussion). Another consequence of this type of alteration is that iron

is removed (leached) from the system so that the bulk Ti:Fe ratio increases with increasing alteration. The intermediate minerals, which have the generalized formula $Fe_2Ti_3O_9$, are likewise affected and TEMPLE (1966) concludes that, "complete removal of iron from the pseudorutile lattice results in a grain composed of crystallites of the mineral rutile".

Reference has already been made to the electron probe data which confirms that a complete rutile oxidation series exists between ilmenite and rutile. It is possible therefore that one of the series corresponds structurally to one of the intermediate minerals arizonite, proarizonite or pseudorutile. The two former minerals may be excluded from the discussion as they are known to be hydrated.

Consideration will now be given to the phase pseudorutile. It is reported (TEMPLE, 1966; TEUFER and TEMPLE, 1966), on the basis of single crystal work that the mineral crystallises with a disordered structure of hexagonal symmetry. X-ray powder data gives the following cell parameters:

(first paper)	(second paper)
$a = 2.867$ Å	$a = 2.872$ Å
$c = 4.608$ Å	$c = 4.594$ Å

FLEISCHER (1967), in a review of new mineral names, regards the data as insufficient to establish the proposed mineral and points out that every line of the powder pattern corresponds closely to rutile, or ilmenite, or both; although the strongest line of rutile is missing. A direct comparison of their data is made even more difficult by the fact that no intensity values for the new mineral are given.

In conclusion, the present study confirms, and supports FLEISCHER'S contention that it is unnecessary to name intermediate members of a progressive series. This applies in particular to the case of the Fe-Ti oxides where compositional variations are known to be extreme within the system.

5.7.4 Pseudobrookite

The cell parameters for the end numbers of the pseudobrookite series and the cell parameters for known synthetic compounds with the structure of pseudobrookite are given below; kennedyite, a mineral having an intermediate composition is also quoted.

		a(Å)	b(Å)	c(Å)	V(Å^3)
Pseudobrookite	(Fe_2TiO_5)	9.767	9.947	3.717	361.1
Ferropseudobrookite	($FeTi_2O_5$)	9.798	10.041	3.741	368.0
Karrooite	($MgTi_2O_5$)	9.774	9.980	3.732	364.0

Teilite	(Al_2TiO_5)	9.436	9.6[illegible]	3.557	323.8
Kennedyite	($Fe_2MgTi_3O_{10}$)	9.770	9.950	3.730	362.5

SMITH (1960) has pointed out that Al may be an important constituent of pseudobrookite, but the small ionic radius of Al (0.51 Å) has the effect of drastically reducing the cell parameter data. A chemically analysed pseudobrookite quoted by SMITH contains 7.22% Al_2O_3, 0.95% MgO, and the volume of the unit cell is 360.1 Å^3; this value is below the range for the pseudobrookite series.

Optical examination of basaltic pseudobrookite shows that it is characteristically inhomogeneous. The two pseudobrookite pseudomorphs which were extracted for X-ray purposes cannot therefore be said to represent the full range of possible compositions. The electron probe data does show however that Mg and Al are only present in small quantities, so that the range in the unit cell values may be entirely attributed to the pseudobrookite series.

The analysed pseudomorphs contained inclusions of rutile and titanohematite but the reflections of these minerals on the X-ray powder photographs were only weakly developed. The cell parameters for pseudobrookite after ilmenite (a and b) are listed below, and for comparison a

pseudobrookite-titanohematite grain (c), after original titanomagnetite-ilmenite (e.g. Plate 6.12c), is also presented. The compositional plot in Figure 5.3b also includes a value for pseudobrookite (point d) which was obtained by reducing ilmenite in hydrogen. The details and the results of these experiments are fully described in a subsequent section (Chapter 14.2).

	a(Å)	b(Å)	c(Å)	V(Å^3)
Grain (a)	9.762	9.959	3.739	363.401
" (b)	9.784	9.972	3.734	364.273
" (c)	9.805	9.983	3.729	364.810
" (d)	9.814	9.952	3.770	368.226

The curve showing the relation between the volume of the unit cell for members of the pseudobrookite solid solution series and the composition of the series in terms of mol.% $FeTi_2O_5$ is reproduced in Figure 5.3b.

The pseudobrookite compositions derived by oxidation vary between 70 and 79 mol.% Fe_2TiO_5; whereas the value for the reduced member corresponds approximately to 2 mol.% Fe_2TiO_5.

Theoretically, an ulvospinel-rich magnetite (titanomagnetite) should produce, on oxidation, a pseudobrookitic

member which is close to Fe_2TiO_5 in composition; this is apparent from a consideration of the oxidation lines on the ternary diagram in Figure 5.2. Although the X-ray data are sparse the value for grain c (oxidized titanomagnetite + ilmenite) indicates that it contains the lowest percentage of the Fe_2TiO_5 molecule, compared to pseudobrookite which is derived from discrete ilmenite. This, perhaps, may be accounted for by the fact that the grain which was chosen showed well oriented pseudobrookite lamellae in a widmanstatten pattern, which indicates that the pseudobrookite was essentially derived not from the original titanomagnetite, but rather from the original "exsolved" ilmenite.

5.8 Oxidation Experiments on Ilmenite

The purpose of the heating experiments has been to determine: the thermal stability of ilmenite under oxidation; the conditions controlling the formation of the direct and the indirect trends shown in natural ilmenites; the relative susceptibility of discrete ilmenite with ilmenite which has "exsolved" from titanomagnitite.

The starting material for the thermal stability oxidation experiments consisted of an ilmenite concentrate from the Urals (R.S.M. Collection). The material was optically homogeneous, unaltered, and an electron probe

microanalysis gave the following composition:-

Fe = 36.97% : Ti = 30.0%

Mn, Mg = Trace amounts

Samples were crushed to pass a -200 mesh screen (< 0.03 mm); the grinding was carried out under acetone to prevent oxidation. Grains of the material were spread out along the length of the ceramic boats to give the sample an adequate reaction surface. In spite of this precaution the powder still tended to sinter after a few hours, the result being that the lower temperature experiments (600°C for example) may not have reached equilibrium.

Runs were made at 100°C intervals from 100° to 1000°C. Additional runs at 550° and 650°C were also made. All runs were quenched in air. X-ray powder photographs were obtained from the material of each run using Fe filtered Co radiation.

5.8.1 Reflection Microscopy

The optical properties of the alteration products were examined in a separate series of experiments from the stability runs. These experiments were carried out on coarse grained ilmenite (a 100 u; b 2-3 mm) as well as on oxidized and unoxidized polished samples of basalt. Additional

material was obtained from these polished sections for X-ray identification using the microsampling technique.

The fine grained material (stability runs) and the polished sections of basalt were aimed and designed as equilibrium runs, whereas the purpose in heating the coarsely granular material was an attempt to trace the progressive breakdown of ilmenite from equilibrium conditions at the grain boundaries to prevailing non-equilibrium conditions which would exist towards the core of the grains.

The starting material is not excessively coarse grained and so thermal gradients may be regarded as having a negligible effect on the products which are produced. The chief factor controlling the breakdown assemblages is undoubtedly the availability and partial pressure of oxygen. Although no quantitative estimates have been made of the thermal and oxidation gradients across ilmenite grains, in the size and temperature ranges under consideration, the thermal gradients may be regarded as being fairly even because of the relatively high thermal conductivity of ilmenite, but it is known that solid state diffusion reactions at these temperatures are relatively sluggish, and hence the oxidation gradients would appear to be relatively steep.

The textural intergrowths of the oxide assemblages are on a very fine scale in all the experiments which were run for less than five days, supporting the above contention. An attempt has been made, therefore, to illustrate these textural phase relationships diagramatically as their finely disseminated nature does not make the intergrowths amenable to good photographic reproduction. These sketches are illustrated in Figure 5.4.

In the course of polished section manufacture the grains are randomly sectioned so that a wide spectrum of oxidation assemblages appear; grains which have only had the surface veneer removed during polishing will show an equilibrium assemblage across the entire grain, whereas a grain which is cut across the maximum oxidation gradient will show the widest variation, ranging from an equilibrium grain boundary assemblage to a non-equilibrium assemblage at the core. The assemblages which form may be regarded as being in equilibrum at the point where they exist but are obviously not in equilibrium with the overall conditions of the experimental run.

A discussion of the phases and the textural intergrowths in these runs may conveniently be made, in the first instance, by considering the grain size fractions separately

(a. 100 u ; b. 2-3 mm.). Table 5.2 lists the grainsize of the starting material used in the experimental runs, the temperature at which the runs were carried out, the duration of the runs and finally the phases in each run as determined optically.

5.8.2 Starting Material 100 u

Run 1 (4 hrs. to 850°C; 2 hrs. at 850°C)

Fine, well oriented and slightly sygmoidal blades of ferri-rutile occur throughout the ilmenite grains. Minute flecks (1-5 u) of rutile, pseudobrookite and titanohematite occur towards the grain boundaries. The orientation and form of the ferri-rutile compares favourably with natural samples as for example Plate 5.6b. Unaltered ilmenite, free from ferri-rutile, occurs extensively towards the core of the grains.

Run 2 (4 hrs. to 850°C; 20 hrs. at 850°C)

What are considered to be three progressive stages of ilmenite alteration in this experimental run are represented in Figure 5.4 a-c.

Figure 5.4a

The grain contains three relatively well defined mineral zones. The core consists of an intersecting network of finely oriented ferri-rutile blades in an ilmenitic

host; occassional coaser blades of rutile occur with this zone but are generally concentrated towards the zone boundary. Unaltered areas of ilmenite may still persist.

The intermediate zone contains a sub-graphic intergrowth of pseudobrookite and titanohematite. Minor amounts of rutile always occur in this zone as irregular patches or as well oriented lenses.

The outer zone consists essentially of a thin diffusion rim of titanohematite. The diffusion rim is rather irregular and is often littered with small blebs of subgraphic pseudobrookite.

The phase inversion boundary between the ilmenite-ferri-rutile assemblage and the pseudobrookite-titanohematite assemblage is relatively sharp but is unmistakably an alteration front, concentric to the grain boundary.

Figure 5.4b

This grain is at a more advanced stage of alteration than (a) above; no original unaltered ilmenite remains; the central core is now crowded with blades of ferri-rutile; the phase-inversion contact is strongly crenulated; the pseudobrookite-titanohematite assemblage has increased considerably as a ratio of the grain area; and finally, the

titanohematite diffusion rim has thickened.

Figure 5.4c

The end product of the alteration trend consists essentially of a sub-graphic intergrowth of pseudobrookite and titanohematite; irregular areas of rutile are also present. The titanohematite diffusion rim is well developed, not only along the major grain boundary but also along minor sub-grain boundaries.

5.8.3 Starting Material 2-3 mm.

Run 3 (4 hrs. to 850°C; 20 hrs. at 850°C)

The degree of alteration in the coarser grained material is far less than the level of alteration reached in runs 1 and 2.

Two main types of grains occur in this run and these are illustrated in Figure 5.4 (d) and (e).

Figure 5.4d

The edge of the grain boundary is zoned by a thin (10-20 u) sub-graphic rim of pseudobrookite and titanohematite. The zone is concentric to the grain boundary and unlike the 100 uruns the titanohematite diffusion rim has not developed.

The central zone of the grain represents the major assemblage. This consists of densely packed blades of ferri-rutile in a pale, anisotropic ilmenitic host. The density of the blades decreases towards the grain centre where large unaltered areas of primary ilmenite may still persist. An X-ray powder photograph of the (ferri-rutile) - (ferri-ilmenite) assemblage gave the following cell parameters:

Ferri-rutile	Ferri-ilmenite	
$a = 4.598\ \text{Å}$	$a = 5.057\ \text{Å}$	
$c = 2.942\ \text{Å}$	$c = 13.883\ \text{Å}$	
$V = 62.210\ \text{Å}^3$	$V = 307.507\ \text{Å}^3$	$= 48\text{mol.\% } FeTiO_3$

The value for ferri-rutile supports and is consistent with the unit cell volume - temperature profile plotted in Figure 5.5. The ferri-ilmenite value, on the other hand, is unique. It is interesting to note, however that a re-examination of the polished section has shown that this phase is almost intermediate in colour (the other optical properties are more difficult to judge) between unaltered ilmenite (core) and titanohematite (edge).

The inversion boundary between the pseudobrookite-titanohematite assemblage and the ilmenite-(ferri-rutile) assemblage is not as sharply defined as the inversion

contacts in runs 1 and 2.

Figure 5.4e

The second type of grain shows a more advanced state of oxidation in which a considerable thickening of the pseudobrookite-titanohematite rim occurs; the central ilmenitic zone is densely packed with ferri-rutile and only small unaltered areas of original ilmenite are present. The essential difference between this rim and the preceding rim is the development of relatively large sygmoidal lenses of rutile. These lenses are concentrated towards the inversion boundary and are oriented along a single preferred crystallographic plane. The rutile is embedded in a host consisting essentially of titanohematite; minor amounts of pseudobrookite, ferri-rutile and the ilmenitic phase may also be present. As Figure 5.6e illustrates the blades are sharply defined and penetrate into the ilmenite-ferri-rutile core. The rutile-titanohematite assemblage develops in this form at the expense of the ilmenite-ferri-rutile assemblage. As the pseudobrookite-titanohematite zone thickens, the assemblage ratio (rutile + titanohematite) : (Ilmenite + ferri-rutile) is seen to increase at a corresponding rate.

Run 4 (5 days at 960°)

In this extended high temperature run no original, unreacted ilmenite remains. The oxidized grains of ilmenite

appear to have reached a mineralogical state of equilibrium. Pseudobrookite plus titanohematite, an assemblage which appears only along the edge of ilmenite grains in previous runs, now appears throughout the entire sample.

Very coarse lenses of pseudobrookite occur towards the centre of the grains (Plate 5.15 a-b). The lenses are elongated along a single preferred directional plan (parallel to the length of the grain); concentrations along subsidiary planes also occur.

At the edges of the grains the lensoidal pseudobrookite breaks down to a graphic form. BRETT'S (1964) experimental work on sulphides suggests that lamellae are stable only as long as the lamellar phase is in crystallographic continuity with the host phase. When no continuity exists the most stable texture is a series of polyhedral grains or spheroids. This structural transformation of pseudobrookite is accompanied by a preferential migration of Fe^{+3} towards the grain boundaries. It is difficult to estimate accurately whether the ratio of lensoidal pseudobrookite to titanohematite, at the core of the grains, is comparable to the ratio of graphic pseudobrookite to titanohematite, at the grain boundaries. It is impossible therefore to say whether the hematite diffusion rim,

which results, is derived simply by a process of phase reorganisation or whether it is also derived by the partial decomposition of the pseudobrookitic phase. The breakdown of pseudobrookite in this manner would, however, necessitate not only the production of hematite (titanohematite) but also rutile, and this latter phase does not occur in great abundance. The optical properties of the core assemblage are very similar to the properties of the assemblage at the grain boundary. Pseudobrookite contains finely textured lamellae of a pale grey to white phase which has tentatively been identified as titanohematite (reflectivity and anisotropy are of the right order). These lamellae have also been observed in natural pseudobrookite. They are well oriented and are either parallel to the length of the pseudobrookite lens or occur at a slight angle to it. The heterogeneous nature of the pseudobrookite has precluded accurate electron probe microanalysis but the following cell parameters have been obtained from X-ray powder photographs.

Centre of Grain	Edge of Grain
Lensoidal Pseudobrookite	Graphic Pseudobrookite
a = 9.786 Å	a = 9.804 Å
b = 9.961 Å	b = 9.982 Å
c = 3.739 Å	c = 3.727 Å

$V = 364.475\ \text{Å}^3 \equiv 70$ mol.% Fe_2TiO_5 $\quad V = 364.383\ \text{Å}^3 \equiv 68$ mol.% Fe_2TiO_5

Titanohematite
$a = 5.036$ Å
$b = 13.755$ Å
$V = 302.090\ \text{Å}^3 \equiv 98$ mol %Fe_2O_3

Titanohematite
$a = 5.063$ Å
$b = 13.642$ Å
$V = 303.010\ \text{Å}^3 \equiv 92$ mol %Fe_2O_3

The compositional differences between the core assemblage and the grain boundary assemblage are probably not significant; the differences in the unit cell determinations are well within the order of experimental error.

A unique feature of this 960°C run is the widespread development of cracks throughout the altered ilmenite. These cracks are generally irregular but an obvious fracture pattern may be seen in Plate 5.15b. TEMPLE (1966) considers that these cracks are the result of "expansion straining of the ilmenite lattice".

Run 5 (10 days at 960°C)

Two grains from this run are represented in Plate 5.15 c-d. Texturally and mineralogically the altered ilmenite compares favourably with the five day experiment on Run 4. The only differences being an increased and purer

(free from pseudobrookitic blebs) titanohematite rim and an increased and well developed sub-graphic pseudobrookite-titanohematite zone.

In summary the progressive alteration stages that have been recognised in the heating experiments on ilmenite are as follows:

(a) Starting Material 100u.

Stage 1. Homogeneous ilmenite

Stage 2. An ilmenitic phase + Ferri-rutile

Stage 3. Pseudobrookite + Titanohematite + minor rutile

(b) Starting Material 2-3mm.

Stage 1. Homogeneous ilmenite

Stage 2. An ilmenitic phase + Ferri-rutile

Stage 3. Rutile + Titanohemite + minor amounts of assemblage 2.

Stage 4. Pseudobrookite + Titanohematite.

5.9 X-ray results

Details of the experimental runs and the cell parameters of the phases produced in each of the runs are given in Table 5.4. The approximate compositions for ilmenite and hematite (LINDSLEY 1964-65) and for pseudobrookite (AKIMOTO et.al. 1957) have been determined from the cell

parameters and are presented separately in Table 5.4.

No optical (megascopic) or structural changes were observed in the temperature range 100-500°C; only ilmenite has been identified in the X-ray powder patterns. The results indicate that ilmenite breaks down between 550° and 600°C to produce titanohematite plus rutile. Pseudobrookite first appears at 650°C and continues to form up to 1000°C in association with rutile and titanohematite.

The X-ray powder patterns of the material from the experimental runs were sharp and well defined with the exception of the 600°C run. A structural breakdown of the ilmenite appears to occur at 600°C; the alteration effect produces a relatively diffuse X-ray pattern but ilmenite, titanohematite and rutile (ferri-rutile) reflections were nevertheless still identified. The runs are of relatively short duration so that the degree of crystallinity of the developing phases may not be expected to be of a very high quality. The presence of "unreacted" ilmenite in the 600°C run, for example, indicates that equilibrium was not fully reached. Since the unit cell parameters vary systematically from ilmenite to hematite the problem of reflection-broadening arises when both phases are present in the same assemblage. A number of reflections are distinct and

these may be separated with some degree of certainty, but others, which are common to both end members, are more difficult to unravel. These latter reflections have not been used in the lattice parameter determinations. Although the reflections, in the 600 °C experiment, have been separated into two distinct phases, this may be misleading as only one phase may be present, having a single and intermediate composition (i.e. between Fe_2O_3 and $FeTiO_3$).

5.9.1 Ilmenite

The cell parameters for ilmenite do not vary systematically with temperature. The unit cell volume of the starting material is 315.17 Å^3, which according to LINDSLEY'S (1964-65) determinative curve is equivalent to 98 mol.% $FeTiO_3$. The only significant variation which was determined occurs at 600 °C, where the corresponding parameter is 313.05 Å^3, this gives a composition of 82 mol.% $FeTiO_3$. Unfortunately, the 650 °C run was totally reactive, so that one cannot say whether or not the trend towards the hematite end member is progressively followed as the process of oxidation gradually proceeds. No similar, intermediate (ilmenite-hematite) members were detected, in the stability runs, in the temperature range 700 °-1000 °C.

5.9.2 Titanohematite

Hematite (titanohematite) develops in all the experimental runs above 600°C. The volume of the unit cell, which does not vary systematically with temperature, ranges from 302.59 Å³ (650°C) to 304.32 Å³ (900°C), with the average of 303.29 Å³. Compositionally, these values correspond respectively to 90 mol.%, 78 mol.%, and 82 mol.% Fe_2O_3. These results compare favourably with the values for natural titanohematite derived from oxidized ilmenite (Table 5.5).

5.9.3 Pseudobrookite

Traces of pseudobrookite first appear at 650°C. Only the high intensity reflections were identified and as these reflections were only faintly visible on the powder patterns they were regarded as being unreliable for accurate cell parameter determination. These remarks also apply to the material of the 700°C run. Pseudobrookite continues to appear up to 1000°C and forms a major phase at these higher temperatures. The volume of the unit cell varies from 364.92 Å (70 mol.% Fe_2TiO_5) at 800°C to 363.92 Å³ (75 mol.% Fe_2TiO_5) at 1000°C with an average value of 364.31 Å³. These values agree very well with the X-ray (Table 5.5) and electron probe results for natural

pseudobrookite from oxidized ilmenite. There is a small decrease in the volume of the unit cell, corresponding to an increase in mole per cent pseudobrookite (Fe_2TiO_5), from 800°C to 1000°C. The significance of this decrease cannot be fully evaluated, however, as only three reliable determinations are available.

5.9.4 Rutile

Rutile, in common with titanohematite, is the only other phase to develop in all the experimental runs above 600°C. The volume of the unit cell varies from 61.88 A^3 at 1000°C to 62.93 A^3 at 650°C, with an average of 62.36 A^3. These results compare favourably with natural rutile from oxidized ilmenite (c.f. Table 5.5). Table 5.5 shows that there is asmall but systematic decrease in the volume of the unit cell from 1000°C to 650°C; the results are plotted in Figure 5.5. The rutile of the 600°C run does not fall within the range as the ilmenite sample did not reach equilibrium. Electron probe microanalyses of natural rutile from oxidized ilmenite has shown pure TiO_2 to be rare (Table 5.1). It seems reasonable therefore to assume that, as in natural samples, rutile which is derived from oxidized ilmenite under experimental conditions probably also contains substitutional iron in its lattice.

The decrease in the volume of the unit cell seems anomalous since one may expect larger ions to be accommodated at higher temperatures, but the reason for this decrease may be related to the presence of iron. There are at least two possible explanations for this observed decrease in unit cell volume with temperature:

(a) A progressive oxidation of substitutional Fe^{+2} (0.74 Å) to Fe^{+3} (0.64 Å) may take place with increasing temperature in non-stoichiometric TiO_2.

(b) Alternatively a purification process towards stoichiometric TiO_2 may develop with increasing temperature. If all the iron is in the Fe^{+2} state (WITTKE, 1967) purification would induce an increase in the ratio Ti^{+4} (0.68 Å): Fe^{+2} (0.74 Å).

5.10 Comparison of products derived by natural and experimental oxidation of ilmenite

There are a surprising number of similarities in ilmenite which has been oxidized in nature and ilmenite which has been oxidized experimentally. The conditions of oxidation however are different in several respects: Firstly, and most significantly of all, is the time factor, or the period

of time over which high temperature oxidation has taken place. Geologically the time involved is relatively short as the initial cooling of a lava may take place over a number of years, or in the case of thin flows effective cooling may take place within a matter of months. The length of time involved in the experimental runs is much shorter than this, the maximum period being ten days. Secondly, the natural high temperature trends which have been discussed are considered to be due to a process of deuteric oxidation. Such a process demands that primary crystallisation is accompanied by, or, is closely followed by oxidation; that is, the process is continuous and takes place slowly on cooling. In the experimental runs on the other hand, oxidation has been carried out isothermally, the samples were rapidly heated to the set temperature, maintained at the temperature for a period of time and then suddenly chilled.

There are some important conditions which have been simulated however and these are: First, oxidation takes place as a solid state reaction; second, no addition or substraction of cations is involved in the alteration process; third, the conditions of oxidation are conditions of high oxygen partial pressure; and fourth, the starting

material is crystalline and of comparable basaltic composition.

5.10.1 Mineral Phases

Ilmenite, titanohematite, pseudobrookite, rutile and ferri-rutile are the phases which have been identified as oxidation products of ilmenite in both natural and experimental samples. The results indicate that although the phases are members of solid solution series, no intermediate or distinct minerals, other than ferri-rutile are present. The polished section data has shown that the ratio of the respective phases which are in equilibrium at the early and intermediate stages of oxidation are comparable, but towards the later stages there is a marked increase in the production of pseudobrookite in natural ilmenite. The heated samples tend to contain larger percentages of titanohematite and smaller percentages of rutile.

5.10.2 Optical Properties

The only oxidation phase that can be said to be similar to the natural product is ferri-rutile. Rutile tends to be much more transparent but nevertheless retains its high degree of anisotropy. Pseudobrookite is comparable in colour, it is more anisotropic than the natural product, has a lower reflectivity and contains disseminated red

internal reflections. Titanohematite is more distinctly anisotropic than the natural product and tends to be whiter in colour.

5.10.3 Composition of Phases

No electron probe results have been obtained from the products of oxidized ilmenite in the experimental runs. The phases which develop on heating are finely textured and precise microprobe analyses are technically difficult to obtain. The exceptional coarseness of the phases in the 5 and 10 day experimental runs has precluded them on the basis of inhomogeneity.

The X-ray data suggests that the natural products are very similar in structural form and composition, where the latter can be determined, to the experimental products.

Table 5.5 compares and contrasts the average values of the cell parameters which have been obtained in this study for natural and experimental products of ilmenite. It has previously been pointed out that compositions which have been determined from cell parameters, in the ilmenito-hematite series and in the pseudobrookite series, are only intended as guides. In determining the composition one needs to assume that the phases fall precisely on solid

solution joins; the chances of this occuring as a general rule in any process of oxidation are remote. The predominance of pseudobrookite in the late stages of oxidation in natural ilmenite and the greater abundance of titanohematite in the experimental ilmenite is a case in point. The cell parameters, and hence the determined compositions, are comparable but the distribution of Fe and Ti must obviously be different. These small differences evidently cannot be accurately determined by conventional X-ray methods.

5.10.4 Textures

The textures produced by ilmenite on oxidation resemble exsolution features. Many of the classical criteria which are used in the textural interpretation of exsolution may be seen in these examples. The heating experiments on ilmenite firmly supports the observation that although the intergrowths have an exsolution appearance they are not the result of exsolution. The bulk composition does not remain constant for example, diffusion does not occur under conditions of slow cooling and the phases which are produced are not solid solution members of the starting material.

The orientation, along basal and rhombohedral parting planes, of rutile and ferri-rutile is exactly the same in both types of oxidized ilmenite. These phases are sharply

defined and texturally are either sygmoidal or flame-like in form.

Lensoidal pseudobrookite and its disruption into a graphic form, described from the 5 and 10 day experimental runs, has not been observed in discrete natural ilmenite. This transformation has been observed, however, in highly oxidized titanomagnetite-ilmenite intergrowths. In heated ilmenite and in oxidized titanomagnetite, relatively larger amounts of titanohematite are present in comparison to natural oxidized ilmenite. The presence or absence of titanohematite therefore seems to exercise some control on the textural stability of the pseudobrookitic intergrowth. The well defined and oriented lenses of pseudobrookite are unique to the experimental runs. In highly oxidized titanomagnetite-ilmenite intergrowths, the pseudomorphed ilmenite lamellae maintain their general orientation along (111) planes in the early stages, but the lamellae are always strongly serrated.

Hematite diffusion rims which have been described in the experimental runs do not occur around highly oxidized ilmenite in nature. These rims resemble the concentric hematite zones which are common around highly oxidized grains of olivine. The rims occur around natural olivine

and also olivine which has been artifically heated. The mobility and preferential migration of Fe^{+2} appears to be a common feature as it has also been noted in highly oxidized Cr-spinels. It has previously been noted that titanohematite only occurs in very small quantities in the late stages of oxidation of natural ilmenite. This apparent lack of titanohematite cannot be adequately accounted for, but it seems possible, although not proved, that the pseudobrookitic phase in natural ilmenite is an iron-enriched member of the solid solution series.

Since lensoidal pseudobrookite has a tendency to invert to the graphic form and since the formation of the titanohematite diffusion rims are characteristic of the experimental runs one may conclude, in common with the study by McCOLLISTER and VAN VLACK (1965), that "high isothermal temperatures accentuates the spheroid process (graphic pseudobrookite) and the accumulation of ferric iron (titanohematite) at the grain boundaries".

10.5 Oxidation Trends

On textural evidence, the polished section analysis of the oxidation products in ilmenite from the experimental runs suggests that the indirect trend is followed; that is, pseudobrookite develops from rutile and titanohematite and

does not develop directly from ilmenite. LINDSLEY (1964-65) has shown that the pseudobrookite series is interrupted by a decomposition gap. This means that the join Fe_2TiO_5 - $FeTi_2O_5$ (Figure 3.2) does not act as a barrier to the formation of rutile and titanohematite. The heating experiments indicate, however, that at high temperatures (850°C) the assemblages which form are controlled by the partial pressure of oxygen. The short term experiments have accidently arrested the progressive and <u>indirect</u> oxidation trend within single grains. Run 3 at 850°C (Figure 5.6e) shows the following assemblages from the grain boundary to the grain centre:-

1. Titanohematite (diffusion rim)
2. Pseudobrookite + Titanohematite
3. Rutile + Titanohematite
4. Ferri-ilmenite + Ferri-rutile

This zonation in mineral assemblages within a single grain has resulted, because of an oxidation gradient across the grain. The long term experiments (5 and 10 days) prove that the rate at which equilibration takes place depends directly on the rate at which oxygen diffuses into the grain.

The conclusion that is drawn from these observations is that the <u>direct</u> trend, which is equivalent to the grain

boundary assemblage of the indirect trend (omitting the diffusion rim) requires a higher partial pressure of oxygen for its formation. It is important to note that any surface reaction will have the effect of monitoring the diffusion of oxygen into the grain centre.

5.10.6 Temperature and po_2 of formation

The above conclusions suggest a re-examination of the electron probe data on the products of natural ilmenite to see whether any further points may be raised from a composition point of view which would support the contention that po_2 is a major property controlling the type of assemblage which forms. The critical assemblages are the rutile series, rutile + titanohematite, pseudobrookite + titanohematite and pseudobrookite; the critical division of these assemblages from the reflection microscopy point of view is between the pseudobrookite solid solution series and the rutile oxidation series.

Previous work (KARKHANAVALA and MOMIN, 1959: FLINTER 1959: TEMPLE, 1966) suggests that pseudobrookite forms at high temperatures, "somewhere in the region of 850 ^{o}C". The present study confirms this high temperature formation but has also shown that it may form as low as 650 ^{o}C. LINDSLEY'S (1964-85) work, in addition, has now conclusively

shown that pseudobrookite is thermodynamically unstable below 580°C with respect to titanohematite + rutile. These experiments were carried out under conditions of controlled oxygen partial pressure using the magnetite-hematite buffer. Intermediate hematite-ilmenite solid solutions show that above 700°C the starting material is oxidized to pseudobrookite (Fe_2TiO_5-rich solid solution) whereas at 600°C the compositionally equivalent assemblage produces titanohematite + rutile. Since there is a simple relationship between the buffered po_2 value and temperature these results effectively mean that the assemblage rutile + titanohematite forms at a lower partial pressure of oxygen than members of the pseudobrookite solid solution series.

The electron probe data are plotted on a po_2 diagram in Figure 5.6, and the range in compositions are represented by the shaded areas. The phases indicated on the diagram represent phases in the FeTiO system at 1200°C, as a function of Fe:Fe + Ti and oxygen partial pressure (WEBSTER and BRIGHT, 1961). Admittedly 1200°C is somewhat high for natural dueteric oxidation but since the phase diagram changes proportionately with temperature it may be used to illustrate the effect of po_2. It is important to note that the diagram gives no direct indication of the

oxygen contents of the condensed phases. The significant feature of the plot is that with increasing titanium content, the stability region of any given oxide assemblage is shifted to lower oxygen partial pressures.

Oxidation-reaction lines on this diagram are vertical. By starting at an ideal composition for ilmenite (point F) the assemblages produced on oxidation will be ferri-ilmenite + pseudobrookite at 10^{-8} atm., and pseudobrookite + rutile at 10^{-3} atm. It is also evident from the diagram that the pseudobrookite line, which divides the pseudobrookite-rutile assemblage from the pseudobrookite-titanohematite (or ferri-ilmenite) assemblage, changes in composition with increasing po_2, indicating that equilibrium can only be maintained by an interphase reaction. This latter point undoubtedly accounts for the wide variation in the optical properties of natural pseudobrookite and probably also accounts for the large numbers of inclusions in this mineral.

TABLE 5.1

Electron probe data for products of oxidized ilmenite

No.	Phase	Fe	Ti	$\frac{Fe}{Ti}$	$\frac{Fe}{Fe + Ti}$	Metal ions	No.	Phase	Fe	Ti	$\frac{Fe}{Ti}$	$\frac{Fe}{Fe + Ti}$	Metal ions
4	$FeTiO_3$	35.1	32.0	1.09	0.52	67.1	14	TiO_2	2.7	62.2	0.04	0.04	64.9
5		38.5	30.5	1.26	0.56	58.8	15		3.7	59.6	0.06	0.06	63.3.
6		37.1	32.8	1.13	0.53	69.8	17		1.5	61.0	0.02	0.02	62.5
7		36.2	31.6	1.15	0.53	67.8	A		6.5	58.3	0.11	0.10	64.8
G		36.5	28.1	1.30	0.56	64.6	B		6.8	58.2	0.12	0.10	65.0
H		36.6	29.7	1.23	0.55	66.3	J		8.8	56.6	0.16	0.13	65.3
I		36.8	29.9	1.23	0.55	66.7	K		7.7	56.4	0.14	0.12	64.1
1	$Fe\text{-}TiO_2$	23.6	47.4	0.49	0.33	71.0	13	Fe_2TiO_5	39.8	27.7	1.44	0.59	67.5
2		21.5	42.9	0.50	0.33	64.4	C		40.6	24.7	1.64	0.62	65.3
3		23.5	40.9	0.57	0.36	64.4	D		41.0	24.3	1.68	0.63	65.4
E		29.3	34.4	0.85	0.46	63.7	M		40.3	26.1	1.54	0.61	66.4
F		27.8	35.2	0.79	0.44	63.0							
10	Int.-TiO_2	9.9	44.7	0.20	0.16	59.6	12(Ti)Fe_2O_3		54.0	17.7	3.05	0.75	71.7
11		16.6	43.2	0.38	0.28	59.8	16		58.1	11.2	5.18	0.84	69.3
L		11.9	55.2	0.22	0.18	67.1	18		62.5	7.0	8.92	0.90	69.5
							N		63.9	6.1	10.45	0.91	70.0

TABLE 5.2

Run No.	Grain size (Starting Material)	Temp. °C	Duration	Phase
1	100u	850°C	4hrs. to 850°C 2hrs. at 850°C	I + F.R + (R + H + Pb)
2	100u	850°C	4hrs. to 850°C 20hrs. at 850°C	Pb + H + R +F.R + (I)
3	2-3 mm	850°C	4hrs. to 850°C 20hrs. at 850°C	I + F.R + R + (H = Pb)
4	2-3 mm	960°C	5 days	Pb + R + H
5	2-3 mm	960°C	10 days	Pb = R + H

Oxidation Experiments on Ilmenite. These experimental runs were made to examine the optical properties of the breakdown products in reflected light. Phases in parenthesis indicate trace amounts. (I = Ilmenite; H = Hematite; R = Rutile; F.R. = Ferri-Rutile; Pb = Pseudobrookite).

TABLE 5.3

A.S.T.M. Values.	a = 4.958 c = 14.060 V = 315.70	a = 5.039 c = 13.760 V = 302.10	a = 4.590 c = 2.960 V = 62.220	a = 9.810 b = 9.950 c = 3.730 V = 364.100
Temp.	Ilmenite	Hematite	Rutile	Pseudobrookite
Starting Material	a = 5.089 c = 14.053 V = 315.170			
550°C	a = 5.091 c = 14.057 V = 315.533			
600°C	a = 5.091 c = 13.945 V = 313.047	a = 4.050 c = 13.766 V = 304.029	a = 4.568 c = 2.988 V = 62.344	
650°C		a = 5.044 c = 13.644 V = 303.591	a = 4.594 c = 2.974 V = 62.926	Trace
700°C		a = 5.071 c = 13.589 V = 302.665	a = 4.603 c = 2.958 V = 62.693	Trace
800°C		a = 5.063 c = 13.647 V = 303.011	a = 4.588 c = 2.960 V = 62.312	a = 9.806 b = 9.983 c = 3.727 V = 364.838
900°C		a = 5.047 c = 13.795 V = 304.320	a = 4.593 c = 2.941 V = 62.033	a = 9.805 b = 9.954 c = 3.731 V = 364.193
1000°C		a = 5.017 c = 13.908 V = 303.127	a = 4.586 c = 2.943 V = 61.882	a = 9.786 b = 9.983 c = 3.726 V = 363.916

Lattice parameters for products of oxidised ilmenite determined between 550° and 1000°C. (a, b and c are in Å; V is in $Å^3$).

Table 5.4

Temp (^{o}C)	% $FeTiO_3$	% Fe_2O_3	% Fe_2TiO_5
Starting Material	95		
550	94		
600	86	21	
650		18	
700		7	
800		15	70
900		22	74
1000		17	79

Heating experiments on ilmenite. Molecular percentage determinations from unit cell parameter data. These results were determined graphically from the curves published by LINDSIEY (1964) and AKIMOTO et. al (1957). The unit cell volume data is presented in Table 5.3.

TABLE 5.5

NATURAL PRODUCTS				EXPERIMENTAL PRODUCTS			
No. of samples	Phase	Mean Unit Cell Values(Å)	a/c	No. of samples	Phase	Mean Unit o Cell Values(A)	a/c
6	Titanohematite	a = 5.037 c = 13.789	0.365	8	Titanohematite	a = 5.048 c = 13.718	0.367
2	Pseudobrookite	a = 9.703 b= 9.966 c = 3.736	2.616	5	Pseudobrookite	a = 9.797 b = 9.973 c = 3.730	2.630
6	Rutile	a = 4.589 c = 2.965	1.548	6	Rutile	a = 4.589 c = 2.961	1.55
1	Ferri-rutile	a = 4.602 c = 2.943	1.564	1	Ferri-Rutile	a = 4.598 c = 2.942	1.56
					sample from polished specimen		

A comparison of the mean unit cell parameters determined from natural occurring products and products of experimental heating.

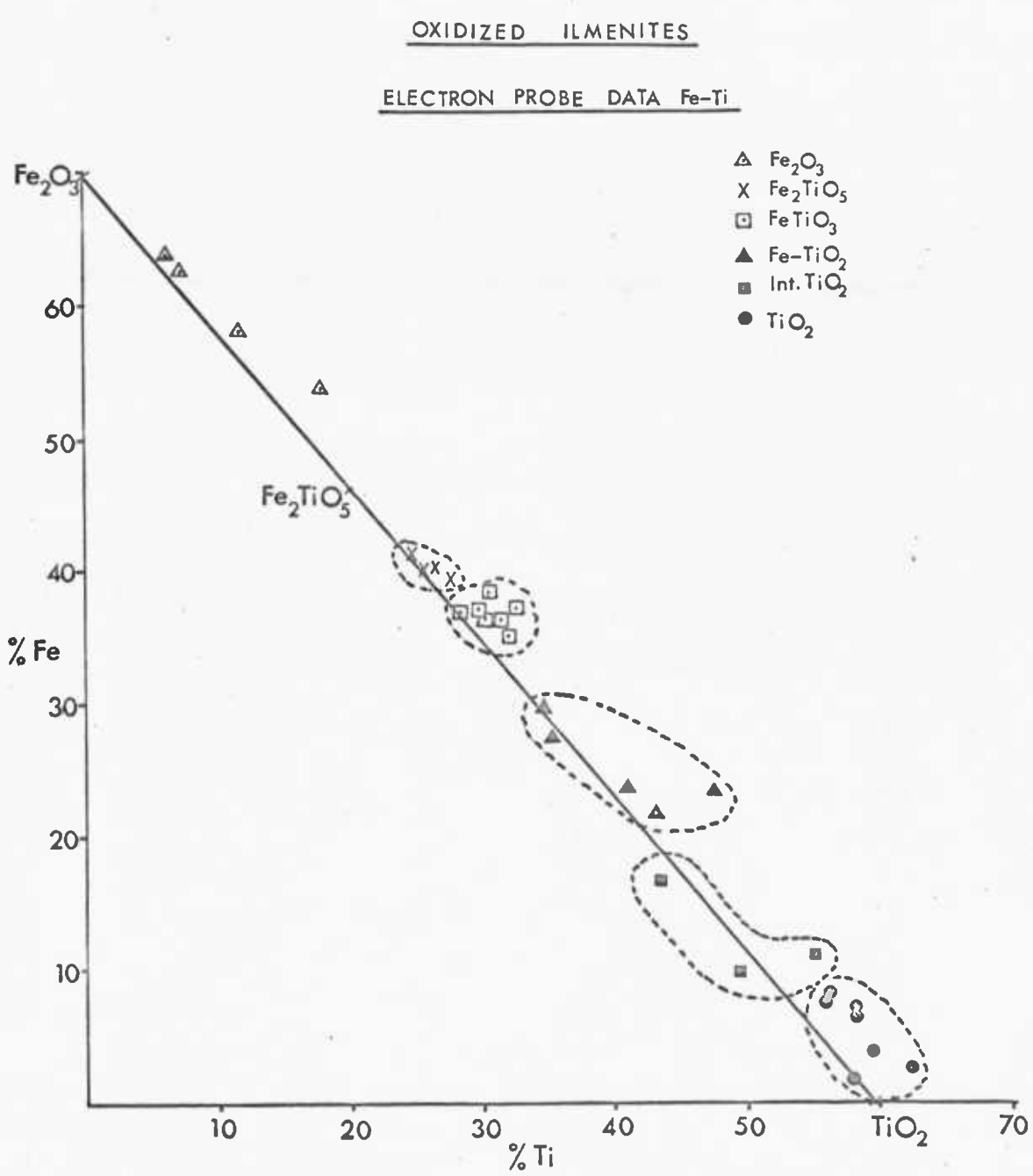
OXIDIZED ILMENITES
ELECTRON PROBE DATA Fe-Ti
Fe2O3
Fe2TiO5
FeTiO3
Fe-TiO2
Int. TiO2
TiO2
Fe2O3
Fe2TiO5
% Fe
% Ti
TiO2
10
20
30
40
50
60
70

Fig 5.1

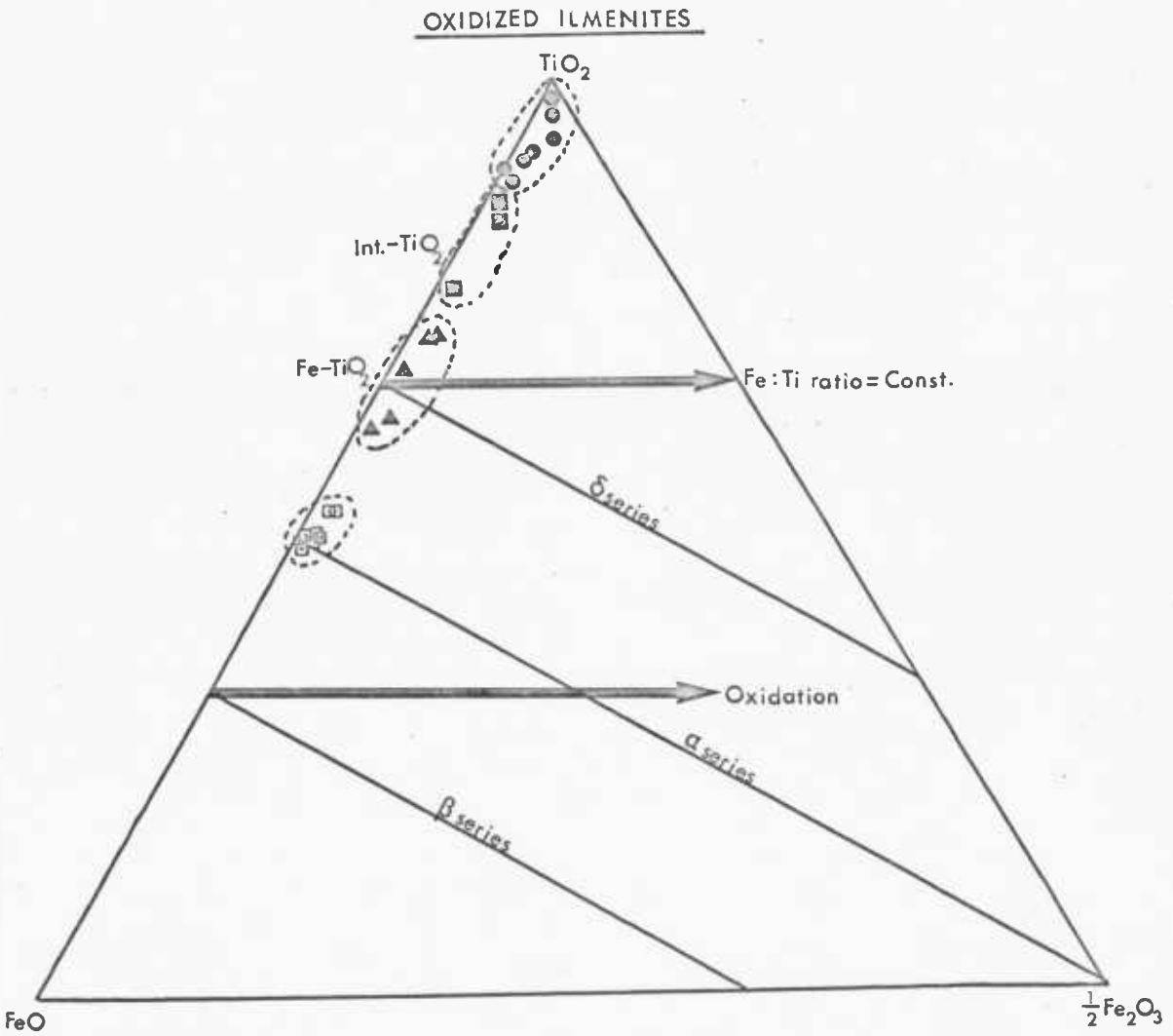

Electron Probe Data Plotted in terms of FeO and TiO_2

- Ilmenite
- Ferri-Rutile
- Intermediate-Rutile
- Rutile

Fig 5.2

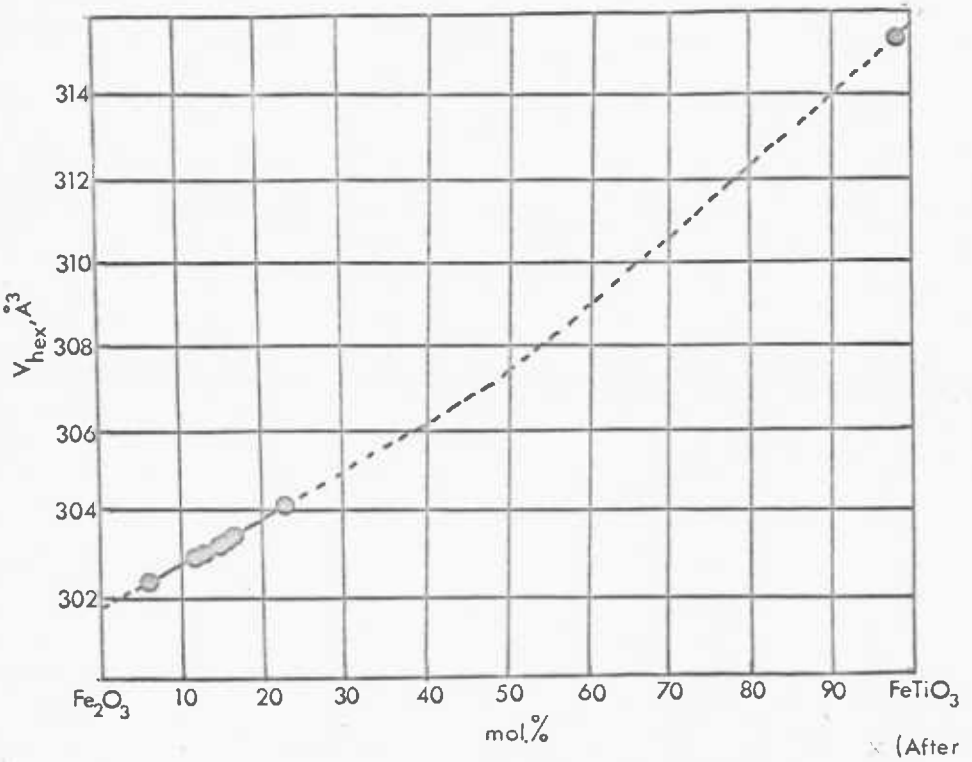

(After Lindsley 1964)

(a)

Composition Determinations from Unit Cell Volume Data.

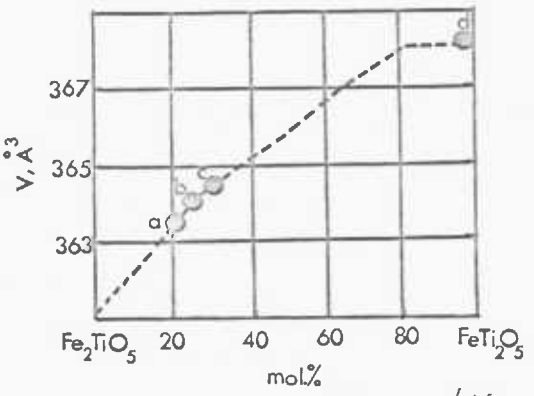

(After Akimoto et al 1957)

Fig 5.3(b)

OXIDIZED ILMENITES

PB Fe_2TiO_5 ; R TiO_2

H Fe_2O_3 ; F-R Fe-TiO_2

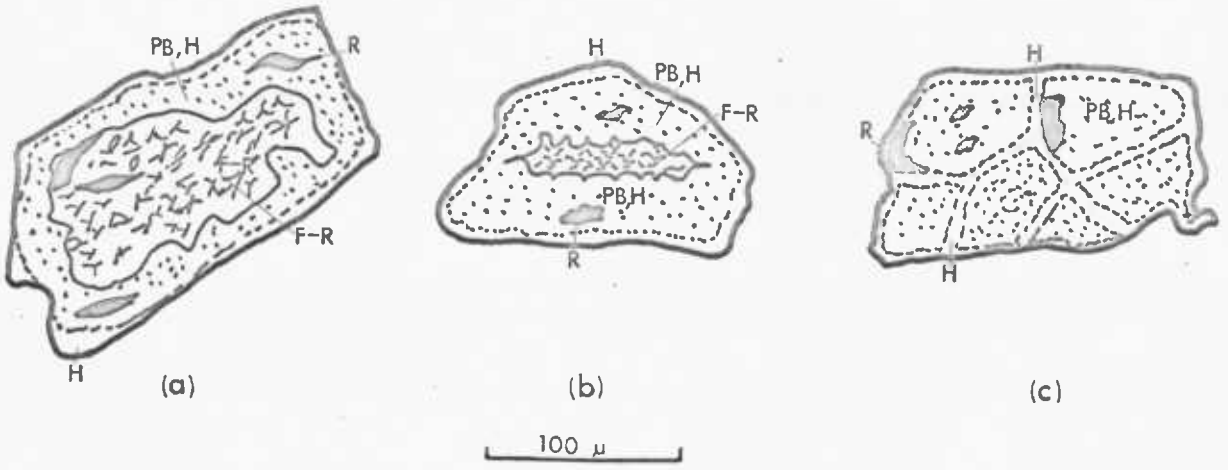

Fig 5·4

FIG

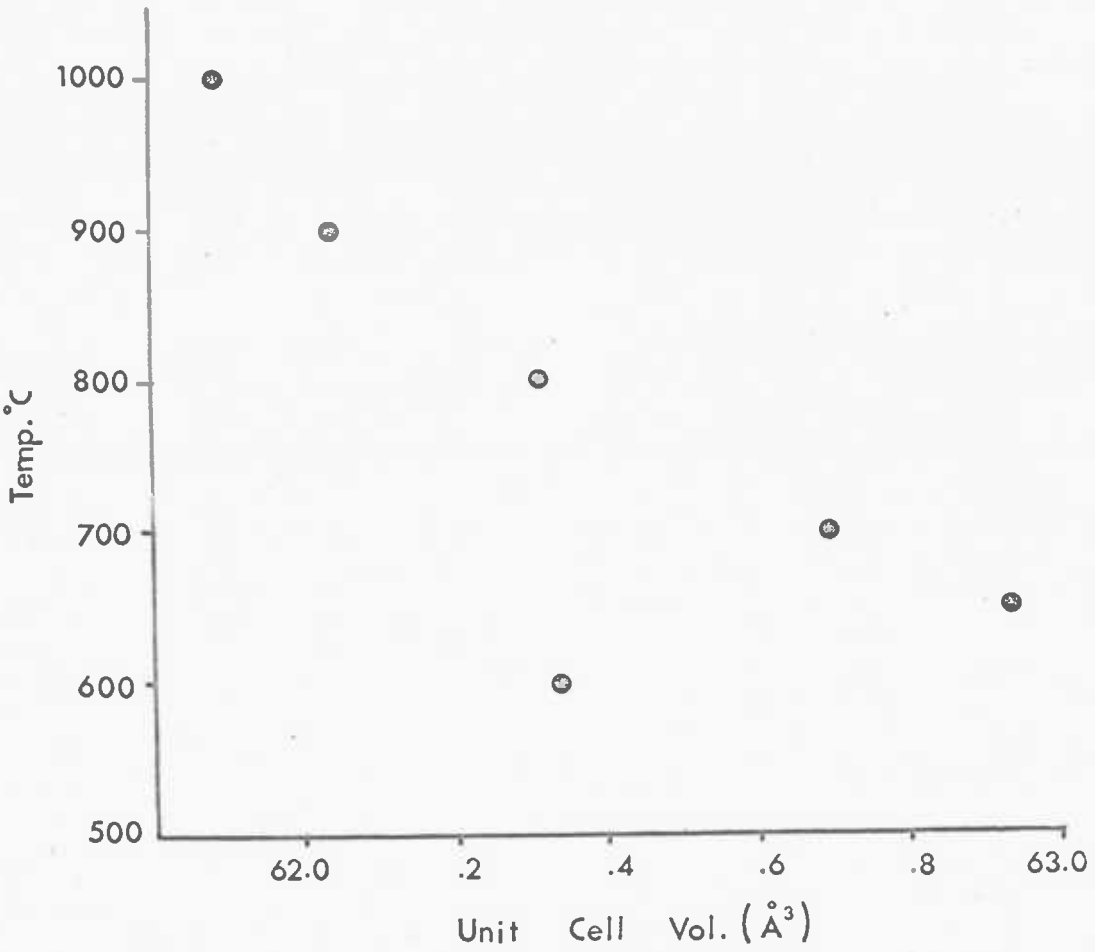

Unit Cell Volume of Rutile as a Function of Temp.

Fig 5.5

Electron Probe Data For Products Of Oxidized Ilmenite.

(Phase Diagram As A Function Of Po_2 At 1200°C)

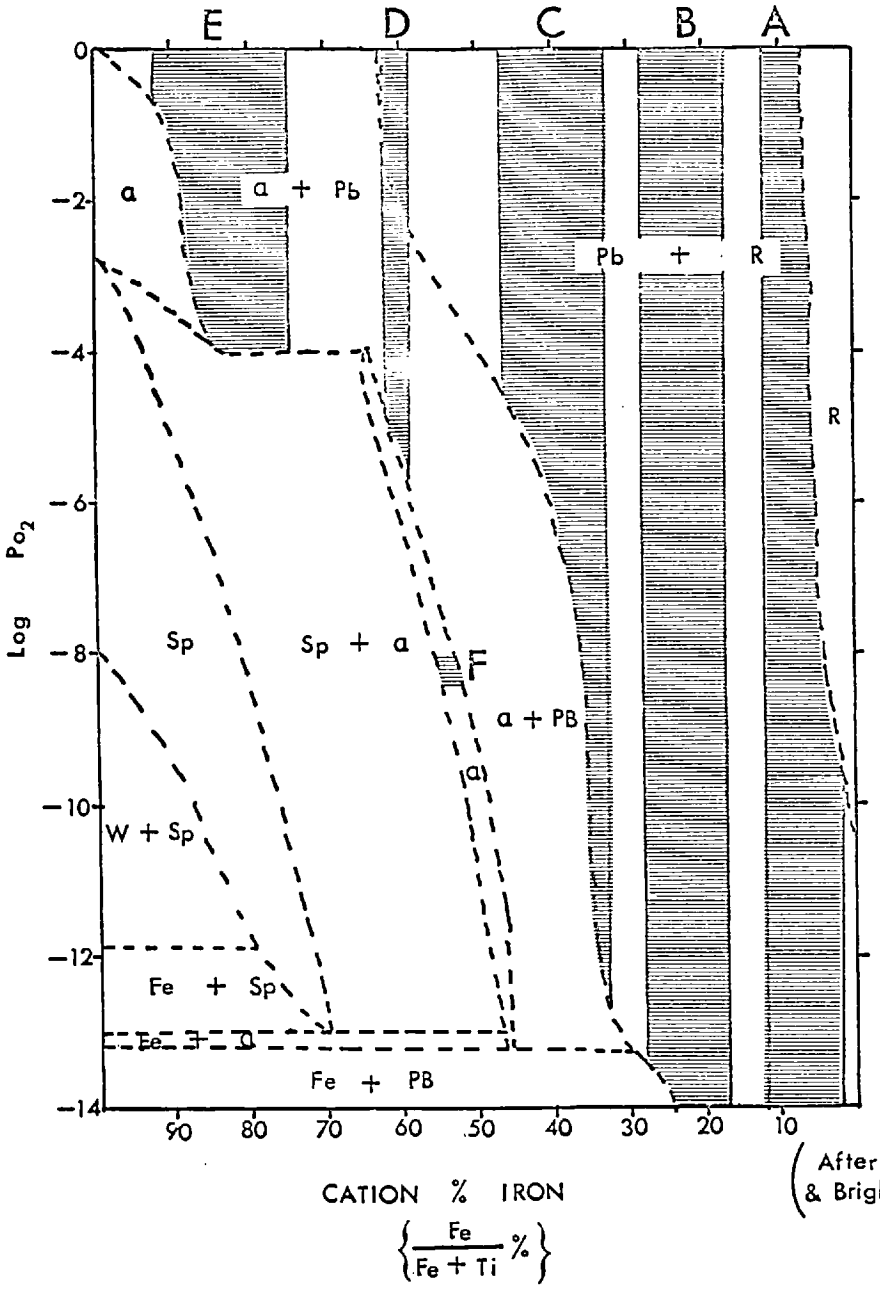

A TiO_2
B Int. TiO_2
C Fe–TiO_2
D Pb
E Fe_2O_3
F $FeTiO_3$

Fig 5.6

CHAPTER 6

TITANOMAGNETITE

6.1 Titanomagnetite Morphology

The shape of titanomagnetite grains is usually very irregular, although the grain boundaries are often linear in parts; completely euhedral grains are not uncommon.

The most spectacular forms of titanomagnetite are those in which sudden quenching of the lava has initiated the development of skeletal crystallites.

The crystal growth of titanomagnetite in the early stages of precipitation rarely seems to take place by the simple enlargement of primary cubic seeds. The textural evidence suggests that many minute crystals are initiated from the melt and these develop by rapid growth along certain crystallographic axes, rather than by a process of successive overgrowth (SCHWARTZ 1926).

6.1.1 Skeletal Crystals

Titanomagnetite crystallites in the Icelandic lavas may be divided into simple (Plate 6.1.) and complex (Plate 6.3) skeletal forms. The simple skeletal class being further sub-divided into crystallites which contain single or multiple dendritic arms.

In the simple skeletal forms, primary crystallites consist of small rod-shaped particles which intersect at right angles, and are parallel to the crystallographic axes (100). Small, sub-cubic, arrowhead crystallites, which are pyramidal in form, develop at the four ends of the intersecting cross arms. The next stage in the formation is the connecting of the ends of the crosses by diagonals from the arrowhead crystallites, which are parallel to (010), thus giving the skeletal crystal a distinctly square outline. Gradual filling in of the skeletal crystal from the diagonals and towards the primary cross-arms results in a fully grown crystal of cubic dimensions in which all evidence of the manner and stages of growth is obliterated.

Plate 6.1a, shows four skeletal crystallites of titanomagnetite in various stages of development. The progressive manner in which these crystallites have grown are depicted from left to right within the same field of view. The individual crystals which are illustrated in Plate 6.1b, c-d represent the same growth series but each of the development stages are shown in greater detail.

The simple skeletal forms of titanomagnetite in these lavas show various similarities with metallic dendrites. No quantitative measurements of the size and distribution of

the dendrites has been attempted, but it is worth noting that in an interesting series of unidirectional solidification experiments by AHEARN and QUIGLEY (1966), dendritic parameters, such as the length of dendritic cross-arms and the inter-dendritic arm spacing, were found to show good positive correlations with the distance from a chilled surface.

The crystallites in Plate 6.2 a-d show varying stages of growth, and differ from the simple skeletal forms described above, in that the single diagonals which link the main vertical cross-arms, do not simply grow from the ends of the primary arms but develop in great numbers along the entire length of the arms. In other words the filling-in process does not proceed exclusively from the outer edge towards the centre of the crystal, but progresses by the enlargement of the many diagonals. A constriction at the intersection of the main cross arms occurs in the single diagonal type, whereas a considerable thickening of the intersection, appears in the multiple type, indicating that crystalline growth in the latter form has also developed from the centre towards the periphery.

The <u>complex</u> skeletal crystallities (Plate 6.3) are characterised by more than two primary intersecting arms

and these frequently do not occur at right angles to each other as is common in the simple skeletal types. In addition, the complex forms also develop multiple rather than single diagonals. These dendritic diagonals vary in length and diameter from coarse subhedral segments of titanomagnetite to fine, delicate barbs, depending on the stage of growth reached in any particular part of a crystallite.

Herringbone textures, consisting of parallel rows of individual cruciform crystallites, with intervening silicate "spines", frequently develop as long attached arms to larger and more complex skeletal crystals (Plate 6.4). Individual crystallites generally become more euhedral as the larger parent grain is approached.

Although the skeletal crystals fall into natural, morphological classes, there are no clear indications in the lavas, as to the factors which are likely to induce or inhibit the development of any one skeletal type. Generally either the simple or the complex skeletal variety is dominant in any one sample. Single or multiple diagonals in the simple type are equally likely to develop, and both types frequently occur in close association (Plate 6.4d).

In Iceland, skeletal crystals of titanomagnetite are commonly found in quenched and glassy mesostases, in fine

grained lavas, in thin pohoehoe flow units, at the tops and bases of thick individual flows, within the chilled margins of dykes, and in basaltic fragments of lithic tuffs. In spite of this distribution skeletal crystals are by no means restricted to rocks which have suffered the effects of rapid chilling. In many cases the skeletal crystals of titanomagnetite are phenocrystic or very coarse grained, as those illustrated in the photomicrographs, and have even been found in a suite of gabbroic rocks examined from south-east Iceland (specimens loaned by J. ROEBOL).

The work by SCHWARTZ (1926) on iron-ore sinters and the skeletal growth pattern of magnetite supports earlier work which has shown that in crystallisation from a solution there are two zones of temperature concentration where crystallisation develops. In the high temperature zone the liquid is metastable or in a condition where crystallisation by "inoculation" takes place. At a higher concentration or in the supersaturated zone (labile zone) crystallisation takes place spontaneously. Experiments have shown that crystallisation in the labile zone is very rapid and results in branching, feathery, denditic forms, whereas from a metastable state it is comparatively slow and there is adequate time for the growth of good crystals. One may

expect therefore that the dendritic forms of titanomagnetite observed in lavas probably crystallised under conditions analagous to the labile state in solutions. SCHWARTZ is careful to point out, however, that the crystallisation of magnetite (titanomagnetite) from a melt is not this simple. Where other material is present both supersaturation and undercooling are involved.

We are not aware of any unusual magnetic effects in skeletal titanomagnetite crystals but there is one general point which has been confirmed in this study; since the surface area gradually decreases with increasing crystal growth, skeletal crystallites are relatively more susceptable to alteration than fully grown crystals.

6.2 Corrosion of titanomagnetite

Magmatic corrosion features of the opaques appear to be uncommon, although some lavas are characterised by large numbers of titanomagnetite phenocrysts which appear to be almost sub-graphic in form (Plate 6.5a). In general, and this is a problem which always arises in the interpretation of graphic intergrowths, it is difficult to decide textually whether the smooth radial fingers, which frequently develop from the opaques are the result of corrosion, or are an expression of primary crystal growth under rather

exceptional magmatic conditions (Plate 6.5b). In the case of good euhedral crystals, it is clear that the limit of the embayments into the opaque are often concentric to the original crystal outlines (Plate 6.5c), indicating that the rate of advance of the alteration front is constant at many different points along the grain boundary. This seems an unlikely corrosional effect even at high temperatures. On the other hand, skeletal forms of growth indicate that renewed generations of titanomagnetite are sharp and well defined, and that crystal growth takes place in a very precise manner along preferred axial directions. Rims of titanomagnetite which link the radial rods (Plate 6.5c), complicate the issue even further, but it does give the impression that the enclosed graphic silicates were trapped in a "fluidal" state, suggesting that the feature is a primary growth characteristic, rather than an expression of corrosion. Alternatively, the normal growth rate of the titanomagnetite may have been impeded by a short and sudden burst of silicate(s) crystallisation. Co-precipitation of the titanomagnetite may have been initiated and the atoll-texture illustrated in Plate 6.5d would have resulted. Since these features are only observed in phenocrysts of titanomagnetite the proposed mechanisms are not unrealistic; there is ample opportunity for the phenocrysts to be moved

and transferred from stable to metastable conditions or from crystallising to non-crystallising environments. It seems unlikely that the atoll texture illustrated in Plate 6.5d could ever have resulted by corrosion, and presumably replacement, of titanomagnetite, as it would have needed to be highly selective.

6.3 Oxidation of Titanomagnetite

6.3.1 General Statement

The common oxidation products of magnetite are hematite and maghemite. The latter γFe_2O_3 phase is metastable and readily inverts to the stable αFe_2O_3 form above 300°C. Hematite on the other hand has a wide thermal stability range under oxidizing conditions. Simple oxidation of magnetite to hematite, resulting from supergene weathering, is shown in Plate 6.6a; and in Plate 6.6b the effect of heating an unoxidized sample (from the same locality, and taken from a mine drill core at a depth of 400 ft.) in air at 700°C for a period of 4 hours, has produced hematite in a somewhat similar, but more advanced form. In basaltic rocks pure Fe_3O_4 is rarely if ever encountered as a primary homogeneous phase, as it invariably forms a solid-solution series with ulvospinel, and is thus appreciably enriched in titanium. From the experimental point of view and from

the work in the FeO - Fe_2O_3 - TiO_2 system, it is evident that ulvospinel-rich solid solutions are more susceptible to oxidation than magnetite-rich end members. This is partly due to an increase in the ferrous:ferric ratio towards the ulvospinel end of the solid solution series. The effect of titanium in magnetite therefore not only increases its susceptability to oxidation but also increases the complexity and number of phases which may form in an oxide assemblage. In contrast to the simple oxidation of magnetite to hematite (Plate 6.6 a-b), Plates 6.7 - 6.18 illustrate the breakdown of titanomagnetite into a systematic series of alteration products.

From a consideration of the ternary diagram it is evident that the complications are due firstly to the fact that solid-solutions and not pure end members are involved; and secondly intermediate members of non-stiochiometric proportion, may be present as metastable phases, whose compositions may therefore be plotted in areas between two solid solution joins. The optical identification and nomenclature of these phases is therefore highly simplified in terms of the ideal compositions invoked by the ternary phase system, FeO -Fe_2O_3 - TiO_2.

The oxidation of titanomagnetite at high temperatures may be divided into a sub-solidus oxidation process which produces ilmenite lamellae along (111) planes, and a pseudomorphic oxidation process in which the titanomagnetite or titanomagnetite-ilmenite intergrowths are completely transformed to pseudobrookite, titanohematite and rutile. The processes may be separated in time but are more commonly continuous. It is significant that in these types of oxidation the bulk Fe:Ti ratio remains constant.

In igneous rocks sub-solidus oxidation takes place above 600°C and may continue to as low as 200°C (BUDDINGTON and LINDSLEY 1964). Pseudomorphic, or more advanced, oxidation of titanomagnetite-ilmenite intergrowths also takes place at relatively high temperatures. The evidence is based first on the lower thermal stability limit of pseudobrookite, which is 580°C (LINDSLEY 1965): and secondly, similar textures and mineralogical assemblages as those found in nature have been reproduced in a series of laboratory heating experiments above 600°C, on homogeneous titanomagnetite and on titanomagnetite with ilmenite lamellae.

A third and more subtle form of oxidation in titanomagnetite, and one which cannot be observed optically, is

the oxidation of Fe^{+2} to Fe^{+3}. COLOMBO et.al. (1964) and O'REILLY and BANNERJEE (1967) have proposed that cations diffuse through the lattice and combine with absorbed oxygen at the surface; the mechanism is dependant on the higher rates of diffusion of the octahedrally sited Fe^{+2} ions. The latter authors have demonstrated that this type of oxidation occurs at 390 °C, but may undoubtedly take place at even lower temperatures. This type of oxidation is of the utmost importance to the fundamental property of magnetism but one which requires sophisticated analytical tools for its thorough investigation.

6.3.2 Sub-Solidus Oxidation

The widespread occurrences of oriented intergrowths of ilmenite along (111) planes in titanomagnetite has provided the basis for assuming the existence of Fe_3O_4 - $FeTiO_3$ solid-solutions at high temperatures. The existence of magnetite-ilmenite solid solutions has been suggested experimentally by RAMDOHR (1926), WILSON (1953) and ROY (1954). These authors reported the successful homogenisation of magnetite-ilmenite intergrowths by heating polished rock samples. They did not chemically confirm that the bulk composition remained unchanged and therefore did not demonstrate a solid-solution series between magnetite and ilmenite.

BASTA (1959) and VINCENT et.al (1954) showed, conclusively however, that exchange reactions between magnetite and ilmenite take place on heating; the ilmenite gains in Fe_2O_3 and the magnetite in Fe_2TiO_4 and therefore a solid solution series does not exist.

NICHOLLS (1955) has suggested that at high temperatures ilmenite enters into solid solution with magnetite in the form of $\gamma FeTiO_3$ which is metastable and has an inverse spinel structure similar to that of maghemite (γFe_2O_3). Exsolution of this phase takes place with falling temperature and inverts to the stable rhobohedral form. Gamma $FeTiO_3$ is hypothetical; it has not been observed in nature and has not been reproduced synthetically or by heating natural magnetite-ilmenite intergrowths. It was also suggested that $\gamma FeTiO_3$ forms a solid solution series with γFe_2O_3, analogous with the ilmenite-hematite series.

Phase equilibrium studies show further that the solubility of ilmenite in magnetite between 600° and 1300° C is far too small to explain the observed amounts of ilmenite in ilmenite-magnetite intergrowths - [WEBSTER and BRIGHT (1961), LINDSLEY (1962), TAYLOR (1964)]. FOSLIE (1928) questioned the existence of magnetite-ilmenite solid solution on crystallographic grounds, suggesting that the

TiO_2 content of magnetites might be present in an iron analogue of Mg_2TiO_4 and that ilmenite lamellae formed by oxidation, of this postulated Fe_2TiO_4 phase. As BUDDINGTON and LINDSLEY (1964) point out, it was the synthesis of this phase by BARTH and POSNJAK (1932) and the discovery of natural ulvospinel by MORGENSEN (1946) that added impetus to the oxidation hypothesis. RAMDOHR (1953) and VINCENT (1960) demonstrated the clear relationship between ilmenite lamellae and pre-existing exsolved ulvospinel, and showed further that the ilmenite was derived from the ulvospinel by a process of oxidation.

LINDSLEY (1962) has made synthetic intergrowths of magnetite and ilmenite directly by controlled oxidation of ulvospinel and magnetite-ulvospinel solid solutions at temperatures from 600°-1000°C and water pressures from 670-2000 bars; this process is reversible upon reduction. VINCENT et.al (1954) also showed that true homogenization of magnetite- ilmenite intergrowths, without a change in bulk composition, could only be effected under reducing conditions.

The oxidation of ulvospinel takes place according to the following reaction:-

$$6Fe_2TiO_4 + O_2 = 2Fe_3O_4 + 6FeTiO_3$$

The reaction is simplified, in that solid solution (SS) relationships are involved in each phase. More accurately the equation would read: ulvospinel rich$_{ss}$ + O_2 = Magnetite-enriched$_{ss}$ + ilmenite$_{ss}$. The theoretical implications of this reaction has been considered by VERHOOGEN (1962) who confirms that magnetite-ilmenite intergrowths result by oxidation of initial magnetite-ulvospinel solid solutions.

Magnetite-ulvospinel solid solutions can also be oxidized, without loss of structure, to produce metastable cationic deficient Fe-Ti spinels. In terms of the FeO-Fe_2O_3-TiO_2 ternary system (Figure 3.2) these spinels fall on the TiO_2 and Fe_2O_3 side of the magnetite-ulvospinel join, and are termed titanomaghemites.

The change from magnetite to maghemite takes place below 600^{o}C (the temperature at which γFe_2O_3 inverts to the stable αFe_2O_3 form) and involves a replacement of $3Fe^{++}$ in 6-fold co-ordination by $2Fe^{++}$ (NICHOLLS 1955). NICHOLLS (1955) and VERHOOGEN (1962) on theoretical grounds have suggested that magnetite-ilmenite intergrowths may result from an oxidation process of this type, in which the metastable titanomaghemite phase, breaks down and subsequently inverts to a member of the ilmenite-hematite solid solution series.

Inasmuch as these (γ) spinels form by oxidation of an original magnetite-ulvospinel solid solution, the concept of cationic deficiency is most useful and more valid than that of the hypothetical γ $FeTiO_3$ phase in solid solution.

In summary, the two alternative ways in which titanomagnetite can be oxidized to a rhomboderal hematite-ilmenite phase are:-

1. Oxidation at low pressures and between 400°C and 600°C to yield cation-deficient spinels of the titanomaghemite series, which may or may not subsequently invert to hematite-ilmenite solid solutions.

2. Oxidation at low to moderate pressures and above 600°C with <u>direct</u> formation of rhombohedral hematite-ilmenite solid solutions.

6.4 <u>Reflection Microscopy of Titanomagnetite-Ilmenite Intergrowths</u>

The ilmenite content of titanomagnetite is extremely variable, in some grains it may reach up to 70%, while in others only a few or a single inclusion of ilmenite is observed.

Texturally ilmenite intergrowths in titanomagnetite have an exsolution appearance. However, exsolution does not take place in the classic sense but results by oxidation of a primary magnetite-ulvospinel solid solution. Ilmenite intergrowths may be produced at high temperatures ($>600^{\circ}C$) by the direct oxidation of a primary spinel or alternatively by oxidation at lower temperatures to yield cationic deficient spinels, of the titanomaghemite series, which invert, owing to instability, to ilmenite-hematite solid solutions.

Ilmenite intergrowths in titanomagnetite may be devided into the following textural forms: (a) trellis networks; (b) sandwich types; and (c) composite (granule) types.

6.4.1 Trellis Type

All transitions from fine spindles of ilmenite along one set of (111) planes to closely crowded lamellae along all sets of the octahedral planes are observed. The latter intergrowth, forms the well known widmanstatten texture. Ilmenite lamellae are usually single crystals which show sharp and well defined contacts with the titanomagnetite host. Although the lamellae are smooth in outline, they are rarely parallel for any distance. At the intersection

of two or more lamellae, the ends of the individual lamellae are tapered. This tapering effect also applies to thin lamellae of ilmenite which do not extend to the titanomagnetite grain boundaries. The width of ilmenite lamellae in any one grain is fairly uniform (Plate 6.9c) but a supertrelliswork of larger laths, infilled by several generations of finer lamellae, are also common.

Ilmenite lamellae are often concentrated along cracks, around silicate inclusions and most significantly of all along titanomagnetite grain boundaries (Plate 6.7). These textural features strongly support the hypothesis that oxidation and not exsolution, is involved in the formation of ilmenite lamellae from a primary spinel solid solution. The ilmenite in these oxidized lamellar-zones increase in size and abundance towards the grain boundaries (Plate 6.7a). Lamellae which project into the titanomagnetite are sharply tapered and gradually disappear as the unoxidized areas are approached. There is a significant change in colour and reflectivity in the titanomagnetite as it becomes whiter and brighter (Plate 6.7 c-d), as titanium is drained from the host. Once a lamellar framework is established at the edge of a grain, microcapillary access to the centre, for further oxidation, is made available through the discontinuities which are formed at the ilmenite-titanomagnetite interfaces.

In spite of the doubts raised by GOLDSCHMIDT (1926) and FOSLIE (1928) for the existence of a magnetite-ilmenite solid solution series, based on the dissimilarity of crystal structure, GRUNER (1929) has nevertheless found that lattice intergrowths only occur on planes in which the atomic arrangement and spacing are most alike. In this light, oxidation-reduction relationships between magnetite, ulvospinel and ilmenite seem reasonable. In the spinel structures of ulvospinel and magnetite (BARTH and POSNJAK (1932)) the oxygen atoms are arranged in cubic close packing, with metal atoms in tetrahedral and octahedral co-ordination; the oxygen layers parallel to (111) in the spinel structure and parallel to (0001) in the ilmenite structure are practically equivalent. This orientation of ilmenite lamellae in titanomagnetite has been confirmed by BERNAL et.al (1957), by single crystal analysis, on material from the Skaergaard intrusion.

6.4.2 Sandwich Type

Thicker sandwich laths of ilmenite along one set of the octahedral planes are also observed (Plate 6.8b). These laths generally occur in small numbers, and a single lath is the most common form. These laths rarely have parallel sides, are not tapered and unlike the fine, trellis-types

of ilmenite continue to the titanomagnetite grain boundaries. The sandwich laths are also controlled by (111) parting planes in titanomagnetite and when they occur in the same grain as the trellis type, it is obvious that the thicker laths pre-date the finer lamellae. Whether these thick sandwich laths are primary inclusions, or whether they result by oxidation from a primary cubic host is controversial. The same problem arises in the composite or granule-type of intergrowth and will be fully discussed in the following section.

6.4.3 Composite Type

Ilmenite also occurs as an irregular composite intergrowth with titanomagnetite, showing sharp contacts. The ilmenite inclusions are terminated by linear, rather than rounded faces and are not crystallographically distributed within the host. These inclusions are referred to as internal or external composite, depending on whether the ilmenite is wholly or partly included in the titanomagnetite (Plate 6.8a). Sometimes these ilmenite inclusions split into thin fingers and extend into the titanomagnetite as normal lamellae. External composite-ilmenite frequently extends beyond the limit of the titanomagnetite grain boundaries. These may develop as euhedral arms or may become intimately associated with the silicates, forming graphic or subgraphic

intergrowths (plate 5.4d). Titanomagnetite zones around primary silicate inclusions are often oxidized, and contain lamellae or internal composite inclusions of ilmenite. These ilmenitic rims are not structurally controlled, but the boundary between the titanomagnetite and the ilmenite is extremely sharp, and usually smooth and gently curving (Plate 5.4d).

The question as to whether composite intergrowths are the result of diffusion at high temperatures (VINCENT et.al 1954, WRIGHT 1961); the result of increasing degrees of oxidation and diffusion (BUDDINGTON and LINDSLEY 1964); or the result of initial "coprecipitation" of titanomagnetite and ilmenite is highly controversial.

The terms internal and external composite, proposed by BUDDINGTON and LINDSLEY (1964) were specifically intended to emphasise the point that higher rates of diffusion are operative with increasing degrees of oxidation. By analogy with sulphide exsolution textures (BRETT 1964), BUDDINGTON and LINDSLEY are of the opinion that increasing degrees of oxidation and diffusion result in a systematic series of fabrics according to the following scheme.

1. Homogeneous titanomagnetite
2. Trellis intergrowths of thin ilmenite lamellae

along all sets of (111) planes in the host.

3. Sandwich intergrowths of thick lamellae, predominantly in one set of (111) planes.

4. Composite (granule) intergrowths within the titanomagnetite.

5. Composite (granule) or occasional lamellae of ilmenite on the external borders of the magnetite.

VINCENT (1960 p.1606) considers that composite intergrowths of magnetite and ilmenite are "clearly fundemental to a full understanding of the petrological role of the opaques"; particular attention has therefore been directed towards the textural form, distribution and mode of occurance of composite intergrowths in the Icelandic lavas.

This study suggests that composite intergrowths result from original co-precipitation of titanomagnetite and ilmenite. The reasons for this are as follows:-

1. The normal precipitation sequence of the opaques from a magma is ilmenite followed by titanomagnetite.

2. Protruding arms, from external composite grains, form either euhedral plates of ilmenite extending into the

groundmass, or graphic intergrowths within the silicates. Extensions of this type are obviously not the result of a primary "exsolution" process.

3. It has now been clearly demonstrated that ilmenite does not exsolve from titanomagnetite in the classic sense, but is the result of a sub-solidus oxidation process. Whether a textural diffusion process is effective under oxidizing rather than slow cooling conditions, to produce lamellar, sandwich and composite intergrowths in successive stages, is uncertain. Classical rim textures as those produced by the solute in exsolving sulphide solid solutions are not observed, and as far as is known have not previously been recorded. The external composites are often subhedral or equant (Plate 6.8a) and as such bear no relation to diffusion rims. Since ulvospinel forms a true solid solution with magnetite, and it is well known that not only low po_2, but also slow cooling conditions are needed for it to exsolve, it might be expected that diffusion rims of ulvospinel should develop, but the published photomicrographs by RAMDOHR (1953) VINCENT (1960), and NICKEL (1958) do not show this feature.

Slow cooling and oxidizing conditions are also required for the exsolution of transparent aluminous spinels from

titanomagnetite (see Chapter 6.6). If composite inclusions of ilmenite are due to exsolution under highly oxidizing conditions, then spinel rods should also be expected to abound - but do not.

4. The presence of all three textural types (trellis, sandwich, composite) of ilmenite in titanomagnetite precludes the possibility that composite inclusions are the result of advanced oxidation. Composite inclusions are often in the centre of a framework of thick ilmenite laths, and/or within a sea of finer lamellae. The lamellae terminate sharply at the composite, titanomagnetite-ilmenite interface, and there is no evidence to suggest that inclusions are enlarged by diffusion of material from oriented lamallae. In all cases it is judge that lamellar structures post-date composite forms of ilmenite. If large composite inclusions develop under conditions of high diffusion rates, and hence at high temperatures, most of the titanium would be leached from the titanomagnetite structure at an early stage, inhibiting any further exsolution of a finer scale.

5. Polished sections of basalt which are characterised by large numbers of titanomagnetite grains, densely packed with ilmenite lamellae along (111) planes, will always show a few grains in which the ilmenite has been further oxidized

to metailmenite. If irregular inclusions of ilmenite are the result of advanced oxidation, one would expect that if the oxidation process continued (not sub-solidus) some effect on the intergrowth, or the host for that matter, should be apparent, but this is not the case; metailmenite only develops in composite ilmenite, when discrete lamellae within the titanomagnetite are also present.

In short, composite inclusions of ilmenite cannot be oxidized independantly of their otherwise homogeneous titanomagnetite hosts, without the cubic phase being affected. Once the titanomagnetite contains a well established framework of ilmenite lamellae, both textural forms of ilmenite (trellis plus composite) may then follow the metailmenite sequence of oxidation side by side. Furthermore, this indicates (supporting 4 above) that although large inclusions of ilmenite may be present in the titanomagnetite, the titanomagnetite is effectively unoxidized, on a gross scale, until ilmenite lamellae appear.

6. No original homogeneous titanomagnetite can have a composition richer in Ti than Fe_2TiO_4, and if this is all oxidized to ilmenite, ilmenite and magnetite will form in the molecular proportions of 3:1 according to the following equation:

$$3Fe_2TiO_4 + \tfrac{1}{2}O = 3FeTiO_3 + Fe_3O_4$$

This 3:1 molecular ratio corresponds to a 2.2 : 1 volume ratio, (HENRIQUES 1966) and many of the composite grains have a volume ratio of ilmenite to titanomagnetite larger than this.

7. The most convincing evidence that composite ilmenite inclusions in titanomagnetite are the result of co-precipitation, is that of composition. In three selected lavas, composite inclusions of ilmenite were measured using the electron probe. Analyses of ilmenite lamellae in these samples were attempted but the count rates were found to vary considerably within the same lamella and also between lamellae within the same grain; this did not apply to the areas of composite ilmenite. In an unpublished report by MILLMAN and KELLY (1962) a 6.0% variation in Fe and a 9.7% variation in Ti was detected inlamellar ilmenite. This variation may be attributed to the fact that the composition of a lamella depends primarily on the degree of sub-solidus oxidation, whereas the composition of composite (and discrete) ilmenite depends on primary crystallisation.

The values for Fe and Ti which were determined in the areas of composite ilmenite are as follows:

	Fe	Ti	Fe:Fe + Ti
Grain (a)	37.4	26.5	0.58
" (b)	38.1	26.7	0.58
" (c)	36.7	25.5	0.59

The average Fe:Fe + Ti ratio that was obtained on discrete ilmenite, in a different set of samples, (Table 5.3), was 0.55; the average value for composite ilmenite is 0.58, compared to the stoichiometric value for $FeTiO_3$ which is 0.54.

The conclusion therefore is that the similarity in composition between discrete ilmenite and composite ilmenite, even within different samples, indicates a common source, which is different from that of lamellar ilmenite.

Arguments have been presented above, in which it is suggested that irregular inclusions of ilmenite in titanomagnetite (composite intergrowths) are not the result of advanced oxidation and exsolution, but rather the result of primary inclusions. Furthermore, titanomagnetite grains which contain concentrations of ilmenite lamellae along grain boundaries (Plate 6.7 a-d), show a gradual decrease in the size and abundance of these lamellae towards the less oxidized central part of the grain. The numberand density of ilmenite lamellae within a titanomagnetite crystal, is therefore a direct indication of the degree of effective sub-solidus oxidation. This feature has been used in the development of an oxidation classification, and one which will be extended in its thesis.

6.5 Pseudomorphic Oxidation of Titanomagnetite

The term pseudomorphic oxidation is used to describe the progressive oxidation of titanomagnetite-ilmenite intergrowths to pseudomorphs of pseudobrookite, rutile, ferrirutile and titanohematite. The variation in iron and titanium in the primary cubic and rhombohedral phases controls the ratio and distribution of the secondary phases which form. One effect of this compositional control is that the phases are also structually controlled. In other words the pseudomorphic assemblage is controlled texturally by the form of the original titanomagnetite-ilmenite intergrowth; the imprints of these relic textures are particularly striking in the case of primary (111) intergrowths (Plate 6.12 b-c).

The sequence of reactions that would take place upon the progressive oxidation of titanomagnetite and ilmenite are as follows:

Initial Subsolidus Oxidation

$$6Fe_2TiO_4 + O_2 = Fe_3O_4 + 6FeTiO_3 \quad \text{.....(1)}$$

Pseudomorphic Oxidation

$$4Fe_3O_4 + O_2 = 6Fe_2O_3 \quad \text{.....(2)}$$

$$4FeTiO_3 + O_2 = 4TiO_2 + 2Fe_2O_3 \quad \text{.....(3)}$$

$$2Fe_2TiO_4 + O_2 = 2Fe_2O_3 + 2TiO_2 \quad \ldots\ldots\ldots(4)$$

$$Fe_2O_3 + TiO_2 = Fe_2TiO_5 \quad \ldots\ldots\ldots\ldots\ldots(5)$$

6.5.1 Reflection Microscopy

With the effective termination of sub-solidus oxidation, although some titanium may still be present in the titanomagnetite, the first sign of pseudomorphic oxidation is marked by an indistinct mottling of the titanomagnetite-ilmenite intergrowth (Plate 6.9d). This mottling is due, firstly, to the fine serrations which develop at the exsolution interfaces; secondly, to the formation of minute exsolved transparent spinels in the titanomagnetite; and thirdly, to the development of micro-bladed ferri-rutile in the ilmenite.

Developing from this mottled stage, the ilmenite becomes whitened, and the titanomagnetite changes from tan to dark brown, (Plate 6.10). Although the entire grain is subjected to the oxidation process the most rapid changes which take place optically, occur within the ilmenite lamellae. Coarse lamellae and fine reticulate lamellae along (111) planes are equally affected; although lamellae towards the edge of a titanomagnetite grain are always more oxidized than those towards the centre. Texturally and mineralogically the progressive alteration stages of the

"exsolved" ilmenite follows the same trend, with certain modifications as that described for discrete ilmenite (Chapter 5.2). The only detectable differences between the "exsolved" and discrete ilmenite lies in fact that titanomagnetite appears to increase the susceptibility of the ilmenite to oxidation.

The whitening of the ilmenite lamellae and the corresponding changes in colour observed in the titanomagnetite suggest that a rapid build-up of ferric iron in the ilmenite areas takes place on oxidation. At high magnifications (x 2100) fine blades of ferri-rutile can be seen within the ilmenite lamellae, developing at an angle to the titanomagnetite-ilmenite interface; that is, at any angle to the (0001) face of the ilmenite. As oxidation proceeds, these blades increase in size and abundance and gradually transform to oriented intergrowths of rutile in a host of titanohematite. Once all the ilmenite has reached a fairly advanced stage of oxidation, the rutile-titanohematite lamellae begin to thicken and are seen to gradually encroach upon the interlamellar titanomagnetite areas (Plate 6.11b). The oxide assemblage which develops from the titanomagnetite is still titanohematite plus rutile, but the relative proportions of each phase is very nearly inversed. The oxidation front

is usually smooth and linear, or gently curving, and is not at all typical of the cuspate textures which may be expected to result from a process of this nature.

Some irregular features do appear (Plate 6.11d) but in general, inversion of the titanomagnetite takes place and is controlled by the sharp interfaces originally defined by ilmenite lamellae. The lattice control of the oxidation front is particularly well shown in Plate 6.12a.

With progressive oxidation the entire grain is eventually pseudomorphed by titanohematite plus rutile, although small triangular or rectangular relic areas of titanomagnetite may still persist (Plate 6.11d). Even at this advanced stage of oxidation the primary (111) fabric displayed by the original titanomagnetite-ilmenite intergrowth may be well preserved. The reasons for this are: firstly, individual lamellae of ilmenite are often replaced by single crystals of titanohematite; secondly, rutile shows a preferred orientation with the titanohematite, which enhances the effect of anisotropy and at the same time produces a greater contrast between different sets of lamellae; and thirdly, because of the relative concentration and distribution of titanium in the cubic and rhombohedral phases, the ratio rutile: titanohematite is greater in the zones

originally occupied by ilmenite.

Within the ilmenite lamellae it was found that only the indirect oxidation trend was followed; that is, pseudobrookite develops from rutile plus titanohematite and does not originate directly from the "exsolved" ilmenite. Plate 6.12a shows the gradual development of pseudobrookite from a rutile-titanohematite assemblage. Concentrations of pseudobrookite along original ilmenite planes is particularly noteworthy, and once again reflects the high rutile:titanohematite ratio within these lamellar structures. The chief factor controlling the formation of the pseudobrookite from a rutile-titanohematite assemblage is an increase in p_{O_2} conditions. This increase in oxidation induces an exchange reaction between the lamellar assemblage and the host assemblage. Diffusion of iron and titanium ions takes place in such a way that pseudobrookite develops almost exclusively along relic (111) planes, leaving an enriched titanohematite host, almost entirely free of crystalline residual rutile (Plate 6.12 c-d). In contrast to the sharp ilmenite-titanomagnetite interfaces that result from subsolidus oxidation, pseudobrookitic pseudomorphes are jagged and uneven in detail, which suggests that the control is compositional rather than structural. With more advanced

oxidation the (111) control is disrupted and graphic intergrowths develop (Plate 6.16 a-d). Lamellae are stable only as long as the lamellar phase is in crystallographic continuity with the host phase. When no continuity exists the most stable texture is a series of polyhedral grains or spheroids (BRETT 1964).

An alternative, less common but equally important, oxidation trend has been found in a series of ankaramite lavas fromTeneriefe (Plates 6.13 - 6.15). In the previous (Icelandic) trend the titanomagnetite-ilmenite intergrowths characteristically show an advanced state of oxidation to rutile plus titanohematite, before pseudobrookite makes its appearance. The Teneriefe alteration trend shows the same sequence of high temperature ilmenite alteration products (ferri-rutile, rutile, titanohematite and pseudobrookite) as the Icelandic trend, but the distinction lies in the relative stability of the host titanomagnetite. The original ilmenite lamellae, in this trend, are completely pseudomorphed by pseudobrookite plus titanohematite before any obvious oxidation effects are observed in the titanomagnetite. Plate 6.13d shows the incipient development of ferri-rutile in a single coarse blade of ilmenite. In Plate 6.14a, the original ilmenite lamellae are replaced by an assemblage of rutile plus titanohematite; and in

Plate 6.14 b-d the gradual development of pseudobrookite can be seen to form selectively from rutile plus titanohematite, in the relic ilmenite lamellae. Inversion of rutile plus titanohematite to pseudobrookite starts at the edge of the grain and proceeds along the lamellar interfaces. The ankaramite lavas are characterised by large phenocrysts (200-300u) of titanomagnetite, which contain appreciable numbers of exsolved rods of transparent spinel. The unusual nature of this spinel and the possible presence of magnesium in solid-solution are factors which may effectively control the stability of titanomagnetite. Once pseudobrookite is well established within the lamellar structures (Plate 6.15c) oxidation of the titanomagnetite-spinel intergrowth proceeds. The only major phase which generally forms from this breakdown is titanohematite, which can evidently not accommodate large percentages of the exsolved spinel phase, which may develop in some grains. This results in an unusual texture of the type shown in Plate 6.15d, where undigested globular relics of spinel persist in the titanohematite.

Provided the temperature is still sufficiently high, a redistribution of the titanohematite and the pseudobrookite takes place. This feature applies to the Icelandic and the Teneriefe oxidation trends. The immediate effect of

this redistribution is that the (111) relic texture is rapidly lost as internal recrystallization takes place. Plate 6.16 a-d shows the destruction of the (111) texture from serrated lamellae (a) to subgraphic intergrowths (b) and finally to clusters of subhedral crystals (d). Heating experiments on homogeneous titanomagnetite has shown that textures similar to Plate 6.16d are produced by rapid oxidation at high temperatures (and high partial pressures) when sub-solidus oxidation is not encountered as an intermediate stage. In other words, the structural and compositional control of "exsolved" ilmenite plays a major role in the texture and distribution of the secondary phases which form. The high titanium content of the ilmenite lamellae reflects once again the higher ratio of pseudobrookite: titanohematite in these areas, as opposed to the titanomagnetite host.

In their highly oxidized forms original titanomagnetite and original discrete ilmenite can be distinguished on the basis of the pseudobrookite: titanohematite ratio. This ratio is higher in the original ilmenite and lower in the original titanomagnetite. This criterion is also useful in detecting titanomagnetite which originally contained composite inclusions of ilmenite. Large amounts of

pseudobrookite, containing some rutile, within a highly oxidized grain immediately suggest the presence of excessive ilmenite. Such grains are shown in Plate 6.17 a and d.

The variety of pseudobrookite intergrowths in titanohematite is enormous and all stages from relatively smooth pseudobrookite lamellae (Plate 6.17 a-b) to graphic intergrowths (Plate 6.17c) and unusual cable textures (Plate 6.15 a-b) are all present.

Precise quantitative electron probe analyses such as those carried out on highly oxidized discrete ilmenite are less meaningful and much more difficult to obtain in highly oxidized titanomagnetite. The reason for this is that the measured area may originally have been "exsolved" lamellar ilmenite, primary composite ilmenite or titanomagnetite, and to conclusively distinguish between these is almost impossible

6.6 Exsolved Alumino-Spinels

In the early stages of incipiently oxidized titanomagnetite and ilmenite intergrowths, reference was made to the formation of minute rods of transparent spinel which develop within the titanomagnetite host. Discrete spinel phases will be discussed more fully in the appropriate

section, but the relevance of spinels here is that they are evidently closely connected with the pseudomorphic oxidation process. These spinels are hercynitic ($FeAl_2O_4$) in composition but minor amounts of magnesium and manganese are also present.

Exsolved spinels in magnetite (titanomagnetite) are common in intrusive rocks and in magnetite ore bodies. Slow cooling conditions seem to be a necessary prerequisite for this formation, as they show all the characteristic textural features of true exsolution. Slow cooling conditions are further in evidence by the widespread association of exsolved ulvospinel with magnetite-hercynite intergrowths. (RAMDOHR 1953, MILLMAN 1957, VINCENT and PHILLIPS 1954). An example of this type of association is shown in Plate 6.19.

TURNOCK and EUGSTER (1962) have shown that a complete solid solution series exists at high temperatures but is limited below 860°C by a symmetrical solvus which widens with decreasing temperature. The only qualitative interpretation suggested by the solvus is that the spinel (magnetite-hercynite) would crystallise as a single phase above 860°C; and at lower temperatures exsolution would take place, although the rock would need to be held in the range 400-600°C "for a long period of time". (TURNOCK 1959).

True exsolution can undoubtedly take place, as has indeed been shown experimentally by TURNOCK, but exsolution

closely allied with the effects of oxidation also seem apparent. The solvus diagrams in TURNOCK and EUGSTER indicate that the amount of hercynite that can be accommodated in magnetite at 800°C is 30 mole. percent, and at 600°C is 14 mole. percent; the corresponding amounts of Al_2O_3 which will enter hematite are respectively 8 and 6 mole. percent. CARMICHAEL (1967) found that the average Al_2O_3 content of 29 titanomagnetite samples, and the average of 21 discrete ilmenite samples was 1.80% and 0.04 % respectively. These figures suggest that a primary partitioning of alumina between the cubic mineral and the rhombohedral mineral will take place during the initial crystallisation of these phases. It is suggested, however, that a similar partitioning, with a preferential enrichment of alumina as $FeAl_2O_4$ in titanomagnetite, takes place as a result of oxidation. This mechanism has been tentatively suggested by WRIGHT and LOVERING (1967) to account for the presence of transparent spinels in titanomagnetite from New Zealand beach sands. On the basis of limited evidence these authors suggest that diffusion of Al takes place during the sub-solidus oxidation of an original magnetite-ulvospinel solid solution member. With reference to the Icelandic lavas, a concentration of Al may well take place during sub-solidus oxidation, but the optical evidence strongly

suggests that the effect of alumina diffusion is accelerated by processes of more advanced oxidation. The effect of this oxidation is to saturate the cubic phase in $Fe(Al, Mg, Mn)_4O_4$ and "exsolution" as a result follows. In other words, spinel rods first appear in the titanomagnetite not at the stage when ilmenite lamellae begin to develop, but at the stage of oxidation when these original ilmenite lamellae show their first signs of alteration to ferri-rutile, rutile, and titanohematite. The percentage of spinel rods increases with increasing oxidation. The association of exsolved spinel with highly oxidized titanomagnetite-ilmenite intergrowths, suggests that the oxidation must have taken place over a period of time at relatively high temperatures.

TURNOCK and EUGSTER state that hercynite is not stable at high partial pressures of oxygen; it readily inverts to a magnetite-hematite-corundum assemblage. At 600°C this inversion takes place at an oxygen partial pressure of 10^{-20}, and at 800°C the corresponding pressure is 10^{-12}. A comparison of the equilibrium partial pressures and the reactions involved in the oxidation of ulvospinel, magnetite and ilmenite indicate that hercynite should break down at considerably lower partial pressures than magnetite or ilmenite. The equations involved and the equilibrium partial pressures

are as follows:-

$$4Fe_2TiO_4 + O_2 = 4FeTiO_3 + 2Fe_2O_3 \quad \ldots\ldots\ldots (1)$$

$$4Fe_3O_4 + O_2 = 6Fe_2O_3 + \quad \ldots\ldots\ldots (2)$$

$$2FeTiO_3 + O_2 = Fe_2O_3 + TiO_2 \quad \ldots\ldots\ldots (3)$$

Temp. (^{o}C)	Log p_{O_2} Ulvospinel (1)	Log p_{O_2} Magnetite (2)	Log p_{O_2} Ilmenite (3)
600	- 18.5	- 14.0	- 13.7
800	- 13.2	- 8.5	- 8.3

The persistance and association of spinel with highly oxidized Fe-Ti oxide assemblages must therefore indicate that some degree of stability is enforced upon the hercynite by the presence of magnesium (TSVETOKOV et.al 1966). WRIGHT and LOVERING (1966) have shown that 3-4% Mg may be present in this exsolved phase.

In most cases once the titanomagnetite and the hercynite are oxidized and the breakdown is complete, both phases are absorbed into the rutile-titanohematite, or pseudobrookite-titanohematite assemblages, without any evidence of their previous existence. The role of aluminium

in hematite has been noted; its corresponding substitutional role in pseudobrookite may take the form of Al_2TiO_5 (Tielite) which is known to be isostructural. The pseudobrookite described by SMITH (1965), for a suite of emery-like rocks, were found to contain between 5.2% and 7.9% Al_2O_3.

Only one sample, an exceptional ankaramite from Teneriefe was found to be quite distinct in its association of exsolved spinel with titanomagnetite and ilmenite. The lava contains a large number of titanomagnetite phenocrysts and also shows a wide range of oxidation states over small areas within individual samples. A selection of grains from this lava are shown in Plates 6.13 - 6.15. Exsolution of a spinel phase has evidently taken place during slow cooling, but without being closely coupled with the effect of advanced oxidation. Exsolution of the spinel phase post-dates the process of sub-solidus oxidation. The spinel rods are coarse grained and occur in large numbers. Their abundance may indicate the presence of substantial amounts of alumina in solid solution but this has not been chemically confirmed. The spinel rods taper and terminate at titanomagnetite-ilmenite interfaces and although finer sub-graphic intergrowths of spinel may occur within the ilmenite (Plate 6.13c) most rods bridge the area between the ilmenite lamellae and do not continue through them (Plate 6.13d).

An additional feature of this ankaramitic lava is that the size of the ilmenite lamellae are proportional to the size of the titanomagnetite grains. Tapering of the ilmenite lamellae, constriction at the intersection of two or more lamellae, internal and external composite features are all present. One obvious feature distinguishes it from any other lava examined; this is, that residual spinel droplets in titanohematite are highly resistant to the effects of oxidation and absorption (Plate 6.15d). Individual spinel rods are generally broken up but resorption of the alteration products is limited. This, perhaps, indicates that the saturation level of phase resorption has been reached, at the temperature and po_2 level at which the reaction took place.

6.7 Conclusions

In summary, the following conclusions have been reached.

1. Titanomagnetite growth patterns may be divided into simple and complex skeletal forms. The simple skeletal class being further subdivided into crystallites which contain single or multiple dendritic arms.

2. Corrosional effects on titanomagnetite are rare and are usually confined to the phenocrystic phase of crystallization.

3. The initial sub-solidus oxidation of titanomagnetite produces "exsolution" lamellae of ilmenite in a trellis or widmanstatten pattern.

4. Sandwich and composite intergrowths of ilmenite are considered to be primary features which result from co-precipitation with titanomagnetite.

5. Titanomagnetite-ilmenite intergrowths are oxidized in several successive stages to ferri-rutile plus titanohematite, rutile plus titanohematite and pseudobrookite plus titanohematite. This oxidation series is referred to as the pseudomorphic sequence.

6. In the initial stages of pseudomorphic oxidation (ferri-rutile, titanohematite) the host titanomagnetite is usually less susceptible to oxidation than the "exsolved" ilmenite. Its relative sensitivity to oxidation, however, appears to depend on the concentration of minor elements (Mg, Mn, Al). This difference in concentration distinguishes the Icelandic trend (low concentration) from the Teneriefe trend (high concentration). In the later stages of oxidation (rutile, pseudobrookite titanohematite) titanomagnetite and ilmenite oxidize simultaneously in the Icelandic trend, but independantly in the Teneriefe trend where ilmenite is followed by titanomagnetite.

7. Exsolved hercynite in titanomagnetite is closely coupled with the pseudomorphic oxidation process.

CHAPTER 7

MAGHEMITE (TITANOMAGHEMITE)

7.1 General Statement

Magnetite (cubic) transforms to maghemite (cubic) on oxidation and γFe_2O_3 (maghemite) inverts on further heating to αFe_2O_3 (rhombohedral-hematite). The transition of $Fe_3O_4 \rightarrow \gamma Fe_2O_3 \rightarrow \alpha Fe_2O_3$ brought about by heating magnetite in air has been studied by several workers. It has been found that synthetic magnetite transforms more readily to γFe_2O_3 than natural magnetite. While oxidizing synthetic magnetite it has also been found that four forms of γFe_2O_3 exist. Three of these maghemite types are cubic and the fourth is tetragonal. (BERNAL and MACKAY 1959). The oxidation of Fe_3O_4 on heating has received considerable attention, mainly because of the differences in response and behaviour of natural magnetites with their synthetic equivalents. Experimental heating by SCHMIDT and VERMASS (1955), LEPP (1957) and BERNAL et.al (1959) has shown that synthetic magnetite oxidizes first to maghemite and then to hematite, whereas natural magnetite oxidizes only to hematite, usually at high temperatures.

Heating experiments by LEPP(1957) indicate that the oxidation of magnetite to maghemite starts at 200 ^{o}C and culminates at 375-400 ^{o}C; the inversion of maghemite to

hematite starts at 375°C and is complete at temperatures between 525-650°C. In contrast, BERNAL et.al (1957) have shown that maghemite, formed by the dehydration of lepidocrocite, inverts completely to hematite at temperatures below 250°C.

In basaltic rocks pure maghemite is rarely, if ever, encountered because of the solid solution series which magnetite forms with ulvospinel. There are little data on the effect of titanium on either the temperature of formation or the temperature of inversion of maghemite (titanomaghemite). The limited synthetic work by AKIMOTO et.al (1957) does however indicate that titanomaghemite probably forms at low to intermediate temperatures (<600°C).

Titanomaghemite has not been clearly defined in terms of the ternary phase diagram but the phase may be considered as an oxidation product of titanomagnetite, having a composition close to the Fe_2O_3 - $FeTiO_3$ join. The chemical data supplied by AKIMOTO and KATSURA (1959) suggests that a complete transitional series from titanomagnetite to titanomaghemite probably exists. BASTA (1959) suggested that maghemite forms a solid solution series with magnetite and hence presumably with ulvospinel but this obviously is not acceptable as the association of magnetite with maghemite is

the result of a process of oxidation and is not the result of "unmixing".

AKIMOTO, KATSURA and YOSHIDA (1957) were able to synthesise a cation deficient cubic phase by the oxidation of various members of the Fe_3O_4 - Fe_2TiO_4 solid solution series, if oxidation was carried out below 500 C. The spineloid phase produced had a composition near the Fe_2O_3 - $FeTiO_3$ join and in some cases the oxidation resulted in the formation of a rhombohedral phase in addition to the cubic phase. Unfortunately no optical data was provided by these authors, so that one does not know whether the cubic phase was some unusual form of titanomagnetite or was in fact titanomaghemite.

7.2 Reflection Microscopy

In reflected light titanomaghemite may be white or pale blue in colour, it is isotropic and has a lower reflectivity than titanohematite, but is brighter than the titanomagnetite which it replaces. Hematite, as is well known, may replace magnetite directly and is frequently controlled by (111) parting planes. Titanomaghemite however, characteristically occurs along curved conchoidal cracks and is not crystallographically controlled. The low temperature origin of maghemite has been emphasised above. A textural feature of this low temperature oxidation effect produces a wide

variation in the degree of maghemitisation within a sample or within any one grain of titanomagnetite.

Two distinct textures are produced by titanomaghemite in homogeneous titanomagnetite. These oxidation textures are illustrated in Plate 7.1.

7.2.1 Type I - Titanomaghemite (Plate 7.1 a-b)

The onset of alteration is marked by the development of fine meandering hair-line cracks. As oxidation proceeds thin selvages of titanomaghemite can be detected along these cracks (Plate 7.1a). The maghemite selvages thicken and gradually spread out and affect larger parts of the neighbouring titanomaghetite (Plate 7.1b). Alteration does not start at the edge of a grain, in major cracks within the grain or around silicate inclusions, but appears to be initiated quite evenly throughout the grain. There is a gradual and even darkening of the titanomaghemite as it approaches the unoxidized titanomagnetite, reflecting the continuous metastable inversion of one phase to another. This feature is strongly emphasised by the presence of ilmenite lamellae (Plate 7.2) which divides the titanomagnetite into a large number of sub-grains. Each segment varies slightly in tone and reflectivity representing and corresponding to the variable state of maghematization reached

in each of the respective areas.

7.2.2 Type II Titanomaghemite (Plate 7.1 c-d)

The main differences between type II and type I titanomaghemites are as follows:

a) In type II titanomaghemites alteration starts at the grain boundaries and in major cracks within the grain proceeding towards the centre of the grain with progressive oxidation.

b) In type II titanomaghemites oxidation does not proceed along smoothly meandering perlitic cracks but rather along budding fronts.

c) Type II titanomaghemite is slightly darker in colour and has a distinctly mottled appearance.

Generally either type I or type II is present in any one sample and at present there is no clear distinction between the distribution, mode of occurrence, or factors which control either textural type of titanomaghemite.

7.2.3 Titanomaghemite - Ilmenite Intergrowths

Titanomaghemite may form by simple oxidation of titanomgnetite, as illustrated in Plate 7.2 a-d. Inversion of this metastable titanomaghemite phase may then take place to

form a member of the ilmenite-hematite solid solution series (AKIMOTO et.al (1957) and VERHOOGEN (1962). In Plate 7.2 a-c, three titanomagnetite grains are illustrated and these show well oriented, coarse and fine ilmenite lamellae along (111) planes. In all cases there is an intimate association of titanomaghemite (replacing titanomagnetite) with the ilmenite lamellae. In grain (a) small unoxidized areas of titanomagnetite still exist (i.e. free of ilmenite lamallae and titanomaghemite); in grains (b) and (c) the ilmenite-titanomaghemite assemblage is concentrated towards the grain boundaries of the host crystals. The textural distribution of the ilmenite lamellae in (b) and (c) leaves no doubt that both phases formed by processes of oxidation. Their close relationship further suggests that this may be an example of the metastable inversion process proposed by VERHOOGEN (1962). The examples illustrated here are rare and the interpretation is therefore only tentative. An equally valid micrographic interpretation would seem to be, that the ilmenite formed at a relatively high temperature, by sub-solidus oxidation of a magnetite-ulvospinel solid solution member. In the case of grains (b) and (c) the oxidation is incomplete. The sub-solidus oxidation was then followed by a lower temperature oxidation of the titanomagnetite to titonomaghemite. But restriction of titanomaghemite to

ilmenite lamellar regions within the titanomagnetite still needs to be explained. The structural discontinuities which develop at the ilmenite-titanomagnetite interfaces on sub-solidus oxidation, act as sub-capillary oxidation channels; that is, avenues along which alteration may take place. The inversion of titanomagnetite to titanomaghemite takes place at low to intermediate temperatures (below 600 °C) and the reaction is therefore sluggish. The restriction of the metastable titanomaghemite phase, along easily accessible channels, within a network of well established ilmenite lamallae may therefore be expected.

The balance between the two interpretations does not favour VERHOOGENS inversion process. The VERHOOGEN process would apparently demand that the titanomaghemite be oriented (along (111) planes) but as Plate 7.1 a-d illustrate, the characteristic texture of the metastable phase is vermicular or colloform and is not crystallographically controlled.

7.3 Distribution of Titanomaghemite

The metastable inversion of titanomagnetite to titanomaghemite is considered by KATSURA and KUSHIRO (1961) to take place during the initial cooling of a lava or during weathering. In the present study evidence for both processes, and an additional one, have been found.

Titanomaghemite occurs most commonly in lavas showing distinct weathering features, particularly at the tops of flows and in weathering rinds; it has an equally common occurrence in the dykes. Further support for the low temperature origin of titanomaghemite is the fact that it has not been found to occur in close association with pseudobrookite, rutile or titanohematite: these minerals are all common high temperature alteration products of titanomagnetite. Titanomaghemite has also been found to occur in all lavas and dykes which contain "iddingsite" as an alteration product after olivine. The significance of this association lies in the fact that goethite is an important constituent of "iddingsite"; goethite has an upper thermal stability limit of 140° C (TUNNELL and POSNJAK 1931).

A number of xenolithic inclusions have been examined in basic lavas from St. Helena (specimens loaned by I.BAKER). The xenoliths are 0.5-4.0 cms. in diameter and are basic to intermediate in composition. In a number of samples the only reheating effect that one can detect under the reflecting microscope is the alteration of titanomagnetite to titanomaghemite, along an outer concentric zone of the xenolith. The host rock is generally free of alteration.

Titanomaghemite has also been found to occur in well defined zones of oxidation, in traverses across single Iclandic lavas (WATKINS and HAGGERTY 1965, 1967). The evidence, which will be dealt with more fully at a later stage, suggests that the development of titanomaghemite may be controlled by the initial cooling of the lava and that it is most likely to develop during the late stages of deuteric oxidation.

While it is difficult to dismiss the possibility that the titanomaghemite zones in these lavas are of deuteric origin, it is certain that in the majority of cases its formation is due to post crystallisation, or more accurately, post deuteric processes (e.g. weathering, reheating, burial).

Maghemite is extremely important magnetically as it is structurally ferrimagnetic and has a saturation magnetization value of 83.5 emu/gm at room temperature (c.f. magnetite = 92 emu/gm).

CHAPTER 8

"AMORPHOUS" Fe-Ti OXIDE

"Amorphous" Fe-Ti oxide is a term which has been adopted from BAILEY et.al (1956) to describe an unidentified oxidation product of titanomagnetite. BAILEY and his co-workers used it to describe one of the progressive stages of alteration of beach sand ilmenite. The optical properties described by these authors are identical to those of the Icelandic product. In the present study a clearly defined X-ray powder pattern of the product has not yet been obtained and this has been ascribed to its ultra-cryptocrystalline nature. The essential difference between the phase described here and the phase described by BAILEY et.al is that in the Icelandic rocks it is titanomagnetite and not ilmenite which is affected by this unusual alteration process. Unfortunately BAILEY and co-workers did not consider the corresponding effects of alteration on titanomagnetite in their beach sand concentrates. It therefore remains uncertain as to whether any chemical or structural similarities exist between the respective phases, described as "amorphous" Fe-Ti oxide.

8.1 Reflection Microscopy

In reflected light the product is medium to dark grey in colour, isotropic, and has bright iridescent internal reflections. The phase is strongly mottled. It is relatively

soft and is easily plucked from the surface of a section if great care is not exercised in the polishing process.

In a few exceptional cases "amorphous" Fe-Ti oxide has been found to replace titanomagnetite directly, but the most typical form of replacement is one in which the "amorphous" phase appears to result from the breakdown of titanomaghemite. No reference to this type of alteration has been found in the literature.

The oxidation of titanomagnetite to titanomaghemite is discussed in the previous chapter of this thesis. It has been pointed out that the gamma phase may be texturally classified into type I and type II titanomaghemites. The breakdown of each of these textural types, into amorphous Fe-Ti oxide, are respectively illustrated in Plates 8.1. and 8.2.

Consider firstly the type I titanomaghemite. Plate 8.1 a-d illustrates the progressive breakdown of titanomaghemite in successive stages. It is evident from these photomicrographs that alteration starts within, and spreads out from, the curved perlitic cracks which characteries the type I variety of titanomaghemite (c.f. Plate 7.1a). At times it

has been observed that the breakdown only occurs when the original titanomagnetite is completely pseudomorphed by titanomaghemite (Plate 8.1b). At other times the breakdown to 'amorphous' Fe-Ti oxide follows very closely on the process of maghematisation and although it may appear that the titanomagnetite is breaking down directly, a close examination will usually reveal a thin veneer of the gamma phase between the amorphous product and the unoxidized titanomagnetite.

Plate 8.2 illustrates the type II titanomaghemite breakdown to "amorphous" Fe-Ti oxide. The cuspate form of the inversion fronts, typical of the type II variety (c.f. Plate 7.1b), are not as clearly defined as the alteration interfaces of the type I variety. In the latter variety the breakdown is strictly controlled by the perlitic cracks and inversion takes place in a piecemeal fashion. In the type II variety, however, the onset of alteration is not restricted but takes place over a wide area within the grain. One effect of this widespread alteration is that one can see that the inversion to the "amorphous" phase is progressive and that there is a complete series of intermediate stages in the alteration process.

Plate 8.3 illustrates the inversion of titanomaghemite to "amorphous" Fe-Ti oxide in the presence of "exsolved"

ilmenite. These titanomagnetite grains are particularly interesting for several reasons.

There is firstly the close association of the "amorphous" phase with the fine ilmenite lamellae. The advanced alteration that is associated with areas of maximum ilmenite concentration may be accounted for by the following point. Large numbers of ilmenite lamellae will tend to break the host up into an equally large number of smaller grains. This will automatically increase the surface area of the host and hence the potential for a higher degree of alteration. The relationship between the amorphous phase and ilmenite implies that a close association must once have existed between the ilmenite and titanomaghemite and this now poses the problem as to whether a metastable inversion of the titanomaghemite to a member of the hematite-ilmenite solid solution series may have taken place. Once again, however, as in previous cases, it is difficult to decide whether the trellis lamellae are the result of sub-solidus oxidation (from a magnetite-ulvospinel solid solution series) or whether the lamellae are the result of titanomaghemite inversion.

The second, and most striking feature of the photomicrographs is the fact that the ilmenite remains completely

unaltered. Note that there are three textural types of ilmenite present; trellis, sandwich and external composite. The trellis lamellae are extremely fine and are concentrated towards the titanomagnetite-titanomaghemite grain boundaries. The external composite overgrowth in grain (d) - Plate 8.3, is a primary graphic intergrowth and has not resulted from alteration. Discrete groundmass ilmenite in the presence of the "amorphous" Fe-Ti oxide phase remains unaffected.

"Amorphous" Fe-Ti oxide is extensively developed in the Icelandic dykes and is also a common product of the lavas, which have reached an advanced stage of maghemitisation. The development and recognition of this phase has obvious magnetic implications. It is unfortunate that its mineralogical character has not yet been fully determined, but its presence, distribution, and mode of occurance should nevertheless still be noted as it is an important alteration product of titanomagnetite.

8.2 Temperature of Formation

The oxidation of Fe_3O_4 to γFe_2O_3 takes place well below 200 °C. The metastable nature of maghemite is well known. It readily inverts to the stable alpha form at 375-550 °C. As hematite has not been produced as an

inversion product, in the Icelandic study, it seems valid to assume that the breakdown of titanomaghemite to "amorphous" Fe-Ti oxide probably occurs below this temperature range. This is supported by the fact that no high temperature alteration products have been observed in ilmenite, olivine, or in the discrete spinels. "Iddingsite", however, has been observed in olivine and as BAKER and HAGGERTY (1967) have pointed out it is an indication of low temperature alteration. An essential component of "iddingsite" is goethite which has an upper thermal stability limit of 140 °C (TUNNELL and POSNJAK 1931). The presence of goethite now raises the question as to whether the "amorphous" Fe-Ti oxide phase represents a hydrated form of titanomaghemite. Whether or not the "amorphous" phase we are dealing with here is a titanium equivalent of lepidocrocite (γ FeO.OH) is uncertain.

CHAPTER 9

SPHENE

9.1 Introduction

Sphene is monoclinic in structure. It is essentially $CaTiSiO_5$ in composition and although substitution for Ti by Fe^{+3} and Fe^{+2} is possible, titanium will always be strongly predominating. The relationship between colour and chemical compostion has been determined by KONTA (quoted in DEER, HOWIE and ZUSSMAN V.1., p.76, 1962). In general the colour may be correlated with the iron content, the green and yellow varieties being low in iron while the brown or black sphenes may carry 1% or more Fe_2O_3.

Sphene is a common accessory mineral in acid to intermediate rocks, in metamorphic rocks and in some types of skarn assemblages. It breaks down to anatase with quartz or occasionally to rutile (DEER, HOWIE and ZUSSMAN, 1962; MITCHELL 1964). Sphene is also known as an alteration product of titanomagnetite and ilmenite.

9.2 Reflection Microscopy

The reflectivity of sphene is considerably lower than that of the common Fe-Ti oxides and although it is extremely variable it is on a par with the Cr-spinels but may also be as low as that of olivine or pyroxene. Primary sphene is

always much brighter than secondary sphene after titanomagnetite or ilmenite. The colour is dark grey in various shades. It has a pronounced mottled appearance and as an alteration product is distinctly porous and obviously rather inhomogeneous. Sphene is strongly anisotropic and shows whitish or light yellow to pale brown internal reflections. This feature is very useful to distinguish sphene, in reflected light from all the other common silicate minerals. It is difficult to generalise on the optical properties of secondary sphene, in reflected light, as the degree of opacity varies, not only on the initial composition of the phase that it is replacing but also on the degree of replacement.

9.2.1 Primary Sphene

Primary sphene occurs in the more intermediate Icelandic lavas and hence is generally associated with relatively small percentages of co-existing Fe-Ti oxides. Typical sphenoidal wedge-shaped crystals are common. Although sphene occurs in accessory amounts it is frequently phenocrystic in form, clusters of smaller groundmass crystals, closely associated with ilmenite or titanomagnetite, are also common.

Plate 9.1a illustrates an intimate association of ilmenite with a twinned crystal of sphene. The ilmenite forms in short, stubby laths and the penetrating nature of the laths, normal to the sphene grain boundary, suggests that ilmenite has formed by reaction and is not simply the product of an initial crystalline overgrowth. This particular lava is extremely fresh and no other alteration effects were noted. Although some transparent minerals are associated with the ilmenite reaction rim these have not been identified in polished section.

Although ilmenite is the most commonly associated opaque mineral, titanomagnetite also occurs. In Plate 9.1b, several euhedral crystals are shown forming a cluster around two embayed titanomagnetite grains. The form of the embayments, the nature of the association and the well developed crystals of sphene all point to the suggestion that the sphene may have resulted, in part, by corrosional breakdown of titanomagnetite at high temperatures.

9.2.2 Secondary Sphene

In contrast to these two examples of primary sphene, attention is now directed to the widespread occurrence of secondary sphene after titanomagnetite and ilmenite. Sphene of this nature probably forms at low to intermediate

temperatures under non-oxidizing conditions. There are many recorded occurrences of Fe-Ti oxides altering to sphene and these have been summarised in an interesting and comprehensive paper by DESBOROUGH (1963). An important feature of this alteration trend, unlike those previously described at high temperatures and under conditions of oxidizing environments, is that the process is metasomatic, since its formation not only implies an addition of Ca and Si but also removal of Fe. There are obvious magnetic implications in this loss of iron and the recognition of sphene as a breakdown product is therefore very import. DESBOROUGH (1963) considers that mobilization of iron on a regional scale and under suitable conditions may contribute significantly to the formation of titanium-free iron ore bodies.

9.2.3 Homogenous Titanomagnetite

Alteration of the groundmass of homogeneous titanomagnetite, to turbid sphene is a widespread form of alteration, particularly in the Icelandic dykes, and more particularly in the Streitishorn composite dyke. This type of alteration has an irregular distribution across the dykes, and even within the same polished section it is possible to find strongly altered areas of titanomagnetite alternating with completely fresh areas. Every gradation from incipient

spotwise alteration along perlitic cracks (Plate 9.2a) to strong alteration where the entire titanomagnetite grain is completely altered (Plate 9.2d) is found. As alteration progresses the sphene transforms from a dark grey phase which is dense and mottled and generally without optical character to one which is weakly anisotropic, lighter in colour and with white internal reflections. The inversion is illustrated in Plate 9.2 a-d. The alteration to sphene is evidently younger than the cracks throughout the titanomagnetite, and the most common way of attack is by spreading out from the cracks, but alteration proceeding inwards from grain boundaries is also found. The perlitic cracks are identical to those formed during the initial alteration of titanomagnetite to titanomaghemite but no correlation between the co-existance of sphene and titanomaghemite has been found. Sphene replacing titanomagnetite along these perlitic cracks may be contrasted with the unidentified "amorphous" Fe-Ti oxide phase which, on textural evidence, is paragentically derived from the breakdown of titanomaghemite (Plate 8.1a). The initial stages of alteration are very similar in colour, reflectivity and degree of anisotropy but the important differences are that "amorphous' Fe-Ti oxide is always closely associated with titanomaghemite and hence is restricted to areas which were

originally titanomagnetite. Sphene on the other hand attacks titanomagnetite and ilmenite with equal severity and is not associated with the characteristic titanomaghemite phase. There is no question of confusing the end products of the alteration trends to either sphene or"amorphous" Fe-Ti oxide.

9.3.4 Titanomagnetite-Ilmenite

Sphene replacement of titanomagnetite-ilmenite intergrowths contrasts strongly with that of homogeneous titanomagnetite. The textural form and nature of the alteration trend is illustrated in Plate 9.3 a-c. For further comparison a discrete grain of ilmenite is included in the same Plate 9.3 - grain (d). There is a close similarity between the alteration trends shown by discrete groundmass ilmenite and "exsolved" ilmenite.

Sphene after ilmenite tends to be dark, strongly anisotropic and is distinctly polycrystalline, whereas sphene after titanomagnetite is cloudy and white, weakly pleochroic with strong internal reflections and is distinctly mottled and obviously porous. The difference in colour may be due to the presence of Ti but more significant perhaps is that it is optically denser and shows a greater degree of crystallinity. The perlitic, vermiform cracks which are characteristic of sphene replacement in homogeneous

titanomagnetite are absent in ilmenite and in ilmenite-titanomagnetite intergrowths. The initial replacement of ilmenite and titanomagnetite takes place along the ilmenite-titanomagnetite interface and also at a large number of different points in planes which are parallel to (0001) in ilmenite and to (111) in titanomagnetite. In the titanomagnetite these centres of alteration coalesce to form short lamellae with strongly serrated boundaries.

Some reaction between the dark sphene which pseudomorphs the ilmenite lamellae and the cloudy sphene which is derived from the titanomagnetite host evidently takes place. The lamellae become jagged and eventually disrupt within the host as alteration, and recrystallisation, progresses. These lamellae are highly resistant however and even in the advanced stages of alteration the original relic (111) pattern may still be discerned under crossed-nicols and low illumination (Plate 9.3c).

9.3 Alteration Susceptibility

As far as susceptibility to alteration is concerned it is evident that at times, ilmenite lamellae along (111) planes are selectively altered to sphene, and it is not until these lamellae are completely transformed, or show an advanced stage of transformation, that alteration is seen

to spread to the adjacent titanomagnetite areas (Plate 9.3a). At other times alteration of the titanomagnetite and the ilmenite takes place more or less similtaneously with the ilmenite lagging perhaps a little behind the titanomagnetite. As far as discrete ilmenite and "exsolved" ilmenite are concerned both types appear to be equally susceptible to alteration. This is at variance with the observations of BARAGER (1960) and JENSEN (1966), where the excellent photomicrographs, particularly those of the latter author, clearly demonstrate that "exsolved" ilmenite is <u>always</u> completely unaffected by this type of alteration to sphene, even when fine lamellae occur at the edges of strongly altered titanomagnetite grains. Discrete grains of ilmenite in their studies showed the same trend in alteration as those found in the Icelandic rocks (Plate 9.3d). No plausible explanation for these differences is offered although the higher Ti:Fe ratio in ilmenite should certainly make ilmenite rather than titanomagnetite chemically more attractive, in a transformation of this nature.

9.4 <u>X-ray Results</u>

Three types of sphene pseudomorphs were extracted from the surfaces of polished sections and X-ray powder photographs were made of the mounts. The type of grain and the

results are as follows:-

a) Sphene pseudomorph after homogeneous titanomagnetite (Plate 9.2d). X-ray pattern rather diffuse but sphene positively indentified with no other phases present.

b) Sphenepseudomorph after titanomagnetite-ilmenite intergrowth gave a well defined X-ray pattern with no trace of any other phases.

c) A near-pseudomorph after discrete ilmenite gave the best pattern; some traces of original ilmenite detected but no other phases were present.

The X-ray data confirm the optical evidence which suggests firstly, that sphene derived from ilmenite is generally well crystalline and secondly that no other major phases are produced in the alteration of the Fe-Ti oxides to sphene.

9.5 Electron Probe Results

Are exceptionally high-iron sphenes likely to form from the breakdown of Fe-Ti oxides? The identification of sphene as an alteration product of titanomagnetite and ilmenite, without the formation of a co-existing iron-rich

phase, has been confirmed by X-ray analysis, but the question of iron removal from an Fe-Ti oxide to the extent demanded by the known analysis of sphene, is still problematical. The analyses of sphene listed by DEER, HOWIE and ZUSSMAN (1962) all have low iron values. One possible explanation for these iron values may be the fact that all the analyses refer to specimens of primary sphene, rather than secondary sphene.

The possibility that natural, high-iron sphene may exist has been tested in a preliminary election probe study and the results are briefly summerised in Plate 9.4. The determinations were purely qualitative but in spite of this it has been confirmed that the composition of secondary sphene is almost entirely free of iron.

An example of the distribution of Fe, Ti and Ca in an ilmenite grain altering to sphene is illustrated in Plate 9.4, and a portion of this grain also appears in a reflected light photomicrograph in Plate 9.3d. On the electron image (EI) photograph (Plate 9.4) ilmenite is white and the dark grey areas of high relief are sphene. The large lens-shaped body in the centre of the ilmenite grain is calcite and the adjacent silicate areas, on either side of the grain, although not positively identifiable under the microscope,

appear to be pyroxene. The most significant feature of the X-ray scanning photomicrographs in Plate 9.4 is that within the zones of sphene a substantial loss of iron has taken place; these areas are now represented by correspondingly higher concentrations of calcium (and silica).

A pseudomorph of sphene after a titanomagnetite-ilmenite intergrowth similar to the grain in Plate 9.3b, was also scanned and although the lamellae showed slightly higher concentrations of Ti and Ca, the iron content throughout was negligible.

9.6 Discussion

Having confirmed mineralogically that low-iron sphene exists as an alteration product of Fe-Ti oxides, the following questions arise:-

a) What is the source of Si and Ca?

b) What evidence is there that remobilisation of iron has taken place?

c) Accepting that iron must of necessity be removed from ilmenite or titanomagnetite to form sphene, has the iron been reprecipitated within the rock or has it been removed from the system?

None of these questions has been adequately resolved but there is one relevant point which should be emphasised with reference to the Icelandic rocks, and it is that sphene is generally associated as an alteration product of the Fe:Ti oxides in dykes and has only rarely been found in lavas. This suggests that sphene may result from the effects of alteration at depth, or its presence may be due to some differences in the deuteric cycles of alteration that occur in dykes and lavas.

In all the dyke samples examined which contain sphene as an alteration product, calcite was found to be present occuring in thin veinlets and in vesicles. The silicates are incipiently altered; plagioclase to secondary mica and the ferromagnesian minerals to pale green chlorite.

It is a general feature of the dykes that they contain high concentrations of sulphides. Pyrite and marcasite are the chief phases but chalcopyrite and pyrrhotite also occur. The sulphides rarely develop euhedral crystals but form irregular aggregates around the Fe-Ti oxides, sometimes penetrating and infilling voids within the oxides, and as thin irregular veinlets along the silicate grain boundaries. Whether or not these sulphides result, in part, from a process of iron remobilisation, is problematical.

CHAPTER 10

PRIMARY SPINELS

10.1 Introduction

The spinel group of minerals has the general formula $R^{+2}O\,R^{+3}_2O_3$. Where the divalent cations may be Mg^{+2} or Fe^{+2} and the trivalent cations Cr^{+3}, Fe^{+3} and Al^{+3}. Spinel can also contain a wide range of other cations, the most important being titanium and vanadium but zinc, nickel and manganese are also known to occur.

The composition of spinel may be expressed in terms of the following end members:-

Hercynite	$Fe^{+2}Al_2O_4$	(H)
Spinel (sensu stricto)	$MgAl_2O_4$	(S)
Magnetite	$Fe^{+2}Fe^{+3}_2O_4$	(M)
Magnesioferrite	$MgFe^{+3}_2O_4$	(MF)
Ferrochromite	$Fe^{+2}Cr_2O_4$	(FC)
Magnesiochromite	$MgCr_2O_4$	(MC)

A spinel composition prism having these six end members at its corners has been constructed by STEVENS (1944) and is redrawn in Figure 10.1. The triangular faces of the prism show variations in the trivalent cation, while variations in

magnesium and ferrous iron are represented along the length of prism.

Experimental studies of phase relations within some parts of the spinel series have been carried out, but there are still many gaps in our knowledge of the extent of solid solution in this series. The magnesiochromite-spinel series is completely miscible from 1600°C down to 510°C (WARSHAW and KEITH 1954), complete solid solution exists above 1400°C between magnetite and ferro-chromite (MUAN and SOMIYA 1960) and the magnesioferrite-magnetite series is complete above 1400°C. (PHILLIPS and MUAN 1962). Solid solution is complete between magnetite and hercynite at high temperatures, but becomes limited below 860°C by a symmetrical solvus (TURNOCK and EUGSTER 1962). A study of published analyses of spinels by DEER, HOWIE and ZUSSMAN (1962) and by IRVINE (1965) indicates that extensive solid solution occurs between the six spinel end members at the temperatures of basaltic magmas, and that solid solution may become limited in the magnetite-hercynite, hercynite-spinel and ferrochromite-magnesiochromite series at lower temperatures.

Spinel is a typical mineral in alpine-type peridotite and serpentinite bodies, in the stratified ultramafic differentiates present in many large intrusions of tholeiitic

and high alumina basalt magmas, and in the picrite facies of basaltic volcanic rocks. Although commonly thought of for its occurrence in concentrated layers, bands, veins, and pods because of their economic value, most spinel is disseminated in amounts of only 1 or 2% through its ultramafic or mafic host rock. However, despite its accessory nature, it is potentially an extremely important indicator of the physicochemical conditions under which its host rocks have formed. Spinel shows a wide compositional range in both divalent and trivalent elements and hence must be relatively sensitive to the chemical or thermal conditions that accompanied its formation. Because of its high density and the fact that it contains large concentrations of major rock forming elements, it may in some circumstances be indicative of high pressures (IRVINE 1965). On the other hand, in terms of depths of tens of kilometers in the mantle, the presence of certain types of spinel may reflect relatively low pressures (MacGREGOR 1964).

10.2 Reflection Microscopy

Spinels are black to dark grey or near-colourless in colour, isotropic and have the lowest reflectivity value of all the common opaque minerals in igneous rocks. The spinels vary a great deal compositionally owing to the complex solid solution relationships which exist between the

numerous end members.

In the Icelandic lavas there are two distinct compositional groups of spinels which may be further classified on their textural form and distribution. The first type, the discrete spinels, are of the Cr - Fe - Al - Mg variety; the second type are the exsolved spinels in titanomagnetite, and these are essentially hercynitic in composition, but the presence of magnesium places them within the $MgFe_2O_4$ - Fe_3O_4 - $MgAl_2O_4$ - $FeAl_2O_4$ field. These fields relate to the spinel compositional prism in Figure 10.1. The discrete spinels are primary high temperature crystalline phases, whereas the exsolved spinels develop at much lower temperatures and are closely related to the oxidation of titanomagnetite.

10.2.1 Discrete Spinels

Discrete spinels are among the first minerals to crystallise from a melt and generally show good euhedral crystal forms. As a result of this early crystallisation the spinels are phenocrystic and are commonly included in olivine or pyroxene. A particularly striking feature of these spinels is that within the groundmass silicates they are always zoned by outer, concentric rims of titanomagnetite (Plate 10.1), whereas in olivine or pyroxene they occur as poikilitic inclusions and are unzoned. Grain (a) in Plate 10.1 shows

an unzoned euhedral spinel enclosed in olivine and in (b)-(d) the variations in zoned spinels are illustrated. The overgrowth principle is so strictly adhered to, that spinels which are only partially included in olivine or pyroxene are unzoned within the ferromagnesian area, but are zoned outside it (Plate 10.6a). The most common type of overgrowth is one in which the titanomagnetite rim follows the outline and crystal shape of the spinel quite faithfully. That is, the overgrowth is euhedral or shows sharp, angular extensions when the spinelcore is a simple cubic form (Plate 10.1b), or the overgrowth is irregular, when the spinel is irregular (Plate 10.1c-d). This control on the shape of the titanomagnetite overgrowth is quite remarkable. In lavas containing skeletal titanomagnetite crystals, the overgrowths on the spinels follow the euhedral shape or general outline of the core and develop as solid titanomagnetite mantles, rather than as dendritic crystals.

The titanomagnetite-spinel contact is usually sharp but gradational contacts are also common (see especially Plate 10.3c). Reaction rims between spinel and chrome-diopside (LEGG, 1967) and between spinel and titanaugite (BABKINE 1965; WRIGHT 1967) have been observed. In contrast, the Icelandic study has shown that unoxidized spinel-silicate contacts are always sharp and optically well defined; these

sharp contacts are supported by the election probe study.

No examples have been found in which the overgrowth on spinel is ilmenite rather than titanomagnetite. The normal crystallisation sequence of these three minerals in spinel, ilmenite and then titanomagnetite; the chemical and structural affinity of magnetite and spinel makes their coexistence a natural choice. Although reverse-crystallisation overgrowths do occur, such as ilmenite on titanomagnetite, spinel has not yet be found as an overgrowth on any other phase.

Euhedral or subhedral poikilitic silicate inclusions as those commonly found in titanomagnetite and ilmenite are generally absent as inclusions in spinel. Co-precipitation of spinel and olivine, suggested by the graphic intergrowth illustrated in Plate 10.2b, is exceptional in the lavas studied. Equally exceptional are the triffed-like voids shown in Plate 10.2 c-d, the variation in colour and reflectivity shown within these globular areas is due to the diffration of light under oil immersion. Their shape strongly suggests that they were originally gas inclusions but in some areas rods or spherules of spinel have precipitated.

Since solid-solution relationships are known to occur between the various end members of the spinel series one

might expect to find not only exsolved spinel in magnetite but also exsolved magnetite in spinel. The latter intergrowth is rare, but an interesting occurrence has recently been described by SMITH (1965) in a suite of emery-like rocks from Sithean Sluaigh, Argyllshire. It has previously been suggested that in the Icelandic rocks the exsolution of spinel from titanomagnetite is in some way induced by the advanced oxidation of titanomagnetite-ilmenite intergrowths. On the basis of this observation, close attention has been paid to the lamellar phases which develop in the spinel, in order to determine whether the exceptional spinel-titanomagnetite relationship is reversible or not. SMITH concluded in his study that the exsolved magnetite took place under conditions of slow cooling, low pO_2 and at temperatures above 860°C. In the Icelandic lavas hematite is the only phase produced within the spinel. Relatively slow cooling conditions have at times been operative in the spinel phenocrysts and although oxidation gradients occur across these phenocrysts it seems evident that the oxidation - induced process for exsolution, in the spinel series, is not reversible. In other words, exsolved magnetite does not occur in spinel; one possible explanation for the absence of magnetite is that it is unstable under conditions of exceptionally high pO_2.

10.2.2 Alteration of Discrete Spinels

Zones of alteration in chrome spinels have been studied by a number of workers. Observation with the ore microscope has shown that the alteration zones occur as "bleached" areas with diffuse margins against the central portions of the chrome spinel, and that the brightest portions are at the centres of veins and hairline cracks and at the margins of chrome spinel grains. TEX (1966) showed by X-ray diffraction measurements that the opaque rims around some Alpine chromites were composed of almost pure magnetite. VAASJOKI and HEIKKINEN (1961) showed by means of the electron probe that alteration veins in Finnish chrome spinels were enriched in iron and impoverished in chromium, magnesium and aluminium relative to the unaltered areas. Similar results were obtained by DE MENEZES and STUBICAN (1966) in an electron probe study of magnesia-chrome refractories. In contrast to these results the electron probe data, of PANAGOS and OTTAMAN (1966), show that the alteration rims around some Greek chromites are enriched, not only in iron, but also in chromium, while the cores are enriched in magnesium and aluminium; similar results have been reported by LEGG (1967) for a collection of chromites from Greenland.

Factors which control the preferential diffusion of iron, or iron plus chromium, towards the edge of a chromite

grain probably depends to a considerable extent on temperature (DE MENEZES and STUBICAN, 1966), but might also be dependent on oxygen and water fugacities and on the composition of the original chrome-spinel. The state of oxidation is evidently low, as Fe_2O_3 is only rarely observed in the alteration zone.

A common factor in all the studies quoted above is that the chromites or chrome-spinels originate from mafic or ultramafic intrusive bodies which have suffered some degree of metamorphism. In recent lavas the effects of magmatic corrosion, since the spinels crystallise at an early stage, and the effects of oxidation at lower temperatures, are the main types of alteration which one may expect to find.

The gradational contacts between titanomagnetite and spinel are undoubtedly due to diffusion and counter-diffusion of cations between the core and the outer margin, at magmatic temperatures and under conditions of low pO_2. The gradational or diffuse zone is, in effect, a zone of selective, solid solution homogenization. BABKINE et.al (1965) interpret the titanomagnetite overgrowths, in part, as due to re-solution of the central chrome-spinel core.

In order to have some idea of the temperature range under which spinel breaks down in a lava, one ideally needs

some experimental data, or alternatively an internal mineral standard with which the various stages of alteration may be compared. The close association of titanomagnetite as an overgrowth on spinel, its sensitivity as an indicator of the temperatures and conditions of oxidation, its ubiquitous nature, and the fact that some temperature data exists regarding its alteration products, makes titanomagnetite an ideal comparitive standard.

Grain (b) in Plate 10.1 shows that low temperature maghemitization of the titanomagnetite has no corresponding oxidation effect on the spinel core. Although the degree of maghemitization in this particular grain is limited to the outer edge of the titanomagnetite, in grains which are completely pseudomorphed by titanomaghemite rims, the alteration effect stops abruptly at the spinel contact. In the case of diffuse contacts, the alteration effects are also diffuse (Plate 10.1c).

Titanomagnetite zones around central spinel cores follow the normal sub-solidus oxidation sequence of ilmenite exsolution. Titanomagnetite crystals with or without spinel cores are equally affected by any process of oxidation but the temperatures and pO_2 conditions which control this initial sub-solidus oxidation is evidently not sufficient

to induce any optical changes within the spinel. In the case when the titanomagnetite-spinel contact is sharp the ilmenite lamellae, within the titanomagnetite, come to an equally sharp termination at the contact and the lamellae are square-ended rather than tapered (Plate 10.4c). In the case of diffuse contacts the ilmenite lamellae gradually fade out in the gradational zone that occurs between the titanomagnetite and the spinel (Plate 10.3 b-c).

The first sign of alteration, that is detected in the spinel, is at the stage of oxidation when titanomagnetite and ilmenite begin to transform to rutile, ferri-rutile, titanohematite and pseudobrookite. It has previously been shown that this oxidation assemblage is the result of high pO_2 conditions at temperatures above 600°C. The effect of oxidation produces hematite rods and lamellae along a system of (111) parting planes in the spinel. The hematite rods become more numerous towards the edge of the spinel grain boundary and in the case of many unzoned spinels the effect of migrating ferric iron creates a narrow and concentric diffusion rim of hematite at the spinel boundary. As in the case of hematite rims around highly oxidized olivines these hematite rims develop within the spinel and do not mantle the spinel in the sense of an overgrowth. In the case of

zoned spinels, an intensely darkened spinel halo develops at the titanomagnetite contact (see especially Plate 10.4 b-c). This darkening of the spinel host is a general feature of spinel grains which have developed hematite lamellae on oxidation. The hematite lamellae are well oriented and sharply defined but vary considerably in thickness. The apparent crystallographic control of the titanomagnetite overgrowths by the spinel cores, as shown in Plate 10.1b and in Plate 10.3d, is further illustrated in Plate 10.4, where, because of the high oxidation state of the primary phases, the presence of oriented hematite and metailmenite lamellae permits the continuity of single (111) planes to be traced across the titanomagnetite-spinel boundary. The hematite lamellae within the spinel are much finer than the earlier formed ilmenite (metailmenite) lamellae within the titanomagnetite.

In summary, observation has shown that titanomagnetite is more susceptible to oxidation than spinel with which it is closely associated. The spinel is not affected by maghemitization or the process of sub-solidus oxidation, but is affected by any process of more advanced oxidation at high temperatures, such as those which transform primary titanomagnetite and ilmenite into pseudobrookite, titanohematite,

rutile and ferri-rutile. The only product of oxidation formed from spinel at these temperatures and under these conditions is hematite.

10.3 Electron Probe Analysis

The grains for the electron probe study were carefully selected microscopically to ensure homogeneity. Magnetite (SMITH 1965), ilmenite and rutile (LEGG 1967; GHISLER and LINDSLEY 1967) are known to exsolve from chrome spinels with hematite as a common oxidation product. The spinels are generally phenocrystic so the choice of sample material is somewhat simplified. Primary homogenous spinels in olivine or pyroxene, and spinels containing titanomagnetite rims were analysed in three samples, one sample was basaltic in composition and the other two samples were cumulative ankaramites.

The elements sought were Cr, Al, Fe, Ti, Mg, Mn, Zn, Si and Ca of which only chromium, aluminium, iron and titanium were determined quantitatively. Magnesium was known to be present but at the time these analyses were carried out it was not possible to determine it quantitatively on the electron probe available. Manganese appeared in concentrations of less than 1% whereas zinc, silica and calcium were not detected.

The quantitative distribution of Fe, Ti, Cr, Al and Si in a zoned spinel assemblage are well illustrated in the X-ray scanning photomicrographs in Plate 10.5. The electron image (E.I.) shows part of a spinel cluster in which the main grain consists of a dark euhedral spinel core zoned by titanomagnetite. Smaller attached grains with diffuse spinel-titanomagnetite contacts may also be seen in the same field of view. It is evident from these images that the spinel is concentrated in Fe, Cr and Al with small quantities of Ti; whereas the titanomagnetite rim is concentrated in Fe and Ti but Cr and Al are also present. The spinels occur in an iron-alumino silicate groundmass. The dark, high-silicate reflectivity, areas are either olivine or pyroxene; these two minerals may be distinguished on the basis of high Al and Ti concentrations in pyroxene. The lighter areas are probably felspar since they are highly enriched in Al.

Line scans across the field of view (the traverse line is shown on the electron image) were determined for Fe, Ti, Cr and Al, and are illustrated in Figure 10.2. The titanomagnetite-silicate grain boundary is compositionally well defined whereas the titanomagnetite-spinel boundary shows a steep but nevertheless gradational profile across the interface; the Fe profile, for example, is distinctly

trough-shaped. There is also some assymetry in composition across the grains and is particularly marked in the zone of titanomagnetite. Similar line scans, vertical in this case, for Mn and Mg are illustrated in the accompanying photomicrograph. Manganese shows a slight preference for the titanomagnetite rim, whereas Mg is distinctly concentrated in the spinel core. The sensitivity and hence the peak height was greatly increased for this purpose.

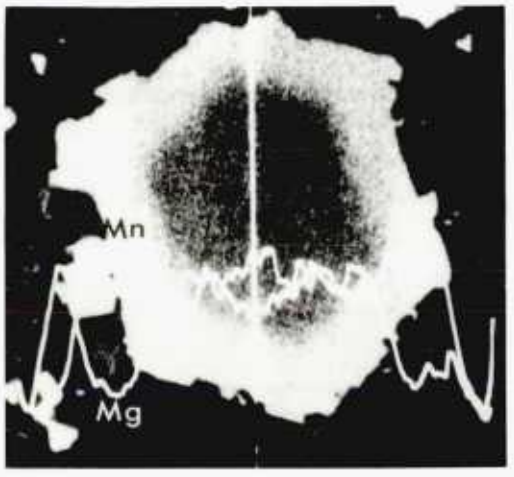

The quantitative analyses which have been determined on spinel are presented in Table 10.1. The difficulty which arises in using the electron probe to distinguish different valency states, has previously been dealt with in the section on oxidized ilmenite (Chapter 5). Since magnesium is known to be present, an arithmetic estimate of its concentration has been made. This was done in the following way: An internal check on the accuracy of a probe analysis can be mad by calculating each cation in terms of its oxide; for example, Cr in terms of Cr_2O_3 and Al in terms of Al_2O_3, the summation should approximate to 100%. Normally, the

iron would be recast in terms of both FeO and Fe_2O_3 and these values would then be suitably apportioned on the basis of stoichiometry or known chemical analysis. The summations in the present study varied between 72.9% and 95.1%, the difference has been assumed to be due to the presence of magnesium. The validity of this assumption is based on the following points: Firstly, magnesium has been determined quantitatively; secondly, since the major part of this study was carried out an analysis for magnesium has been determined by P.SUDDEBY on sample Number 4 in Table 10.1. This determination gave a value of 8.55%; the determined concentration based on the oxidized summation method gives a value of 8.25% Mg (the estimated error is 2-3%); thirdly, in an X-ray powder pattern obtained from an unzoned spinel, the reflections were found to correspond closely to the d-values for magnesiochromite. The determined unit cell edge is $a = 8.286 \pm .005$ Å. The cell edges for members of the spinel compositional prism vary systematically from the hercynite-spinel join to the magnesioferrit-magnetite join and also from the hercynite-spinel series to the magnesiochromite-chromite series (DEER, HOWIE and ZUSSMAN 1962). Thus giving a series of steeply inclined equi-unit-cell surfaces across the compositional prism. The surface value for $a = 8.286$ Å is plotted in Figure 10.1, and clearly

indicates that the determined value forms an intergral part of the prism, in which magnesium is present.

On the basis of this evidence, magnesium is quoted for each determination as an arithmetic estimate, the data are included with the other analyses in Table 10.1.

An elegant way of plotting spinel compositions in terms of the compositional prism is the one used by IRVINE (1965), the method is graphically illustrated in Figure 10.3. In order to have some idea of the region covered by the present analyses and in order to graphically illustrate the differences in composition between the zoned and unzoned spinels, an attempt has been made to show the distributions by using part of IRVINE'S plot. Only the base of the prism may be considered since it involves only one valency state for iron (Fe^{+2}). For the sake of this plot all the probe-determined iron is assumed to be in this lower valency state. The cation ratios, Cr : Cr + Al and Mg : Mg + Fe^{+2} which are used in the plot (Figure 10.3), are noted separately in Table 10.2.

It is evident from the plot that analyses within the same sample can be grouped, but that the groups of analyses from zoned and unzoned samples are separated. There is a preferential separation of the unzoned groups towards

higher values of Mg : Mg + Fe^{+2}. Another point which emerges is that the basaltic spinels (full circles) not only show an abscissa variation in Mg : Mg + Fe^{+2} but also a considerable ordinate variation in Cr : Cr + Al which is not apparent in the ankaramitic samples. Unfortunately, on the basis of the assumptions that have already been made, the significance of these trends cannot be fully evaluated. It is interesting, nevertheless, to note that the range in ratios which have been transferred from Figure 10.3 to the base of the prism in Figure 10.1 (shaded area) are of the order of the unit cell surface.

10.4 Heating Experiments

The sharply defined and well oriented nature of the hematite lamellae in spinel, suggests that the hematite may be a product of exsolution rather than oxidation. Compare, for example, the jagged form of the hematite lamellae in magnetite (Plate 6.6) with the well defined hematite lamellae in spinel (Plate 10.4). The intergrowths contain a common rhombohedral phase (hematite) oriented along common (111) phanes within their respective cubic hosts, and both result from a process of oxidation. In spite of all these common factors the obvious distinguishing feature between them is the initial composition of the primary cubic phase, which undoubtedly exercises some control on the texture of

the alteration products that form. In spite of the well defined textures, there are two lines of evidence in favour of an oxidation process. Firstly, in an associated spinel assemblage, olivine and the Fe-Ti oxides show evidence of advanced oxidation at high temperatures. Secondly, the exsolution phases which are derived from spinel are more likely to be members, or intermediate members, of the spinel compositional prism, rather than simply hematite.

A series of heating experiments were carried out, not for the purpose of defining the thermal stability limits of spinel, but rather to test the unusual textural evidence for signs of true exsolution or simple oxidation; and further, to examine the possibility than hematite may in fact be derived by oxidation of previously exsolved magnetite.

Starting material for the heating experiments consisted of an olivine-rich beach sand from Mull (kindly loaned by P. HUDLESTON), in which large numbers of poikilitically enclosed spinels occur. In a number of olivine phenocryts, spinels which are partly included along the silicate margins are zoned by overgrowths of titanomagnetite (Plate 10.6 a). Attached fragments of basalt, which are common in the concentrate, were deliberately heated with the phenocrystic olivines. This permitted a comparison to be made between

the mineralogical state of oxidation of the discrete Fe-Ti oxides and the degree of alteration reached by the spinel inclusions.

The samples were heated in open, high temperature, ceramic boats for 24 hours at 600 and 950°C. The grain-size of the starting material varied from 0.5-1.0 mm. in diameter. Polished mounts of the material were made and the products were studied under the ore microscope.

The results of the 950°C experiment are shown in Plate 10.6; no alteration effect in the spinel was detected in the 600°C run. These photomicrographs demonstrate quite clearly that the hematite lamellae are comparable to those found in natural spinel examples (c.f. Plate 10.4).

In most cases, except for spinel at an olivine grain boundary, the Fe-Ti oxides in the groundmass are more susceptible to oxidation than the spinels enclosed within the olivine. As one might expect, the olivine acts as a buffer to the effects of oxidation. Thermal oxidation gradients develop across the olivine and across individually included grains of spinel, giving a progressive series of oxidation states. All gradations, from incipiently oxidized rims containing a few lamellae per unit area, to examples which are highly oxidized and contain closely packed lamellae

throughout the grain, are present. In spite of these gradients there is no evidence to suggest that hematite is derived from an earlier, exsolved phase of magnetite. The samples were quenched in air which clearly confirms that a process of conventional exsolution has not taken place; diffusion of iron has been induced by oxidation at high temperatures.

The primary Fe-Ti oxides, titanomagnetite and ilmenite, in the groundmass of the 950°C run, have inverted to pseudobrookite plus titanohematite associated with minor amounts of rutile and ferri-rutile; while olivine enclosing the spinels has inverted to a symplectic intergrowth of magnetite plus enstatite, with forsterite plus hematite occuring towards the edge of the olivine grains (see Chapter 13). The photomicrograph in Plate 10.6a is particularly instructive as it illustrates the composite features described here for the oxidation of titanomagnetite, spinel and olivine.

The effects of oxidation on the silicate-spinel contacts and on the Fe-Ti oxide - spinel contacts are illustrated in Plate 10.6. The degree of material exhange across either of these phase boundaries depends on the reactive properties of the minerals involved, on the temperature of the reaction, and in this case on the degree of alteration.

The rate at which these reactions take place is undoubtedly enhanced by the fact that new minerals are produced during the thermal decomposition of the primary phases. Feldspar, for example, is inert under the conditions of the experimental run and hence no obvious reaction results at the spinel boundary (Plate 10.6c). In contrast (Plate 10.6a-b), the reaction of the Fe-Ti oxides with the spinel has induced the pseudobrookite-titanohematite assemblage (after an original overgrowth of titanomagnetite) to divide into its component phases. The titanohematite tends to concentrate towards the spinel boundary, and along this contact meets with the spinel to form a pseudographic intergrowth. The spinel-olivine contact (Plate 10.6d) is also affected by the thermal oxidation process. Once again the hematite, which in this case is derived from symplectic magnetite, forms a pseudographic intergrowth with the spinel. Symplectic magnetite, after olivine, is always more coarsely crystalline, and is frequently found to be more highly oxidized, in areas which are immediately adjacent to spinel inclusions.

It is uncertain whether any new phases actually develop at the spinel reaction contacts. The optical examination is made extremely difficult by virtue of the narrowness of the reaction zones that develop and by the delicate nature

of the intergrowths. It is proposed that a detailed study of these reactions contacts, using the electron probe, will be made at a later date.

10.5 Conclusions

In the light of these heating experiments, which now confirm that the hematite has been produced directly by oxidation, further consideration may be given to the magnetite -hematite analogy which was discussed earlier and illustrated by comparison of hematite lamellae in magnetite (Plate 6.6) with hematite lamellae in spinel (Plate 10.4 and 10.6). Complete pseudomorphs of hematite after magnetite are the common end-products of oxidation, but this does not apply to the multi-cation spinels under discussion. Oxidation induces a preferential segregation of Fe^{+3} ions from the spinel lattice. The hematite is structurally monitored by the newly formed and iron-deficient cubic spinel host. This crystallographic control of the rhombohedral phase accounts for its well defined lamellar form. Although some differences do exist, one is, nevertheless, tempted to draw a comparison between the cubic-rhombohedral (titanomagnetite-ilmenite) relationship in the Fe-Ti oxides, and to consider whether the well substantiated sub-solidus oxidation process, which produces exsolution-like features, may not also apply to the spinels.

Plate 10.1

Zoned Spinels

Sample No.	MA	15	MA	23	WK	30-1			
Grain No.	1	2	3	4	5	6	7	8	9
Element									
Fe	23.8	25.1	23.1	22.9	21.9	24.4	24.9	23.5	23.5
Cr	18.0	17.5	18.0	17.3	25.6	25.8	25.9	25.7	25.4
Ti	2.5	2.5	1.8	0.8	0.4	0.7	0.7	0.5	0.5
Al	11.2	11.2	13.4	12.6	12.6	12.2	12.7	11.9	12.2
Mg	10.7	10.1	10.0	8.3	5.8	4.1	2.9	5.2	5.3

Unzoned Spinels

Sample No.	MA	15	MA	23	WK	30-1
Grain No.	10	11	12	13	14	15
Element						
Fe	18.4	18.2	23.0	23.3	19.1	18.9
Cr	17.6	17.3	17.3	17.3	20.3	20.4
Ti	1.5	1.5	1.9	1.9	0.5	0.6
Al	12.0	12.0	12.4	12.0	17.7	16.9
Mg	15.3	16.5	11.1	11.3	6.9	7.9

Electron probe analyses for zoned and unzoned spinels. Samples MA-15 and MA-23 are ankaramites and sample WK 30-1 is basaltic. Mg is determined by difference - see text for explanation.

Table 10.2

Zoned Spinels

Sample No.	MA 15		MA 23		WK 30-1				
Grain No.	1	2	3	4	5	6	7	8	9
Cr: Cr + Al	0.62	0.61	0.57	0.58	0.67	0.68	0.67	0.68	0.67
Mg: $Mg+Fe^{+3}$	0.11	0.29	0.30	0.26	0.21	0.14	0.11	0.18	0.18

Unzoned Spinels

Sample No,	MA 15		MA 23		WK 30-1	
Grain No.	10	11	12	13	14	15
Cr: Cr + Al	0.59	0.59	0.58	0.59	0.53	0.55
Mg: $Mg + Fe^{+3}$	0.45	0.48	0.32	0.39	0.27	0.29

Cr : Cr + Al and Mg : Mg + Fe^{+2} ratios derived from electron probe analyses given in Table 10.1.

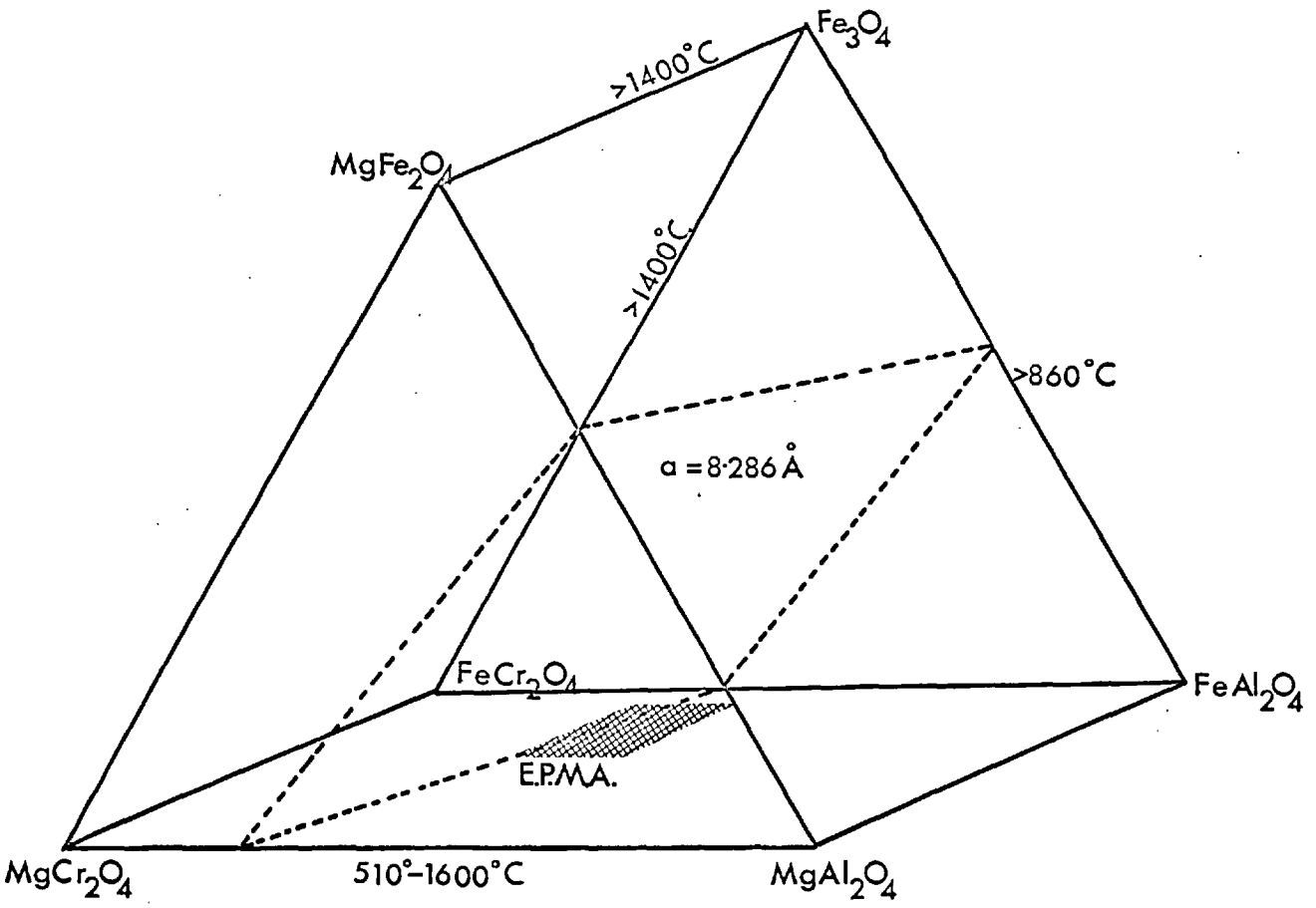

Spinel Compositional Prism (STEVENS 1944)
showing
Solid soln. temp.; Unit cell surface; Probe values.

Fig. 10·1

ELECTRON PROBE SCANS

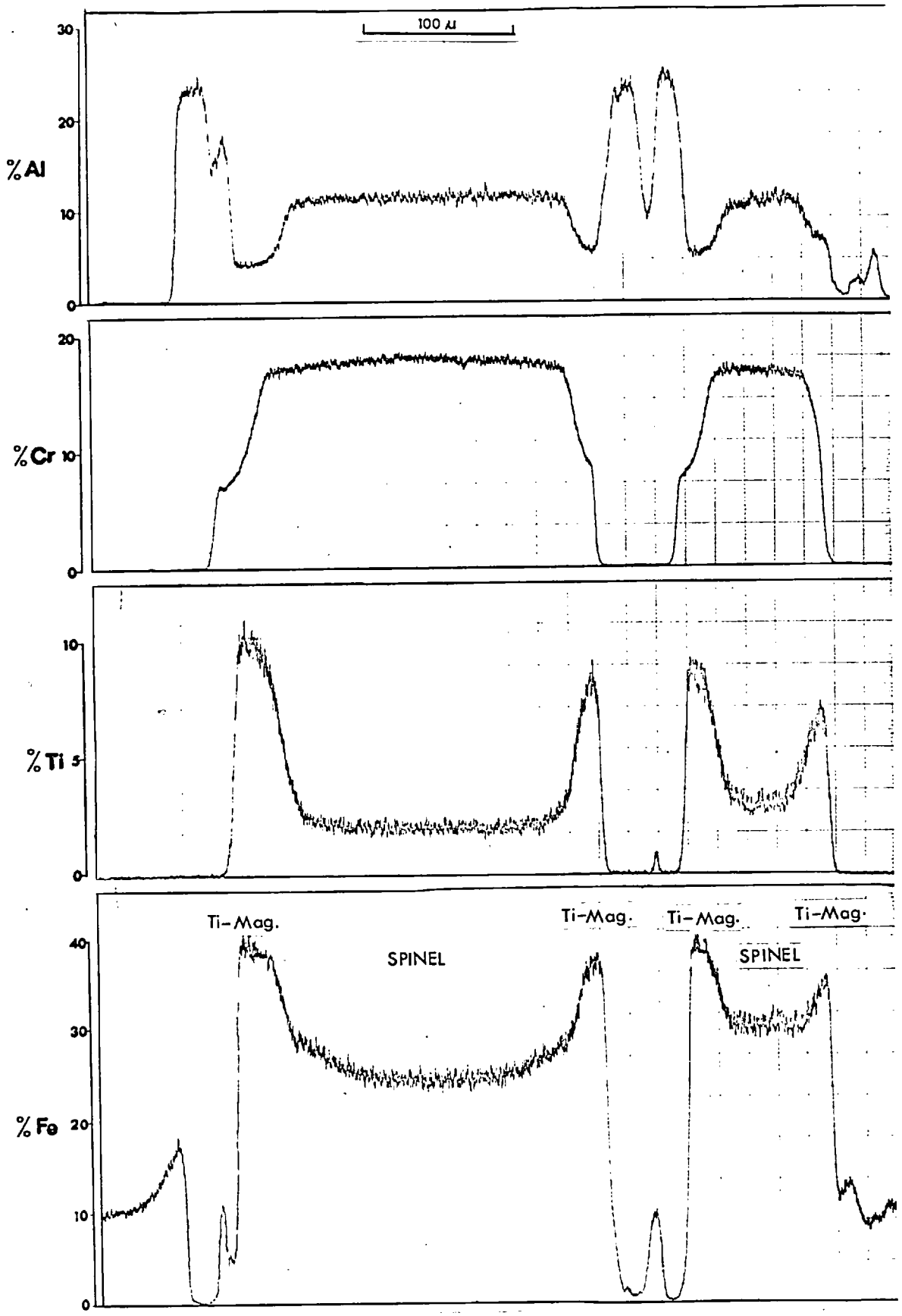

Fig 10.2

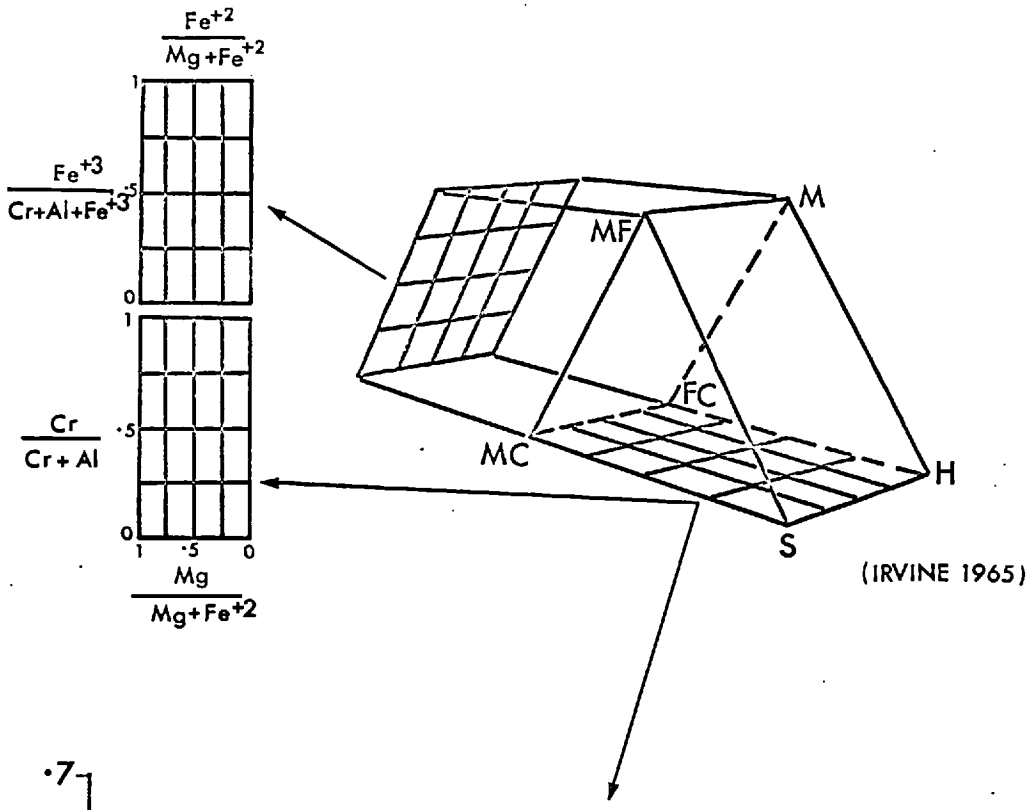

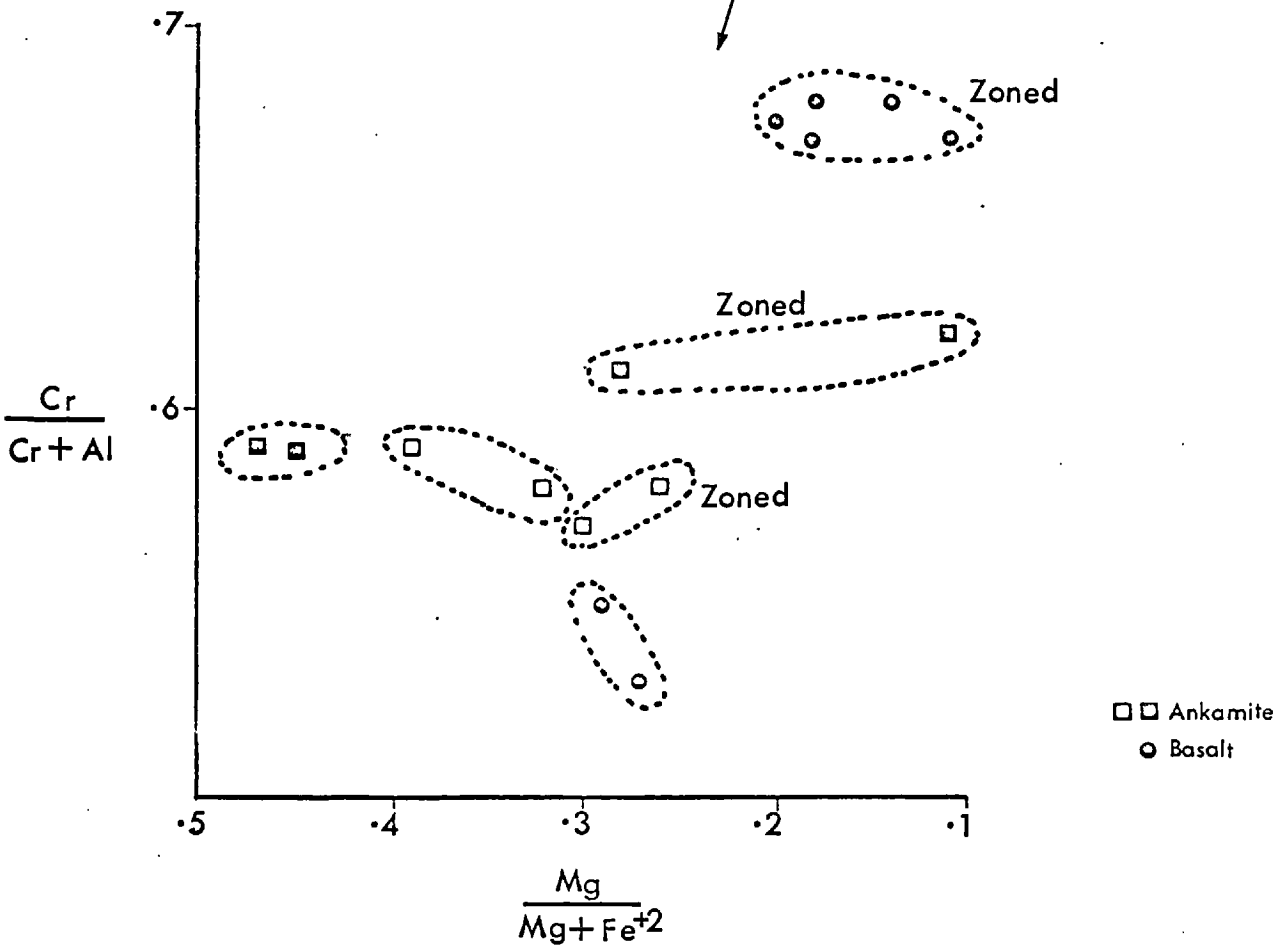

Fig 10-3 Spinel Compositions

CHAPTER 11

SULPHIDES

11.1 Relection Microscopy

The chief iron sulphides which occur in the Icelandic rocks are pyrite and marcasite. Pyrrhotite occurs in minor amounts. Pyrite and pyrite-marcasite inversion products after pyrrhotite also occur. The sulphides of copper are rare.

Sulphides generally occur in accessory amounts but in expectional cases may form as much as 20% of the total opaque content.

Texturally the sulphides may occur as small euhedral disseminated crystals, as rounded inclusions in titanomagnetite, in irregular clusters and in microveinlets along silicate grain boundaries. The sulphides are generally not haphazardly distributed throughout a sample but tend to show a close affinity for the Fe-Ti oxides (Plate 11.1 a-d). This association may take the form of a matrix overgrowth (Plate 11.1c) or may simply occur as an attached grain (Plate 11.1d).

Paragenetically the sulphides are among the last phases to crystallise. In some cases the field evidence and the textural form of the sulphides, in polished section,

indicates that the minerals may have been introduced at a later period, during a phase of hydrothermal activity. In such cases entire sequences of lavas are affected. In general though, the sulphides may be regarded as products of primary crystallisation.

Iron sulphides are characteristic of the dykes and are only rarely found in lavas. There are three main lines of evidence suggesting that the sulphides in these dykes originate directly from a melt, in spite of their irregular crystal form. Firstly, sulphides were found in all the dykes examined (203 samples); secondly, lavas cut by the dykes do not contain sulphides; and thirdly, sulphides occur in the quenched marginal contacts of the dykes and are seen to increase in grain size and abundance towards the centre of the dykes - a feature which is not likely to occur epigenetically.

The question as to whether the sulphides are primary or secondary in origin is an important consideration for the following reasons; firstly, the characteristic association of sulphides with intrusives rather than extrusives indicates that there are important underlying differences to be taken into account, such as rates of cooling and rates of volatile loss, when considering the effects of denteric oxidation;

secondly, the availability of iron is at a minimum towards the end of crystallization and the effects of sulphidization must therefore also be considered; thirdly, from the magnetic point of view, the production of pyrrhotite and the distruction of magnetite by sulphidization may have drastic effects on the property of thermal remanance.

Photomicrograph (a) in Plate 11.1 illustrates the most typical form developed by pyrite and shows in addition the manner in which it is texturally related to the silicates and titanomagnetite. A large mass of pyrite has accumulated around the titanomagnetite, and pyrite stringers branch out in all directionsfrom this mass. A close inspection of the pyrite-silicate contacts and the pyrite-Fe-Ti oxide contacts, at high magnifications, shows that the former interface is crenulated while the latter is relatively smooth. It is surprising that although the pyrite and the Fe-Ti oxides are in such close contact there are no obvious interactions between them. KULLERUD and DONNAY (1965) have shown that by sulphidation, and at temperatures as low as 300 ^{o}C, pyrite and an iron-deficient magnetite may be produced from primary magnetite, without destroying the original spinel structure. Alteration of the grain in photomicrograph (a) Plate 11.1, also shown at a higher magnification in (b), is the result of later

oxidation to titanomaghemite and amorphous Fe-Ti oxide, and is not the result of sulphidization. The voids in the titanomagnetite are areas of secondary material which have been plucked from the surface of the section during polishing.

By contrast to the pyrite-Fe-Ti oxide contacts, it is interesting to note that these rocks may show some evidence which supports the work of KULLERUD and YODER (1964) on sulphidization of the silicates. The sulphides tend to penetrate and become intimately associated with the ferromagnesian minerals but only occur as thin filaments along the relatively non-reactive felspar grain boundaries. Their work showed however that sulphidization of pyroxene and olivine not only produced pyrite but also magnetite or hematite. These latter phases have not been observed in this study.

CHAPTER 12

ACCESSORY MINERALS AND RARE MINERAL INTERGROWTHS

12.1 Native Metals

The only native metals that have been observed in the Icelandic basalts are native copper and native iron.

Native copper is a primary crystalline phase, it occurs in typical dendritic grains which are usually attached to crystals of titanomagnetite or ilmenite. It also appears as a late stage precipitate and is commonly found in the glassy mesostases. It rarely occurs in grains which are larger than 20 microns, it has a high metallic reflectivity and is optically isotropic. Native copper is easily tarnished but no other alteration products have been observed, even in highly oxidized samples.

Metallic iron, on the other hand, is a "secondary" product after titanomagnetite. It occurs in association with trapped fragments of wood which have effectively reduced the iron to its metallic state. One sample (loaned by G.P.L. WALKER) was examined from Iceland in which textural intergrowths were found to be extremely fine grained. A description of this type of reduction process will be discussed in **Appendix I.** Many examples of native iron and

native nickel-iron are known to occur in basic igneous rocks (CHAMBERLAIN et.al 1965). The best known localities are the Disko basalts of Greenland which at one time were thought to contain meteoritic iron. It has now been shown, however, that reduction of the Fe-Ti oxides to the metallic state was brought about by the inclusion of carbonaceous sediments (MELSON and SWITZER, 1966).

12.2 Hydroxides

It has come as somewhat of a surprise that iron hydroxides (goethite α FeO.OH; lepidocrocite γ FeO.OH) are relatively uncommon in the Icelandic basalts, particularly since these lavas are known to have been buried to depths of at least 500-800 meters. These figures are based on WALKER'S (1960) zeolite zones, which in addition require a hydrous environment for their production.

Goethite (lepidocrocite has not been conclusively identified) is confined to tuffaceous lavas, to basaltic fragments in lateritic sediments, and to vesicle or fracture infillings in basaltic lavas.

Goethite is medium to dark grey in colour, weakly anisotropic and with reflectivity values considerably lower than the Fe-Ti oxies; it invariably shows red or bright

irridescent internal reflections.

In the tuffs and in the sediments goethite occurs as a complex replacement product of titanomagnetite. Some examples of this type of alteration are shown in Plate 12.1. In some cases the textures resemble those of "amorphous" Fe-Ti oxide as in Plate 12.1b, but often the replacement front is not along curved perlitic cracks but along flame-like (Plate 12.1a) or botryoidal surfaces (Plate 12.1c). Hematite is commonly associated with goethite (Plate 12.1a) and in these cases the zone between the two end products is completely gradational. Shrinkagecracks are a common feature (Plate 12.1c).

Some further examples of goethite as a vesicle in filling are shown in Plate 12.2. The goethite in these cases is fibrous (Plate 12.2a) vermiform (Plate 12.2 b-c) or colloform (Plate 12.2d). Hematite, chalcedony, zeolites and calcite are common association products.

12.3. Ilmenite-titanomagnetite Intergrowths

The sub-solidus oxidation process which produces "exsolved" ilmenite from titanomagnetite is now well substantiated. In a solid solution series, between two end members, members of intermediate composition may produce either of the end members by conventional exsolution below the solvus. Well known examples are ulvospinel-magnetite and ilmenite-hematite.

There are very few descriptions in the literature of ilmenite exsolving titanomagnetite. The process is probably rare and it is certainly an uncommon feature in the rocks examined for this study. A few examples of this type of intergrowth are shown in Plate 12.4. The ilmenite grains are always phenocrysts and the common plane of exsolution is (0001); this is the same crystallographic plane along which titanohematite exsolves. These intergrowths are sometimes difficult to detect but become well marked when they are selectively oxidized to titanomaghemite (e.g. Plate 12.4b). The exsolved lamellae are rarely parallel sided but tend rather to pinch and swell along the length of the plate. Grain boundary migration of titanomagnetite has been observed (Plate 12.4c) but is regarded as being exceptional.

It has been suggested (BUDDINGTON, FAHEY and VLISIDIS, 1963) that these intergrowths are the result of a sub-solidus reduction process of Fe_2O_3 in solid solution, with contemporaneous exsolution of titanomagnetite; similar textures have been duplicated synthetically by LINDSLEY (BUDDINGTON and LINDSLEY 1964) in precisely this manner.

Since the observed intergrowths in the Icelandic rocks are exclusively confined to phenocrystic ilmenite it seems

reasonable to assume that these crystals have undergone a complex magmatic history which was different from the finer grained Fe-Ti oxide minerals in the host rock.

12.4 Controls on Crystal Growth

Plate 12.5 shows the type of crystalline habit that is exceptionally found in highly vesicular lavas where titanomagnetite and ilmenite are separately precipitated on the surfaces of gas vesicles.

In Plate 12.6 a selection of photomicrographs are shown to illustrate the mesostasis effect on crystal growth. It is important to note that the phenocryst-mesostasic contact forms an ideal point source to initiate crystallization. Both titanomagnetite and ilmenite are present in these zones but it is invariably the latter mineral that tends to line the mesostasic cavity.

CHAPTER 13

FERROMAGNESIAN SILICATES

13.1 Introduction

From the magnetic standpoint the silicates do not contribute to the overall magnetic properties, conventionally measured in palaeomagnetic practice, since they are essentially paramagnetic and not ferrimagnetic. WILSON (pers. comm. 1966) has found however that the main magnetic source material in highly oxidized basic lavas does not lie in the Fe-Ti oxides but in highly altered olivines. This has now been confirmed; heating experiments on olivine under oxidizing conditions show that it is retentive, strongly magnetic and very stable (A. RIDING pers. comm. 1967).

In order to supplement these magnetic observations, the mineralogy of olivine and its associated breakdown products has been investigated. Brief consideration has also been given to the alteration products of primary pyroxene; this mineral produces not only secondary iron oxides but frequently also Fe-Ti oxides.

During the high temperature oxidation of olivine it has been found that iron gradually exsolves from the lattice as an opaque oxide phase. The segregation of iron in this manner

produces a simultaneous enrichment of magnesium in the silicate host. The iron oxide phase which forms is either magnetite or hematite depending on the availability and the partial pressure of oxygen, and on the temperature of formation. The silicate phase which co-exists with the iron oxides is either enstatite or forsteritic olivine and there is a close association between magnetite and enstatite on the one hand and hematite and forsteritic olivine on the other. It is suggested that the magnetite-enstatite trend is an intermediate stage in the oxidation of olivine, but that the stable high temperature assemblage is hematite plus forsterite.

The characteristic textural trend of the intermediate oxidation assemblage is a symplectic (graphic or sub-graphic) intergrowth of magnetite in enstatite. The secondary silicate phases are difficult to identify optically in fine grained lavas owing to the densely packed nature of the symplectite which renders the "olivine" very nearly opaque in thin section. The silicate phases present have, however, been determined by X-ray powder photography.

MUIR et.al (1957) suggested that the oxidation breakdown of olivine may take place according to the following chemical reactions:-

$$(3Fe_2SiO_4 + 3Mg_2SiO_4) + O_2 = 2Fe_3O_4 + 6MgSiO_3$$

Olivine — Magnetite — Enstatite

i.e. for every mole of fayalite converted to magnetite, sufficient silica is released to convert one mole of forsterite to enstatite. The chemical breakdown suggested by these authors, however, did not satisfy their own finding that hypersthene (Fs_{18-24}) and not enstatite had developed in the picritic basalts studied. It was concluded that an introduction of iron and a loss of magnesium and silicon had taken place.

Symplectic corona structures around olivine need not necessarily form by processes of oxidation but may result from magmatic or thermal metamorphic reaction with plagioclase feldspar (SHAND, 1945).

KUSHIRO and YODER (1966) in considering anorthite-forsterite and anorthite-enstatite reactions, have reviewed and summarised in detail a number of publications in which spinel (sensu stricto $MgAl_2O_4$) -pyroxene symplectites have been recorded from the breakdown of olivine. All the intergrowths described are from basic intrusive rocks which occur in metamorphic environments. Altered plagioclase is thought to be the source of alumina for the production of spinel.

There are several important differences between oxidation symplectites and metamorphic symplectites. In the oxidation symplectites, magnetite and enstatite are derived solely from the breakdown of olivine on oxidation. In the metamorphic symplectites, however, the breakdown of olivine is more complex, as an introduction or exchange of Mg, Al, Ca or Fe ions may take place, resulting in single or successive reaction zones around the olivine. Within these zones the characteristic spinel phase may occur in close association with orthopyroxene, clinopyroxene, cummingtonite, actinolite or hornblend (SHAND, 1945). An interesting comparison between metamorphic and oxidation symplectites has been revealed in an examination of a number of polished and thin sections from the Hamar meta-gabbro, Somalia (specimens loaned by W. SKIBA). The opaque oxide phase in these symplectites is either magnetite or spinel plus enstatite, indicating that simple oxidation without metamorphic reaction has at times been operative.

With reference to the MgO - FeO - Fe_2O_3 system, MUAN and OSBORN (1956) have discussed the effect of the partial pressure of oxygen on paths of primary equilibrium crystallization. MUAN (1958) has broadly defined paths of equilibrium crystallization in a closed system as "a continuous

description of the changes in phase assemblage taking place as the temperature is lowered from liquidus temperature, and equilibrium maintained among the phases".

It is well known that a continuous compositional change may take place in a solid solution series as a result of magmatic equilibration. The oxidation reactions referred to in this study, however, are considered to be effected during the late stages of crystallization and as such are dominantly gas-solid, rather than liquid-solid reactions. The latter reaction results in a fayalitic enriched component, whereas an oxidizing gas-solid reaction induces a separation of the olivine into two component phases (forsterite plus hematite).

On the basis of MUAN and OSBORN's work, if one considers a continuous increase in pO_2 taking place with increasing crystallization, an increase in the MgO : (MgO + FeO) and Fe_2O_3 : FeO ratios is to be expected. MUELLER (1961) points out that both these ratios may reflect pO_2 conditions during late stages of consolidation, irrespective of previous pO_2 conditions, but adds that the Fe_2O_3 : FeO ratio is the better of the two indicators.

An increase in the MgO : (MgO + FeO) and Fe_2O_3 : FeO ratios is evident in the progressive high temperature

oxidation breakdown of olivine. The former ratio is reflected in the development of the silicate phases (enstatite or forsterite) and the latter ratio is expressed in the opaque oxides (magnetite or hematite).

13.2 Reflection Microscopy

13.2.1 Secondary Iron Oxides in Altered Olivine

A wide variety of textural forms exist in the secondary opaque oxides associated with the oxidation breakdown of olivine at high temperatures. The progressive oxidation of each type may occasionally be followed within a single polished section, where oxidizing conditions have varied over small distances. Gross variations have been traced in vertical traverses across single lavas in which high temperature oxidation zones have been found to occur (WATKINS and HAGGERTY, 1965). These zones commonly occur towards the centre of a lava, and several factors suggest that the oxidation process is of a primary deuteric nature (see Chapter 18).

The coarser magnetite symplectites (Plates 13.1 and 13.2) that have been observed in polished sections of basic lavas, may vary from true vermicules (single or multiple worm-like forms of the opaque phase) to rods, lamellae and irregular plates. Generally, individual vermicules are extremely fine, and at magnifications of x2000 are only just within

the resolving power of a good reflecting microscope. These magnetite vermicules constitute the microsymplectites (Plates 13.4 and 13.5).

In the coarser symplectites, massed vermicules of magnetite occur in jagged symplectic units which may be spheroidal, semi-spheroidal, lensoid or lamellar in form. Examples of these units are illustrated in Plate 13.8. These units frequently show a perfect gradation of one form to another, in the order listed, as they develop from the centre towards the edge of a crystal. Symplectic units are generally oriented within the oxidized olivines, but local crystallographic control of individual vermicules does not seem apparent. Particle coarsening and gradual growth of the symplectites to solid lamellae and irregular plates takes place by a process of diffusion and agglomeration, and in this respect a very close analogy may be drawn between this process and the textural transformation which have been observed to take place in annealing experiments of eutectic binary alloys (GRAHAM and KRAFT, 1966; HUNT, 1966). Although the maximum oxidation reached in a grain is towards the edge of the grain, nucleation and particle coarsening of the magnetite is not restricted to any particular area or zone within the crystal.

The microsymplectites occur more commonly than their coarser counterparts. They characteristically occur in lens shaped bodies and yet may show some degree of orientation in one or more crystallographic directions (Plate 13.4). Fine filamental symplectite stringers occur between the larger bodies and in irregular cracks, which give the grain an intricate net-like appearance (Plate 13.5). These bodies tend to coalesce and become densely packed at the grain boundaries, where no apparent orientation occurs. A perfect transition of this deterioration in orientation is evident in crystals which show a steep oxidation gradient from the crystal boundary to the centre of the crystal.

The micrographic nature of the microsymplectites is not evident in the photomicrographs. This feature is best observed under the microscope by racking the stage into and out of focus. Optically the opaque phase in the microsymplectites is isotropic, somewhat darker in colour, and has a lower reflectivity than the magnetite in the coarser symplectites. Microsampling and X-ray powder photography of a number of altered olivines of this type have confirmed that the opaque phase is magnetite. The optically anomalous nature of the magnetite is considered to be partly due to its extremely fine grain size and to the fact that the Fe-oxide: Mg-silicate ratio is far less than in the coarser symplectites.

It follows that subsequent or continued oxidation of the magnetite phase produces hematite. Hematite may also be produced directly from the olivine without passing through this intermediate magnetite-enstatite assemblage.

Olivine grains which are highly oxidized are characterised by thick diffusion rims of Fe_2O_3 along the grain boundaries (Plates 13.3 - 13.5). These hematitic rims develop within the olivine, and do not mantle the olivine in the sense of an overgrowth. The outer margin of the rim tends to be irregular, whereas the inner contact frequently shows sharp, straight edges (Plate 13.4b). A concentric opaque-oxide deficient zone generally forms adjacent to this rim (Plate 13.3a); the Mg-enriched silicate phase assumes a spongy appearance and becomes intensely reddened when viewed under oil immersion. The rate and direction of solid diffusion of the iron seems to be variable, and as a result, perfectly continuous oxidation hematite rims are rarely seen. While in a majority of cases the diffusion rim is hematite, a small number of samples also showed associated hercynite (Plate 13.3 a-b). The identification of this phase has been confirmed by electron probe microanalysis. The Al, as pointed out by KUSHIRO and YODER (1966), is probably derived from reaction with adjacent plagioclase.

Two distinct textures are produced in the oxidation of magnetite to hematite. The micrographic form of the magnetite phase may give rise to fine orientated laths of hematite (Plate 13.3), or to solid microcrystalline areas of hematite (Plates 13.4 - 13.5). The former texture is the result of a direct transformation and recrystallization of vermicular magnetite to lamellar hematite, whereas the latter texture appears to be the result of an internal migration and nucleation of Fe^{+2} ions into well-defined lens-shaped bodies. These bodies gradually invert to hematite as diffusion and oxidation proceed (Plate 13.4 a-d). Plate 13.3a illustrates the structural transformation that takes place towards the grain boundaries in the oxidation of magnetite to hematite. It is important to note that pseudomorphic hematite after magnetite only occurs when the magnetite is in a lamellar or plate form; vermicular hematite is only rarely seen. The vermicular to lamellar transformation is typical of the coarser symplectites (Plate 13.3), whereas a gradual concentration with accompanying oxidation of the ferrous iron into flame-like bodies is typical of the microsymplectites. (Plate 13.4).

Olivines from samples which show positive reheating effects, as in thin pahoehoe flow units, olivine nodules, and scoriaceous crusts at the tops of lava flows, tend to contain

hematite rather than magnetite in their secondary assemblage. This applies equally to samples immediately adjacent to the high oxidation zones within single lavas. The hematite characteristically segregates into irregular cracks throughout the olivine (Plate 13.6), and also diffuses towards the grain boundaries, as in the symplectites. Flame-like segregations of Fe_2O_3 are typical of thin pahoehoe flow units. These may be crudely orientated, and are indistinguishable from the massive microcrystalline Fe_2O_3 lenses referred to above. There is no evidence from the large number of samples examined, in spite of the fact that variable oxidation conditions may exist with one grain (Plate 13.5c) or within one sample, to suggest that these lenses are the oxidized equivalents of magnetite microsymplectites. They appear to be derived directly as hematite.

13.3 Stability of Symplectic Magnetite

In spite of the high oxidation states shown by the discrete Fe - Ti oxides, symplectic magnetite may be well preserved and unaffected in many highly oxidized olivines. There are two possibilities which may account for this fact. Firstly, the formation of the Fe_2O_3 diffusion rim, which appears to form early on in the oxidation process, may protect the magnetite-pyroxene assemblage from being extensively oxidized.

It may act almost as a semi-permeable membrane, allowing oxidation to continue, but only to a very limited extent. The alternative is that small amounts of MgO which may be present in the magnetite will have a stabilizing effect on it (TSVETKOV et.al 1966).

There is some evidence to suggest that a well established diffusion rim of hematite may act as a preventative barrier against further oxidation. Olivine grains in the state of oxidation shown in Plate 13.5c illustrate the preservation of a well-defined symplectite zone between the hematite diffusion rim and the rest of the grain. Mass diffusion of iron has taken place only in part of the grain, towards what appears to be a natural crystal termination. It would appear that oxidation may have terminated, or was prevented from continuing, once the symplectite and diffusion rim had been produced. The initiation of fresh oxidizing conditions, or sustained oxidation at low temperatures (since the rate of diffusion has been rather sluggish) has effectively attacked the olivine away from the diffusion rim. In these areas, limited segregation of the iron has taken place within the olivine, into thin stringers and irregular lenses, and has not migrated in the normal sense towards the grain boundaries. The oxidation front now moves towards the hematite rim from within the crystal, gradually disrupting not only the magnetite vermicules, but also the

well-defined symplectite lenses. The arrow in Plate 13.5c illustrates a perfectly gradational transformation in the oxidation of magnetite to hematite.

The effect of thermal-oxidation gradients across single crystals of olivine will be dealt with more fully in a discussion of the heating experiments. The oxidation asymmetry of the type shown in Plate 13.5c is extremely common, and one which probably reflects, in addition, the effectiveness of grain boundary seal to oxidation processes at different temperatures.

13.4 Associated Fe-Ti Oxides

Lavas which contain highly altered olivines also contain highly oxidized Fe-Ti oxides. The progressive oxidation trends followed by titanomagnetite and ilmenite, and the importance of pseudobrookite in particular as a high temperature oxidation-indicator has been discussed in previous chapters. The distinction between high temperature oxidation and oxidation at lower temperatures, where the latter is characterised by the presence of titanomaghemite has aided the classification of the alteration of olivine into assemblages which result from primary or deuteric processes and those which result from post depositional processes.

Pseudomorphic assemblages which contain pseudobrookite in the discrete Fe-Ti oxides are found to co-exist with altered olivines, which contain intergrowths of sympletic magnetite or hematite, which is derived from magnetite. In lavas containing predominantly titanohematite and rutile, hematite rather than sympletic magnetite is produced directly from the olivine. The heating experiments on olivine and the determined lower thermal stability limit of pseudobrookite, demonstrate that the primary formation of hematite from olivine is temperature controlled. It is nevertheless emphasised that in a lava volatile activity and/or rate of cooling may also influence the conditions of its formation.

The importance of maghemite in these lavas has been to show that it is a common low temperature oxidation product, but more important that this is the fact that it has been found in each and every lava containing "iddingsite" as an alteration product after olivine.

Although the thermal stability of titanomaghemite as opposed to pure maghemite, is not known accurately, the close association of this phase with "iddingsite", which contains goethite, having an upper stability limit of 140° C (TUNELL and POSNJAK, 1931), lends support to the evidence that this assemblage owes its origin to a low temperature formation.

This assemblage contrasts strongly with the oxidation group of minerals formed at temperatures in excess of 600°C, in which the Fe-Ti oxides are replaced by pseudobrookite, rutile and titanohematite, and the olivine by either symplectic magnetite plus enstatite or hematite plus forsterite.

13.5 Associated Spinels

Primary spinels occur in very small quantities in normal olivine basalts. They tend to crystallize at an early stage, and hence are frequently included within grains of olivine. They are less susceptible to oxidation than the Fe-Ti oxides, but nevertheless may give some indication, internal to the olivine, of the temperature at which oxidation takes place. When these spinels occur as discrete grains within a basaltic groundmass they are usually homogeneous. Plate 10.6a shows an oxidized spinel partly included in a high temperature oxidized olivine crystal, mantled in the groundmass by a pseudomorphic assemblage of rutile, titanohematite and pseudobrookite, after what was an original titanomagnetite overgrowth. Fine oxidation lamellae of hematite are evident in the spinel along octahedral parting planes. A thin diffusion rim of hematite, from the olivine, has developed adjacent to the spinel. Note that the density of hematite lamellae within the spinel increases

towards the spinel grain boundary. Oxidation of these spinels (which are of the Cr, Al, Fe type) has the effect of darkening the spinel; this is probably caused by diffusion of the iron into (111) parting planes. Spinels, whether partially or totally included within highly oxidized olivines, provided they are closely associated with magnetite symplectites or derived hematite, are themselves highly oxidized. It seems a relevant point to emphasize that primary titanomagnetite and ilmenite, associated with spinels in this high oxidation state are replaced by the high temperature ($>600^{\circ}$ C) assemblage pseudobrookite, titanohematite and rutile.

By contrast, spinels have also been found in highly "iddingsitized" olivines, but they in no way show any sign or form of alteration. This applies equally to those spinels occurring in cores of "iddingsite" around olivine. As far as the Fe-Ti oxides are concerned, titanomagnetite always shows signs of maghematization, whereas ilmenite remains completely unaffected.

The importance of pseudobrookite and maghemite as temperature indicators has already been stressed. The spinels therefore provide additional proof that the characteristic associations produced simultaneously in olivine and

the Fe-Ti oxides under highly oxidizing, high temperature conditions are quite different from those associations formed under conditions of lower temperature oxidation.

13.6 Heating Experiments

The purpose of the heating experiments has been to determine the thermal stability of basaltic olivine under oxidizing conditions in the temperature range 600-1000°C at atomspheric pressure. An attempt has been made through these experiments to throw some light on the obvious mineralogical and textural changes that are effected within olivines of highly oxidized basaltic lavas.

Starting material for the oxidation experiments consisted of hand picked, unzoned basaltic olivine grains of composition Fa_{20}. The grain size of the starting material was of the order of 0.5 mm. but additional runs were also made on material which was crushed to pass a -120 mesh screen (< 0.01 mm.). X-ray powder photographs were made from the material of each run using conventional glass fibre mounts. Diffractometer traces were made of several of the alteration products when sufficient material was available. Polished sections, for obvious reasons, were made only of the coarser grained material.

The experiments were carried out in air in a muffle furnace, with a temperature control unit accurate to $\pm 10^{\circ}$C.

Runs were made in open high temperature ceramic boats; silver capsules and silica glass tubes were used in a series of further experiments. Samples from all runs were quenched in air.

Details of the duration, temperatures and results of the oxidation experiments carried out on these basaltic olivines at atmospheric pressure are summarized in Table 13.1.

The results of these experiments indicate that on oxidation in air at temperatures above 600°C, olivine 'exsolves' its iron to form hematite, leaving behind a forsteritic enriched matrix. At 820°C ± 10°C a metastable and intermediate magnetite-pyroxene assemblage makes its first appearance. This metastable assemblage was detected in all the non-equilibrium runs up to 1000°C. It is evident from microscopic examination that the assemblage forms a symplectic intergrowth. The symplectite inverts, with continued oxidation at constant temperature, to the stable forsterite-hematite assemblage.

13.6.1 X-ray Data On Runs From Heating Experiments

X-ray powder photographs were taken of samples from each run. Diffractometer traces were also made using Ni filtered Cu radiation. Small amounts of additional material

were extracted from polished sections using the microsampling techniques.

The interpretation of X-ray powder photographs or diffractometer traces of multi-component assemblages may be extremely difficult. A large majority of the runs, however, contain simply hematite and forsteritic olivine of varying composition. It was only in the coarse grained material heated above 820° C, where equilibrium had not been reached, that four components were detected. These phases were identified as magnetite, hematite, enstatite and forsteritic olivine. Some difficulty naturally arises where a single reflection may be attributed to more than one phase.

Table 13.2 lists the d(Å) values of the ten strongest lines of each phase present in samples from two runs (data obtained from X-ray powder photographs). These were made at 950° C on coarse grained and powered material. The results indicate quite clearly that the non-equilibrium run contains the metastable magnetite-pyroxene assemblage. The unit cell values which were derived from these measurements are as follows:

	(Å)	A.S.T.M.Index (Å)
Magnetite	a = 8.404	a = 8.391
Hematite	a = 5.049 c = 13.759	a = 5.039 c = 13.760

Enstatite	a = 8.836	a = 8.829
	b = 18.211	b = 18.220
	c = 5.114	c = 5.192
Forsterite	a = 4.761	a = 4.758
	b = 10.203	b = 10.207
	c = 5.989	c = 5.988

The diffractometer traces from the equilibrium and the non-equilibrium runs are shown in Figures 13.1 and 13.2 respectively. The gradual growth of peak intensities with increasing temperature may be followed in successive stages from one profile to next. The first appearance of a reflection is marked by an arrow and the division of a reflection into two or more reflections by X. Note that in the non-equilibrium run, the first sign of any new phase is at 820 ^{o}C, whereas in the equilibrium run the corresponding temperature is 600 ^{o}C. In each of the respective diagrams the reflections for olivine move to higher order values of 2θ as the temperature increases, reflecting an increase in the forsteritic end member. The peaks are well defined which indicates that a reasonably high degree of crystallinity has been attained in the experimental runs.

The composition of the olivine formed during each of the runs has been calculated according to the method of JAMBOR and SMITH (1964). The forsterite content of the olivine is determined by substituting the d($\AA$) value of the

(174) back reflection line in the equation:

$$(\text{mole } \%)\ Fo = 4151.46 - 397\%.45d_{174}$$

The error at 100 mole % Fo is ± 0.87% and at 80 mole % Fo is ± 0.57%. The d_{174} values and the forsteritic compositions of the olivines formed between 600° and 1000° C are listed in Table 13.3.

Samples from all runs above 820° C were found to be highly magnetic. It is known that continued replacement of Fe^{+2} by Mg may take place in magnetite to form magnesioferrite, $MgFe_2O_4$ (DEER, HOWIE and ZUSSMANN, 1962). The possible presence of magnesioferrite rather than magnetite has been considered in the high temperature oxidation of olivine, but has as yet not been detected. While only small differences exist in the unit cell dimensions (Fe_3O_4, a = 8.391; $MgFe_2O_4$, a = 8.383) the intensity of the (111) reflection at 4.84 Å is quite distinct (BERRY and THOMPSON, 1962). The X-ray data are supported by the mineralogical evidence in polished sections, suggesting that the opaque symplectic phase is magnetite and not magnesioferrite. The reflectivity of the (Mg, Fe, Al, Cr) spinel group is lower and the colour darker than that of magnetite. Small amounts of MgO may nevertheless be present in the magnetite. The fineness of

the magnetite symplectite, and the fact that it is closely associated with enstatite, has precluded the positive confirmation or absence of Mg even by electron probe microanalysis.

Microsampling traverses across four olivine grains, selected from polished sections of non-equilibrium runs, has confirmed that towards the edge of an olivine grain forsterite is associated with hematite, and that towards the centre, the symplectite consists of enstatite and magnetite.

13.6.2 Reflection Microscopy of Heated Material

By using relatively coarse grained material, the oxidation and temperature gradients that are set up within single grains, has permitted a detailed study to be made optically of the progressive textural and oxidation changes that occur from the edges, where equilibrium is reached, to the centre, where in the experiments of shorter duration the olivine is completely unaltered.

Samples heated above 820 ^{o}C all showed hematite diffusion rims and the magnetite-pyroxene symplectite. The degree of development and complexity of these intergrowths, and the thickness of the rims varied with the duration of the experiment. A common feature in all of these experiments is the initial development of small spherical to sub-spherical

symplectic nucleii. As these nucleii grow and become more numerous they tend also to become lens shaped. Individual units may show a remarkable degree of orientation (Plate 13.8). The gradual coalescing of these lens shaped units produces the symplectic pinch and swell structures illustrated in Plate 13.8c. Symplectites also develop from narrow cracks and flaws in the olivine. Branches, sub-branches and budding of the symplectite may take place, which then result in a herring bone structure of the type shown in Plate 13.8d.

Towards the grain boundaries and concentric to it, lenses, pinch and swell symplectites and fine inter-unit symplectic lamellae all merge into a densely packed halo adjacent to the hematite zone. These grains, in common with the naturally occurring olivines, show the vermicular to lath transformation that occurs during the oxidation of sympletic magnetite to hematite (Plate 13-9). It is within this outer zone that equilibrium conditions are reached, and it is here that forsterite is the chief magnesium silicate.

Hematite diffusion rims are extremely well developed in the higher temperature runs. These rims are generally continuous but tend to be irregular (Plate 13.9b) and are often of a rather bulbous nature. This feature is undoubtedly related to the fact that the grain boundaries in the heating experiments are unrestricted and not confined as in a crystalline

basaltic host. Jagged saw tooth intergrowths of diffused hematite frequently develop within the olivine along fine hair-line cracks (see for example Plate 13.6d).

Although hematite diffusion rims around olivine were found to be extremely common in the highly oxidized lava samples examined, it was nevertheless considered that these rims may owe their origin, in part, to primary marginal fayalitic zoning. The textural evidence however, supports the idea that diffusion and migration does take place, not only within the crystal, but also towards the crystal boundaries. Great care was taken in the initial choice of the starting material to ensure that the olivines were free of magnetite, and Cr-spinel inclusions, and were unzoned. The textural interpretation that Fe_2O_3 concentrations at the crystal boundaries are the result of an oxidation-diffusion process at high temperatures is supported by the heating experiments. The starting material for the heating experiments was fragmented. It is unlikely therefore, that continuous oxidation diffusion rims of hematite are in any way related to iron-rich zones within the olivines, and although fayalitic zoning will undoubtedly effect a concentration of iron towards the margins, processes of diffusion play the major role.

The Fe_2O_3 : Fe_3O_4 ratio increases rapidly with longer periods of heating. No magnetite was detected in the coarse grained material at 950° C for example after 100 hours. The final product in polished section contains thin oriented laths of hematite in an intensely reddened forsteritic matrix and is zoned by the characteristic Fe_2O_3 diffusion rim. The textural form of this assemblage is identical to the natural sample and is illustrated in Plate 13.9c.

A series of preliminary experiments were carried out in an attempt to coarsen the magnetite symplectite by prolonged heating at 900° C. Runs were made for periods of ten and fifteen days. The problem is to capture the intermediate magnetite-pyroxene phases without extensively developing forsterite and hematite at the same time. Two series of experiments were carried out with the idea that the availability of oxygen to the samples should be restricted. In the first series, samples were heated in narrow silica glass tubes, sealed at one end and drawn to a fine capillary at the other; in the second series, olivine samples were heated in 2 mm. diameter silver capsules which were tightly crimped, but not sealed, at both ends. No attempt was made to coarsen the symplectite by cooling the samples slowly to room temperature because of the forsterite-hematite field which exists below 820° C.

A moderate degree of success in coarsening the symplectite was achieved in the silver capsule experiment which ran for ten days. In the silica-glass runs, as well as in the silver-capsule 15 day run, however, large amounts of forsterite and hematite were produced.

Samples heated below 820°C all showed the direct segregation of hematite from within the olivine. Hematite rims were found to be common but generally less well developed than in the higher temperature runs. In the 600°C run, after 100 hours, the olivine became intensely reddened and only small amounts of hematite were detected at the grain boundaries. The rather unusual textural forms of the opaque phase in the 600°-810°C experiments are illustrated in Plate 13.10. Unlike the spherical nucleii of the symplectites, the onset of alteration is marked by the development of minute star shaped bodies and en echelon lenses of hematite. These gradually develop with intriguing structural complexity towards the crystal boundaries. It is evident from the photomicrographs that these bodies are crystallographically controlled. The phases and textural form of the alteration products in these runs compare favourably with naturally reheated olivine in pahoehoe flow units and in olivine-bearing xenoliths.

The X-ray data indicates that with continued exsolution of the iron the olivine becomes more forsteritic in composition.

An important point to note with reference to the high temperature alteration of olivine, is that only oxygen needs to be added to effect the mineralogical changes that are observed in nature. No further introduction or removal of material is necessary. This contrasts greatly with the low to intermediate temperature of alteration, where an introduction of water and alumina (and in some cases alkalis) to the olivine occurs, and removal of iron, magnesium and silicon takes place (BAKER and HAGGERTY, 1967).

Similar high temperature oxidation experiments have been carried by CHAMPNESS and GAY (CHAMPNESS, pers.comm. 1967) using more refined single crystal techniques. Their results confirm that magnetite and hematite are the chief iron oxides which form and it is interesting to note that they have also detected super-lattice effects in these phases. Their results show, however, that pyroxene only forms above 1000°C in association with cristobolite. They suggest that free SiO_2 is present throughout the oxidation reaction and assume that it is amorphous at lower temperatures. No evidence has been found in the present study for this suggested SiO_2 phase although, of course, it may be obscured in the X-ray analysis

if it occurs in small quantities. There seems little doubt that the phase identified as enstatite in this study is in fact a pyroxene, although its composition may not be stiochiometric $MgSiO_3$. The instability of olivine in the presence of free silica is well known and in view of these results it is evident that much more work needs to be done, particularly from the chemical aspect, on the high temperature alteration of olivine.

13.7 Alteration at Low to Intermediate Temperatures

From the reflection microscopy point of view the most important alteration products of olivine that can be identified, and attributed to a lower temperature of formation than those discussed above, is "iddingsite". The phase that makes it optically characteristic is the goethite component. Examples of "iddingsitised" olivine are illustrated in Plate 13.11 and 13.12. In most cases the goethite is closely associated with hematite which must have been brought about by partial dehydration of the iron hydroxide; the examples all have a history of reheating during burial. The Fe-Ti oxides in these "iddingsitised" lavas are strongly maghemitized which supports low-intermediate temperature ($>550^{o}C$) origin.

In contrast to samples which have suffered high temperature alteration, "iddingsitised" samples do not develop

hematite diffusion rims and are not intensely reddened when viewed under an oil immersion lens. In common with the high temperature product, however, is the densely packed nature of the secondary intergrowth and the high concentration of the iron oxide/hydroxide phase. Yet another feature which distinguishes the high temperature assemblage from the lower temperature process is the fact that well developed parting planes result in the latter assemblage. Such samples are highly ordered and appear strongly pleochroic in thin section.

A low to intermediate temperature process which will not be considered here is the process of serpentinization. It is well known, however, that such processes produce secondary iron oxides and in some cases even native iron and native nickel-iron (awarite) have been reported (CHAMBERLAIN et.al 1965). Serpentine is a relatively rare mineral in the Icelandic Tertiary basalts although it occurs extensively in the gabbros (ROEBOL pers.comm. 1967).

13.8 Pyroxene Alteration

Pyroxene is a relatively minor phase in the Icelandic basalts and when it does occur it is usually associated with the groundmass silicates. The examples discussed here are from the BORLEY-ABBOTT Teneriefe collection.

The opaque oxide minerals which develop from pyroxene are titanomagnetite, ilmenite, rutile and titanohematite. The most common association is titanomagnetite plus ilmenite; rutile is always associated with ilmenite and titanohematite is always an oxidation product of either titanomagnetite or ilmenite.

There are two distinct types of alteration assemblages. In the first, where either titanomagnetite or ilmenite may be present, there is a general lack of mineral orientation and no evidence of alteration in the discrete Fe-Ti oxides (Plate 13.13). In the second, the alteration product, which is usually ilmenite or rutile, is well oriented and the discrete Fe-Ti oxides are highly oxidized (Plate 13.14 c-d). These pyroxenes are titanaugites and the rocks are characterised in having low primary concentrations of ilmenite. The former type of alteration is considered to be a high temperature magmatic alteration of the type discussed by VERHOOGEN (1960), and the latter a lower temperature product resulting from deuteric oxidation.

These secondary minerals are important magnetically because of their fine grainsize and because the phases are titanium-enriched. Titanomagnetite, for example, follows the same oxidation trend as its discrete counterpart. At

the sub-solidus stage, when ilmenite lamellae are produced, these small grains will be sub-divided into even smaller particles. Grainsize is known to be directly related to magnetic stability and the particle size in these cases would approach single magnetic domain size, which for magnetite is of the order of 1 micron.

13.9 Conclusions

1. The high temperature oxidation of olivine may produce either magnetite plus enstatite or hematite plus forsterite.

2. Heating experiments on basaltic olivine (Fa_{20}) at atomspheric pressure in the temperature range 600 -1000 C have shown that forsterite plus hematite is the stable assemblage.

3. Magnetite plus enstatite is an intermediate and metastable assemblage. Its first appearance has been noted at 820 C, and it continues to appear up to 1000 C. With sustained oxidation, magnetite plus enstatite inverts to forsterite plus hematite. This latter assemblage also develops between 600 C and 820 C.

4. The discrete Fe-Ti oxides, which accompany the development of magnetite + enstatite or derived forsterite +

hematite assemblages in altered olivine, are typically pseudo-brookite, rutile and titanohematite, which have formed by oxidation after original titanomagnetite and ilmenite. The presence of pseudobrookite in particular, having a lower thermal stability limit of $580^{\circ} \pm 15^{\circ}C$, supports the high temperature origin of iron oxide intergrowths in altered olivines.

5. Texturally the opaque phases of oxidized olivines are characterised in polished section, by the following features:

i) Vermicular magnetite forms symplectic and micro-sympletic intergrowths.

ii) A progressive transformation of vermicular magnetite to lamellar hematite takes place with progressive oxidation.

iii) Hematite derived directly from olivine is lensoid or flame-like in form.

iv) Hematite or hematite-spinel rims develop towards the edge, but within, the crystal boundaries of highly oxidized olivines.

v) "Iddingsitised" olivine is a low to intermediate temperature product because of its component

goethite, which has an upper thermal stability limit of 140°C, and because it is associated with titanomaghemite in the discrete Fe-Ti oxides.

vi) The high temperature alteration products of pyroxene are titanomagnetite, ilmenite and rutile.

vii) The secondary opaque oxide minerals which develop in olivine and pyroxene are important magnetically because of their grainsize, which is known to be related to magnetic stability.

TABLE 13.1

Temp. °C	Duration of run in hours	Phases present Grain size of starting material	
		>0.01 mm	approx.0.5 mm
600	100	Fo+Fe_2O_3	Fo+Fe_2O_3
750	100	Fo+Fe_2O_3	Fo+Fe_2O_3
800	100	Fo+Fe_2O_3	Fo+Fe_2O_3
810	100	Fo+Fe_2O_3	Fo+Fe_2O_3
820	24	Fo+Fe_2O_3	Fo+Fe_2O_3
	100	Fo+Fe_2O_3	$FoFe_2O_3$ (En+$Fe_3)_4$)
830	24	Fo+Fe_2O_3	Fo+Fe_2O_3
	100	Fo+Fe_2O_3	Fo+Fe_2O_3 (En+Fe_3O_4)
850	48	Fo+Fe_2O_3	En+Fe_3O_4+Fo+Fe_2O_3
	100	Fo+Fe_2O_3	
950	24	Fo+Fe_2O_3	En+Fe_3O_4+Fo+Fe_2O_3
	48		En+Fe_3O_4+Fo+Fe_2O_3
	72		En+Fe_3O_4+Fo+Fe_2O_3
	100	Fo+Fe_2O_3	Fo+Fe_2O_3
	120		Fo+Fe_2O_3
	360		Fo+Fe_2O_3
1000	24	Fo+Fe_2O_3	(En+Fe_3O_4)+Fo+Fe_2O_3

Temperature, duration of experiment and phases present in equilibrium (0.01mm) and non-equilibrium (approx.0.5mm) runs. Note that enstatite + magnetite make their first appearance at 820°C and also that equilibrium is reached in the 950°C experiment after 100 hours. The phases in parentheses indicate trace amounts. En = enstatite; Fo = forsterite.

TABLE 13.2

950°C/100hrs. 0.01mm	950°C/48hrs. Approx.0.5mm	Olivine	Enstatite	Magnetite	Hematite
5.12	5.10	5.11			
3.89	3.88	3.88			
	3.28		3.30		
	3.17		3.17		
	2.96			2.96	
			2.94		
	2.87		2.87		
			2.83		
2.76	2.76	2.77			
			2.71		
2.69	2.69				2.69
2.52	2.53		2.53	2.53	2.52
2.51	2.51	2.51			
			2.49		
2.45	2.46	2.46			
	2.47		2.47		
2.27	2.27	2.27			
2.25	2.25	2.25			
2.20	2.20				2.21
			2.11		
	2.10			2.09	
1.839	1.842				1.843
1.747	1.750	1.748			
	1.714			1.712	
1.693	1.695				1.697
	1.616			1.611	
1.511	1.497	1.497			
1.476	1.481	1.479		1.481	1.488
1.453	1.454				1.457
	1.278			1.280	
1.154	1.149				1.143
	1.125			1.122	
1.102	1.106				1.106
	1.092			1.094	
1.055	1.065				1.058
	1.049			1.050	
$Fo+Fe_2O_3$	$En+Fe_3O_4+$				
	$Fo+Fe_2O_3$				

X-ray data for an equilibrium and a non-equilibrium run at 950°C. The d values (Å) listed are for the ten strongest lines of each phase present. Note that only five of the ten values for enstatite could be conclusively attributed to a particular reflection; the unallotted values are all of low intensity.

TABLE 13.3

	Temp. °C	Duration of run in hours	Olivine Composition d_{174} (Å)	Mole % Fo
Starting Material		?	1.0238	80.4 ± 0.6
	600	100	1.0238	80.4 ± 0.6
	750	100	1.0230	83.5 ± 0.6
	800	100	1.0228	84.3 ± 0.7
	810	100	1.0228	84.3 ± 0.7
	820	100	1 0206	93.1 ± 0.8
	830	100	1.0205	93.5 ± 0.8
	850	48	1.0202	94.7 ± 0.8
	950	24	1.0200	95.5 ± 0.8
		48	1.0192	98.7 ± 0.9
		72	1.0192	98.7 ± 0.9
		100	1.0189	99.9 ± 0.9
		360	1.0190	99.5 ± 0.9
	1000	24	1.0197	96.7 ± 0.9

Temperature, duration of experiment, the d_{174} value from X-ray powder photographs, and the mole % forsterite as determined on coars grained olivine (approximately 0.5 mm).

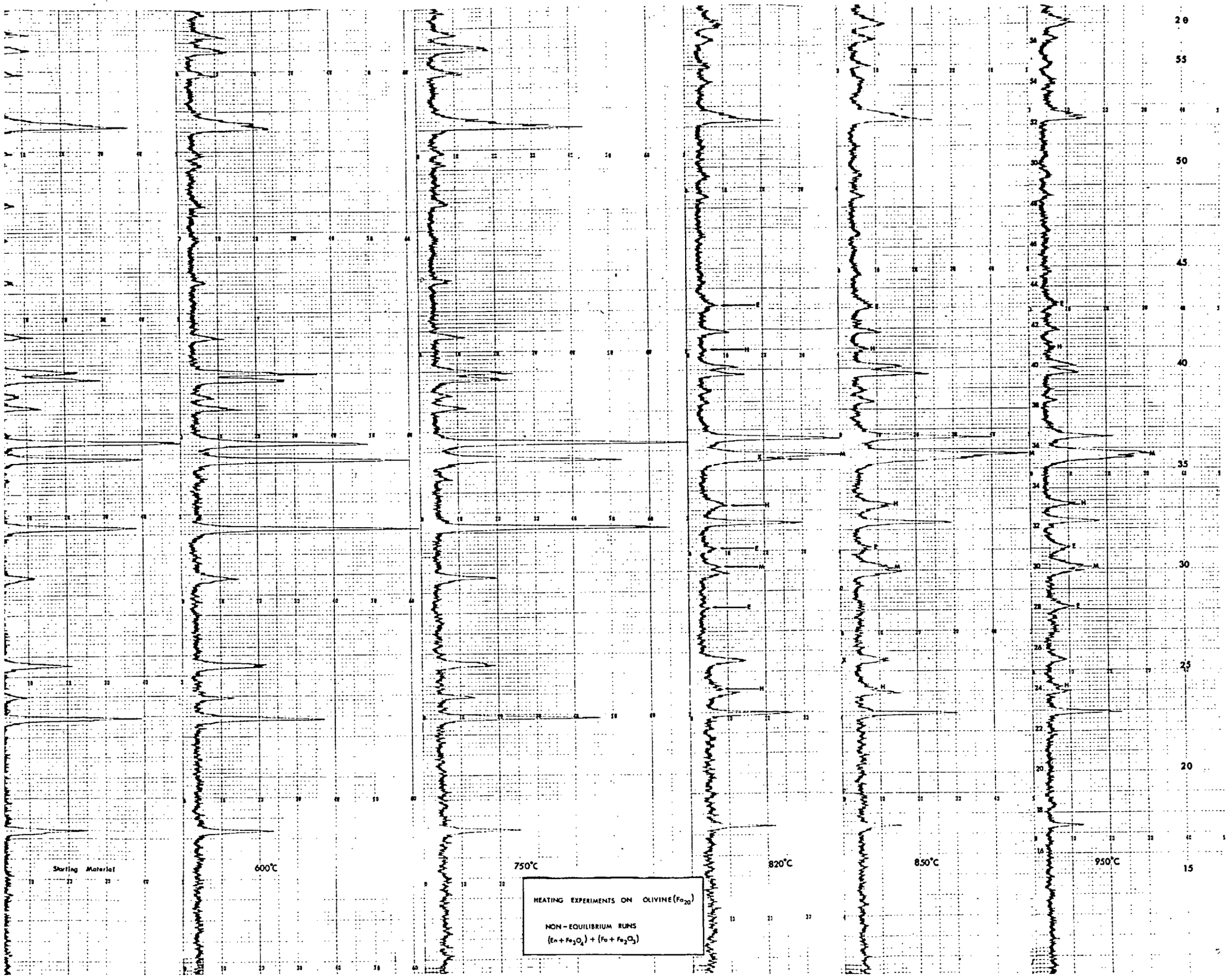
Starting Material
600°C
750°C
820°C
850°C
950°C
HEATING EXPERIMENTS ON OLIVINE (Fo_{20})
NON-EQUILIBRIUM RUNS
$(En + Fe_3O_4) + (Fo + Fe_2O_3)$
2θ
55
50
45
40
35
30
25
20
15

Fig 13.1

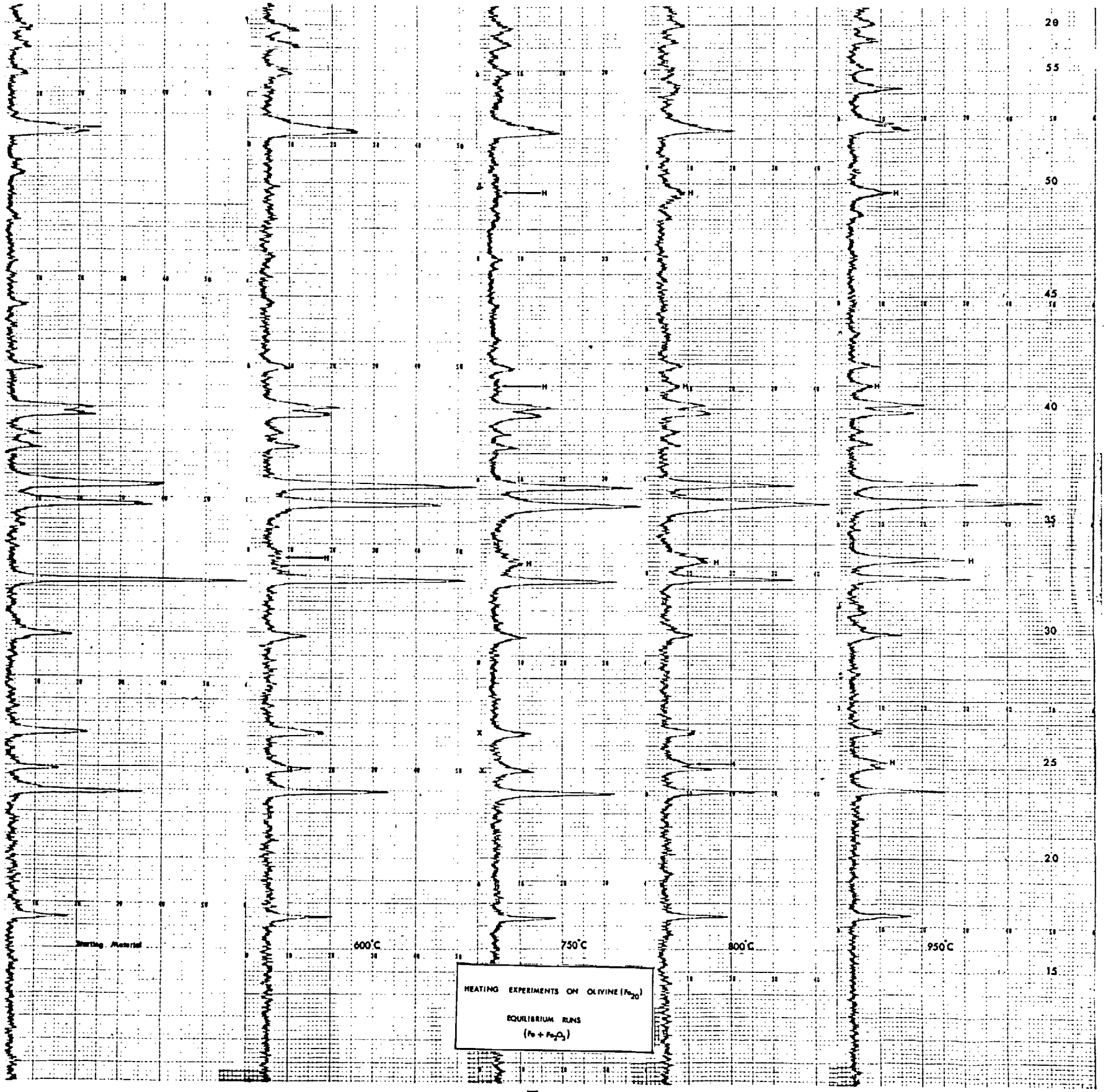
Starting Material
600°C
750°C
800°C
950°C
H
HEATING EXPERIMENTS ON OLIVINE (Fa_{20})
EQUILIBRIUM RUNS
($Fe + Fe_2O_3$)

Fig 13·2

CHAPTER 14

SINGLE UNIT STUDY

14.1 Introduction

In a large collection of lavas, like the present Icelandic study, it is extremely important to know what background effects there are magnetically and mineralogically within single lavas, so that a generalised basic norm can be established with which direct comparisons can then be made. It is tacitly assumed by both palaeomagnetic research workers and petrologists that very little variation may be expected within the limits of a relatively thin lava or dyke. This assumption makes itself manifest by the fact that small numbers of specimens, generally no more than one or two, are usually taken from a single unit, and it is then generally regarded that these samples are totally representative of the body. Chemical differentiation trends in volcanic provinces are frequently quoted in the literature, without any reference or due consideration to the possible internal variations that may be active within single units. Even more serious is the fact that such trends are often extrapolated for the use of inter-continental or inter-oceanic petrological comparison.

The present study is an attempt to rectify this situation, by demonstrating that large variations are to be expected between the cooling faces of an extrusive igneous body.

Vertical traverses across 14 lavas and 7 dykes have been obtained in Iceland. The thickness, number of specimens and the location of these units is given in Table 2.1.

The Fe-Ti oxide minerals will be discussed according to the general principles that have been established in the preceding section. These principles include the progressive state of mineral oxidation, the identification of the phases produced, and the textural form and mode of occurrence of these phases. Their general distribution in traverses across the units and their correlation with the magnetic properties will also be considered.

Oxides of iron and titanium are the chief opaque phases in these rocks. The primary minerals are titanomagnetite and ilmenite and the secondary products are rutile, ferri-rutile, titanohematite and pseudobrookite. It has been established that the process of oxidation is the most active of the natural chemical agencies that affect and modify the minerals in igneous rocks. The Fe-Ti oxides are highly susceptible to oxidation and it is this process of oxidation that has the greatest effect on the magnetic properties of the rock. The prime consideration in this study therefore has been to classify the opaque mineralogy according to the prevailing state of oxidation of the Fe-Ti oxides.

Only two of the lavas will be described in detail; an olivine-rich basalt and an olivine-poor basalt. Both lavas are relatively thick (11.0 and 16.8 m. respectively), and both are reversely magnetized. These lavas were particularly chosen from those sampled because they have several distinct mineralogical and magnetic differences. They were also chosen because a detailed study shows them to have both typical and atypical features of the remaining lavas. The olivine-rich basalt has a fairly uniform grainsize throughout its central portion and a constant titanomagnetite: ilmenite ratio; the olivine-poor basalt, in contrast, has a variable grainsize throughout, and its titanomagnetite:ilmenite ratio is also variable. The remaining differences are that the olivine-rich lavas has a single NRM direction and a uniform state of oxidation within single specimens, whereas the olivine-poor lava has mixed NRM directions (due to instability) and widely varying states of oxidation in single samples.

14.2 Classification of the Fe-Ti Oxides

The following optical scheme of mineral oxidation has been used to classify the Fe-Ti oxides:

I Primary homogenous titanomagnetite (magnetite-ulvospinel solid solution) (Plate 6.9a).

II Titanomagnetite with a single or small number of "exsolved" ilmenite lamellae along (111) planes. (Plate 6.9b)

III Titanomagnetite with abundant "exsolution" lamellae of ilmenite. (Plate 6.9c).

IV The sharp, well defined lamellae of III assume a mottled appearance. These lamellae gradually become lighter in colour as oxidation proceeds, indicating a build-up of ferric iron; the host titanomagnetite becomes correspondingly browner in colour. The mottled effect in the lamellar ilmenite, by analogy with discrete ilmenite, is due to the generation of finely textured rutile, ferri-rutile and titanohematite. The titanomagnetite shows signs of incipient alteration to titanohematite and the host may also contain minute exsolution rods of hercynite. (Plate 6.9d)

V With increasing oxidation the products become more coarsely crystalline. Partitioning of the oxidation products into separate, optically identifiable, mineral phases, takes place. The characteristic phase at this stage is rutile. Both the

titanomagnetite and the ilmenite are oxidized to oriented intergrowths of rutile in a host of titanohematite. The ratio of rutile to titanohematite is greatest in areas of original ilmenite, simply reflecting the distribution of iron and titanium in the primary titanomagnetite intergrowth. Relic, triangular or rectangular, areas of brown titanomagnetite may still persist. These areas invariably show fine exsolution rods of hercynite. (Plate 6.10-11)

VI This class represents the maximum degree of oxidation and is characterised by the high temperature, $585^{o} \pm 15^{o}$ C (LINDSLEY 1965) index mineral pseudobrookite. The original titanomagnetite-ilmenite intergrowth is completely pseudomorphed by an assemblage of sub-graphic pseudobrookite in a host of titanohematite, in which accessory rutile may or may not be present. The pseudobrookite may be well oriented in a Widmanstätten pattern or may be graphically intergrown with the host titanohematite. (Plate 6.12)

The above scheme is an index of the state of oxidation of the Fe-Ti oxides. By limiting the classification to

titanomagnetite the index is reduced to a single number. This has the added advantage that the effect of oxidation on discrete ilmenite may also be taken into account since ilmenite features prominently in the initial stages of titanomagnetite oxidation. Mineralogically the progressive alteration of discrete ilmenite is exactly the same as ilmenite which has "exsolved" from titanomagnetite; discrete ilmenite is slightly less susceptible to oxidation however.

Oxidation indices I - III are due to sub-solidus oxidation and are restricted to titanomagnetite, whereas IV - VI are due to pseudomorphic oxidation and include both titanomagnetite and ilmenite. Discrete ilmenite remains completely unaffected in class I - III, it shows incipient signs of alteration in IV to ferri-rutile, and V to rutile + titanohematite, and in VI to pseudobrookite.

Evidence has previously been presented which suggests that composite and sandwich intergrowths are the result of primary precipitation and are not due to sub-solidus oxidation. (Chapter 6.4.3).

Composite inclusions of ilmenite and thick sandwich laths of ilmenite are therefore classified in index I and are indicated as such by subscripts c and s respectively, thus

Ic or Is or Ics. When these textural forms of ilmenite are associated with lamellar ilmenite then the subscripts are also added, thus IIcs or IIIcs depending upon the density of ilmenite lamellae.

In the systematic classification of the specimens it is sometimes difficult to allocate a single oxidation number to describe the state of oxidation of the entire polished section. A single index number has been used in this study to indicate that there is at least an 80% predominence of that assemblage. Where the value is judged to be less than 80% the index number is described as being between two assemblages, for example III/IV. If more than two assemblages are present, as is common at the edges of lavas, then the range in oxidation assemblages is noted, for example, as I-IV.

In some exceptional cases it has been necessary to point-count titanomagnetite grains (or highly oxidized pseudomorphs after titanomagnetite) in a polished section and to classify each grain in terms of one of the oxidation classes. Where the state of oxidation is highly variable over very small distances (100-200u) this has amounted to counting at least 300 separate grains. The mean oxidation state (WILSON, HAGGERTY and WATKINS 1968) was then determined as a number between 1 and 6 by multiplying each of the six index numbers,

I, II, III, IV, V and VI by the number of grains in that class and then forming the quotient:

$$\text{Magnetite Oxidation Number} \equiv \frac{(n_1 \times I)+(n_2 \times II)+(n_3 \times III)\ldots(n_6 \times VI)}{n_1 + n_2 + n_3 \ldots\ldots n_6}$$

The ilmenite oxidation number has been determined in the same way by using the seven stages of oxidation described in Chapter 5.4.

The scheme of classification is considered to be a high temperature classification. Sub-solidus oxidation of titanomagnetite, to produce ilmenite lamellae, has been shown to occur above 600 °C (LINDSLEY 1963). Heating experiments on ilmenite suggest that rutile, ferri-rutile and pseudobrookite are all high temperature oxidation products, and LINDSLEY'S (1965) work on pseudobrookite confirms that it cannot form below 580 °C.

An attempt has also been made to include the lower temperature oxidation products in this classification. Titanomaghemite only occurs in I-III and its presence is noted by a capital M, thus IIIM. The phase described as amorphous Fe-Ti oxide is paragenetically associated with titanomaghemite, it is also considered to be a low temperature product,

and its presence is noted as follows, IIIAM. The distribution of these phases within any single unit, within any one sample and within any one titanomagnetite grain is extremely variable, and quantitative assessment is made practically impossible. The process of maghemitization does not affect discrete ilmenite.

The importance of the alteration products of olivine on the magnetic properties of a rock have already been noted. Magnetite and/or hematite are the chief oxidation products and are associated with high indices assemblages in the Fe-Ti oxides. These products are not noted directly with the index of classification but are recorded separately.

14.3 Validity of the Oxidation Classification

The classification is divided into two parts. In the first part (I-III), which involves only titanomagnetite, a process of subsolidus oxidation is operative, and in the second (IV-VI) the titanomagnetite-ilmenite assemblage is modified in several successive stages. The classification (I-VI) is a high temperature classification and the higher indices refer to higher states of oxidation.

The classification is based in the first instance on the paragenetic sequence of mineral assemblages which are

observed to form from primary homogeneous titanomagnetite and primary homogeneous discrete ilmenite.

Initial subsolidus oxidation of titanomagnetite produces oriented lamallar intergrowths of ilmenite. This form of oxidation has been demonstrated on natural titanomagnetite by VINCENT et. al (1957) and on synthetic titanomagnetite by LINDSLEY (1963). The density of these lamellae is taken to indicate the degree of sub-solidus oxidation and distinguishes index II from index III. The preferential development of ilmenite lamellae adjacent to cracks and along titanomagnetite grain boundaries supports the evidence for a process of sub-solidus oxidation.(Plate 6.7).

Pseudomorphic oxidation may develop from this titanomagnetite-ilmenite intergrowth, in which case relic (III) textures persist; or alternatively, the higher oxidation phases may develop directly from the primary homogeneous minerals. The order of the assemblages which develop in titanomagnetite are (a) ilmenite (sub-solidus oxidation) (b) ferri-rutile + titanohematite (c) rutile + titanohematite (d) pseudobrookite + titanohematite. The textural evidence supporting this assemblage-sequence is illustrated in the photomicrographs (titanomagnetite, Plates 6. 9 to 6. 12 ; ilmenite, Plates 5.6 to 5.12) and is fully described in the preceeding chapters.

From a mineralogical point of view, the phases which develop from titanomagnetite and ilmenite are all "high-oxides" of iron and titanium. A brief consideration of the oxidation reaction lines in the ternary diagrams (Figure 3.1 and Figure 3.2) will demonstrate this point.

The minerals which are produced, and the sequence in which these minerals are formed, at high levels of oxidation in nature, have been reproduced in laboratory experiments at high temperatures. These heating experiments were directed to the pseudomorphic oxidation section of the scheme and to ilmenite in particular. The nature of the oxidized intergrowths and the development of pseudobrookite rims around the assemblage rutile + titanohematite is highly significant. This sequence of mineral assemblages supports the evidence put forward for the natural oxidation trend and is described in Chapter 5.8.

High oxidation-index assemblages are accompanied by high oxidation states in olivine and spinel. The oxidation products produced in these minerals are high temperature products, which not only supports the oxidation nature of the product but also the temperature classification of the Fe-Ti oxides.

A sequence of specimens from an Icelandic single lava (S) has been classified according to the scheme of oxidation. The

results are presented in Table 15.1. Whole rock chemical analyses for FeO, Fe_2O_3 and TiO have also been determined on the same specimens. The results are listed in Table 15.1. The ratio FeO : Fe_2O_3 is plotted as a function of the oxidation index in Figure 14.1. It is apparent from this graph that although there is a spread within classes and some overlap between classes, there is nevertheless a positive correlation between the oxidation state of the rock and the index of oxidation of the Fe-Ti oxides. The total iron and total titanium content of the lava is constant throughout.

In a separate series of 71 basic lavas from Teneriefe, the Fe-Ti oxides have also been classified according to the oxidation scheme. The results are plotted in Figure 14.2 as a function of the chemically determined ratio Fe_2O_3 : FeO. Once again, a positive correlation is present. These rocks are of particular interest as they range in composition from phonolites to cumulative ankaramites. The shape of the curve is very similar to that of the single lava curve, with the exception that the phonolites (open circles) do not fall within the oxidation range. These rocks are characterised by low concentration of opaque minerals (>1%); the ferromagnesian minerals aegerine, barkevikite and anegmatite are present. Since these rocks show a low optical state of

oxidation (80% are index I) the rock reflects the initial moderately high ferric iron content of the magma. This contrasts with the remaining rocks in the series and also with the single lava example, where deuteric and post-crystallization oxidation has been active.

There is one further point of interest in these rocks. Those samples which contain titanomaghemite (full squares), but otherwise in class I (i.e. there are no "exsolution" lamellae of ilmenite), form a separate and distinct range in chemical oxidation. This range is higher than those samples which contain only homogeneous titanomagnetite and homogeneous ilmenite.

It is apparent from these chemical plots that sub-solidus oxidation is only weakly reflected in the Fe_2O_3:FeO ratio, and further, that the relationship is not linear.

In summary, the texturally-defined paragenetic sequence for the progressive oxidation of titanomagnetite and ilmenite is supported by the fact that the secondary minerals are oxidation products, by sub-solidus and pseudomorphic oxidation experiments and finally by chemical analyses on whole rock samples.

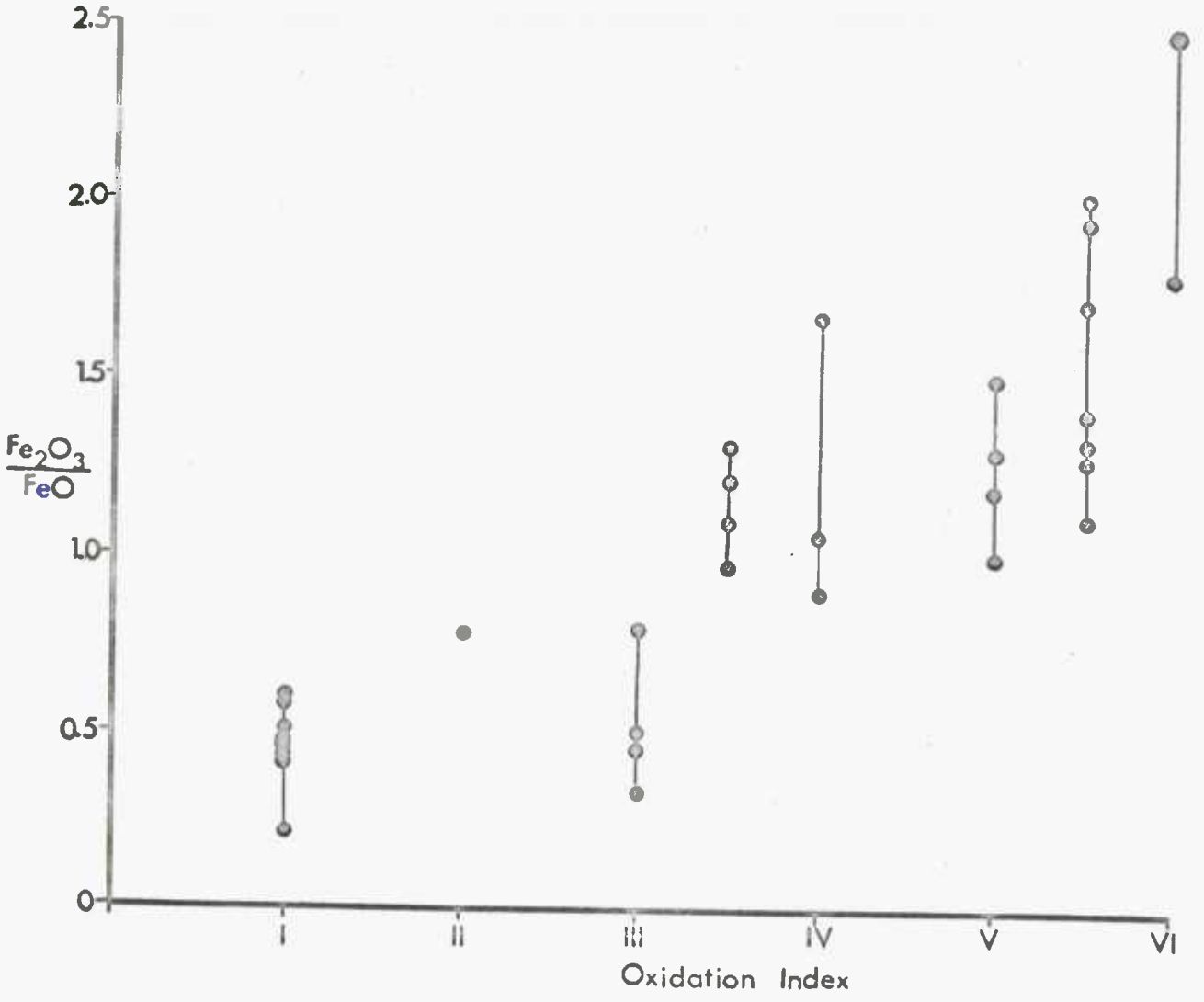

Fig 14.1

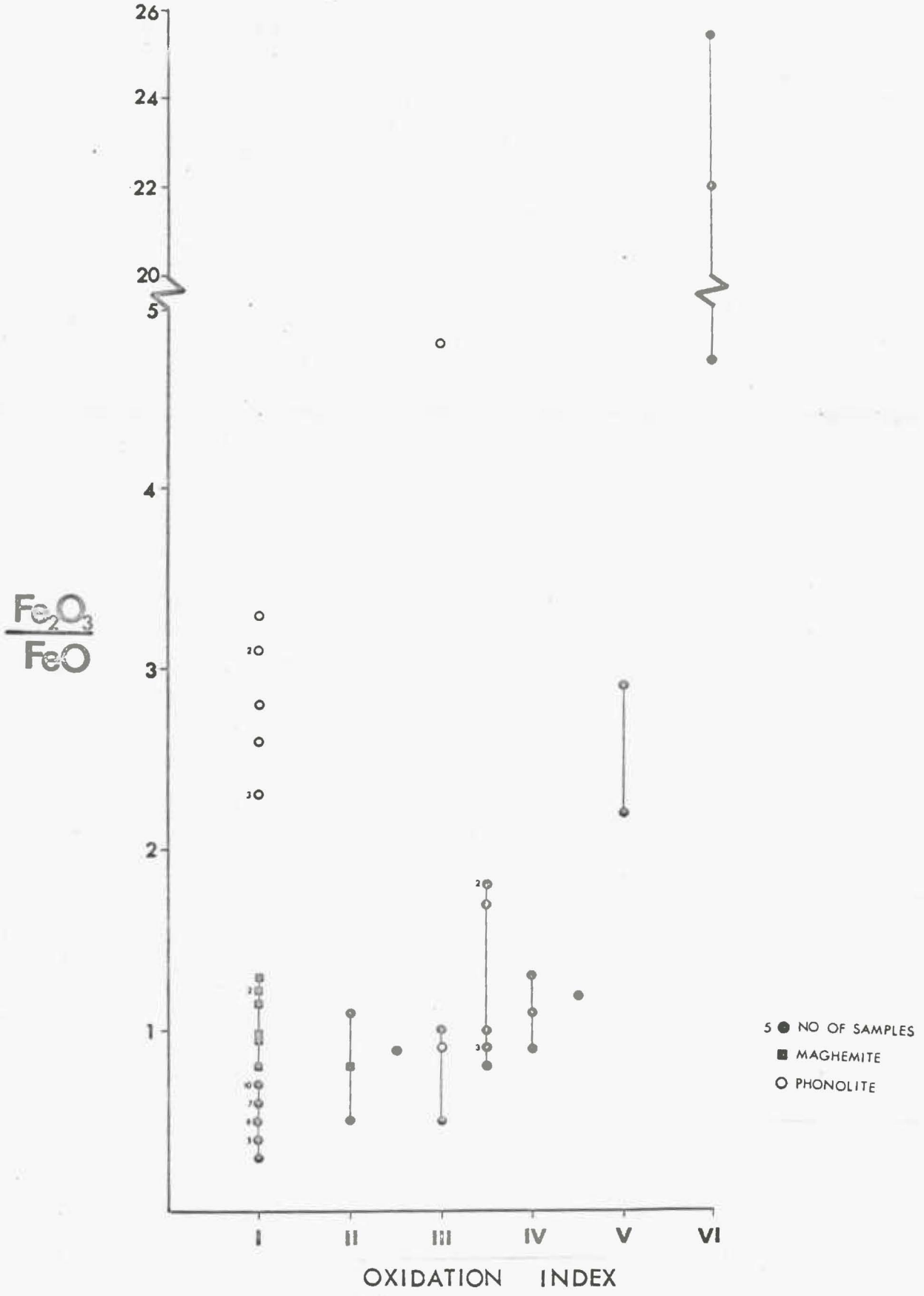
26
24
22
20
5
4
3
2
1
$\frac{Fe_2O_3}{FeO}$
I
II
III
IV
V
VI
OXIDATION INDEX
5 NO OF SAMPLES
MAGHEMITE
PHONOLITE

Fig 14·2

CHAPTER 15

THE OLIVINE-RICH BASALT

15.1 General Features

The lava occurs at an altitude of 35m. above sea level on the north side of Hamersfjordur, 7km west of Djupivogur. It is 11m. in thickness and is laterally exposed for approximately 0.75km.

Two vertical profiles were obtained from the lava. In profile S, 35 geographically oriented cores were drilled with an average sample spacing of 25cm. In profile MS a total of 62 unoriented cores were obtained and the sample density was almost twice as great. The profiles are 110m. apart.

The lava occurs in a clean-out glacial valley. It has a massive appearance in the field with narrow, vesicular upper and lower contact zones. It is underlain and overlain by 1-1.5m. thick acid vitric tuff beds. The underlying tuff is friable, well banded and green in colour away from the lava contact. Approaching the contact it is reddened and solidly baked. The upper tuff is welded and is whitish-grey in colour.

The lava is not jointed and there are no exposed dykes in the vicinity.

15.2 Petrography

The flow is a typical coarse grained olivine basalt. It contains large (2-3mm) euhedral plagioclase phenocrysts which are set in a finer grained groundmass of feldspar, olivine, some pyroxene, and iron-titanium oxides. The texture may be described as intergranular.

The feldspar phenocrysts are incipiently replaced along finecracks to a secondary mica. The distribution of this type of alteration is restricted to the margins of the flow and is more strongly developed at the base than at the top of the flow. The olivines are also altered. The type of alteration and the distribution of the alteration products is ideally dealt with in the following section as the phases are opaque.

The base of the flow and the uppermost part of the flow are highly vesicular. The base is characterized by amygdaloidal inclusions of zeolite and fibrous rosettes of pale green chlorite. This zone varies from 10 to 30 cm. in thickness.

From a thin section point of view, no systematic variations occur throughout the thickness of the flow. This feature has been confirmed in two separate examinations by

Drs. G. BORLEY and I. BAKER.

15.3 Reflection Microscopy

The iron-titanium oxides form approximately 8% of the total, by volume. This concentration does not vary throughout the depth of the lava, but the ratio of primary titanomagnetite: primary ilmenite varies between 0.54 and 0.89. There is no systematic distribution or preferential concentration of one or other of the primary phases throughout the flow.

Ilmenite and titanomagnetite occur in two generations; the larger crystals are 70-100u across and the smaller crystals are in the 1-5u range. Titanomagnetite crystals are anhedral and ilmenite is generally euhedral to subhedral in form. The base of the flow is characterised by fine grained (1-10u) skeletal titanomagnetite and ilmenite. The grain size of the opaque minerals is surprisinglyuniform throughout, the exception being in the chilled lower edge.

15.4 Oxidation Classification

Polished sections (2.5cm. in diameter) from both traverses have been classified according to the titanomagnetite-ilmenite oxidation scheme. The results are presented in Table 15.1. In Figure 15.1 the index of oxidation is plotted as a function of depth within the lava; the two

profiles are plotted separately. Titanomagnetite and ilmenite "oxidation numbers" have also been determined on the cores from profile S by point count analysis. These values are listed in Table 15.1, and their relationship is shown in Figure 15.2.

The immediate results that arise from the plots in Figure 15.1 are as follows:

(i) the state of oxidation is not constant throughout the flow.

(ii) the maximum state of oxidation does not occur at the edges of the flow.

(iii) there is a general similarity between the oxidation profiles but the peaks are of varying thickness and are slightly displaced.

All six types of optically-defined oxidation assemblages occur in both traverses. The sub-solidus oxidation group (I-III) is made up of 57% of the total number of specimens and the pseudomorphic oxidation group (IV-VI) makes up the remainder.

Of the samples classified in the I-III range, 95% were found to contain titanomaghemite or amorphous Fe-Ti

oxide, replacing titanomagnetite. The degree of replacement within any one sample is relatively small and a qualitative estimate of its distribution within the flow suggests that it is concentrated towards the lower part of the flow. Discrete ilmenite in these specimens remains completely unaltered.

The maximum state of oxidation is represented by the pseudobrookite class. The presence and importance of pseudobrookite as an indicator of high temperature alteration has been stressed. This class occurs in a narrow-zone at the base of each traverse and at a point within the traverse.

With regard to the Fe-Ti oxides at the base of the lava they are fine grained (1-5u range) and skeletal. The state of oxidation is highly variable and although the specimens have been classified as index VI, because pseudobrookite is present, it is none the less possible that the assemblage is below the defined 80% level. Its extremely fine grain-size precludes an accurate estimate of its concentration and from a practical point of view it is impossible, on this scale, to distinguish highly oxidized pseudomorphs after ilmenite from highly oxidized pseudomorphs after titanomagnetite.

The second pseudobrookite zone occurs at 2.5m above the base of profile S and at 4.6m above the base of profile MS.

The profile S zone is represented by only one specimen (S-15). The second profile (MS) was drilled after profile S had been magnetically and petrologically analysed. The "anomalous" high oxidation zone towards the centre of the flow was densely sampled in order to define it vertically and in order to prove its continuity laterally within the flow. This high oxidation zone was easily detected in the field; the drilling mud was distinctly red, in contrast to the grey-brown colour of the unoxidized zones.

In both traverses the central zone of high oxidation is flanked, on both sides, by specimens classified as V or V/VI. The concentration of pseudobrookite-titanohematite pseudomorphs gradually increases to a maximum as the zone is approached. This peak is somewhat better defined in profile MS than in profile S. In profile S once the central zone has been reached, from the base of the flow, it then gradually tapers off towards the top of the lava. This contrasts with profile M3 where the cut-off is relatively sharp and within one or two samples the oxidation class jumps from a predominent index VI assemblage to an index III or III/IV assemblage. Other cases of equally sudden jumps occur at different positions in the flow over distances as small as 25 cm.

The pseudobrookite zone gives way to the class V assemblage rutile + titanohematite; some incipient pseudobrookite may nevertheless also be present. This zone has a thickness of 3m in profile S and is less than 1m thick in profile MS. It is apparent from the plots (Figure 15.1) that this difference in thickness essentially controls the form and shape of the oxidation profiles; in the one case the high oxidation zone is symetrical and is relatively sharply defined (MS) and in the other (S) the zone is assymetrical and is gradually approached.

One final point needs to be made with reference to the two oxidation profiles. The uppermost samples in traverse S are classified as index III whereas the corresponding MS zone consists of samples with variable oxidation indices ranging from I to V. No plausible explanation can be offered to account for this variation.

The silicates in the highly oxidized samples appear intensely red when viewed under an oil immersion objective. Olivine is the chief silicate which is altered. The type of alteration product that develops in association with the highly oxidized discrete opaque phases has been fully described in Chapter 13. To summerise these results, magnetite or hematite may develop directly from olivine; the magnetite

may subsequently be oxidized to hematite. It has been shown in a series of oxidation heating experiments that magnetite is only produced at temperatures above 820°C. In the Icelandic lavas the production of magnetite (and derived hematite) in olivine, is very definitely associated with the formation of pseudobrookite in titanomagnetite and ilmenite; hematite, on the other hand, is more generally associated with the class V zones which are characterised by the assemblage rutile + titanohematite.

The secondary production of iron oxides in ferromagnesian silicates has now become important in terms of the magnetic properties of the rock. A quantitative estimate of its concentration is therefore desirable if any significance is to be attached to magnetic-petrological correlations. Unfortunately, serious difficulties are encountered in determining the mineral concentration of the secondary assemblage. The photomicrographs (Plates 13.1 - 13.10) clearly demonstrate the ultra-fine nature of the intergrowths and the Plates show further, that the development of magnetite and hematite is highly variable within single crystals of olivine; the ratio of oxidized to unoxidized magnetite is equally variable. When these highly oxidized samples are viewed in thin-section, the olivines appear as "spongy" opaque phases and so it is difficult to be absolutely sure whether the grain under observation is an oxidized

olivine or whether it is a primary poikilitic phase. Similar difficulties arise in the polished section examination where it is almost impossible to distinguish an unaltered olivine from any other silicate. Point-counting and area distribution analyses are therefore impracticable. An indirect estimate of the concentration of secondary magnetite in olivine is however reflected in the concentration of pseudobrookite. Qualitatively this feature is immediately apparent when highly oxidized samplesare viewed in polished section. The distribution profile of pseudobrookite is therefore considered to reflect the approximate distribution of magnetite in olivine.

A detailed analysis of the distribution of pseudobrookite has therefore been made in profile S. This has taken two forms. In the first, class VI pseudomorphs after titanomagnetite have been determined as a percentage of the titanomagnetite concentration, and in the second, Stage 6 (incipient pseudobrookite) and Stage 7 (pseudobrookite pseudomorphs) discrete ilmenite oxidation classes have also been determined, as a percentage of the discrete ilmenite concentration. The results of the three plots are presented in Figure 15.3; the numerical data is abstracted from Table 15.1. There is a striking similarity in the shape of the curves. The lower part of the curve is sharply defined where pseudobrookite is

suddenly generated over a distance of 50 cm. The uppermost part of the curve is gently sloping and reflects the shape of the oxidation profile shown in Figure 15.1. The influx of pseudobrookite in two samples, 7.5m above the base of the lava is supported by the development of magnetite in olivine and is also apparent in the profile produced from the general classification. The distribution of pseudobrookite after original titanomagnetite and discrete ilmenite therefore defines the high central-oxidation zone, it confirms the shape of the profile derived from the general classification, and, in addition, reflects the distribution of magnetite in olivine. These features have also been found in other lavas and their true significance will become apparent when the magnetic properties are discussed.

16.5 Chemical Analyses

FeO, Fe_2O_3 and TiO_2 contents of whole rock samples from traverse S have been determined by conventional wet chemical analysis. The results are presented in Table 15.2. Total iron and titanium do not vary throughout the flow but there are significant systematic variations in the ratio Fe_2O_3:FeO. Values of this ratio are reflected in the opaque mineralogy and the relationship has been shown in Figure 14.1. This relationship is presented again in Figure 15.4, not as

a function of the oxidation index but as a function of the more refined magnetite oxidation number. A good correlation exists between these two parameters. Clearly, this relationship is due to the fact that a large part of the total iron is contained in the opaque minerals. The oxidation variation of whole rock samples is, therefore, adequately defined by an examination of the state of oxidation of the Fe-Ti oxides.

15.6 Magnetic Properties

The magnetic properties of this lava have been fully described by WATKINS (WATKINS and HAGGERTY 1965; 1967) and the results will only be briefly summarised here.

The direction and intensity of magnetization of all cores from both traverses were measured using an astatic magnetometer.

The intensity of magnetization in all samples from both traverses are shown separately in Figure 15.5 a-b. The intensity of magnetization is highly variable throughout the flow. It varies in traverse S from 0.27×10^{-3} emu/g to 12.85×10^{-3} emu/g and reaches a maximum at 2.45 m above the base of the flow; the corresponding range in traverse MS is 0.18×10^{-3} emu/g to 9.68×10^{-3} emu/g and the maximum value is at a distance of 5 m from the base of the lava.

The directions of the original natural remanent magnetism (NRM) in the oriented cores (traverse S only) are shown in Figure 15.6. A close grouping of directions exists, but several directions are well removed from the mean direction. Three examples of the treatment in alternating magnetic fields of specimens with NRM directions outside the main group are presented in Figure 15.7, showing clearly the removal of unstable components, as indicated in the movement of the NRM directions towards the main group direction, by step demagnetization. Unstable components of NRM are those which have been added since the initial cooling of the lava, and hence result in directions of NRM frequently quite different from the original NRM direction. Figure 15.8 shows the NRM directions of all the oriented cores following the removal of unstable magnetic components by treatment in high alternating magnetic fields. A close grouping of the directions results, and the lava is reversely magnetized.

The magnetic intensities from traverse S may be divided into two groups, those with values higher than 2.5×10^{-3} emu/g and others with values less than 2.5×10^{-3} emu/g. These two groups are plotted in Figure 15.9. The specimens possessing higher magnetic intensities have closely grouped NRM directions, whereas those specimens with relatively low intensities

of magnetization have scattered NRM directions. This variation is not a function of the sensitivity of the astatic magnetiometer but, as will be shown in the following section, is directly related to the mineralogy.

The magnetic stability of a sample is a difficult parameter to quantify but one method by which this may be illustrated is shown in Figure 15.10. Higher alternating magnetic fields are required to demagnetize magnetically-"hard" specimens whereas correspondingly lower fields are required to demagnetize magnetically-"soft" specimens. Magnetically-"hard" specimens may be regarded as specimens which show the greatest magnetic stability and it is these specimens which reflect the original TRM direction. Figure 15.10 shows the magnitude of the maximum alternating magnetic field (H) required to reduce the original intensity of magnetization (Jn) by 10% of its initial value. In other words, specimens with high values of H(0.9 Jn) are magnetically stable and specimens with low values (magnetically-"soft") are relatively unstable. The shape of the profile, with slight modifications, is very similar to the intensity profile shown in Figure 15.5 a.

15.7 Correlation between Magnetic Properties and Oxidation State

Examination of Figure 15.1 and Figure 15.5 reveals the

close relationship between the oxidation state of the lava, defined by the opaque mineralogy, and the intensity of magnetization. This point is more precisely illustrated in Figures 15.11 and 15.12 where the intensity is plotted, in the first instance, as a function of the optical oxidation index, and in the second as a function of the chemical oxidation index.

The resemblance between the two intensity profiles and the two oxidation profiles throughout the lava is quite remarkable. At first sight this relationship would appear to be completely anomalous in view of the fact that the highly oxidized samples are characterized by pseudobrookite, rutile and titanohematite, which, at ordinary temperatures, are considered to be only weakly magnetic (NAGATA 1961). The relationship between the production of secondary magnetite in olivine and the formation of pseudobrookite in the Fe-Ti oxides has been noted. This secondary magnetite would therefore appear to be the chief source of the magnetic moment, a feature which has been demonstrated experimentally by WILSON and RIDING (pers. comm 1967). By plotting the percentage of pseudobrookite (+ titanohematite) pseudomorphs after titanomagnetite (Ox. Index VI) as a function of the intensity of magnetization (Figure 15.13) it is clear that there is a good correlation between the two parameters and that the

relationship is almost linear. An interesting feature of this plot, from the point of view of olivine alteration, is that there are three values (marked H) which show a slightly steeper gradient than the general trend; these samples have less than 10% Class VI pseudomorphs and in addition show a predominance of hematite, rather than magnetite, as the chief olivine oxidation product (the Fe-Ti oxides are classified as Class V - rutile plus titanohematite).

A measure of the magnetic stability H(0.9 Jn), as a function of the oxidation index is shown in Figure 15.14. A considerable spread of the values within each of the oxidation indices exists but there is nevertheless a systematic increase in stability with increasing oxidation. Grain size is known to be the most significant single mineralogical factor which contributes to the overall magnetic stability of a rock but it has already been stressed that, except for two narrow zones at the edges of the flow, there is very little variation in the grainsize of the Fe-Ti oxides. Oxidation may also induce stability in an indirect way. LARSON et.al (1966) have suggested that the formation of ilmenite lamellae in large titanomagnetite grains effectively sub-divides the large grain into a large number of smaller grains, the net effect is that the grain now has a more stable magnetic moment. The maximum number of lamellae are

produced in clase III grains so that these samples may be expected to be more stable than any of the others, but this is not the case. Once again since the high intensity specimens are the more stable specimens the source of this increased stability seems most likely to be due to the ultrafine nature of the secondary symplectic magnetite, which is produced in highly oxidized olivine. The stability of the magnetic properties increases as the grainsize approaches single magnetic domain size. In the case of symplectic magnetite the grainsize is often of the order of 1 micron or less, which is close to the size of a single domain.

The magnetic susceptibility has also been determined on these samples but it does not appear to be directly dependent on the state of oxidation of the Fe-Ti oxides.

The Koenigsberger Q-Ratio ($Q = \frac{Jn}{X.H}$; where Jn = Intensity of magnetization, X = Susceptibility, H = Strength of the Earth's magnetic field = 0.51 oersteds) shows a reasonably good correlation with the oxidation index (Figure 15.15). This relationship is to be expected and one can see that the shape of the curve is similar to the relationship Jn versus oxidation index (Figure 15.12).

15.8 Conclusions

The following conclusions may be drawn from a study of this olivine basalt (traverse S and MS):

(a) the state of oxidation is highly variable throughout vertical traverses in the basalt.

(b) the maximum state of oxidation reached, occurs towards the central part of the basalt.

(c) the oxidation state of the Fe-Ti oxides, defined optically in polished section on a scale of indices I-VI, is reflected in whole rock chemical analyses.

(d) intergration of the polished section analysis with the magnetic data results in the following strong correlations:

i) Unoxidized zones in the lava are magnetically unstable and possess relatively low intensities of magnetization.

ii) Oxidized zones in the lava have a relatively much higher intensity of magnetization and are magnetically more stable.

(e) The relative increases in intensity of magnetization and magnetic stability in highly oxidized samples are considered to be due

to ultra-fine, secondary symplectic magnetite, which is produced in strongly oxidized olivine.

TABLE 15.1

Sample No.	% Oxidation Index I	II	III	IV	V	VI	VII	Titanomagnetite Ox.No.	Titanomagnetite % Conc.	Ilmenite Ox. No.	Ilmenite % Conc	Chemical analyses TiO_2	Total Fe.	Fe_2O_3: FeO
I 1 M	Fine grained and skeletal											1.94	11.53	0.80
I 2 M	100									1.00	53.16	1.94	11.13	1.36
	19. 4	9. 7	22. 6	48. 3				2.99	46.84					
I 3 M	100									1.00	50.23	2.05	11.05	1.05
	27. 3	15. 2	57. 5					2.30	49.77					
I 4 M	100									1.00	52.32	1.91	11.00	0.75
	31. 0	20. 7	48. 3					2.17	47.68					
I 5 M	100									1.00	51.37	1.86	11.13	0.46
	25. 0	18. 2	56. 8					2.31	48.63					
I 6 M	100									1.00	49.45	2.00	11.48	0.51
	83. 8	6. 7	10. 0					1.26	50.55					
I 7 M	100									1.00	50.21	2.08	11.29	0.48
	98.0	0. 9	1. 1					1.03	49.79					
I 8 M	100									1.00	52.28	1.94	11.58	0.41
	97.0	2. 0	2. 0					1.04	47.72					

CONT.

TABLE 15.1.

Sample No.	% Oxidation Index I	II	III	IV	V	VI	VII	Titanomagnetite Ox.No.	Titanomagnetite % Conc.	Ilmenite Ox. No.	Ilmenite % Conc	Chemical analyses TiO_2	Total Fe.	Fe_2O_3:FeO
I 9	100									1.00	53.43	2.00	11.29	0.41
M	98. 0	2. 0						1.04	46.57					
I 10	100									1.00	52.31	2.02	11.28	0.43
M	100							1.00	47.69					
I 11	100											1.76	10.58	0.22
M	36.67	63.33												
I 12	6.17	9.26	15.43	7.41	1.85	14.20	45.68			5.14	54.00	1.93	10.89	1.51
M			3.62	25.36	44.93	26.09		4.93	46.00					
I 13	1.54	9.74	21.54	1.54	1.54	9.74	54.36			5.38	55.87	2.17	11.21	1.33
M				20.13	33.12	46.75		5.26	44.13					
I 14		2.65	5.96		6.61	13.91	76.82			6.77	50.17	1.14	11.01	1.82
M					6.00	36.67	57.33	5.51	49.83					
I 15		2.19	2.92		0.73	12.41	81.75			6.64	45.67	2.05	11.42	2.50
M				13.50	27.61	58.89		5.45	54.33					
I 16		0.55	25.82		1.10	19.78	52.75			5.72	54.17	1.85	10.93	1.24
M			0.65	15.58	44.81	38.96		5.22	45.83					

TABLE 15.1 CONT.

Sample No.	% Oxidation Index I	II	III	IV	V	VI	VII	Titanomagnetite Ox.No.	Titanomagnetite % Conc.	Ilmenite Ox. No.	Ilmenite % Conc	Chemical analyses TiO_2	Chemical analyses total Fe.	Chemical analyses Fe_2O_3: FeO
I 17	0.57	1.71	20.57	2.86	0.57	18.86	54.86			5.77	51.02	1.89	10.83	1.43
M				17.26	41.07	41.67		5.24	48.98					
I 18	5.71	11.43	25.72	1.14		16.00	40.00			4.86	51.47	1.13	11.05	1.15
M			1.21	3.09	31.52	36.36		5.03	48.53					
I 19	0.49	2.45	25.98	3.43	1.96	12.26	53.43			5.54	53.97	2.16	11.20	2.03
M			0.57	13.79	42.53	43.11		5.28	46.03					
I 20	9.52	13.33	29.05	2.38	1.43	11.43	32.86			4.38	52.37	1.95	11.48	1.67
M			2.62	25.13	43.46	28.79		4.98	47.63					
I 21		1.15	40.46	3.47	1.73	15.62	37.57			5.03	52.42	1.96	11.10	1.94
M								5.25	47.58					
I 22		5.88	42.48	7.85	1.96	17.65	24.18			4.56	50.83	2.06	10.59	1.34
M								5.11	49.17					
I 23	7.11	20.38	42.18	5.69	21.80	2.37	0.47			3.24	63.75	2.12	11.26	0.97
M			30.83	40.00	27.50	1.67		4.00	36.25					
I 24	0.97	11.11	56.52	5.79	12.08	6.28	7.25			3.65	61.24	2.06	11.04	1.04
M			18.32	25.19	49.62	6.87		4.45	38.76					

CONT. TABLE 15.1.

Sample No.	% Oxidation Index I	II	III	IV	V	VI	VII	Titanomagnetite Ox.No.	Titanomagnetite % Conc.	Ilmenite Ox. No.	Ilmenite % Conc	Chemical analyses TiO_2	Total Fe.	Fe_2O_3: FeO
I 25	4.27	20.51	48.72	5.98	16.67	3.42	0.43			3.22	61.74	1.96	11.14	1.28
M			29.66	41.39	28.26	0.69		4.00	38.26					
I 26	98.46	1.54								1.02	64.68	1.97	11.18	0.82
M	28.17	40.84	26.76	4.23				2.07	35.32					
I 27	99.34	0.66								1.01	59.60	2.03	11.04	0.41
M	79.21	20.79						1.21	40.40					
I 28	38.50	9.62	29.95	1.07	3.21	3.74	13.91			2.88	56.33	1.85	11.21	1.07
M			23.45	19.31	44.14	13.10		4.47	43.67					
I 29	44.65	13.84	18.87		3.14	11.32	8.18			2.70	51.13	1.88	10.88	1.20
M		1.32	42.10	6.58	39.47	10.53		4.17	48.87					
I 30	100									1.00	65.79	1.98	10.95	0.61
M	31.73	52.88	15.39					2.15	34.21					
I 31	100									1.00	63.69	2.17	11.20	0.41
M	23.85	60.77	15.38						36.31					
I 32	95.04	1.49	3.47							1.08	66.67	2.04	11.07	0.51
M	12.87	30.69	49.51	6.93				2.50	33.33					

CONT. TABLE 15.1

Sample No.	% Oxidation Index I	II	III	IV	V	VI	VII	Titanomagnetite Ox.No.	Titanomagnetite % Conc.	Ilmenite Ox. No.	Ilmenite % Conc	Chemical analyses TiO_2	Total Fe.	Fe_2O_3: FeO
I 33	94.92	5.08								1.05	63.21	2.01	11.27	0.41
M	12.08	22.15	56.38	9.39				2.63	36.79					
I 34	94.92	5.08								1.02	59.44	2.02	11.36	0.34
M	12.08	22.15	56.38	9.39				2.59	40.56					
I 35	100									1.00	58.09	1.96	10.95	0.82
M		23.49	74.24	2.27				2.79	44.91					

Table 15.1.

Lava S: Mineralogical and Chemical Data.
The oxidation classification for titanomagnetite is based on the I - VI system (page 275); ilmenite is on the I - VII system (page 45).

Lava.S Sample No.	Position(m)	H öe for 0.9J	$Jx10^{-3}$ emu/g	Q. Factor	Susceptibility $X \times 10^{-5}$ emu/g.oer
35	11.10	110	2.04	2.73	1.46
34	10.75	75	1.67	2.27	1.44
32	10.05	95	1.24	1.71	1.42
31	9.65	82	0.59	0.68	1.70
30	9.15	110	0.39	0.54	1.43
29	8.65	92	4.85	5.61	1.70
28	8.20	130	4.48	5.61	1.56
27	7.75	10	0.78	0.93	1.65
26	7.05	40	0.78	1.00	1.52
25	6.30	165	4.68	5.94	1.55
24	6.05	150	6.14	7.73	1.56
23	5.70	120	5.32	7.32	1.43
22	4.80	210	7.02	9.20	1.50
21	4.45	165	7.88	10.30	1.50
20	3.85	135	6.00	0.15	1.92
19	3.35	110	9.57	11.30	1.68
18	3.25	155	7.59	8.99	1.68
17	300	165	8.46	10.90	1.52
15	2.55	205	12.85	16.50	1.53
14	2.40	215	11.79	16.60	1.39
13	2.20	175	6.88	7.63	1.77
12	2.05	155	7.12	8.23	1.70
11	1.72	8	1.16	1.15	2.00
10	1.61	10	0.57	0.51	2.20
9	1.47	25	0.42	0.38	2.16
8	1.40	85	0.27	0.25	2.12
7	1.30	10	0.56	0.43	2.56
6	1.25	15	0.57	0.75	1.48
5	1.11	85	1.32	1.45	1.79
4	0.79	140	1.03	1.13	1.79
3	0.30		1.24	4.06	0.60
2	0.40		4.12	6.42	1.26
1	0.17		1.58	3.04	1.02

Lava traverse S showing the position of samples within the vertical profile and some of the derived magnetic data.

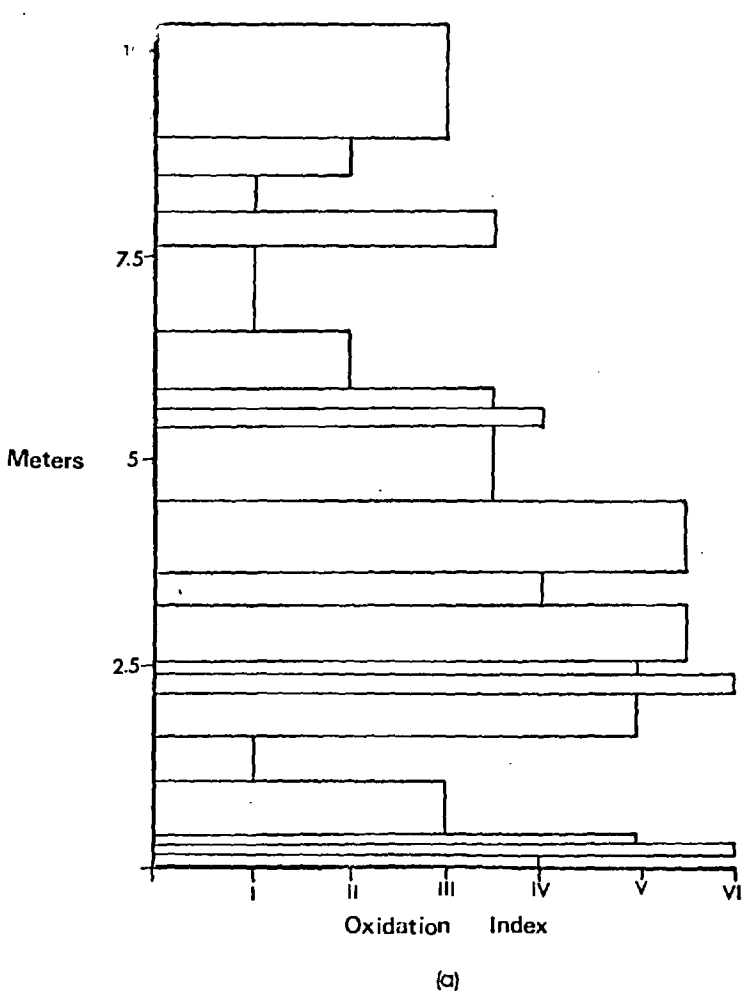
Meters
10
7.5
5
2.5
I
II
III
IV
V
VI
Oxidation Index

(a)

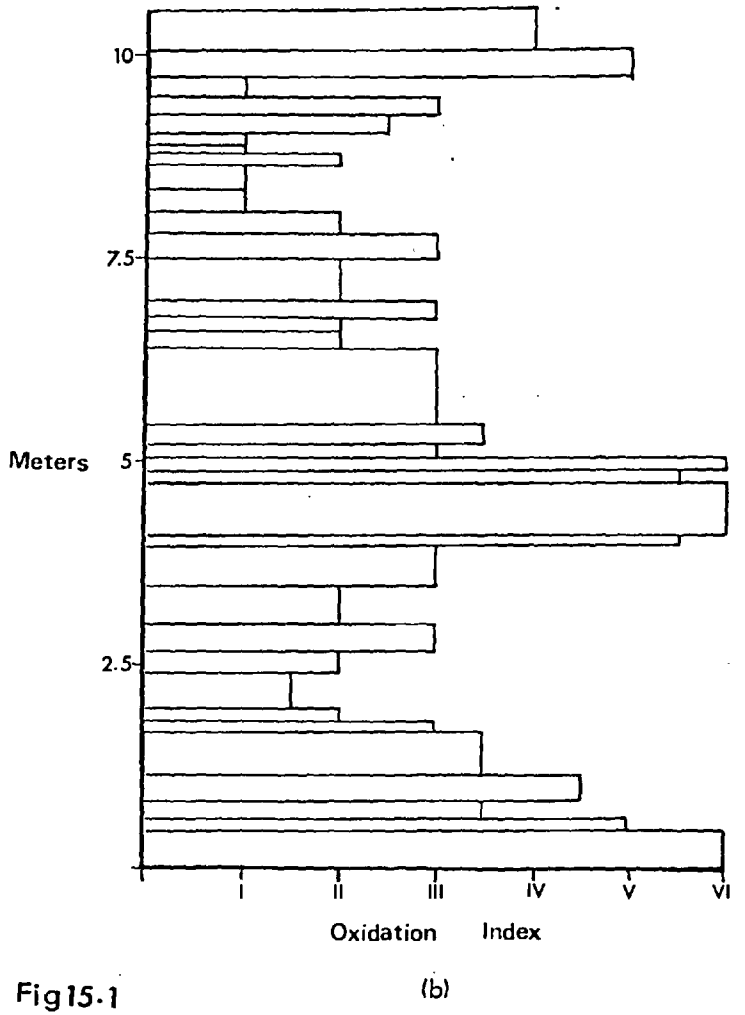
Meters
10
7.5
5
2.5
I
II
III
IV
V
VI
Oxidation Index

(b)

Fig 15.1

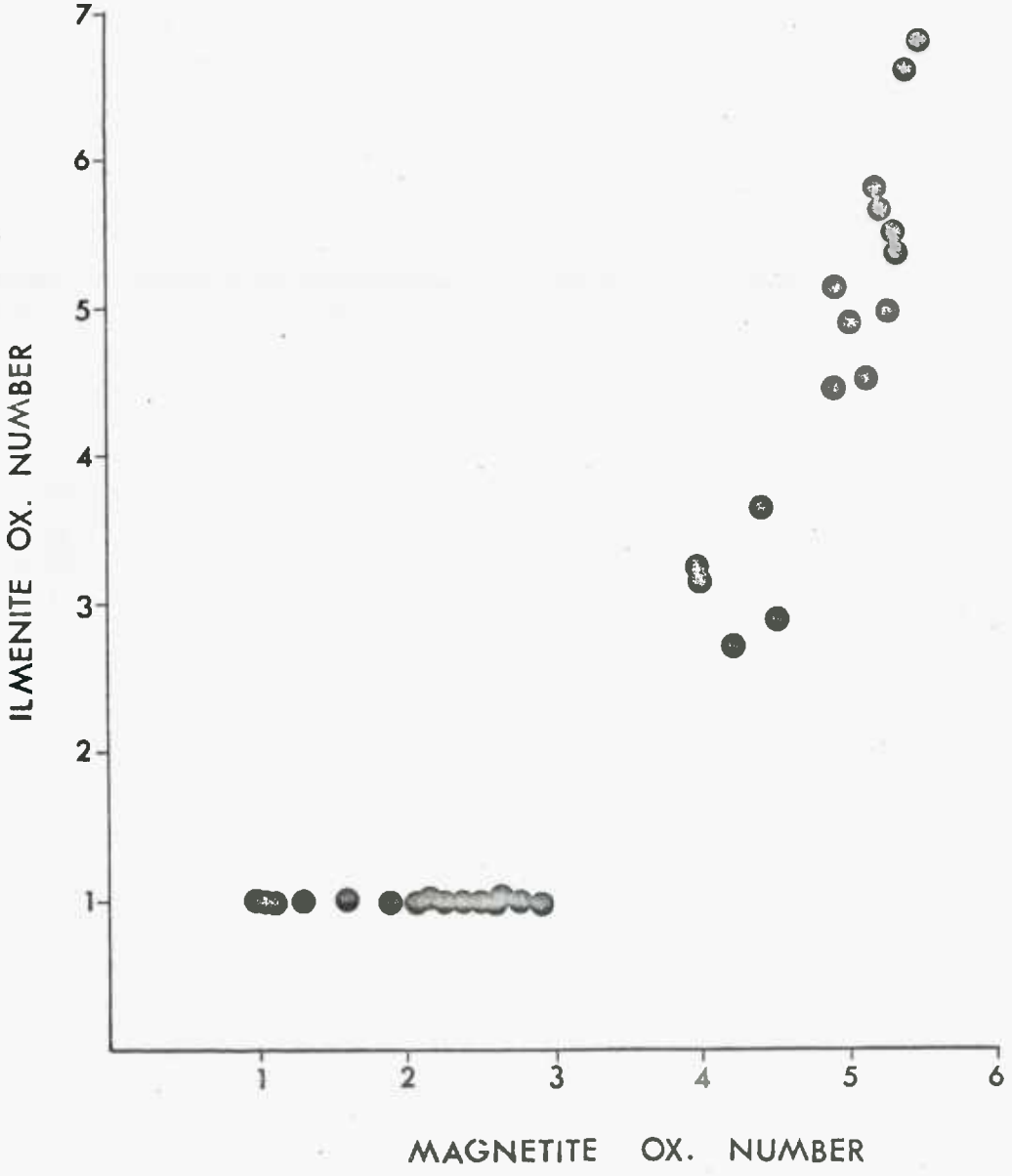

Fig 15·2

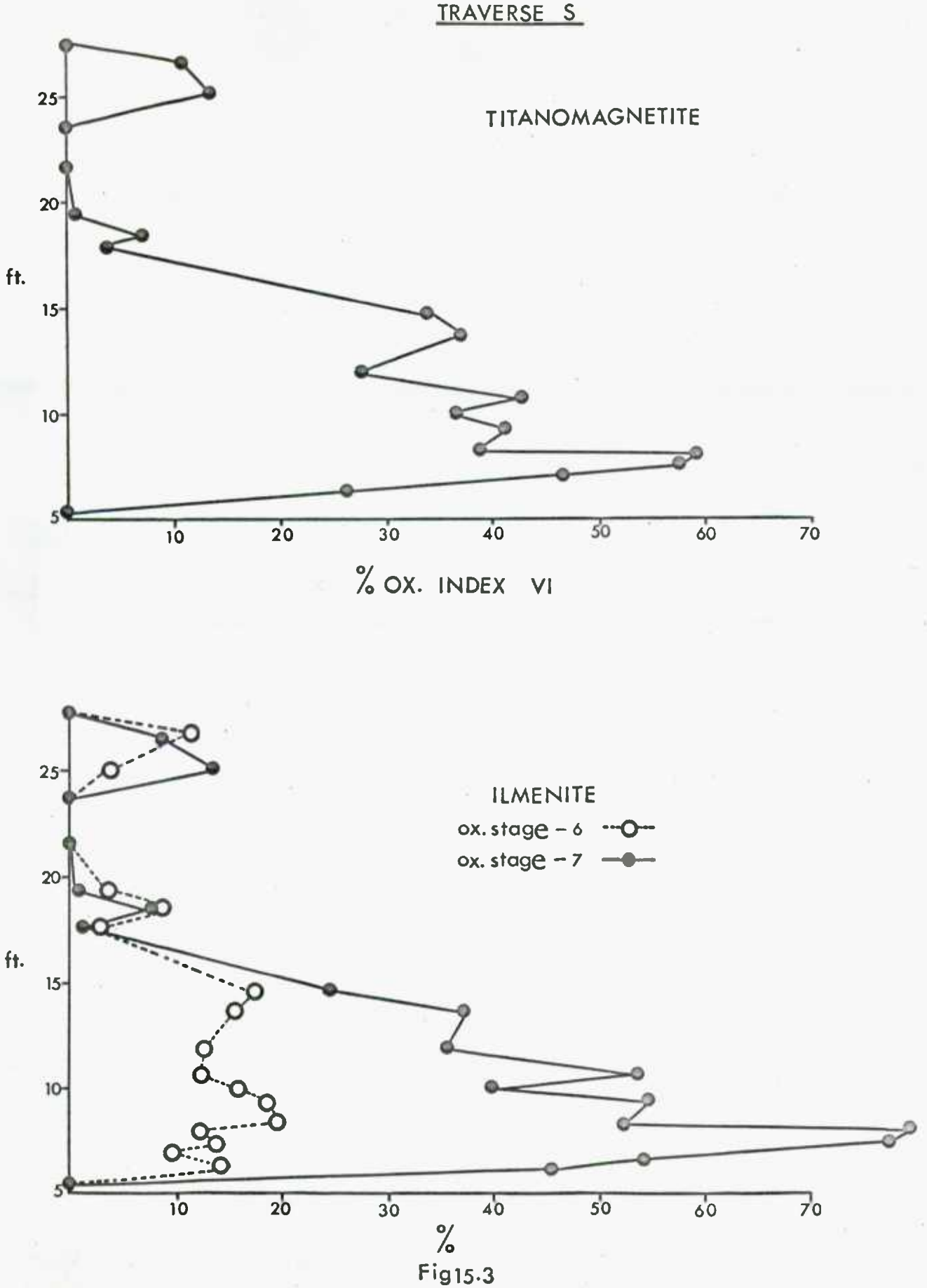
TRAVERSE S
TITANOMAGNETITE
ft.
25
20
15
10
5
10
20
30
40
50
60
70
% OX. INDEX VI
ILMENITE
ox. stage – 6
ox. stage – 7
ft.
25
20
15
10
5
10
20
30
40
50
60
70
%

Fig15.3

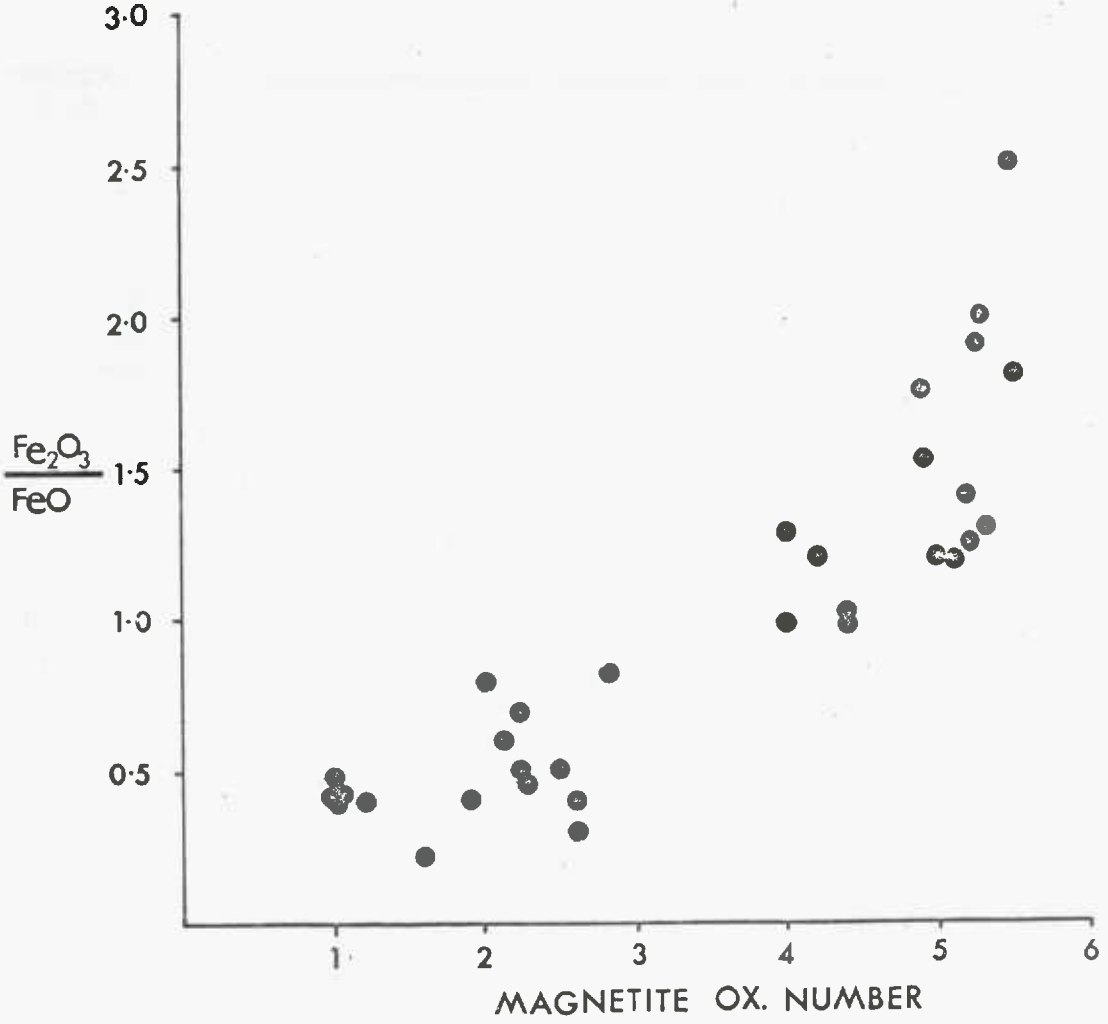

Fig 15.4

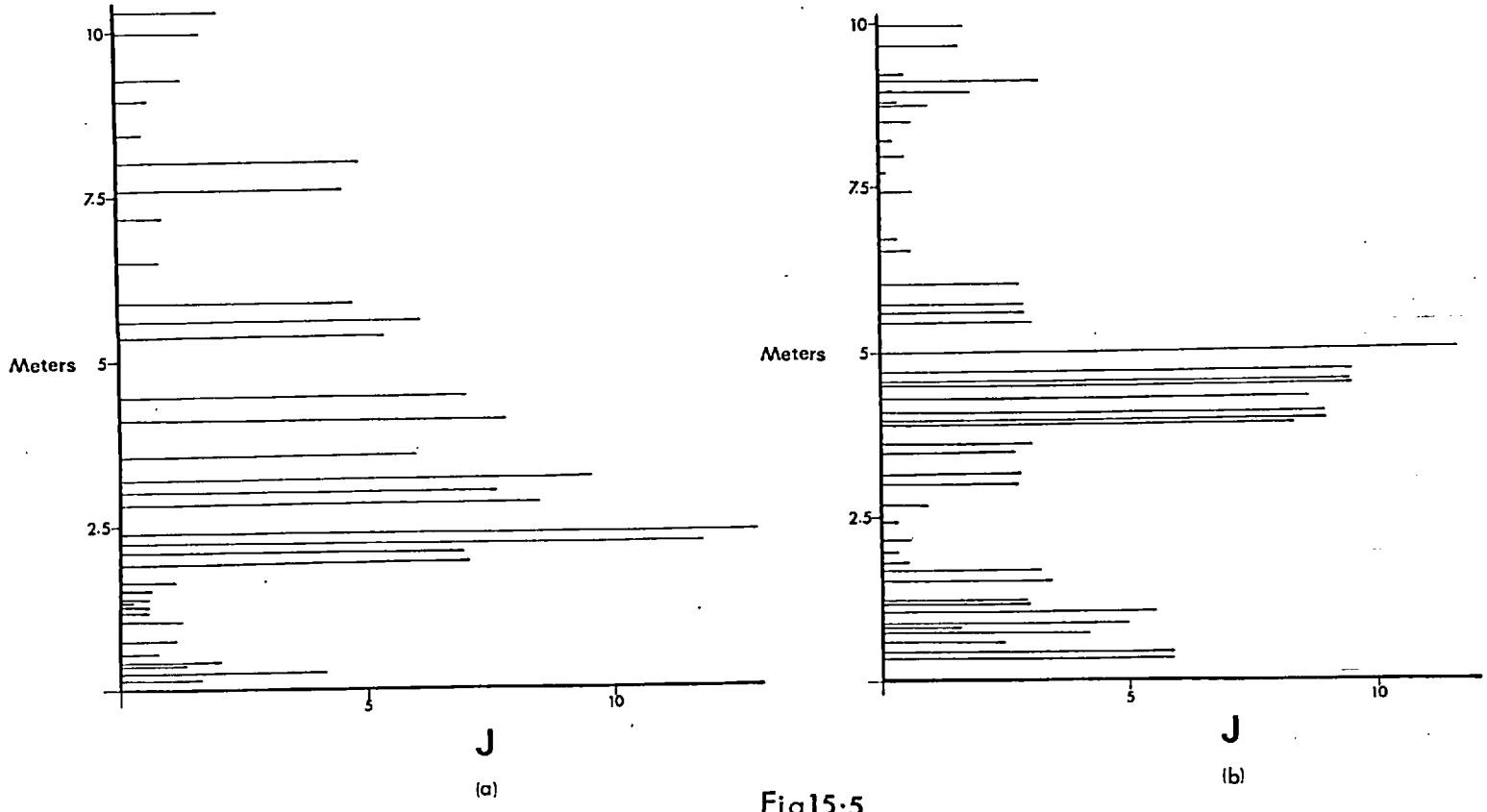

Fig15·5

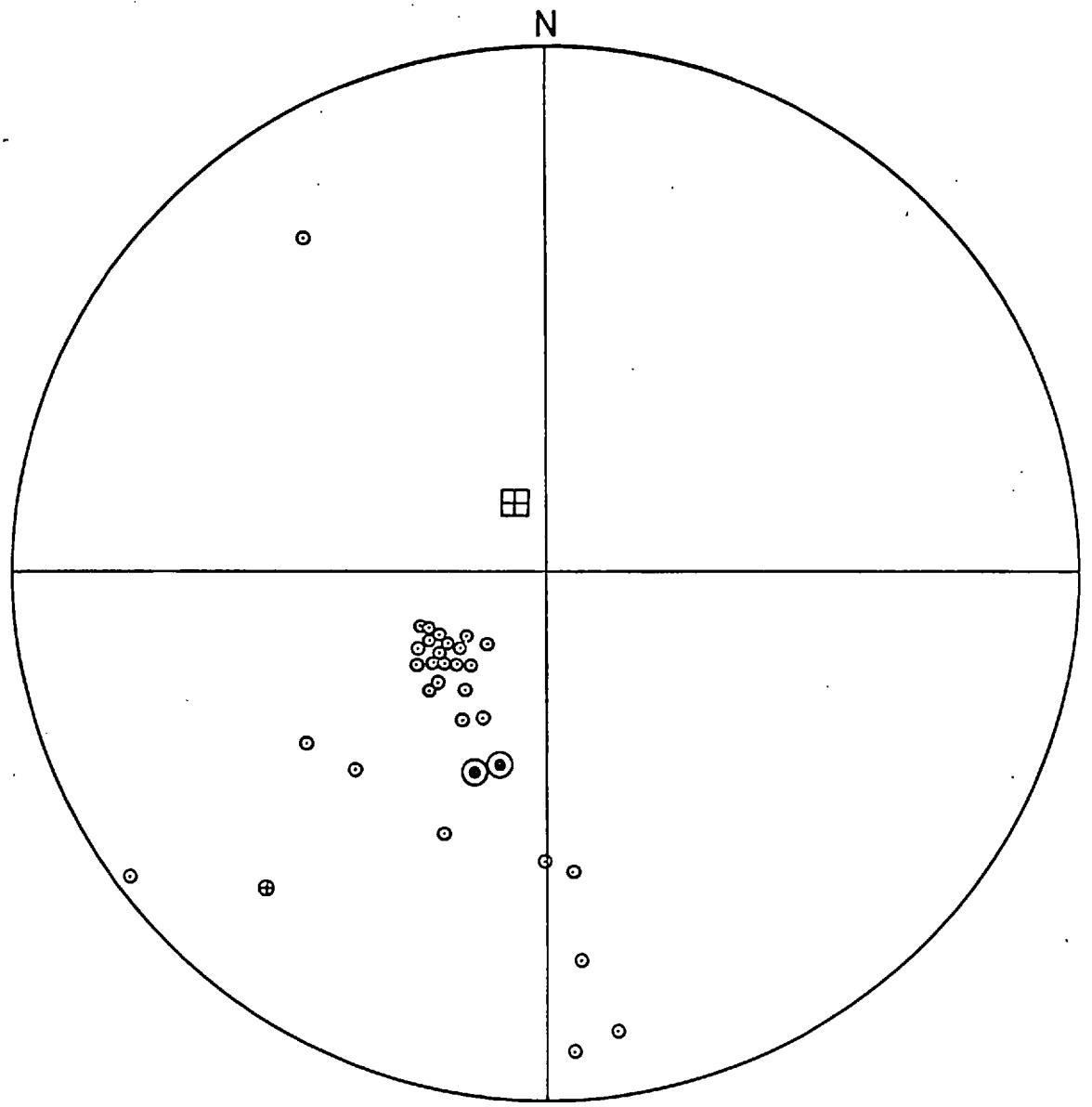

Fig 15·6

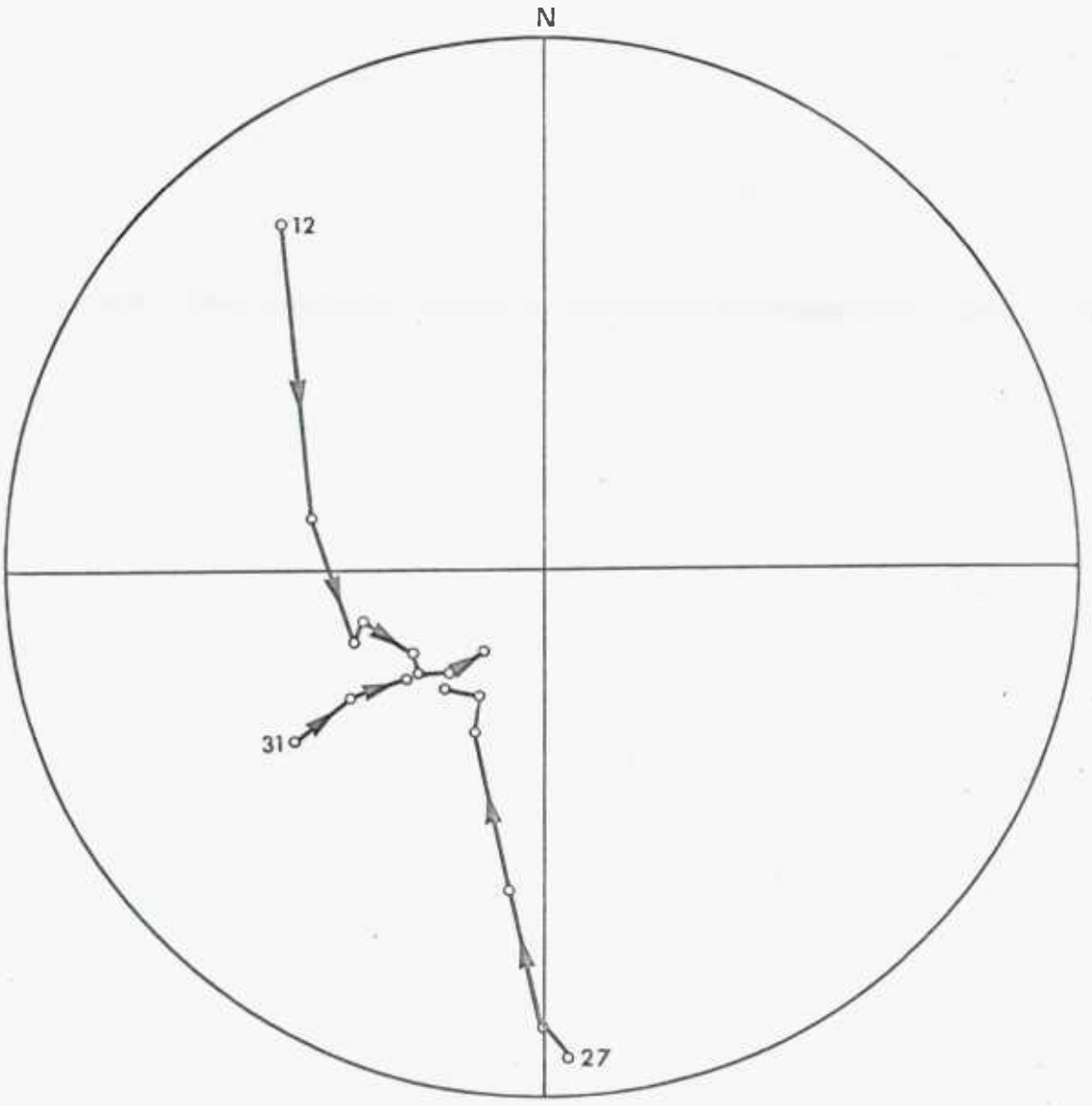

Fig 15·7

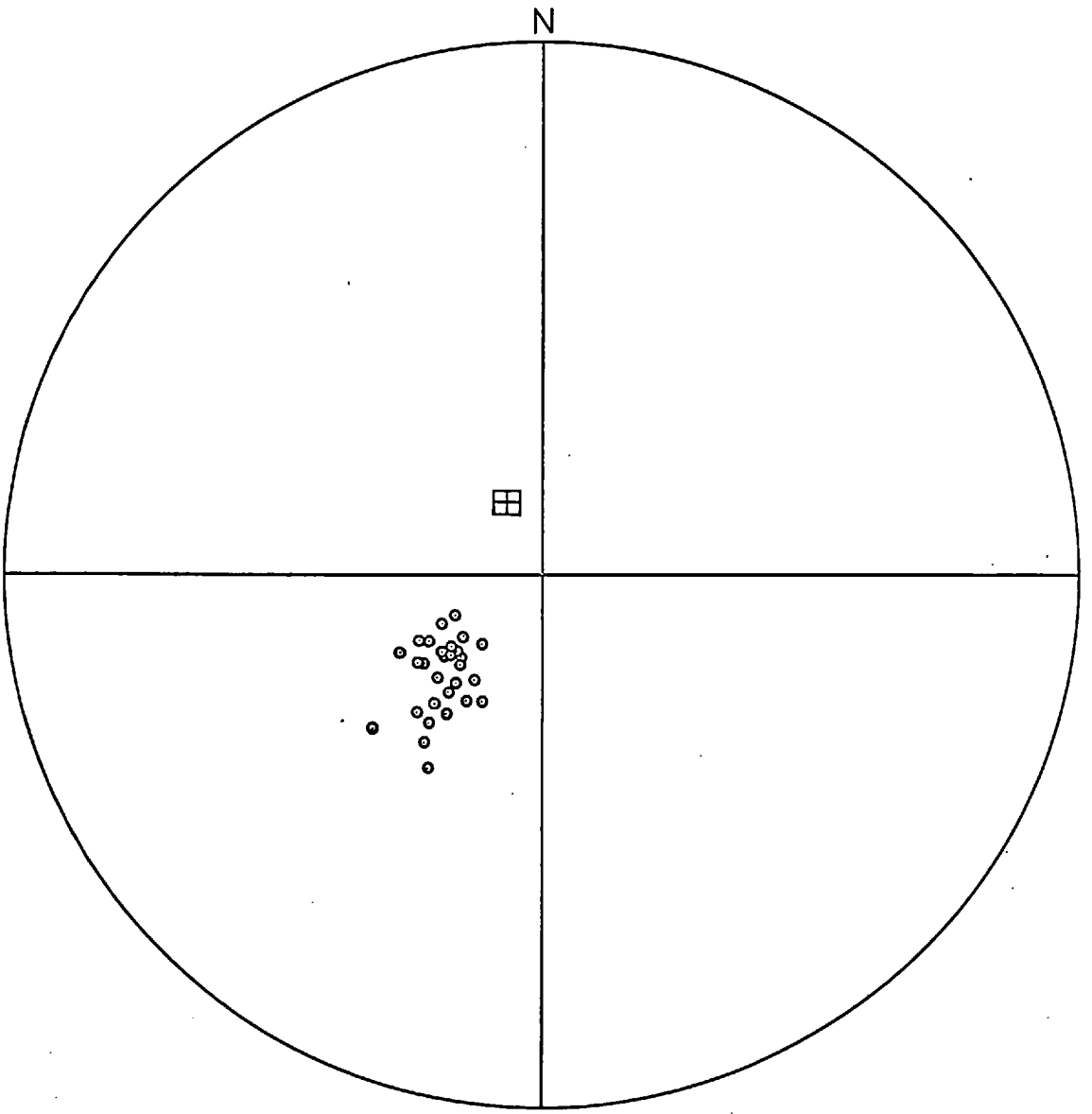

Fig 15·8

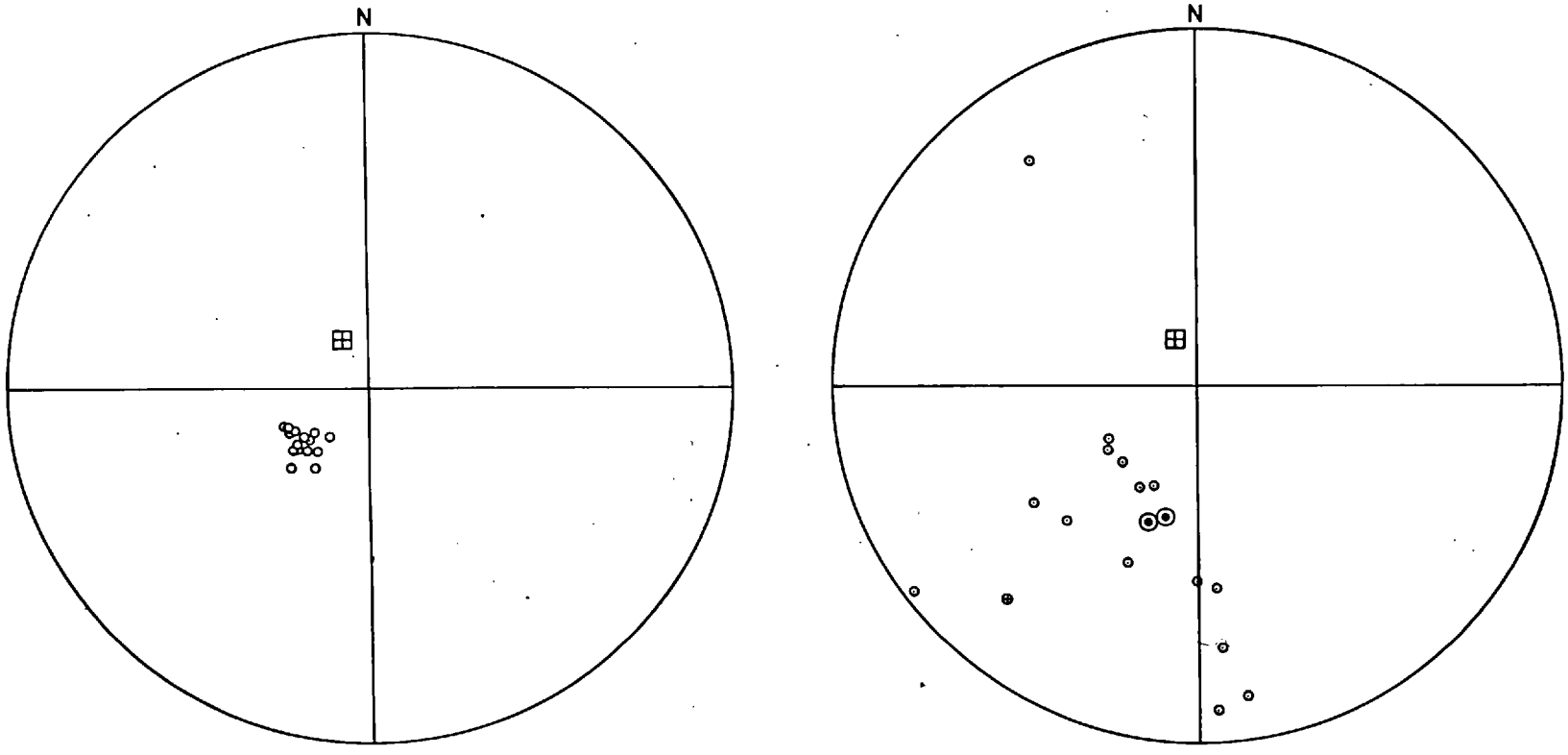

Fig 15.9

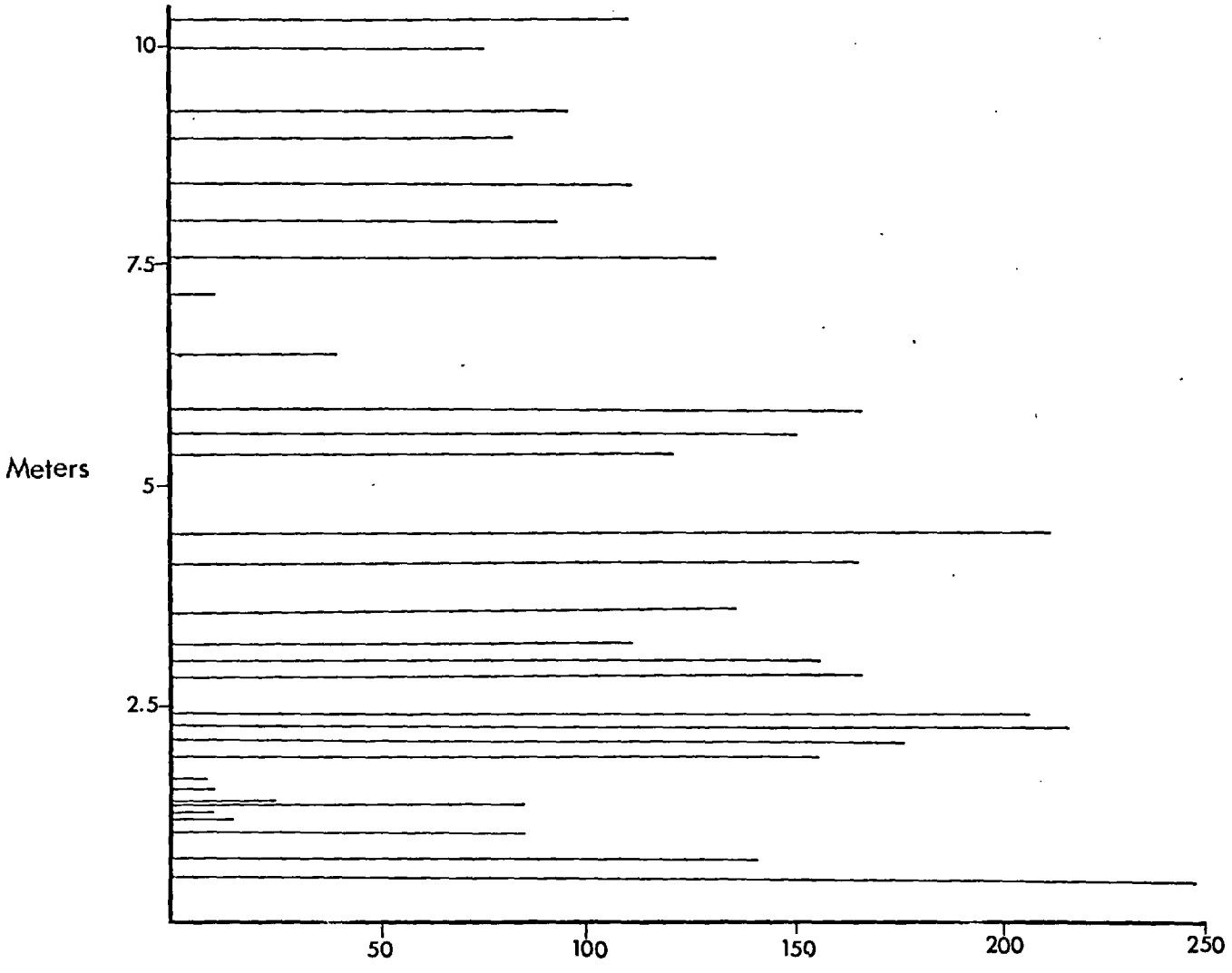

Fig 15·10

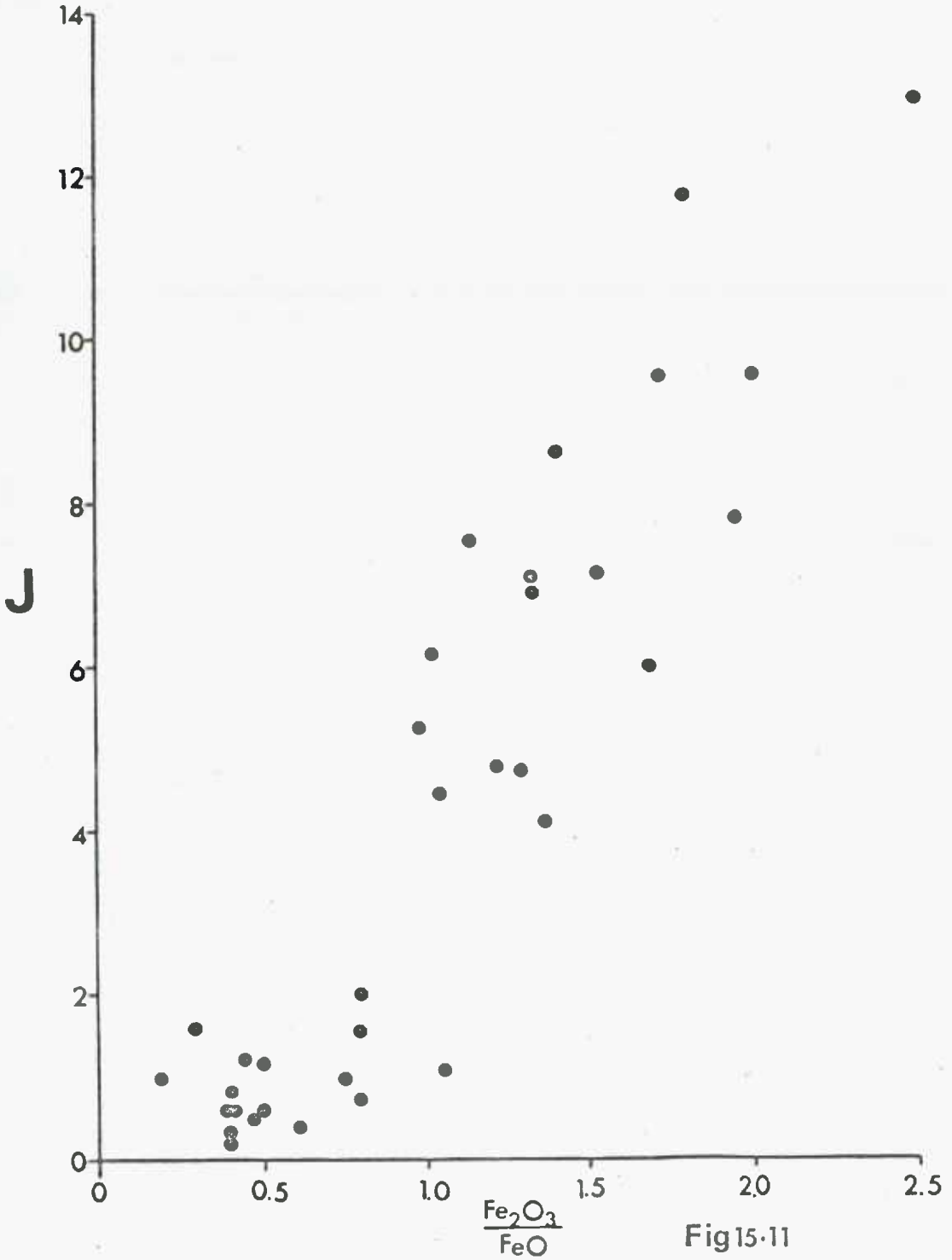

Fig 15·11

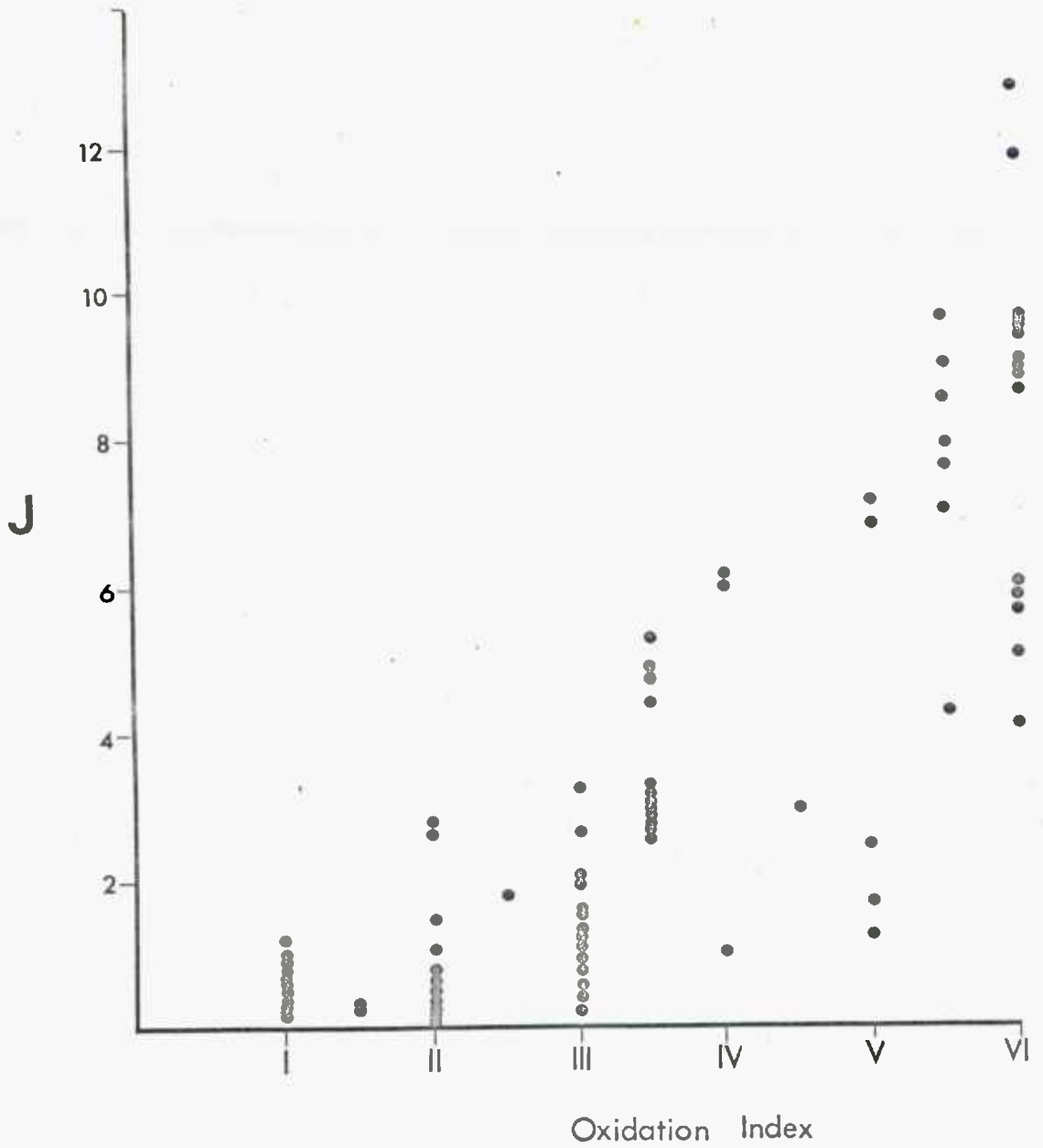

Fig 15·12

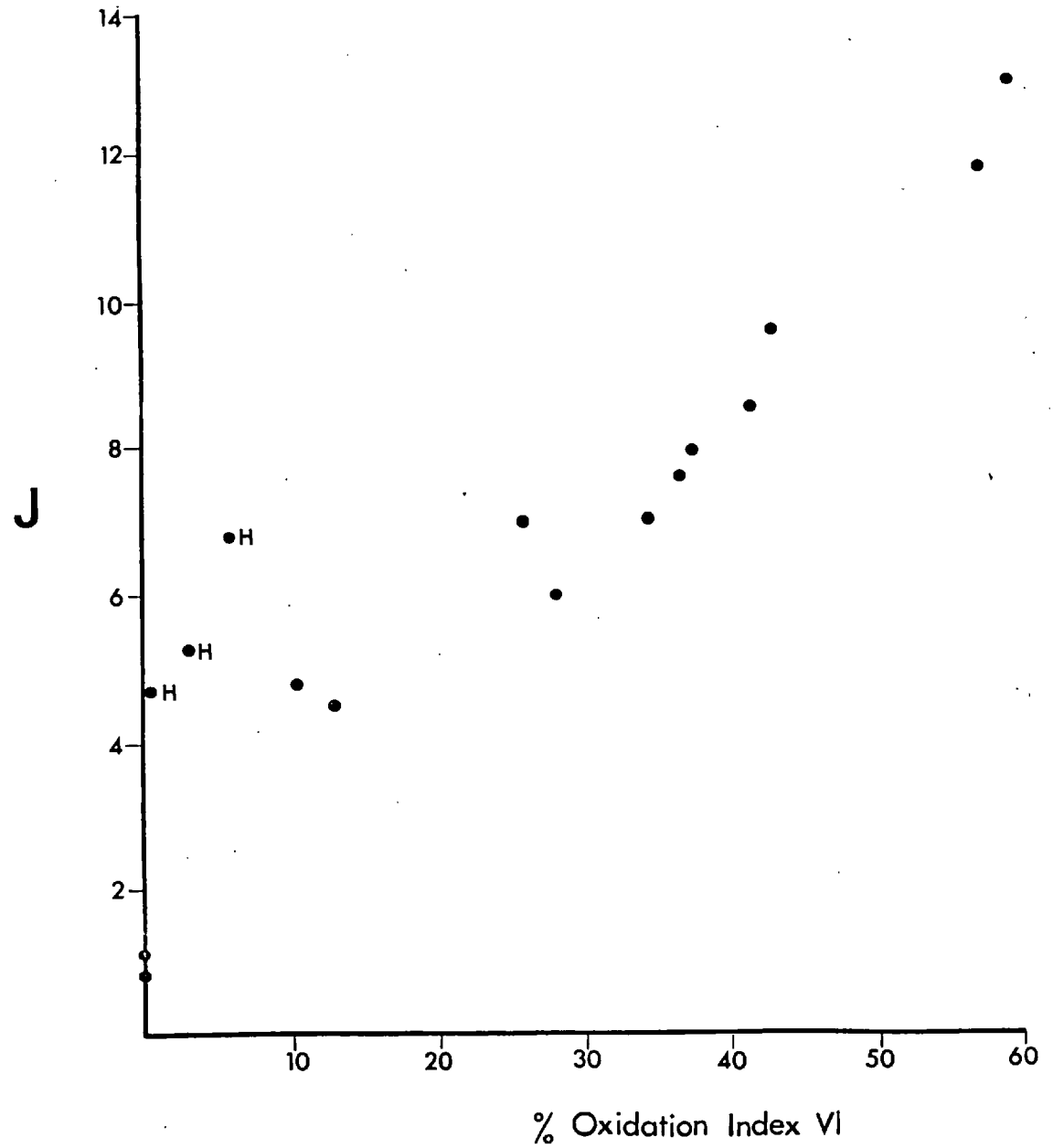

Fig 15·13

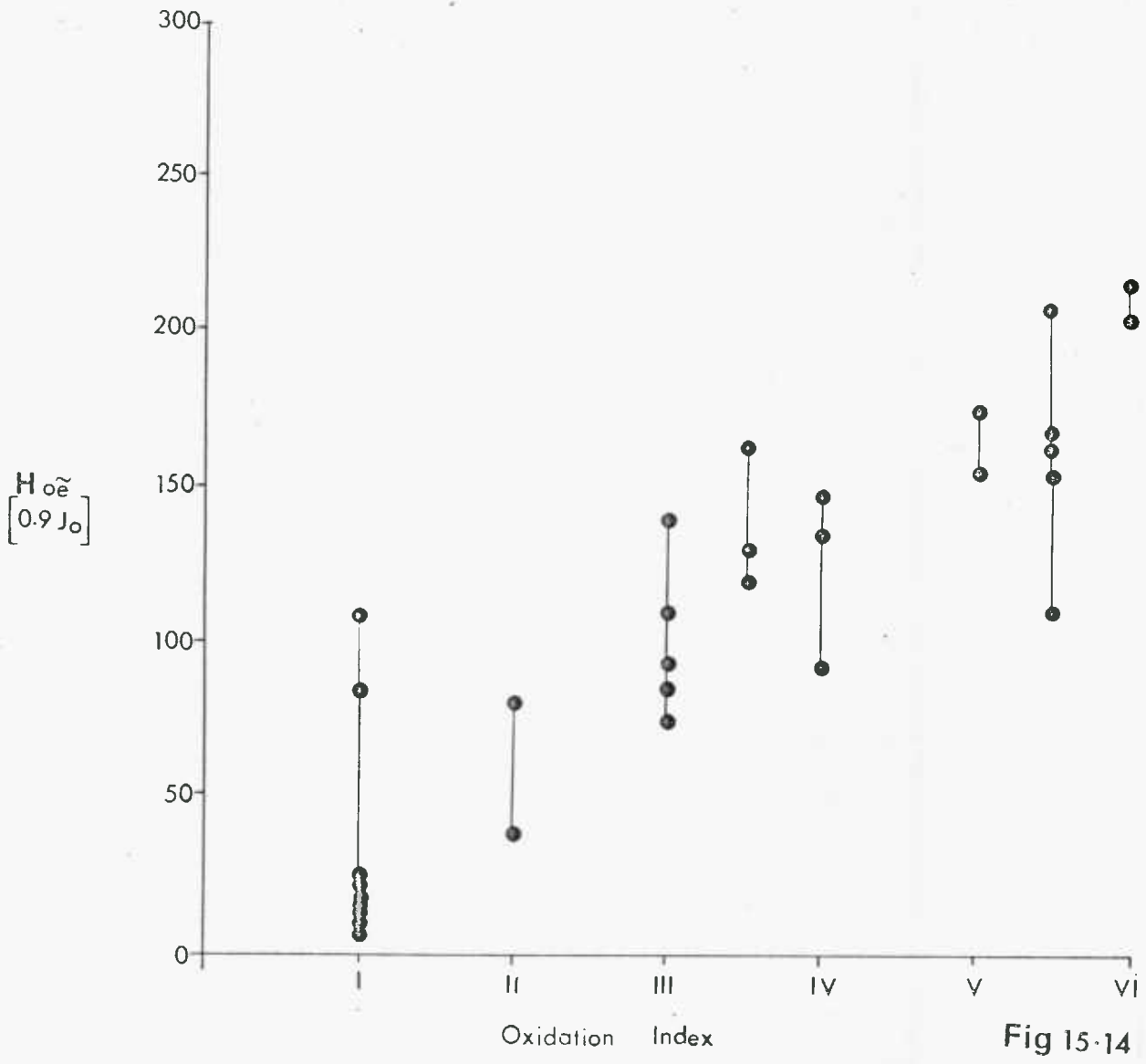
300
250
200
150
100
50
0
H oẽ
[0.9 Jo]
I
II
III
IV
V
VI
Oxidation Index

Fig 15·14

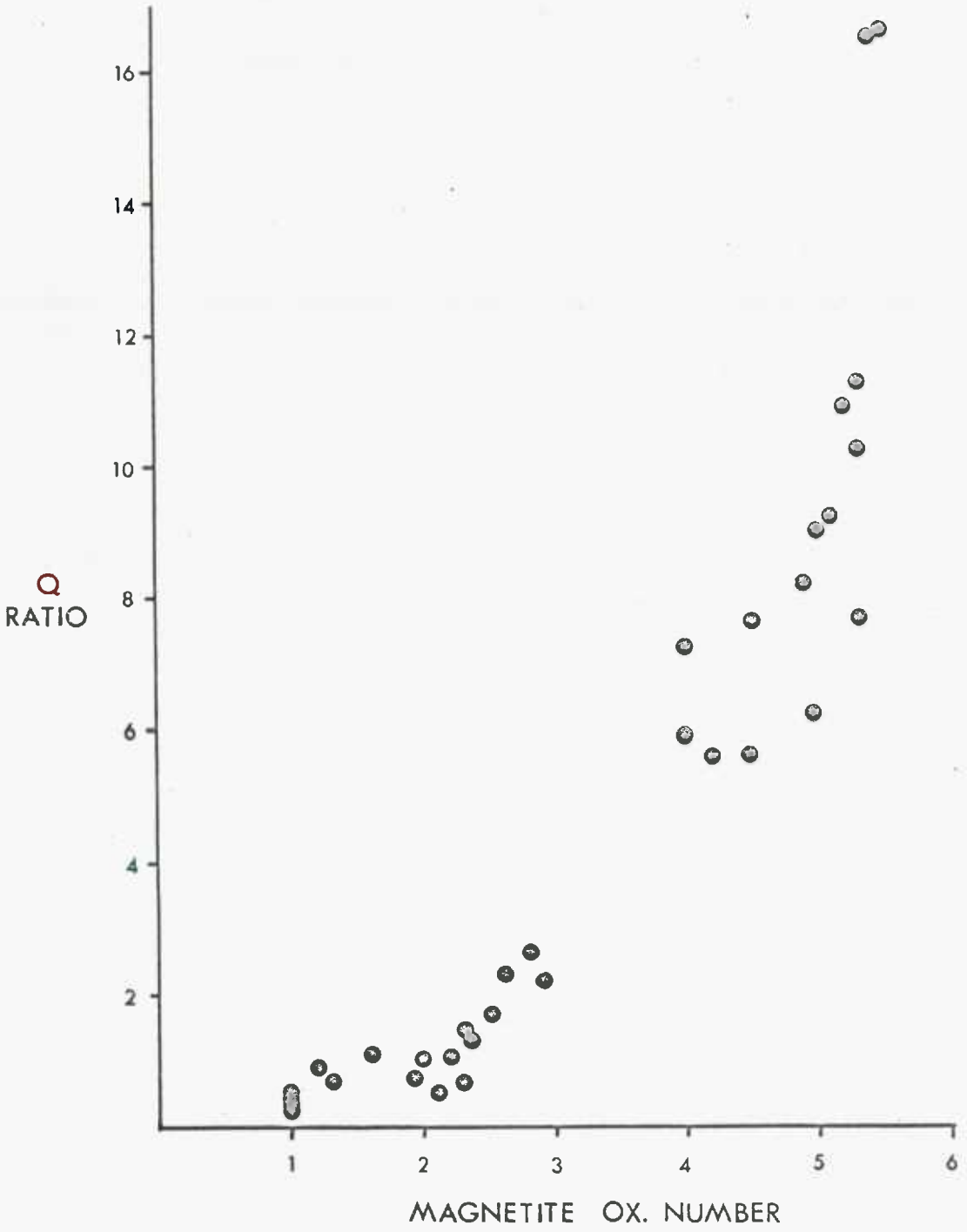

Fig 15·15

CHAPTER 16

THE OLIVINE - POOR BASALT (HS)

16.1 General Features

The lava occurs on the south side of Berufjaurdur, 18 km. north west of Djupivogur and 2 km. south east of the Berufjardara river, at the head of the Fjiord. The lava outcrops at an altitude of 105m and is one of a long series of plateau basalts which are characteristic of the area. The lava is 16.8m in thickness and is exposed laterally for approximately 300m. It is a prominent lava in the sequence and has well defined upper and lower contacts.

Thirty geographically oriented cores, 2.5cm. in diameter and 15-20cm. in length were obtained from a vertical traverse across the lava, using the petrol-powered field drill. The average spacing of samples within the lava is 55cm., but owing to ease of access the flow was more densely sampled towards the base. Two additional cores were obtained from the 30cm. thick baked clastic tuff which underlies the lava.

16.2 Petrography

In contrast with the previous lava, this flow is olivine-poor. It contains plagioclase and occasional iron-

titanium oxide phenocrysts which are set in an intergranular groundmass of feldspar, pyroxene, olivine and finer grained opaque minerals.

As far as the silicates in thin section are concerned, the degree of alteration throughout the flow is difficult to determine optically and may only be assessed in the broadest terms. As in the previous lava, the progressive and obvious variations which occur in the Fe-Ti oxides do not develop to the same extent in the silicates. At the base of the flow, however, plagioclase phenocrysts are fractured and strongly corroded and the ferromagnesian minerals show a chloritic type of alteration. Pale green chlorite and fibrous zeolites occur in the vesicles and the fine grained groundmass is severely altered.

The upper and lower parts of the lava are highly vesicular. There is a distinct variation in grainsize throughout the flow; the lower two-thirds (0 -9.7m) of the lava is medium to coarse grained while the upper part (10.3 - 16.8m) of the lava is relatively fine grained.

16.3 Reflection Microscopy

The iron-titanium oxides form approximately 5% of the rock by volume and this concentration does not vary throughout the thickness of the flow. The ratio titanomagnetite:ilmenite,

however, varies considerably with depth in the flow. Almost equal proportions occur in the lower two thirds of the flow but the titanomagnetite concentration is an order of magnitude greater than that of ilmenite near the top of the flow. A sharp break in the ratio occurs between specimens 21 and 22; the average ratio for specimens 1-21 is 1.25 and for specimens 22-30 is 5.94 . Because of this sudden change in mineral character, which is also reflected in other parameters, the lava has been divided into two groups of specimens, an upper (22-30) and a lower (1-21) group. The upper group is marked by solid dots in the diagrams(Figures 16.7 - 16.10) and the lower group by open circles.

There is a gradual and systematic increase in the size of titanomagnetite grains towards the centre of the lava (Figure 16.1). Although this feature is to be expected, it has not been observed to occur in the remaining fourteen lavas in this study. The edges of a flow are usually characterised by skeletal crystals, but these fine grained zones are, in general, rather narrow. Sandwiched between these two outer zones one finds that the grainsize is surprisingly uniform. In this particular lava the range in mean titanomagnetite grain size varies from 4 microns at the base of the lava, to 187 microns 9.0m above the base.

The grain size of discrete ilmenite, on the other hand, is less variable throughout the flow but varies, nevertheless, from 4 microns at the base, to 57 microns, 4.1m above the base.

This variation in grain size is undoubtedly related to the cooling process of the lava, but the large differences and variation in grain size between titanomagnetite and ilmenite, and their variation within the lava, are more difficult to explain. Under normal circumstances the grain sizes of titanomagnetite and ilmenite are sympathetically related. It may be argued that larger titanomagnetite grains are pre-eruption crystals but their concentration and gradual increase towards the centre of the flow eliminates this suggestion. Chemical analyses on samples from the lava (Table 16.1) show that the total iron and titanium contents do not vary throughout the flow so that relative grain size does not appear to depend on the (bulk) Fe:Ti ratio. It is important, at this stage, to note that the titanomagnetite maxima and the ilmenite maxima, in Figure 16.1, are displaced relative to each other and a possible explanation, in terms of oxidation, will be discussed in a subsequent section.

In the coarser grained parts of the flow the titanomagnetite crystals are strongly poikilitic and contain olivine, pyroxene and feldspar inclusions. These coarser

grains are generally irregular in outline, while the finer grains tend to be euhedral or subhedral in form. The number of poikilitic inclusions decreases markedly with decreasing grain size. Ilmenite crystals, in contrast, are non-poikilitic and tend to be euhedral in form.

16.4 Oxidation Classification

All specimens have been classified according to the titanomagnetite-ilmenite oxidation scheme. It has been necessary to use the quantitative magnetite oxidation number, rather than the qualitative overall oxidation index, because widely varying states of oxidation exist within single specimens. In specimens 2, 28 and 29, for example, grains in all six stages of titanomagnetite oxidation (Indices I-VI) are present, and superimposed on this (high temperature) classification are grains, in states I-III, which show added titanomaghemite.

Magnetite Oxidation Index (%)

Spec.No.	I	II	III	IV	V	VI	Mag.No.
2	2.33	26.74	31.97	15.70	20.35	2.91	3.34
28	2.30	18.75	39.14	12.50	23.03	4.28	3.48
29	1.11	45.56	31.11	5.55	10.00	6.67	2.98

Ilmenite Oxidation Index (%)

Spec.No.	I	II	III	IV	V	VI	VII	Ilm.No
2	56.92	4.62	3.08	2.31	31.08	-	-	2.50
28	30.26	2.63	13.16	1.32	42.10	10.53	-	3.54
29	55.00	-	-	-	45.00	-	-	2.80

This lava is quite exceptional in this respect and no plausible explanation can be offered to account for the extreme variations that occur within areas of 100-200 microns. Data derived for magnetite and ilmenite oxidation numbers are given in Table 16.1.

The variation in the state of oxidation, defined on the optical classification, as a function of depth in the lava is shown in Figure 16.2a. Because of the variety of assemblages that are present within single specimens, no distinct zones of oxidation are immediately apparent across the vertical traverse. A major zone does occur at a point 4.7m. above the base of the lava, but its significance is somewhat "blurred" by the background effect of adjacent samples. This is partly due to the method by which the magnetite oxidation number is calculated. This number gives an average value of the oxidation state by giving each of the mineralogical assemblages (indices I-VI) equal, and progressive, arithmetic weight (i.e. I x 1 + II x 2 etc.) It has been pointed out, however, that the spread in the chemical oxidation indices (Fe_2O_3 : FeO) is much more significant for higher values of the optical index than for correspondingly lower values. This means, in effect, that although some specimens may contain large percentages (10% for example)

of highly oxidized grains the magnetite number will be moved to a lower order because of the dominance of lower order indices. This point is demonstrated in Figure 16.2b, where the percentage of type III grains (pseudobrookite + titanohematite) is plotted as a function of depth. We now see that the high temperature oxidation zones are clearly defined and that the absolute maximum occurs at a point 4.7m above the base. This maximum towards the lower third of the lava supports the trend of the oxidation profile that was previously discussed for the olivine-rich lava (S and MS).

Oxidation has been active to some extent in all specimens of the lava. In fact no single specimen contains 100% homogeneous titanomagnetite, which is the lowest state of oxidation in the classification. Small concentrations (2.8%) of the unoxidized mineral occur in a single specimen (No.2) at the base of the flow and larger percentages are present in the five uppermost specimens. In the central region homogeneous titanomagnetite is totally absent. In contrast, homogeous discrete ilmenite occurs in every specimen throughout the flow, which is a reflection of its relatively higher stability. "Exsolution" lamellae of ilmenite, which are produced in titanomagnetite by subsolidus oxidation, occur throughout the flow and its concentration varies from 2.9% (Specimen 25) to 73.7% (Specimen17).

In the lower part of the lava (0-6.4m.) the average concentration of index III grains (densely packed lamellar ilmenite) is approximately 45%. This value gradually increases to a maximum (73.7%) at 8.3m and the concentration then tapers off towards the top of the flow. It is of interest to note that the mean titanomagnetite grain size value (Figure 16.1) reaches a maximum in the adjacent specimen (Specimen 18, 9.0m).

In reflected light the olivines from samples 1, 2, 8 and 13 all show fine irregular stringers of hematite, while specimens 9 to 12 show very fine incipient intergrowths of a secondary symplectic magnetite, together with hematite. Although the overall percentage of olivine in the lava is small the distribution of samples showing highly altered olivines is coincident with those samples which show large percentages of highly oxidized Fe-Ti oxides. This distribution is reflected in the concentration of pseudobrookite in Figure 16.2b, a curve which has already been referred to.

As in all other cases, the distribution of titanomaghemite as an oxidation product of titanomagnetite is extremely variable throughout the lava, throughout any one specimen and within any single titanomagnetite grain. Its concentration is almost impossible to access quantitatively. Although titanomaghemite may occur in fairly close proximity

to a grain containing the assemblage pseudobrookite + titanohematite or rutile + titanohematite it is nevertheless confined to those grains with indices I, II or III. It is less prevalent in the highly oxidized pseudobrookite specimens and so, therefore, it is more concentrated in the upper parts of the flow. Titanomaghemite is always paragenetically later than the formation of lamellar ilmenite, it is known to form at relatively lower temperatures and since it only affects those grains which did not undergo the process of high temperature pseudomorphic oxidation (IV-VI), it seems most likely that it formed at a very much later period of time and was <u>not</u> part of the primary deuteric process.

16.5 <u>Grain Size Variations</u>

The origin of the variation in the grain size of the opaque minerals throughout flow HS will be discussed. It is important to note, firstly, that the maximum mean titanomagnetite grain size occurs 2.1m. above the corresponding ilmenite maximum, and secondly, that there is little or no variation in ratio or bulk concentration in either of these zones. The significance of this grain size variation is that (a) it is known to be directly related to magnetic stability, and (b) zones which have taken the longest period

of time to crystallize should be chemically, and magnetically, different from zones which have cooled relatively quickly.

This grain size variation cannot simply be due to differential rates of cooling in various parts of the lava although the position of the titanomagnetite maximum (towards the centre of the lava) strongly suggests that this is the case. The point is that ilmenite does not vary sympathetically with this relationship and there are at least two plausible explanations which may account for this fact.

(a) Conditions of crystallization, which are known to be variable throughout the flow, may have favoured an increased rate of growth for titanomagnetite. What these conditions are likely to be is open to debate.

(b) It is known that the partial pressure of oxygen (pO_2) controls the partitioning of iron and titanium between silicates and (Fe-Ti) oxides during crystallization, and also controls the formation of the respective solid solution series within the Fe-Ti oxide system. Considering the latter effect, low pO_2 conditions will favour the formation of the magnetite-ulvospinel series and relatively higher pO_2 conditions the formation of the ilmenite-hematite series.

If any primary crystalline zonation exists within a lava it seems reasonable to assume that the process, or the effect of the process, will continue during deuteric cooling. If higher pO_2 conditions are needed to crystallize members of the ilmenite series, then its maximum development should coincide with zones of high overall deuteric oxidation. Similarly, the maximum development of titanomagnetite may be expected to occur in zones of minimum oxidation; this is indeed the case.

The grain size profile for ilmenite is matched in Figure 16.4, with the high temperature oxidation profile (defined by oxidation index (Fe_2O_3 : FeO)). The correspondence between these trends is good and the conclusion which is reached is that the restricted zones of high partial pressure which developed during deuteric cooling were the (oxidation) conditions which prevailed during the crystalline phase. Grainsize is controlled, therefore, not only by the rate of cooling, but also by effective oxidation.

16.6 Magnetic Properties and their relationship to mineralogical parameters

Certain basic correlations were established for the olivine-rich basalt and the validity of these correlations will now be tested on a lava which is mineralogically and magnetically dissimilar in many respects.

The magnetic properties were measured by WILSON and WATKINS (1968) and the following results were obtained (Table 16.2):

1. The Curie point does not vary significantly throughout the lava.

2. Large variations in (a) Magnetic stability,
(b) Intensity of magnetization,
(c) Susceptibility, and
(d) Koeningsbergs Q Ratio were found to occur throughout the lava.

These variations are all reflected to some degree in the Fe-Ti oxide mineralogy. Each parameter will be treated separately, mineral-magnetic correlations will be presented and the importance of these correlations will be discussed.

16.6.1 Stability

The lava shows both normal and reversed NRM directions which is entirely a function of instability. The stable direction is reversely magnetized, and the behaviour of the directions upon demagnetization at 200 and 400 oersteds alternating magnetic field is shown in Figure 16.5. If the inclination values are considered separately, as a function of depth within the lava, we see that on the whole, the lower part of the lava is more stable (i.e. reversely magnetized)

than the upper part (Figure 16.6). In fact in the lower half only two specimens (13 and 17) have normal directions.

An improved magnetic stability factor has been devised by WILSON which takes into account not only the change of intensity on demagnetization but also the change in direction. The stability factor varies betweeen 0 and ..; high values indicate greater stability. Since both normal and reversed directions are present within this lava, a quantitative measure of the rate of change in direction, at each demagnetization step, is particularly important.

Magnetic stability depends primarily on the grain size of the magnetic minerals and although large variations in the primary grain size are present within the flow, there is still no direct correlation. It has been noted previously that indirect grain size effects may be caused by oxidation. In the case of exsolving ilmenite lamellae, a lattice network is established; this effectively subdivides large primary titanomagnetite crystals into a large number of smaller crystals. A second, size-stability effect may be induced in highly oxidized olivine by the development of ultra fine symplectic magnetite.

Large percentages of type III index grains (densely packed lamellar ilmenite) are present in all specimens, but

a very poor correlation is shown with the stability factor (Figure 16.7a). A very much better correlation (Figure 16.7b is shown with index VI grains, which is used here to define the distribution of secondary symplectic magnetite (see discussion on page 293). This latter correlation is surprising in view of the relatively low olivine concentration.

It is suggested that the unusually large oxidation variations which exist within single specimens, makes neither of the above correlations perfect. However, if the average magnetite oxidation number is considered, a more refined correlation results (Figure 16.8 a). This indicates that magnetic stability, in this lava, is due partly to symplectic magnetite and partly to the subdivided, effective (rather than actual) magnetic grainsize of titanomagnetite (i.e. type III grains).

In all of these correlations, the upper (22-30) and lower groups (1-21) of specimens are separated; the lower group are more highly oxidized and are relatively more stable.

16.6.2 Intensity of Magnetization

The natural intensity of magnetization varies from a maximum of 10.31×10^{-4} emu/g at 4.7m from the base of the lava to a minimum of 0.48×10^{-4} emu/g at 10.3m. The

vertical distribution of the intensity values within the lava is shown in Figure 16.9a. The shape of the curve and the pronounced maximum towards the lower third of the lava clearly resemble the intensity and the oxidation profiles which were described for the olivine-rich lava. In fact, as one can see from Figure 16.9b, the intensity of magnetization of the olivine-poor basalt also correlates well with the magnetite oxidation number. Note that the upper and lower specimens fall into quite distinct groups the upper specimens (less stable magnetically) form a separate group because they have lower intensities and correspondingly lower magnetite oxidation numbers.

An interesting point emerges from a comparison of the intensity profile and the high temperature oxidation profile across the lava (Figure 16.9). In this case the distribution of pseudobrookite (pseudomorphous after titanomagnetite) has been chosen to define the oxidation zones. The major peak towards the centre of the lava (at 4.5 meters) is well matched in both curves but the sensitivity of the pseudobrookite profile to changes in intensity is much more sensitive than was previously expected. Even those samples containing less than 10% of the type VI assemblage (pseudobrookite + titanohematite) show marked increases in intensity.

It should not be inferred from these correlations that pseudobrookite is the magnetic source material. This mineral is chosen, firstly because it represents the maximum state of oxidation reached by the lava, and secondly, because it gives an indirect measure of the concentration of symplectic magnetite in oxidized olivine.

16.6.3 Susceptibility

A non -systematic increase in susceptibility occurs from the top of the lava to the base. This profile is unlike any of the other parameter-profiles across the lava, and in terms of the variation in mineralogy it is difficult to equate this increase in terms of a single mineral parameter.

Susceptibility is known to depend chiefly on the volume of magnetic material present. It also depends, to a lesser extent, on composition and grainsize.

Figure 16.10a shows that a relatively good negative correlation exists between susceptibility and the magnetite oxidation number. This infers that there is less magnetic material in the highly oxidized specimens. There are similar negative correlations between susceptibility and the magnetic stability factor, and between susceptibility and intensity of magnetization. The magnetite oxidation number and the stability factor are independant of the volume of magnetic

material, in contradiction with the above statement that it probably varies rather little throughout the lava. Furthermore, if the overall volume of magnetic material is the significant controlling factor, then the intensity should correlate positively with susceptibility.

As far as grainsize is concerned, no clearly defined correlation exists with either the primary grain size or the effective magnetic grain size.

The lower specimens in the lava are tightly grouped around 7×10^{-4} emu/g.oer while the upper specimens show a considerable spread in values.

In conclusion, specimens which are highly oxidized have relatively low susceptibility values; these values are concentrated towards the lower part of the lava, which is magnetically more stable.

16.6.4 Koenigsberger Q-Ratio

The Koenigsberger ratio is the traditional measure of magnetic stability. It correlates well with WILSON'S stability factor although they are entirely different quantities. It is obvious from these remarks that the Q-ratio should correlate with the magnetite oxidation number, and indeed it does (Figure 16.10b).

Specimens from the upper part of the lava are more highly oxidized and therefore have higher values of Q.

16.7 Conclusions

a. The state of oxidation is highly variable throughout the single vertical traverse.

b. The maximum state of oxidation reached is confined to a well marked zone in the lower third of the lava.

c. There is a 94% increase in the grain size of titanomagnetite crystals from the edges of the flow towards the central interior.

d. The mean ilmenite grain size is not as variable as that of titanomagnetite. The maximum peak for ilmenite does not coincide with that of titanomagnetite but rather with the zone of highest oxidation.

e. The lava contains normal and reversed directions of magnetization within the flow; the reversed (stable) directions are concentrated towards the lower half of the lava and the normal (unstable) directions towards the upper part.

f. Integration of the magnetic data with their mineral properties results in the following strong correlations;

(i) Specimens which are highly oxidized are magnetically stable and show high intensities of magnetization;

(ii) Specimens which show lower states of oxidation are magnetically unstable and have relatively lower intensities of magnetization;

(iii) Susceptibility shows a negative correlation with oxidation.

g. The highly oxidized specimens are magnetically retentive. This is chiefly due to the stability of untra-fine magnetic material in the rock. This material takes two forms (a) symplectic magnetite in oxidized olivine (b) effective magnetic grain size reduction of titanomagnetite by lamellar ilmenite.

h. The large variations in primary grain size do not affect the magnetic properties to any great extent. If the lava had been totally unoxidized this would obviously not have been the case.

TABLE 16.1

Lava HS		% Oxidation Index							Titanomagnetite			Ilmenite			
Sample		I	II	III	IV	V	VI	VII	Ox.No.	%Conc.	Grain size (u)	Ox.No.	%Conc.	Grain size (u)	Fe_2O_3:FeO (whole rock)
I	2	56.92	4.62	2.08	2.31	33.08						2.50	53.05	11	1.13
M		2.33	26.74	31.97	15.70	20.35	2.91		3.34	46.95	19				
I	3	48.75	6.25	8.75	5.00	31.25						2.64	53.35	14	0.88
M			8.57	51.43	19.29	18.57	2.14		3.54	46.67	36				
I	4	47.40	9.25	5.78	4.05	30.06	3.76					2.72	57.66	20	0.78
M			7.88	38.58	25.20	26.77	1.57		3.75	42.34	29				
I	5	50.80	8.87	7.26	3.23	29.84						2.52	43.13	27	
M			5.10	61.15	19.10	14.65			3.43	55.87	58				
I	6	38.83	8.82	20.59	2.94	25.88	2.94					2.77	49.13	33	0.60
M									3.52	50.87	58				
I	7	7.14	8.93	21.43	21.43	41.07						3.80	23.14	37	
M			17.20	45.16	23.66	13.98			3.34	76.86	85				
I	8	33.85	7.05	26.47	1.17	14.12	13.52	4.12				3.12	45.04	32	
M				55.53	17.14	22.24	5.09		3.77	54.96	94				
I	9	25.58	18.16	6.98	4.65	2.32	4.65	37.21				4.02	41.35	32	0.72
M				49.18	23.78	15.57	11.47		3.89	58.65	120				
I	10	20.90	14.92	3.73		0.75	12.69	47.01				4.71	48.88	57	0.95
M			3.82	55.73	22.14	10.69	7.62		3.63	51.12	118				
I	11	6.32	11.58	9.47	3.15		22.11	47.37				5.34	47.50	52	1.14
M				37.14	27.62	5.71	29.53		4 28	52.50	111				
I	12	26.83	14.63	8.54	1.22	17.05	29.27					4.06	40.80	32	0.87
M			0.84	51.26	26.05	12.61	9.24		3.78	59.20	132				

TABLE 16.1 (continued)

I 13	22.45	20.41	13.26	3.06	12.24	17.35	11.23				3.59	47.80	37	1.03
M		2.80	51.40	19.63	12.15	14.02		3.83	52.20	143				
I 14	22.65	29.25	7.55	8.49	9.43	10.37	12.26				3.33	51.96	31	0.82
M		6.12	48.98	25.52	13.26	6.12		3.64	48.04	112				
I.15	34.44	20.00	18.90	3.33	13.33	10.00					2.71	45.23	35	0.85
M		4.59	59.63	25.69	7.34	2.75		3.44	54.77	135				
I 16	75.82	5.88	7.84	2.62	7.84						1.61	46.65	32	0.74
M		12.00	70.86	11.43	5.71			3.11	53.35	98				
I 17	60.58	15.38	11.54	3.85	8.65						1.85	34.89	30	
M		8.25	73.71	10.31	7.73			3.18	65.11	143				
I 18	33.80	6.35	11.97	4.93	16.20	7.75	19,00				3.62	40.92	30.	0.81
M			65.36	15.62	14.63	4.39		3.58	59.08	187				
I 19	42.14	11.95	21.38	5.03	19.50						2.48	52.13	34	0.92
M		13.01	30.82	30.14	26.03			3.69	48.87	167				
I 20	99.32	0.68									1.01	47.42	36	
M	73.62	25.15	1.23					2.28	52.58	141				
I 21	100										1.00	47.48	26	0.70
M		71.23	28.77					2.29	52.52	140				
I 22	100										1.00	26.50	29	1.11
M		91.84	8.16					2.08	73.50	90				
I 23	34.15	10.97	3.66		31.70	19.52					3.43	20.20	32	1.23
M		15.12	46.00	8.64	26.54	3.70		3.58	79.80	45				
I 24	56.41	2.56	5.13	7.69	28.21						2.26	10.96	23	1.13
M		37.85	37.85	6.95	17.35			3.04	89.04	34				
I 25	100										1.00	19.05	10	
M	94.12	2.94	2.94					1.09	80.95	18				
I 26	100										1.00	15.20	12	0.98
M	80.21	15.51	4.28					1.24	84.80	10				

TABLE 16.1 (continued)

I 27	100								1.00	7.14	7		
M	65.38	16.92	10.00	7.69			1.60	92.86	11				1.27
I 28	30.26	2.63	13.16	1.32	42.10	10.53			3.54	14.47	14		
M	2.30	18.75	39.14	12.50	23.03	4.28	3.48	85.53					0.88
I 29	55.00								2.80	11.11	5		
M	1.11	45.56	31.11	5.55	10.00	6.67	2.98	88.89	9				1.27
I 30	53.85		7.69		38.46				2.69	9.03	11		
M	23.66	25.96	29.00	12.98	8.40		2.56	90.97	19				1.24

Lava HS - Mineralogical and Chemical Data. Oxidation classification of titanomagnetite is on a scale of I-VI (page 275), ilmenite is on a scale ofI-VII (page 45).

TABLE 16.2

Sample No.	Position(m)	Stability Factor	J x 10^{-4} emu/am	Q Factor	Susceptibility x 10^{-4} emy/g.oer
30	16.80	0.20	0.94	0.10	18.3
29	16.10	0.26	1.74	0.25	13.9
28	15.65	0.48	2.95	0.68	8.73
27	14.95	0.24	1.01	0.11	19.2
26	14.00	0.02	0.07	0.006	25.9
25	13.40	0.10	0.77	0.09	18.1
24	13.10	0.34	3.76	0.66	11.3
23	13.25	0.38	2.29	0.23	9.91
22	11.65	0.07	0.51	0.07	14.8
21	11.25	0.11	0.72	0.12	11.8
20	10.30	0.05	0.48	0.10	10.0
19	9.69	0.31	3.14	0.78	8.12
18	9.00	0.53	4.53	1.30	6.92
17	8.33	0.34	3.03	0.86	6.98
16	7.78	0.49	3.12	0.66	9.42
15	7.13	0.44	4.31	1.20	7.21
14	6.45	0.61	4.99	1.46	6.87
13	5.98	0.30	4.50	1.30	6.78
12	5.35	0.60	8.69	2.30	7.54
11	4.75	0.64	10.31	3.00	6.86
10	4.11	0.63	8.36	2.36	7.08
9	3.43	0.61	7.09	2.06	6.87
8	2.86	0.55	5.65	1.74	6.49
7	2.36	0.46	3.96	1.10	7.14
6	1.95	0.48	4.55	1.18	7.73
5	1.54	0.45	3.80	1.02	7.48
4	1.20	0.55	3.64	1.22	5.99
3	0.82	0.53	3.99	1.30	6.12
2	0.33	0.60	3.48	0.94	7.47
1	0.20	0.70	6.03	2.12	5.70

Lava No. HS giving the position at which samples were obtained in the vertical traverse and the determined magnetic parameters.

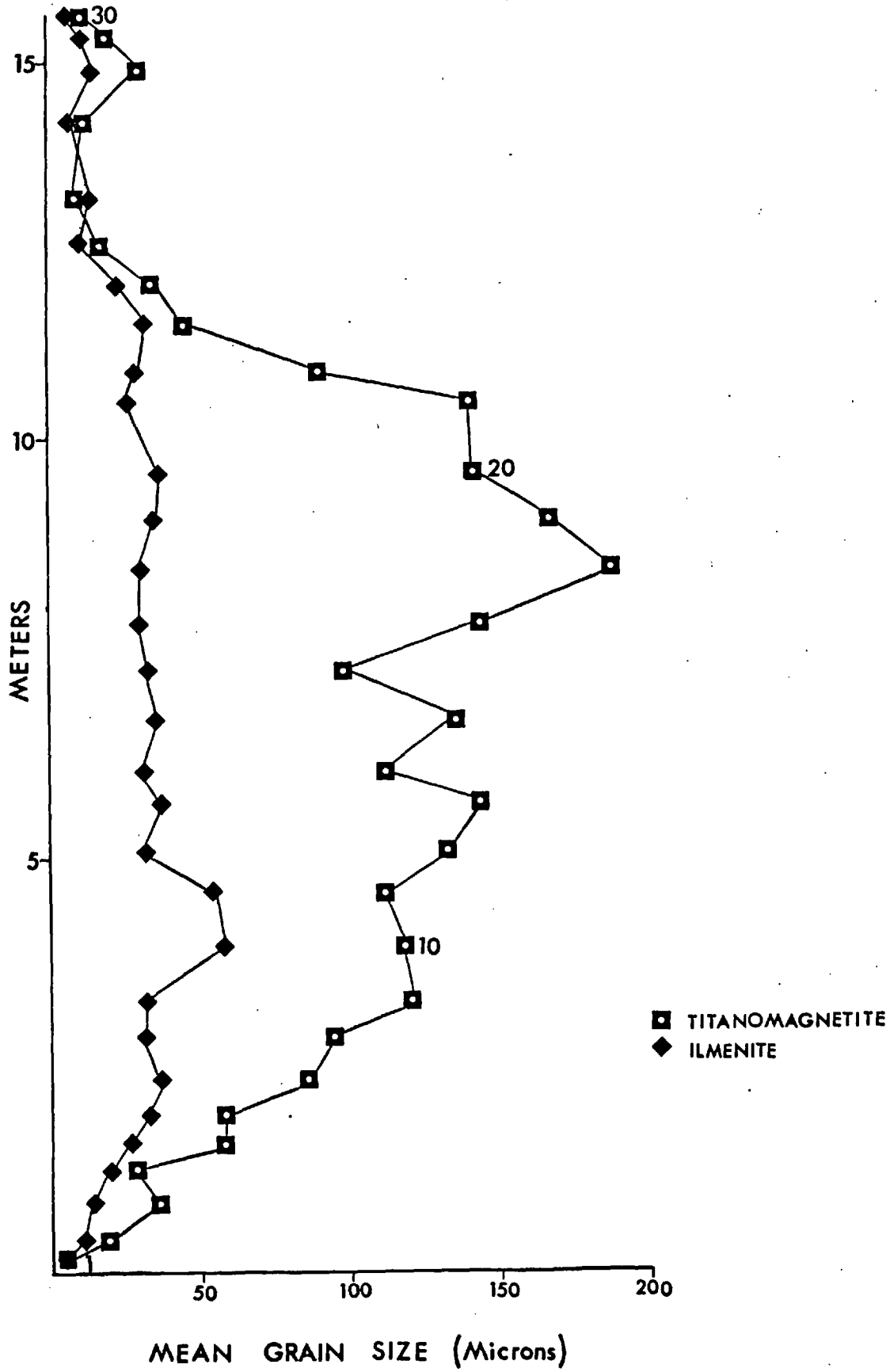
30
15
10
20
METERS
5
10
50
100
150
200
MEAN GRAIN SIZE (Microns)
TITANOMAGNETITE
ILMENITE

Fig 16-1

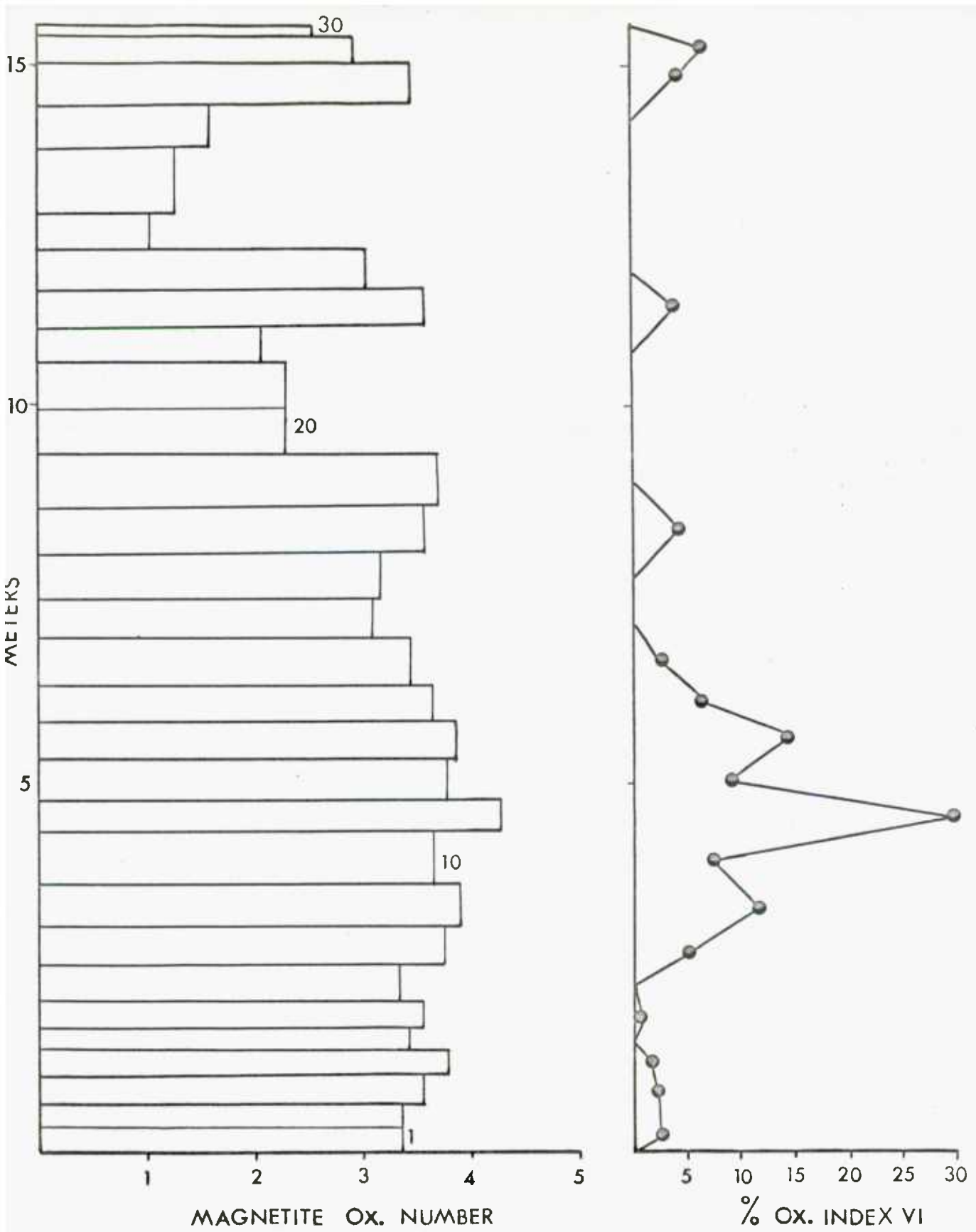
30
15
10
20
METERS
5
10
1
1
2
3
4
5
MAGNETITE OX. NUMBER
5
10
15
20
25
30
% OX. INDEX VI

Fig 16.2

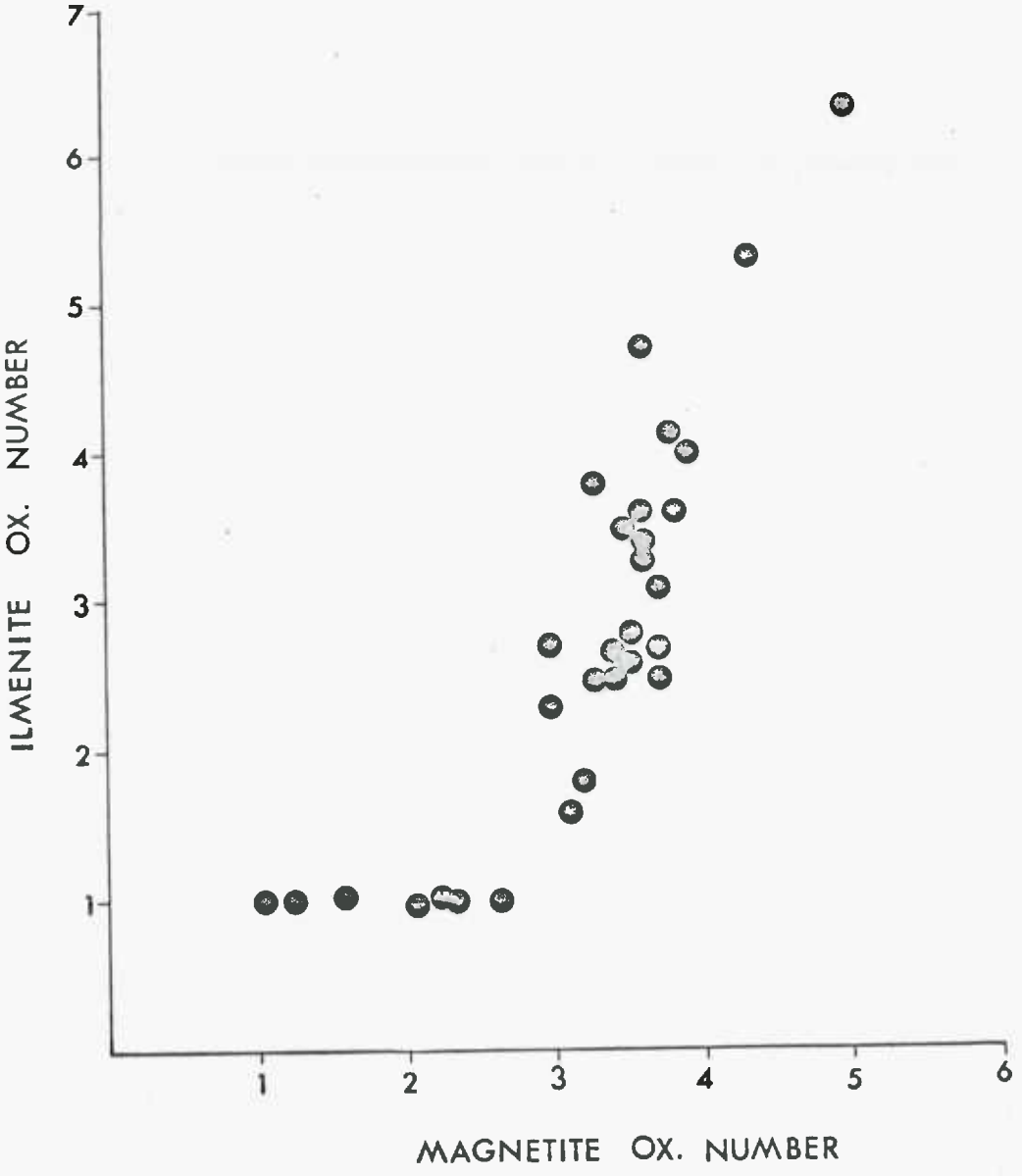

Fig16.3

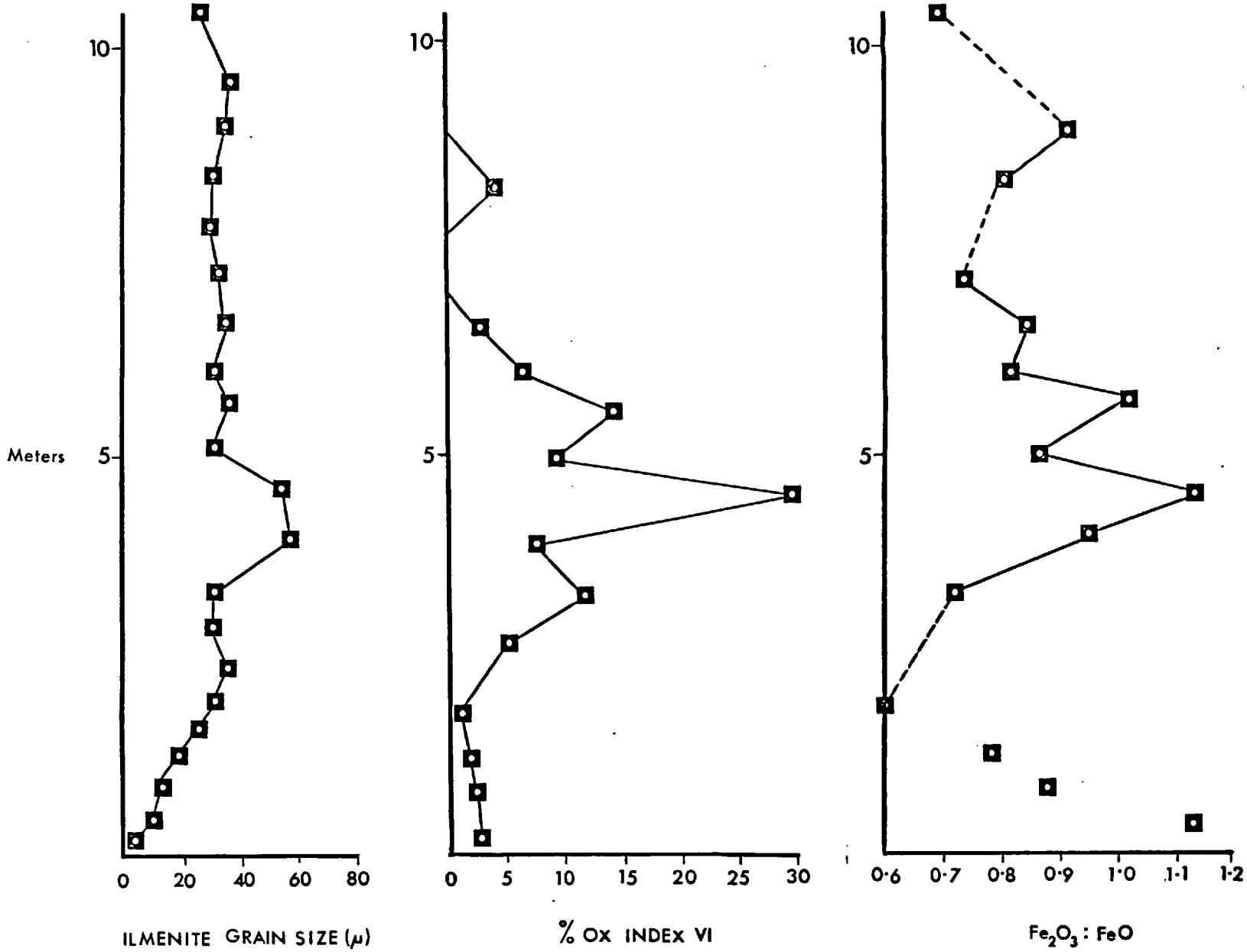
Meters
10
5
0
20
40
60
80
ILMENITE GRAIN SIZE (μ)
10
5
0
5
10
15
20
25
30
% OX INDEX VI
10
5
0·6
0·7
0·8
0·9
1·0
1·1
1·2
Fe_2O_3 : FeO

Fig 16·4

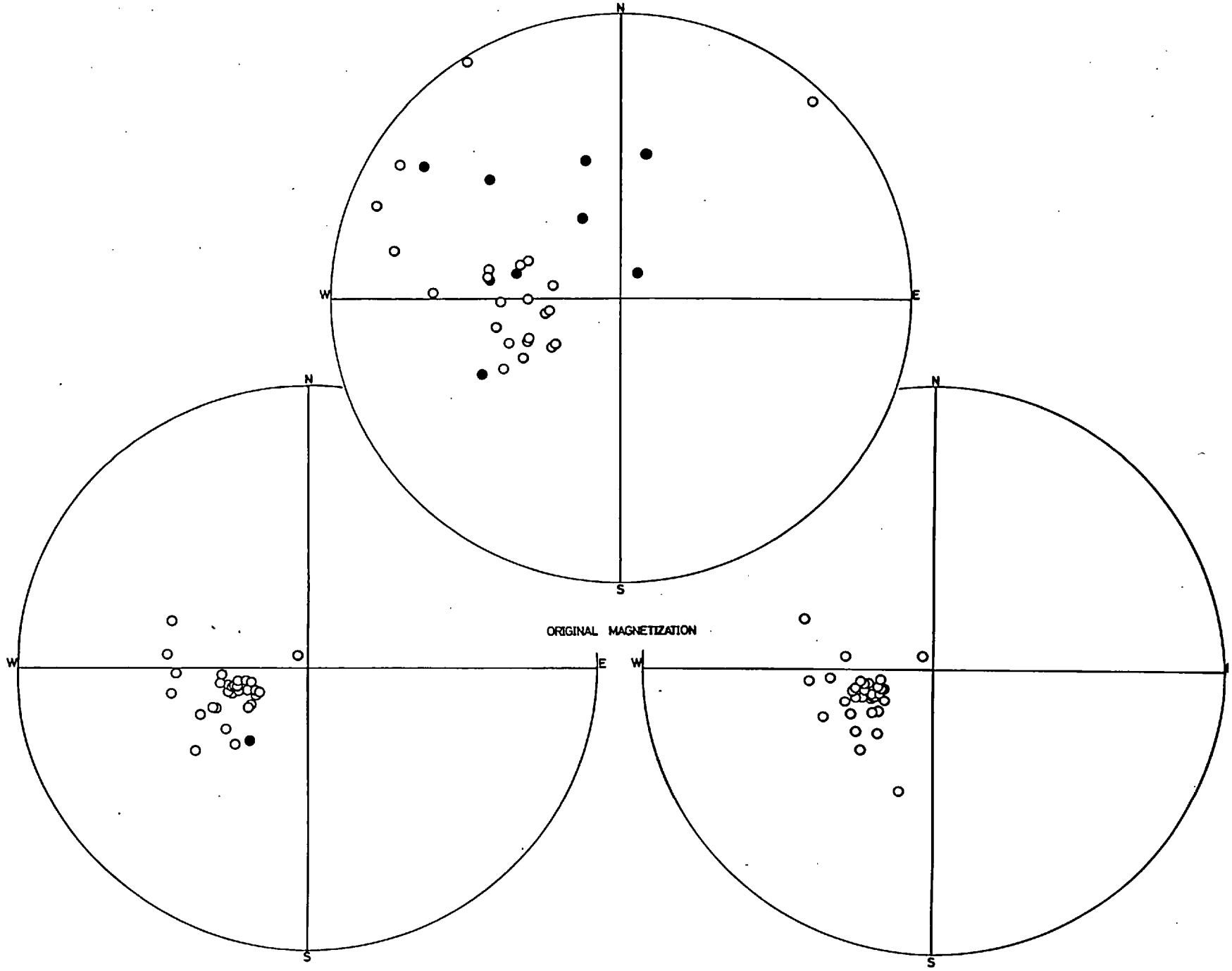
N
W
E
S
ORIGINAL MAGNETIZATION
AFTER 200 OERSTEDS A.C.
AFTER 400 OERSTEDS A.C.

FIG 16.5

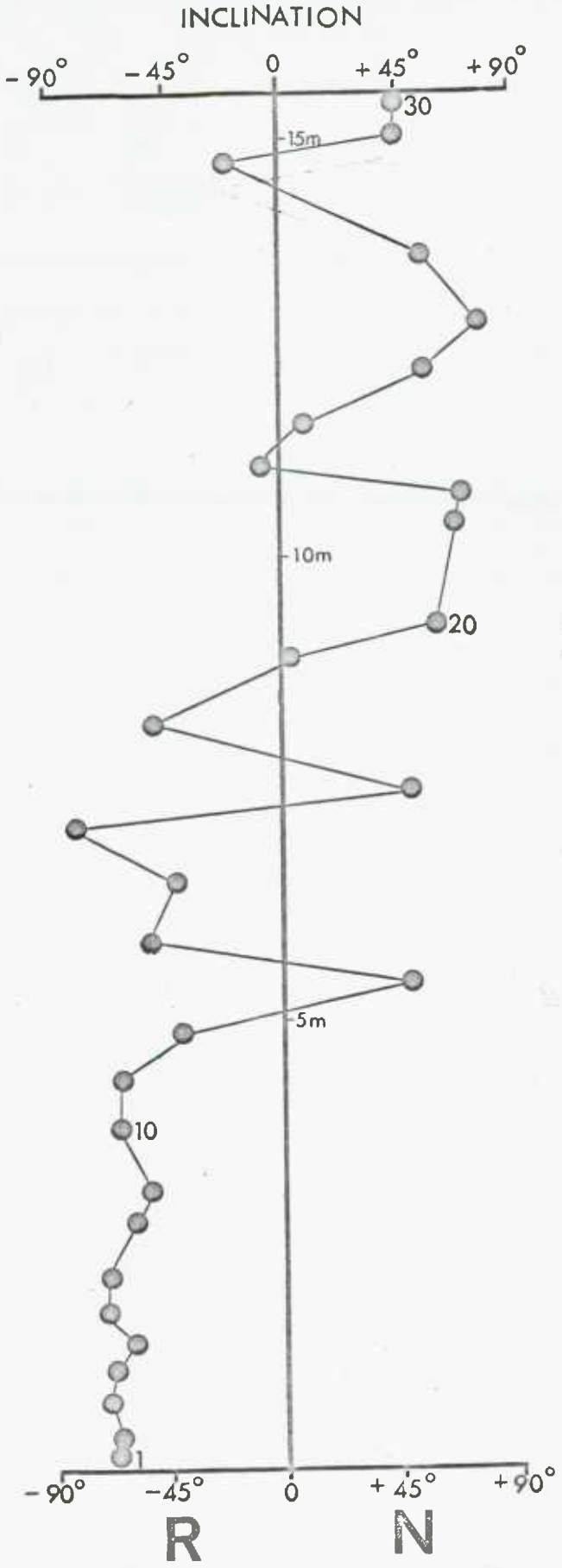

Fig 16·6

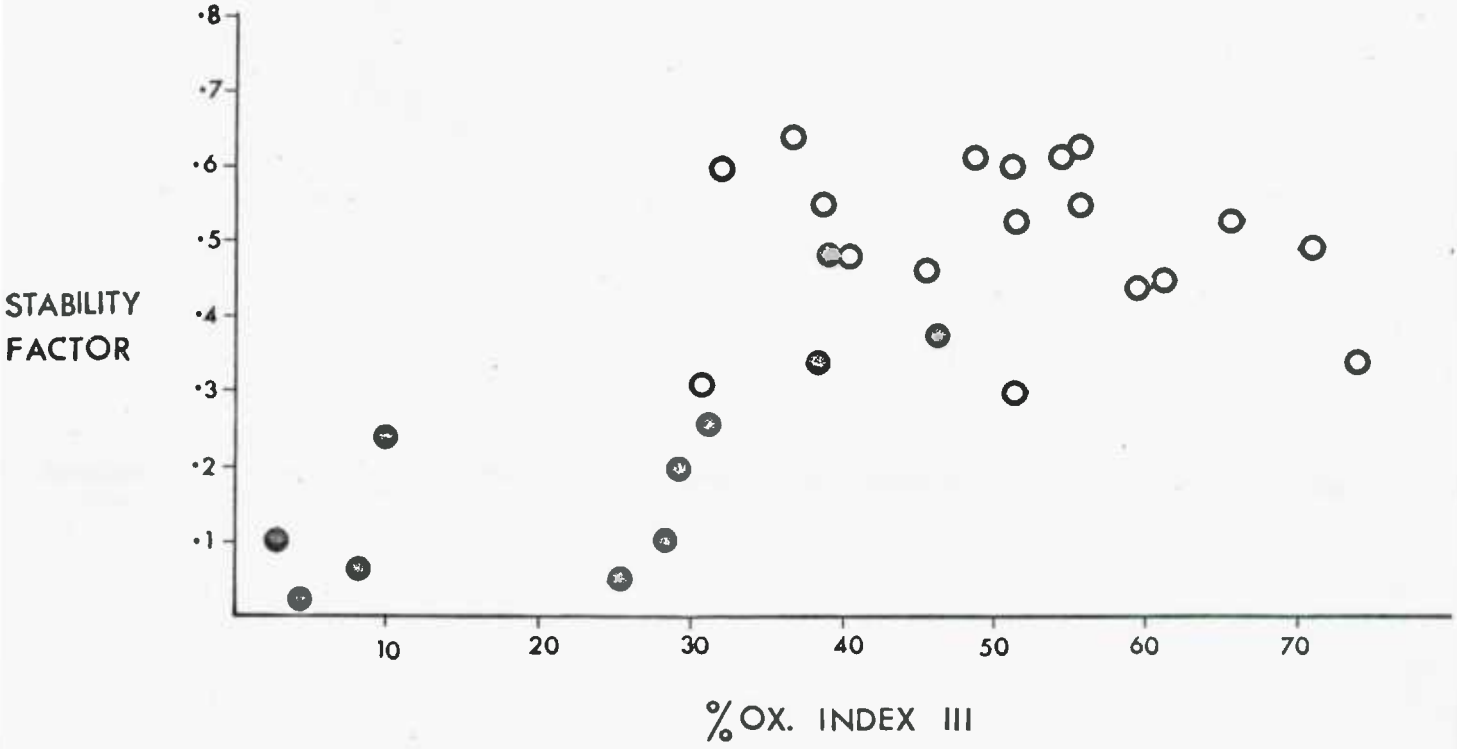

● UPPER GROUP OF SPECS.
○ LOWER " "

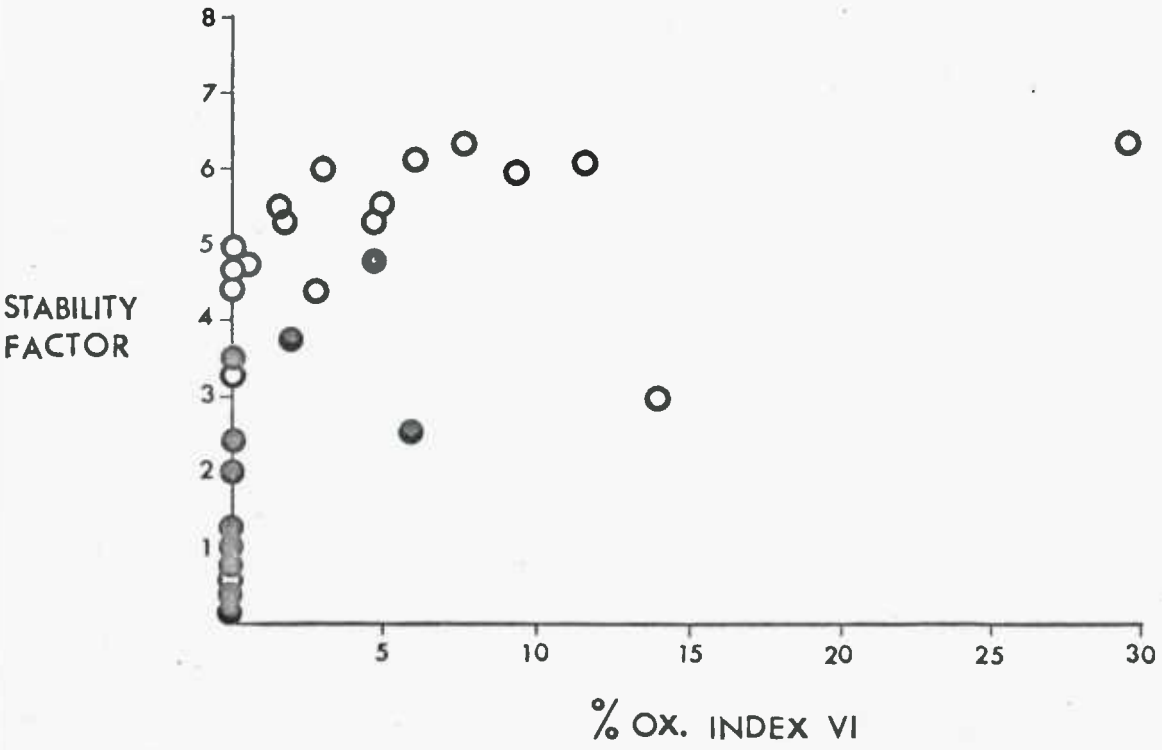

Fig 16.7

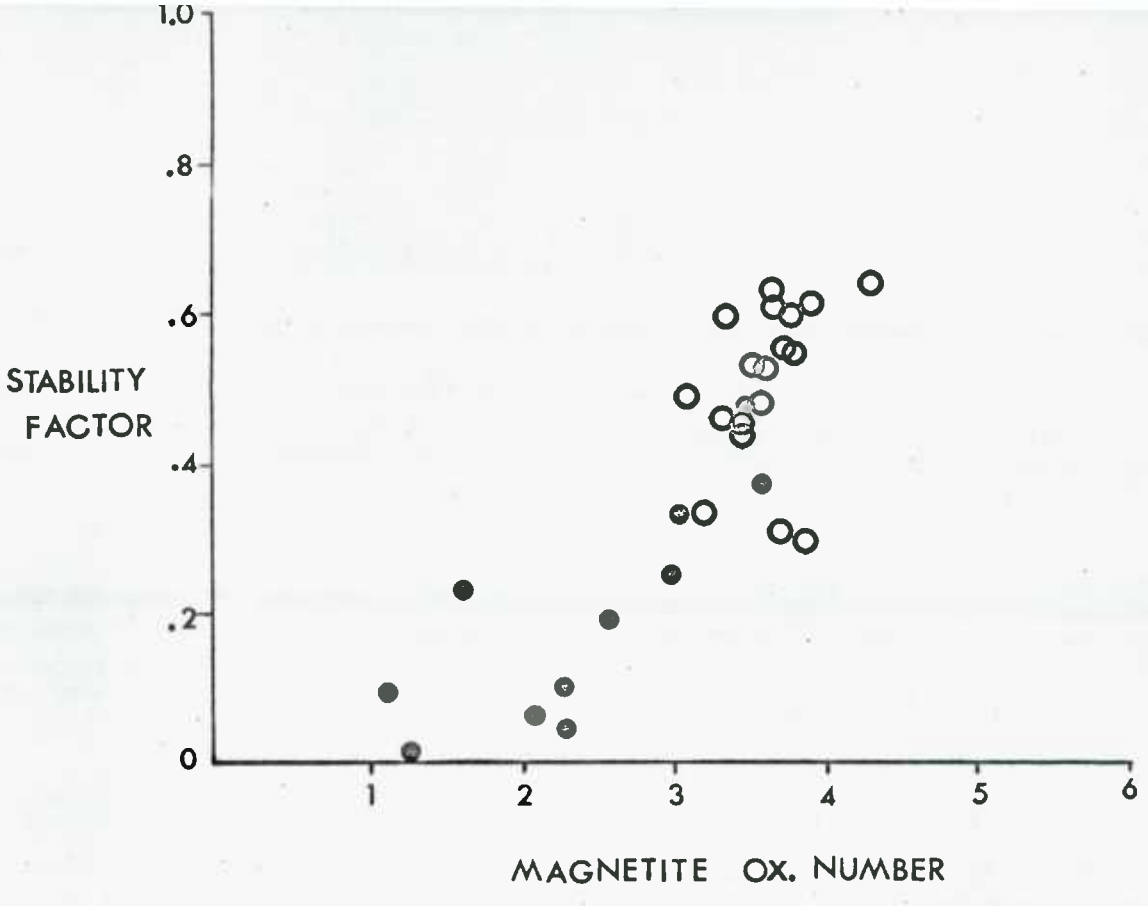

(a)

● UPPER GROUP OF SPECS.
○ LOWER " "

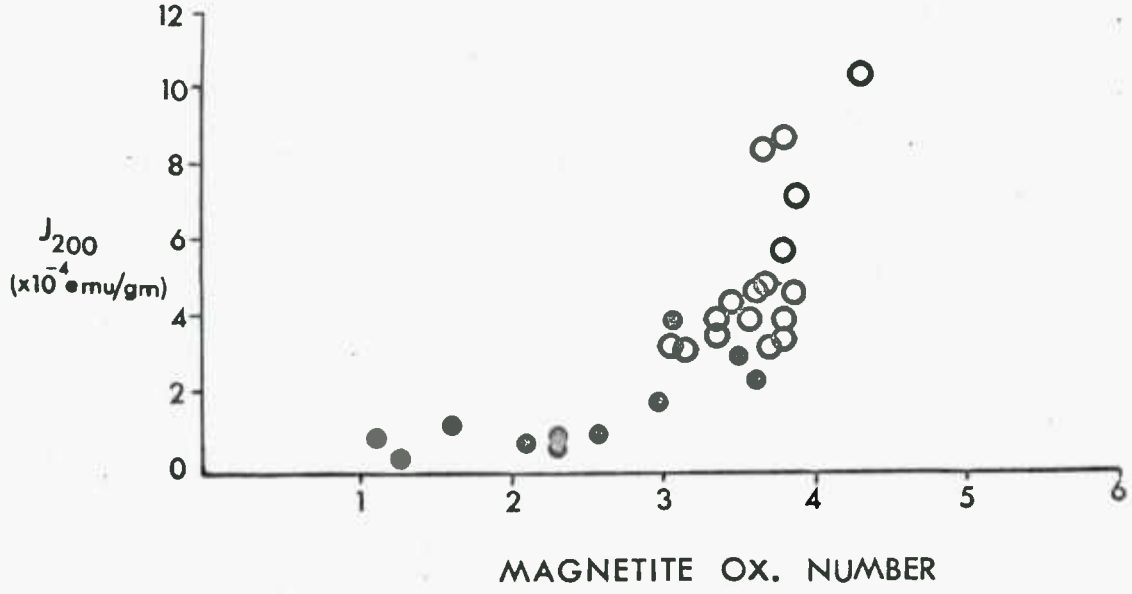

Fig 16·8(b)

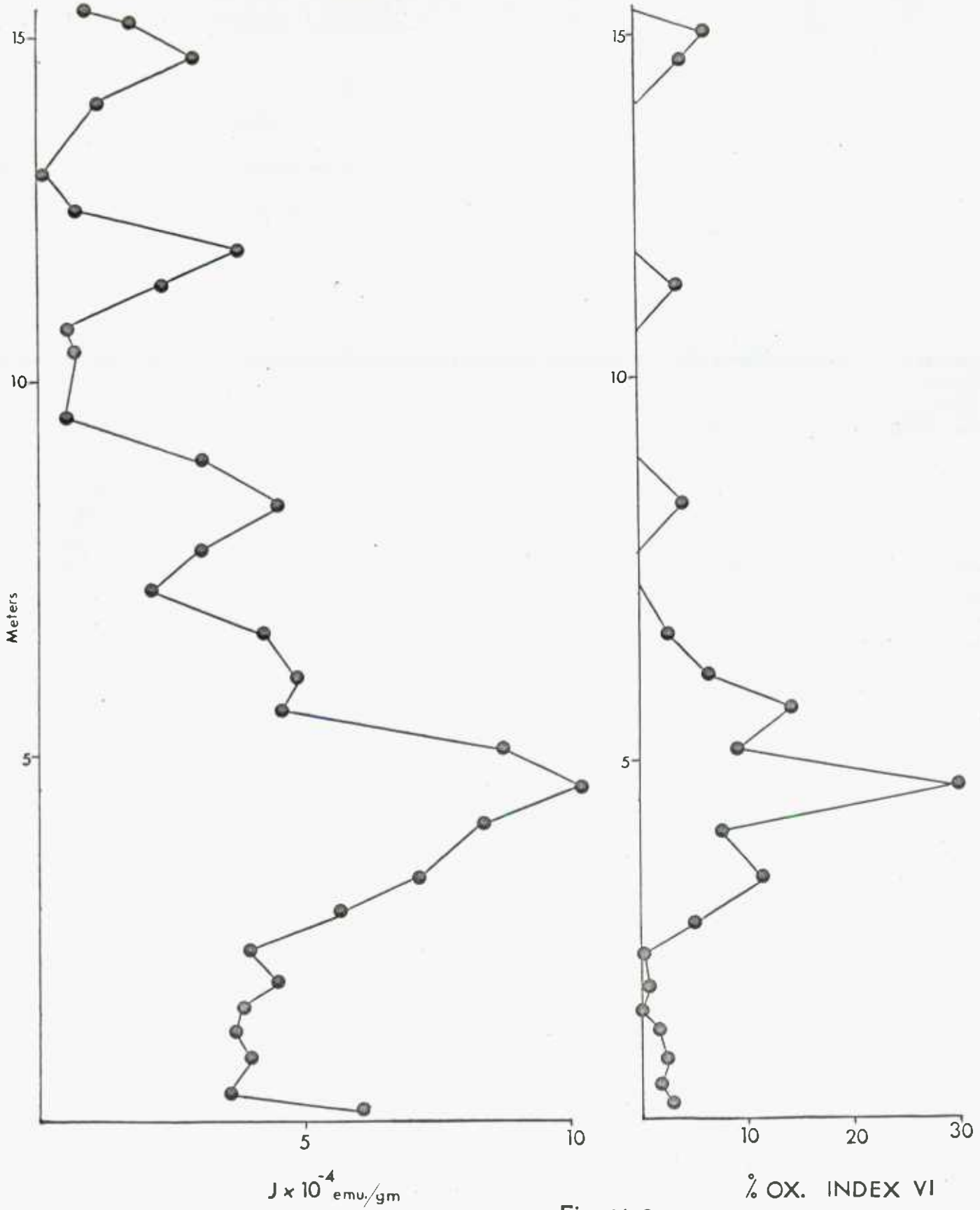

Fig 16·9

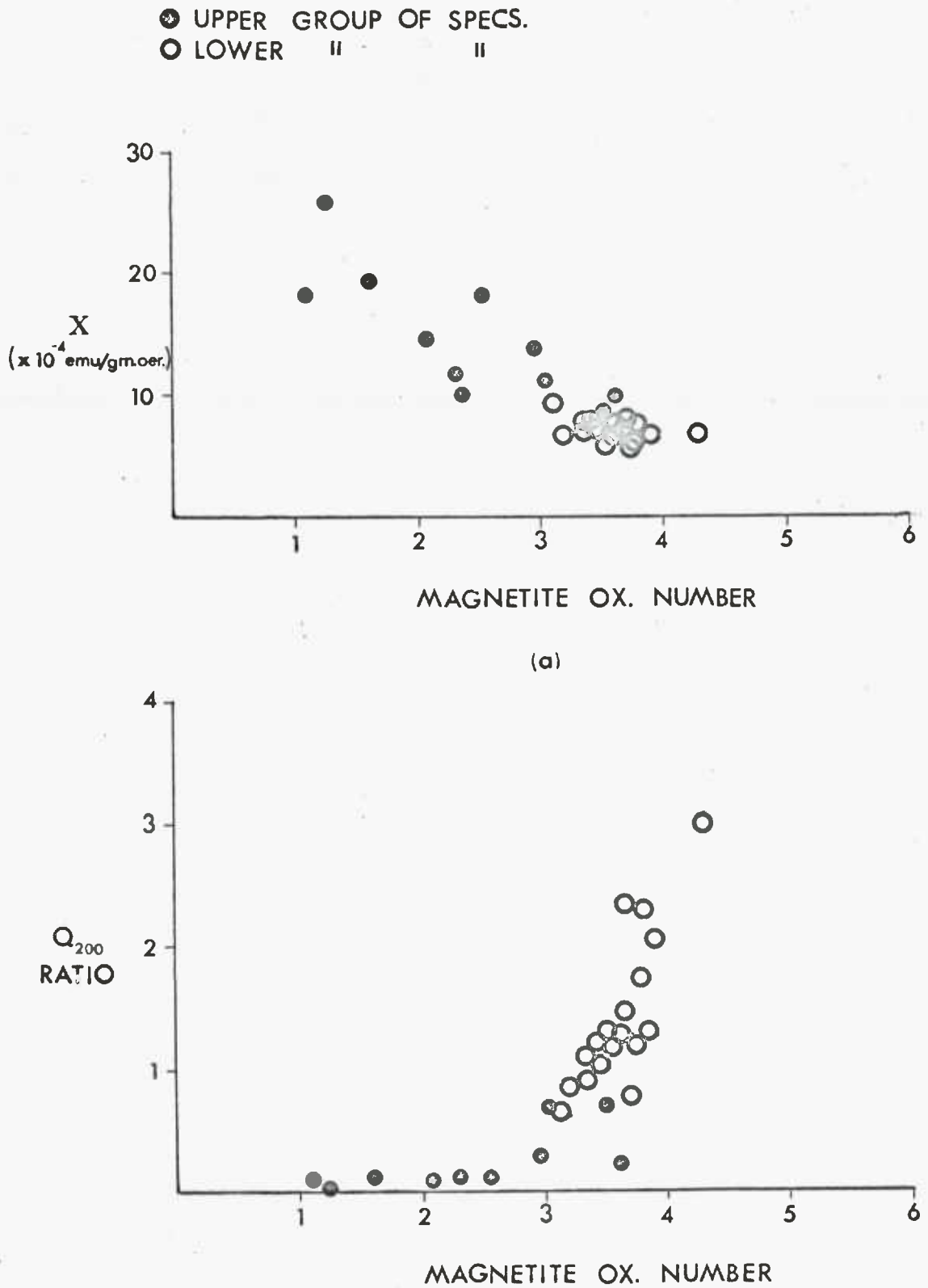
UPPER GROUP OF SPECS.
LOWER " "
30
20
10
X
(x 10⁻⁴ emu/gm.oer.)
1
2
3
4
5
6
MAGNETITE OX. NUMBER
(a)
4
3
2
1
Q200
RATIO
1
2
3
4
5
6
MAGNETITE OX. NUMBER

Fig 16.10(b)

CHAPTER 17

RESULTS FROM OTHER LAVAS

In detail, each lava is slightly different in petrological character and in its magnetic properties. The broad generalities, of oxidation zones, distribution of zones within a lava, and the correlation between certain magnetic properties and the state of oxidation of the Fe-Ti oxide minerals, still hold for the remaining lavas.

17.1 Mineralogy and Petrology

All the lavas are moderately rich in olivine and are characteristically basaltic in composition. All show a fairly constant grain size towards the central parts of the lava and all contain skeletal crystallites towards the outer margins.

No exceptions were found to the classification system, in spite of the variations, in opaque mineral content, in the ratio titanomagnetite: ilmenite and in the state of oxidation of the respective transverses. The present study, which has allowed the systematic changes in oxidation to be progressively followed, suggests that a seventh oxidation class should be introduced to distinguish the incipient development of pseudobrookite from complete pseudomorphs, as is the case for discrete ilmenite.

The problem of sandwich and composite inclusions of ilmenite in titanomagnetite has been dealt with in considerable detail (Chapter 6.4.3 page 146) and from this earlier study it was hoped that these textural forms would show some positional or oxidational characteristic which would further distinguish them from the trellis type. The data available at present suggest that the various textural forms of ilmenite do not vary systematically within the flow. Unfortunately, interpreting highly oxidized pseudomorphs in terms of their primary or intermediate textures is an extremely difficult task and so, although some characteristic distribution may exist, it is somewhat obscured by the effect of superimposed oxidation.

In the case of titanomaghemite, the general principle that it is confined to type I, II or III titanomagnetite grains is strongly confirmed. There does not seem to be a positional preference for maghemitization in terms of depth within the flow but its presence is characteristically associated with those zones which have escaped high temperature oxidation. In all cases ilmenite is unaffected. These remarks apply equally to the distribution of "amorphous Fe-Ti oxide" which is derived from titanomaghemite.

It is a surprising feature that simple "martitization" (i.e. the oxidation of $Fe_3O_4 \rightarrow Fe_2O_3$) does not occur more extensively as a low to intermediate temperature oxidation product. It has been argued that the presence of titanium seems to favour the formation of maghemite rather than hematite at these lower temperatures. Grains in the class III state of oxidation do of course have titanium - poor magnetite hosts, so the argument is not entirely valid. In fact specimens from the absolute tops of lavas do sometimes show (titano) hematite as an oxidation product. It is interesting that in these cases it migrates along controlled (111) planes which is typical of this form of oxidation. It is considered that this may be evidence for partial reheating, and has certainly been proved in material from the regional collection. The temperature of formation would be below that of pseudobrookite (585°C) and above that of maghemite 250-550°C. Ilmenite remains unaffected.

Specimens from the base of a flow present a rather special problem. In the field the base is frequently rather blocky and it is invariably highly vesicular. Classification of the Fe-Ti oxides is made extremely difficult by its fine grain size, and also by the fact that the type of oxidation assemblage is somewhat different from that of any other part

of the lava. There is usually a predominance of titano-hematite rather than the characteristic pseudobrookite and associated rutile. The silicates at the base are also rather badly altered but this always applies only to the specimen from the absolute base. In polished section, and in particular under an oil immersion lens , the entire surface appears intensely red, calcite, zeolites and thin hematite stringers along the grain boundaries and around vesicles are also all common features. FAWCETT (1965), describing the variation in olivine and pyroxene alteration throughout a Mull Tertiary lava, observed that ferromagnesian minerals were replaced by calcite at the base of the flow and he attributed this to the effect of "boiling mud" from below the lava at the time of extrusion. Several of the Icelandic lavas are underlain by tuffs and lateritic soils and however chemically inert these may be regarded to be it seems probable, nevertheless, that the underlying rock may still exert some influence on the process of oxidation at the base, while the lava is cooling. These underlying rocks are always solidly baked and are intensely oxidized. Since the base of the lava is rapidly chilled on extrusion, the observed differences may well be related to the period of time involved during which active oxidation takes place.

The earlier suggestion that hematite in olivine is characteristically associated with index V assemblages and that symplectic magnetite is associated with index VI assemblages is borne out in all the remaining lavas.

The olivine-rich lavas contain an abundance of Cr-spinel inclusions which are unaffected in zones I-V but become highly oxidized in zone VI.

Sulphides are almost totally absent in the lavas, but occasionally fine disseminated specks of pyrite occur in the interstitial, glassy groundmass.

17.2 Oxidation Zones

In all cases the state of oxidation of the Fe-Ti oxide minerals is extremely variable throughout vertical tranverses across the lava. The thinner lavas tend to have a far more uniform state of oxidation than the thicker lavas. In general, the exception being lava HS, the state of oxidation within single samples can usually be classified quite simply by a single oxidation index number on a scale of I-VI because most grains tend to reach the same level of oxidation within a restricted zone, in this case the diameter of the polished section - 2.5cms.

The vertical variation in oxidation of all lavas, S, MS and HS are included for comparison, is shown in Figure 17.1.

The most striking feature of these oxidation profiles is that, with one exception, the maximum state of oxidation is away from the edges of the lava. In most cases this maximum zone of oxidation is towards the centre of the lava but its position may vary by a distance of one third to two thirds from the base. The zone is usually flanked by transitional oxidation zones which grade into lower oxidation horizons towards the upper and lower margins. Most lavas are limited to one zone of maximum oxidation. The zones vary in width, but this does not appear to be a function of lava thickness.

The one lava (HS) which does not conform, in having the central high oxidation zone, is one of a series of Post-Glacial flow units from Ásbergi (North Ireland). The field relationships suggest that the interval of time between lava extrusions was extremely short and in fact some contacts in the series can only be defined on the basis of vesicle distribution, and a thin red colouration at the upper and lower edges. It will be shown in the following section that the zones of oxidation are related to their cooling histories. In the case of this lava its thermal pattern would have been somewhat disturbed by the outpouring of another flow immediately above it. This upper maximum should be seen therefore in the context of a group of lavas cooling as one unit, rather than separate flows with individual patterns. Had this

upper maximum been recognised in the field, the lava above it would also have been sampled for a similar single unit study.

The spectrum of oxidation (I-VI) is greater in the thick lavas than in the thinner lavas. Low states of oxidation are relatively rare (I - homogenous titanomagnetite, homogenous discrete ilmenite). Of the 15 traverses only one lava (LS) has more than half (51.5%) of its specimens in this state, and two lavas do not contain a single specimen which would be classified as oxidation index I. The maximum index of oxidation reached by each lava is plotted as a function of lava thickness in Figure 17.2. There is a reasonably good correlation suggesting that although thin lavas may in general have relatively lower levels of (deuteric) oxidation, such states may not be expected to occur throughout thicker lavas.

17.3 Magnetic Properties and Mineralogical Correlations

Seven of the lavas have normal directions of magnetization and eight have reversed directions (the latter include two traverses from the same lava, S and MS). The variation of the magnetic parameters between lavas is high, but the variations within lavas, although variable, are strongly dependent on the state of oxidation of the Fe-Ti oxides. All the magnetic-mineralogical correlations previously discussed are found to hold for the remaining lavas.

Stability has been found to be directly related to high temperature oxidation, and is less influenced by the presence of titanomaghemite or the effect of overall grain size.

There are no major magnetic differences (e.g. stability, intensity of magnetization, susceptibility) between lavas of normal or reversed polarity. The Post-Glacial lavas (AS-DS), which have normal directions, as may be expected, are magnetically more stable than the other lavas.

Two, thick normal lavas (KS and LS) are shown in Figure 17.3. The natural intensity of magnetization is matched against the oxidation index as a function of depth. The correlation is good and compares well with the reversal lavas discussed previously. For comparison, two thin lavas are shown in Figure 17.4, one normal (ES) and one reversed (ES).

One final point needs to be made with reference to samples at the absolute base, a problem already referred to in this section. In most cases the intensity of magnetization is much lower than the intensity which the state of oxidation would indicate, relative to other samples within the same lava. The fine grain size, the presence of large percentages of titanohematite and the overall oxidation appearance probably means that the index of oxidation is being over-estimated.

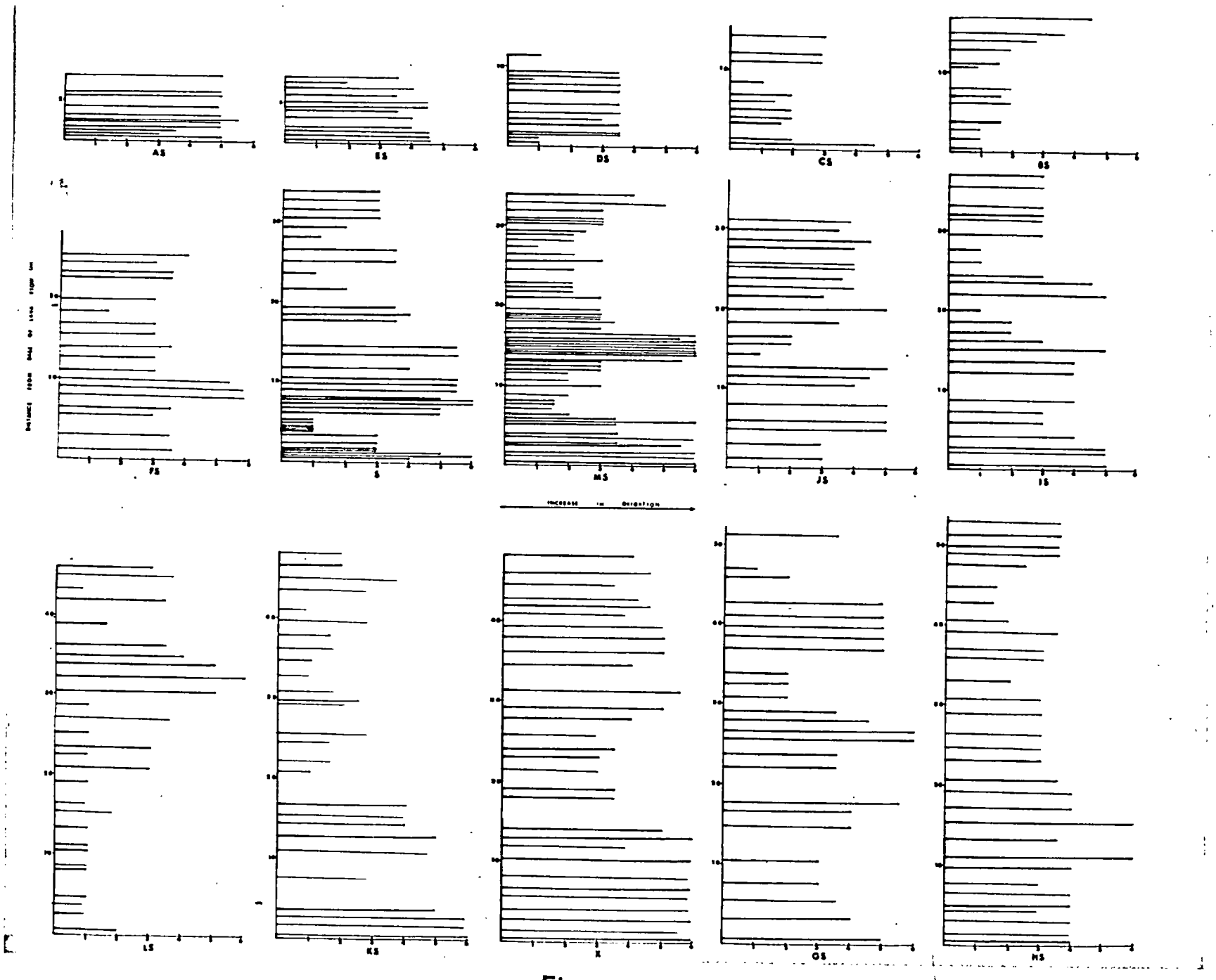

Fig 17.1

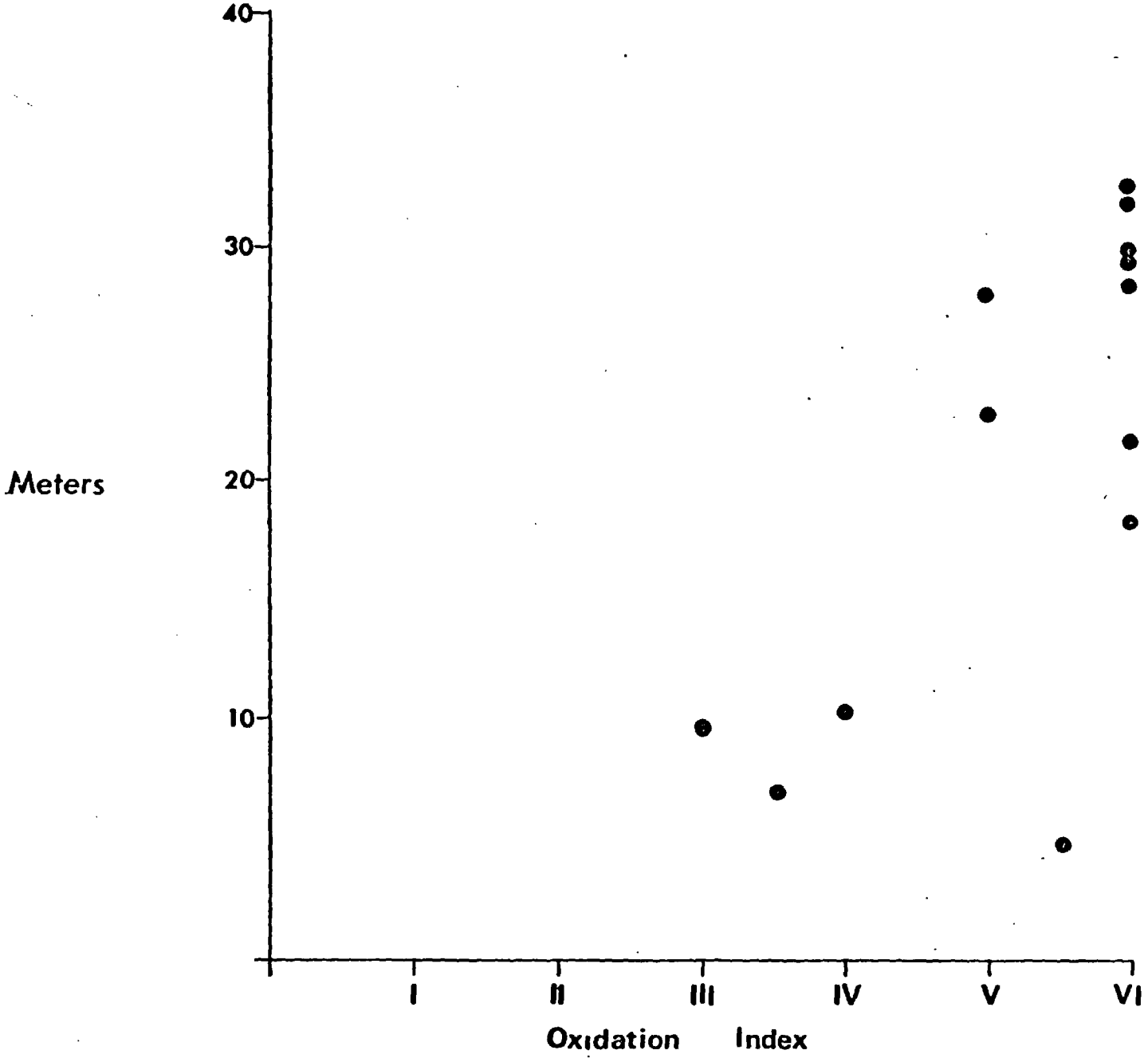

Fig 17.2

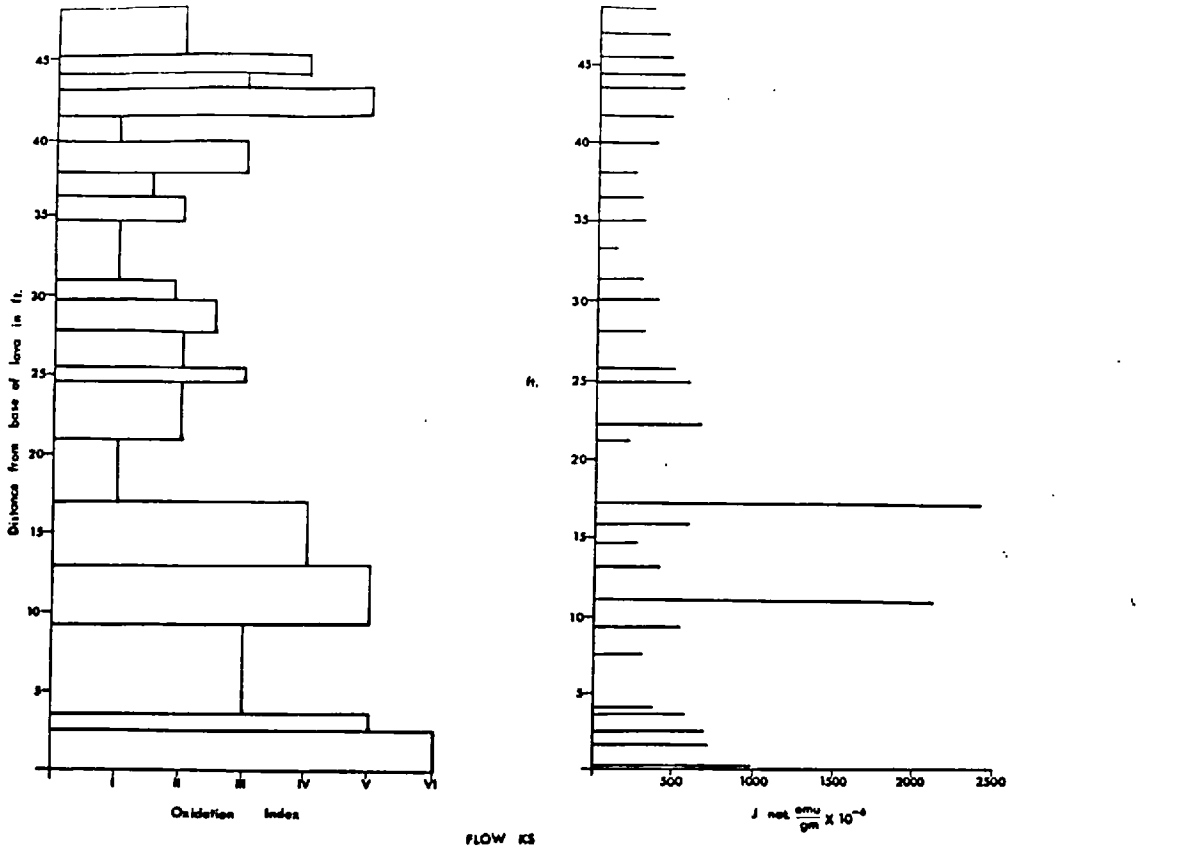

FLOW K5

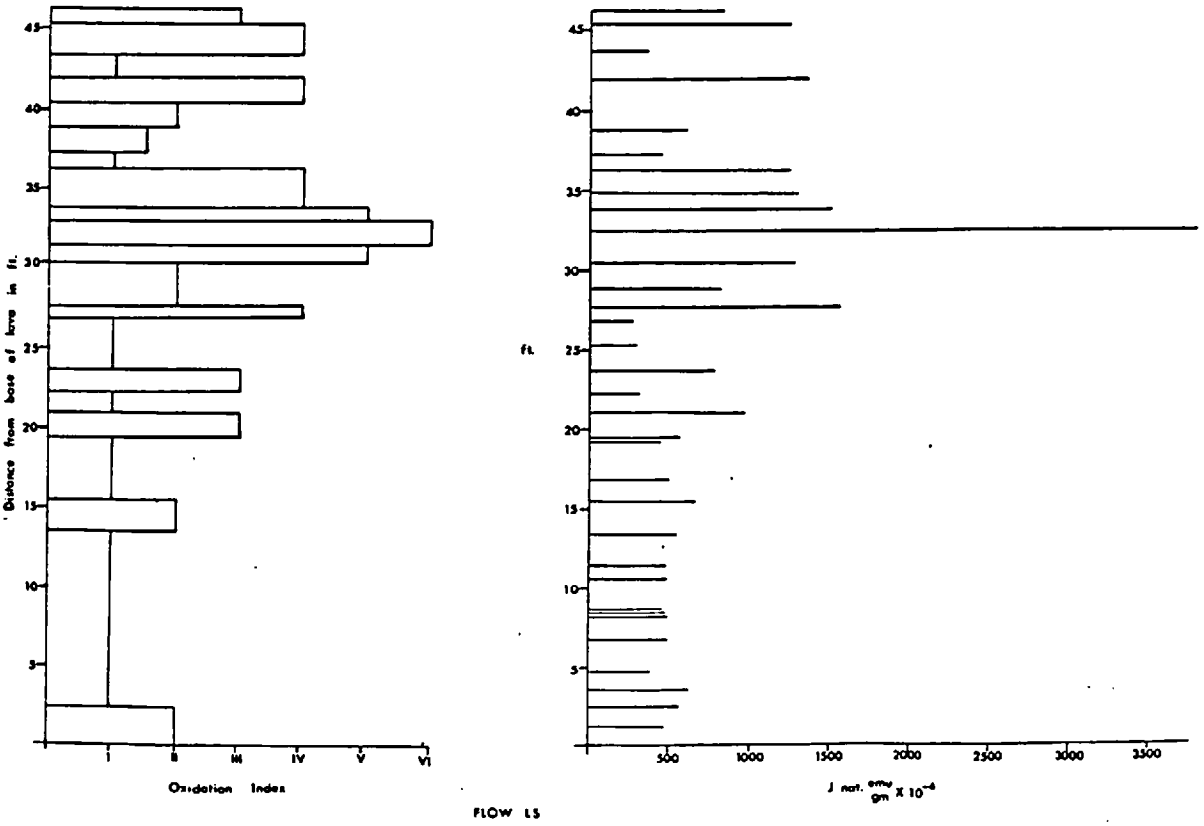

FLOW L5

Fig 17.3

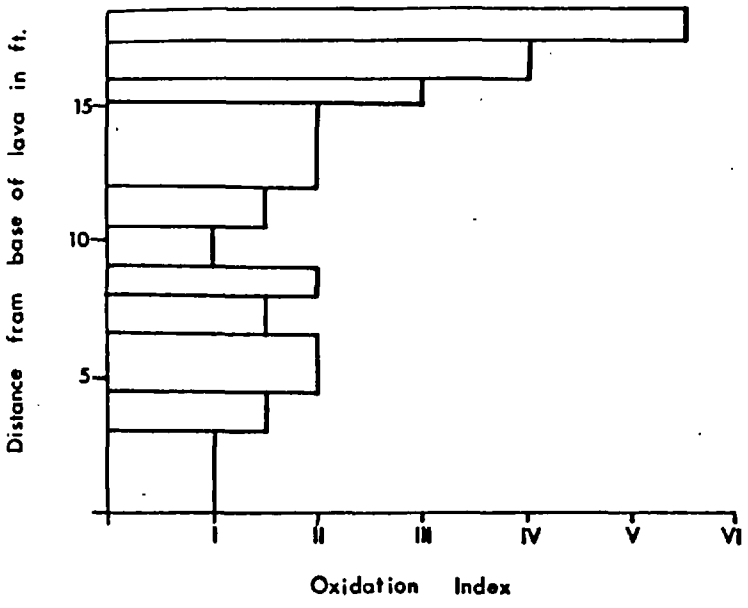

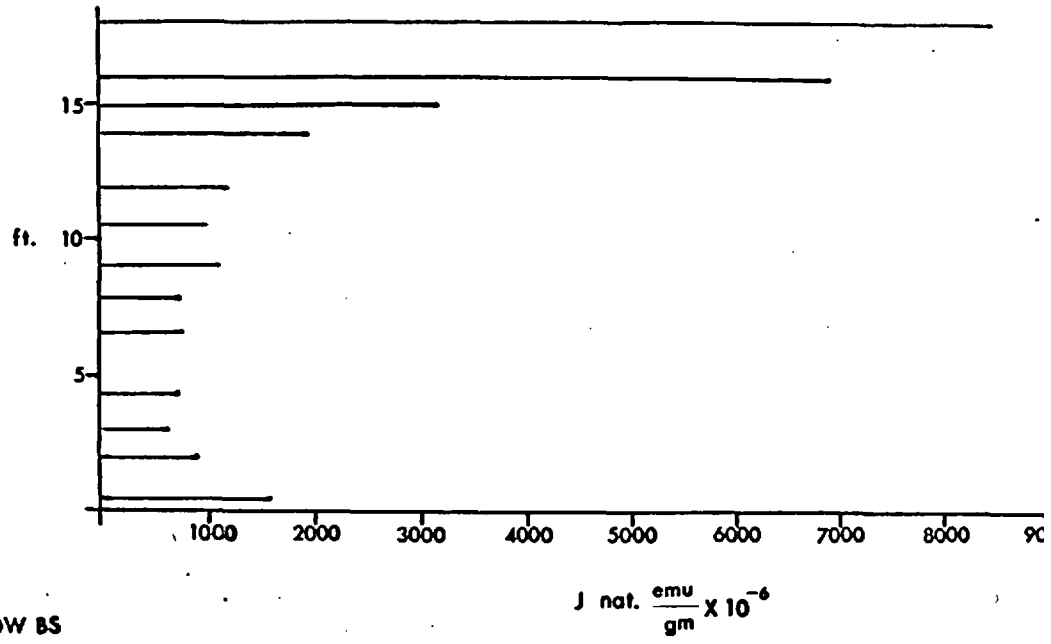

FLOW BS

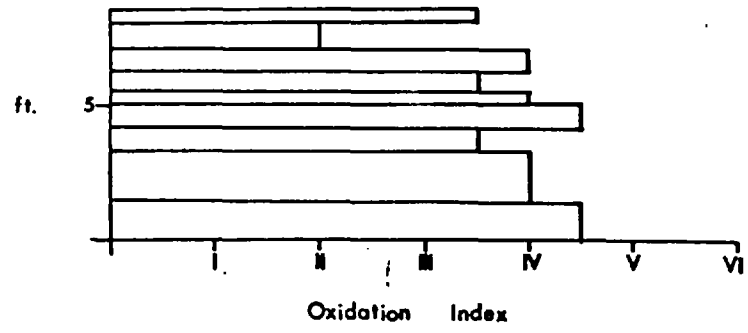

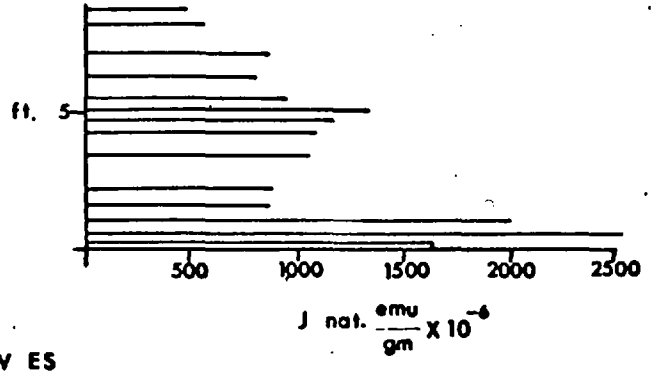

FLOW ES

Fig 17.4

CHAPTER 18

DISCUSSION AND CONCLUSIONS

18.1 Oxidation and Distribution of Fe and Ti

The importance of oxidation processes in petrogenesis has been stressed by many petrologists. There are three fundamental processes of oxidation which are commonly operative and these all have profound effects on the Fe-Ti oxides. Broadly these may be classified as (a) magmatic oxidation (pre-extrusion), (b) deuteric oxidation, and (c) post-depositional or post-cooling oxidation.

18.1.1 Effects of pre-extrusion oxidation

KENNEDY (1948) and OSBORNE (1959) have shown that the oxidation state of iron has an intense effect on the crystallisation history and therefore on the differentation trends in basaltic magmas. The partial pressure of oxygen in the melt controls the amount of titanium which will enter an Fe-Ti oxide solid-solution series, and also has a controlling effect on the distribution of titanium between oxides and silicates.

KENNEDY (1948) has shown experimentally that in a basaltic magma crystallizing at high pressures of oxygen, much of the iron is converted from the ferrous to the ferric state and among the first phases to appear, at approximately

1280°C, is a member of the magnetite-magnesioferrite (Fe_3O_4 - $FeMg_2O_4$) solid solution series. The spinel comes out in great abundance and impoverishes the liquid in both iron and magnesium. The early precipitation of spinel enriches the residuumin silica and the familar BOWEN differentiation trend follows.

If, on the other hand, crystallisation takes place in an environment of low oxygen pressures (high FeO/Fe_2O_3) no ferric iron, and thus no spinel is formed. The residuum is enriched in iron and magnesium, and the basaltic magma does not proceed in a granitic direction, but instead proceeds towards a ferrogabbro, following the Fenner trend. In the Skaergaard intrusion, for example, it was not until 70% of the whole magma had crystallised, that sufficient ferric iron had accummulated for the active precipitation of Fe-Ti oxides (VINCENT 1954). By this stage a great part of the available magnesium had already been removed in the earlier olivines and pyroxenes.

The distribution of titanium between silicates and oxides has been discussed by VERHOOGEN (1962). When silicates and iron oxides coexist, titanium will preferentially enter the oxide phases at low partial pressures of oxygen, forming members of the Fe_2TiO_4 - Fe_3O_4 and $FeTiO_3$-Fe_2O_3

solid-solution series. TiO_2 has about the same affinity for MgO and FeO; it has a larger affinity for CaO and none at all for SiO_2. Titanium will enter the silicates during the stage of crystallisation preceeding the appearance of the iron oxides, and will also enter under high partial pressures of oxidation, when primary Fe-Ti oxides are present. The entry of titanium into pyroxene, in particular, is determined by the "free energy of mixing" and is therefore possible only at high temperatures; the higher the temperature of crystallisation of pyroxene, the more titanium it is likely to contain. Iron-bearing pyroxenes are not expected to contain much titanium, since they would break down in the presence of TiO_2 to form ilmenite. Titanomagnetite and ilmenite, resulting from an equilibration process of this nature, have been observed in pyroxenes in phonolites from Teneriefe. Plate 13.14 contrasts "titanium-reacted" pyroxenes and amphiboles in unoxidised lavas, with pyroxenes which have suffered dueteric oxidation. In the latter case the discrete Fe-Ti oxides are also highly oxidized.

In considering the primary oxidation effects on the crystallization of individual mineral phases, it is evident that in the case of the Fe-Ti oxides, at high pressures of oxygen, members of the ulvospinel-magnetite solid solution series are more likely to form than members of the ilmenite-

hematite solid solution series. Secondly, LINDSLEY (1963-4) has shown that, in the system $FeO-Fe_2O_3-TiO_2$, at low oxygen partial pressures, more titanium is likely to enter into an individual solid-solution series than at high partial pressures; that is, ulvospinel-rich members will form in preference to magnetite, and ilmenite-rich members will form in preference to hematite. Furthermore, there is a systematic decrease in the range of TiO_2 (and equivalent Fe_2TiO_4) in magnetite from basalts through to rhyolites.

In summary, at high partial pressures of oxygen, opaque oxides will form in preference to iron-rich silicates. At low partial pressures, the potential opaque and silicate phases will compete for the available iron and titanium. When one considers the opaque phases only, high partial pressures of oxygen favour the formation of the ilmenite-hematite solid-solution series and low partial pressures the ulvospinel-magnetite series. Within each series, the titanium-rich end-members (ulvospinel and ilmenite) will prevail at low partial pressures.

18.1.2 Deuteric Oxidation

The term deuteric oxidation was originally defined by SEDERHOLM (1929) as "oxidation which takes place in direct continuation of the consolidation of the magma of the rock

itself". Unfortunately, the type of mineral assemblage which is likely to form under these conditions, in an igneous rock, is not uniquely identifiable in terms of the process. The process has a wide temperature range and all one can say is that effective oxidation may be expected to be greater at higher temperatures.. Oxidation becomes effective the moment crystallization ceases, which in itself is indefinable, and continues until the lava is thoroughly cooled. It is unlikely, however, that any process other than deuteric oxidation, or oxidation induced by direct-contact reheating, by another igneous body, will be active above 600 ^{o}C. Knowing the thermal stability of a mineral assemblage therefore may give some hint as to its origin. Other factors, such as the systematic oxidation zoning of recent lavas, may also lend support to a process of deuteric alteration.

18.1.3 Post-Crystallization Oxidation

This form of oxidation may result from supergene weathering, from processes of burial, from hydrothermal or pneumatolitic activity or from thermal and dynamic metamorphism. Field relationship studies can obviously help in eliminating one or several of these possible processes when deciding upon the origin of a secondary mineral assemblage. But once again the final assemblage may not be entirely

characteristic of the process. In this study the processes of weathering and burial are considered to have a negligible effect on the igneous mineralogy. Since these processes are of the low to intermediate temperature range some confusion may still arise in distinguishing an assemblage derived from low temperature deuteric alteration from one derived by a process of burial or weathering.

18.2 Origin of the Oxidation Zones

Since it has now been demonstrated that the magnetic properties are strongly dependant on the state of oxidation of the Fe-Ti oxides, and since these are highly variable within single lavas, it is important to know whether oxidation takes place deuterically (i.e. during the initial cooling) or at some indeterminate time later (hydrothermal activity, burial, weathering). This point is critical because we need to decide whether the magnetization records the field (and its polarity) during the initial cooling, or whether perhaps the oxidation process remagnetizes the lava at a later date ina field which is possibly of different polarity.

The position of the maximum oxidation zones towards the central part of a lava, the fact that the oxidation profile is asymmetrical about the edges of the flow, the observation that transitional states of oxidation exist on either side

of the maximum, and the mineral evidence that it is a high temperature oxidation, all strongly suggests that oxidation takes place deuterically at the time of cooling.

If oxidation was caused by some external process then one might expect the upper and lower margins of the flow to be more highly oxidized than the interior. After all, the contacts are easily accessible and in addition are vesicular and highly porous.

The high temperature nature of the oxidation phases, in particular "oxidation-exsolution" of ilmenite in titanomagnetite and the formation of pseudobrookite, suggest that the temperature of maximum oxidation must have been near to, or in excess of 600°C. Effective sub-solidus oxidation of titanomagnetite falls off sharply below this temperature (BUDDINGTON and LINDSLEY 1964) and it has now been established from heating experiments on titanomagnetite and ilmenite (this study) and from LINDSLEY'S 1965) synthetic stability work that pseudobrookite cannot form below 580° ± 15°C. Further, the assemblages (a) rutile + titanohematite and (b) pseudobrookite + titanohematite, as high temperature products of ilmenite, form an important contrast to the murky amorphous products (e.g. "leucoxene") that develop during supergene weathering (see Appendix I).

Co-existing with high states of oxidation in the Fe-Ti oxides one finds that olivine and Cr-spinel are also in advanced states of oxidation. The oxidation products have been reproduced in heating experiments and their high temperature nature has been confirmed.

More significant than any of the above features perhaps, is the fact that when unoxidized samples from the edges of a flow are heated in an oxidizing medium, above 600°C, the textures and mineral phases of the central oxidized interior are replicated.

Temperatures as high as 600°C are unlikely to develop under conditions of burial but may, in exceptional circumstances, be operative during hydrothermal activity. The lavas were carefully chosen for this study so that major disturbed areas, areas in regions of high density dyke swarms, and areas in the vicinity of central volcanoes, were deliberately avoided to minimise the risk of secondary alteration.

The zones of maximum oxidation cannot therefore be due to any process of weathering, but weathering has undoubtedly played some part in oxidizing those zones which remained unaffected by the high temperature process. Titanomaghemite plays the most important role in this respect and since it is

known to be metastable well below 600°C we can place an upper limit on its temperature of formation. The problem arises, however, that in these circumstances it is impossible to distinguish a low temperature deuteric effect from a low temperature weathering or hydrothermal effect. The fact remains that evidence for the transformation of γFe_2O_3 to αFe_2O_3, has been systematically searched for but has, as yet, not been detected, suggesting that later reheating effects (i.e. above 550°C), to produce the central zone, may be completely discounted. Preferential reheating towards the centre of a body is an unlikely event anyway.

With reference to the asymmetry of the oxidation zones, in relation to the edges of the flow, we (WATKINS and HAGGERTY 1965) originally suggested, on the basis of one lava only (No.S), that the position and distribution of the oxidation zones was probably controlled by the rate of deuteric cooling. A quantitative analysis was made of the temperature distribution at various times during the cooling history of the lava using the constants and theory by JAEGER (1961) for extrusive sheets. For this lava several generalities emerge: during the first three months of cooling, virtually no decrease in temperature occurred at the centre of the lava; a maximum temperature of 100°C in any part of the lava did not occur until six years after the beginning of

cooling, assuming that its initial extrusion temperature was 1000°C; and the section of the lava which remained hottest for the longest period of time was towards the lower third of the flow. An example of the 650°C isotherm after 58 weeks is shown in Figure 18.1c and is matched with the oxidation and intensity profiles previously discussed. The second profile (MS) from this lava (Figure 15.1) shows that although they are essentially similar in both having central zones of high oxidation, in detail the profiles are somewhat variable. Whether this is due partly to thermal convective turbulence, a variable rate of chemical reaction, or some entirely different process, is not known. The fact that some lavas have maximum zones of oxidation one third of the distance from the top of the flow and also that thinner lavas do not behave in the same oxidation manner as thicker flows may mean that the 650°C isotherm is not greatly significant; the coincidence of the oxidation profile is nevertheless quite remarkable, especially in view of the upper (titanomaghemite) and lower (pseudobrookite, rutile, olivine symplectic magnetite) thermal stability limits of the phases involved.

In considering the possible origins for oxidation in these lavas it is of general interest to note that the Fe_2O_3 : FeO ratio is commonly much higher in <u>acid</u> igneous rocks, that have consolidated at relatively low temperatures,

than in basalts which have cooled from a relatively high temperature. The ratio is also higher in slowly cooled gabbros than in basalts (VERHOOGEN 1962). CORNWALL (1951) has suggested that in deep-seated intrusives, the partial pressure of oxygen builds up as the total volatile pressure increases during crystallization, but in lavas the total volatile pressure is low and nearly constant because the lavas are not a closed system and are exposed to the atmosphere. In general terms this is probably correct but as KENNEDY (1955) points out, even if the total volatile concentration is constant throughout, partial pressures will nevertheless be higher in hotter portions of the "magma" than in the cooler marginal portions.

Undoubtedly the most valuable contribution that has been made in recent years to the problems of oxidation in lavas is the work by the U.S. Geological Survey on the now actively cooling and crystallizing lava lakes of Hawaii (RICHTER and MOORE, 1966; PECK, WRIGHT and MOORE 1966; SATO and WRIGHT 1966). The work is chiefly petrological but it has been demonstrated, by taking in-situ measurements of the oxygen partial pressure, that zones of high (deuteric) oxidation exist within these lava lakes. The temperature profiles show that the maximum pO_2 values are obtained in the range 550 -750 °C. These zones migrate downwards as the lava cools

and the rate of migration corresponds with JAEGERS (1962) theoretically predicted rate. RICHTER and MOORE'S (1966) results show the descent of isotherms below 600°C is virtually linear during the early periods of cooling whereas the isotherms above 600°C are relatively steep, but these show a marked tendency to flatten with time (see for example Figure 18.1c - Lava S).

A highly significant fact emerges from SATO and WRIGHT'S (1966) pO_2 data. Except for the "amomalous", maximum high oxidation zone, all measured po_2 values fall within the stability field of magnetite. The stability boundaries are those according to the data of EUGSTER and WONES (1962). The maximum pO_2 values are of the order of 10^{-5} atm. The pO_2 probe data from the bore-holes has been checked by Fe_2O_3 : FeO ratios on core samples. Unfortunately the effects of oxidation on the mineralogy have not yet been fully investigated but the core section from this highly oxidized zone is intensely red. WRIGHT reports that a megascopic examination shows ilmenite to be tarnished and from a thin-section examination, olivine is red and contains opaque stringers. In view of the high pO_2 reached in this zone and from these descritions it seems entirely probable that ilmenite is oxidized to rutile + titanchematite, or pseudobrookite + titanohematite and that the olivine contains hematite or

symplectic magnetite.

Water is known to be a major volatile component in igneous rocks and it has been variously suggested that oxidation becomes effective once the water has dissociated into hydrogen and oxygen. EUGSTER (1959 and pers. comm. 1966) points out that the dissociation of water does not in itself control the pO_2 but depends either on a solid-state assemblage (e.g. an oxygen buffer such as magnetite-hematite, or quartz-magnetite-fayalite) or on the bulk composition of the gas phase. The gas phase appears to control the oxidation state of the solids rather than the other way around, so that the hydrogen: water (gas) ratio is the relevant factor. Hence, an oxidation maximum in a lava may be caused by a decrease in the $H_2 : H_2O$ ratio. Three obvious mechanisms are available: addition of oxygen, addition of H_2O, loss of hydrogen.

SATO and WRIGHT (1966) have suggested a model which is based on this mechanism. They propose that a certain horizon in the lava lake cools to the temperature range in which oxygen and water molecules can no longer diffuse through the basalt freely, while hydrogen continues to escape towards the surface because of its greater diffusion rate. In other words the basalt acts as a "semipermeable membrane" for

hydrogen in the critical temperature range 550-750°C. The preferential escape of hydrogen induces further thermal decomposition of water and locally generates high oxygen partial pressures which effectively oxidizes the surrounding basalt.

A significant point which is not made by these authors is the fact that the rate of hydrogen diffusion is going to be greatest in those parts of the lava which remain hottest for the longest period of time (viz. towards the lower central part of the lava). Loss of hydrogen in the way suggested by SATO and WRIGHT is attractive in terms of the Icelandic study because this means that although some parts of the lava are undergoing oxidation, other parts are being effectively reduced. This would account for the lower states of oxidation above the maxima and also, since the diffusion rate of hydrogen is probably rather delicately balanced, the asymmetry between profiles of the same lava.

It is also of interest to note that BUDDINGTON and LINDSLEY (1964) showed by consideration of the stability curves for magnetite-ulvospinel and ilmenite-hematite solid solutions, with respect to pO_2 and temperature, that in many igneous rocks sub-solidus oxidation of the cubic series to form members of the ilmenite series will take place as the temperature falls. EUGSTER (1959) has

calculated the effect of the pO_2 on a gas mixture having H:O = 2:1 and shows that the partial pressure decreases with decreasing temperature but decreases less rapidly than that of the assemblage hematite + magnetite; in other words the gas becomes more oxidizing with respect to the solids as the temperature decreases.

In conclusion, the high temperature zones of oxidation defined by the opaque Fe-Ti oxides, are deuteric zones of oxidation which have probably resulted from the preferential diffusion loss of hydrogen during the initial cooling.

The results obtained from the Iceland dyke study have not been considered in detail, but it is relevant to note that the dykes do not show the systematic zones of high temperature oxidation which are common in the lavas; nor do they reach the same degree of oxidation as the lavas. The maximum state of oxidation observed in any of the dyke samples was the index III assemblage. The dykes are characterised by high concentrations of primary sulphides and by a dominance of titanomagnetite over ilmenite. These factors all indicate that a relatively lower partial pressure of oxygen is operative in the dykes. It is considered that the significant differences in oxidation state are due partly to high confining pressures, which effectively inhibits

vesiculation, and partly to the monitoring of sulphurous volatiles in a "closed system" at depth.

18.5 Magnetic and Petrological Implications of Oxidation Zones

From the magnetic point of view there is at least a 50% chance that any part of a lava which is preferentially remagnetized at some later period will have a polarity direction which is different from the original direction. Since none of the present group of lavas have mixed (stable) polarities, we may assume that all parts of the lava have recorded a single ambient geomagnetic field direction which prevailed during the initial cooling. The fact that such a wide spectrum of oxidation may exist within a single lava, and the fact that only a single polarity is present, raises serious objections to the theory that there is a link between reversed directions of magnetization and oxidation; such correlations will be discussed in the final section of this thesis.

Other magnetic properties are strongly dependent on the state of oxidation of the Fe-Ti oxides and so, therefore, on the position of sampling within the lava. It is common palaeomagnetic practice to make spot determinations of magnetic stability in regional surveys, in order to choose a single demagnetizing field which would then be applied to

each of a collection of samples. This is obviously not recommended in view of the wide ranges of stability than can exist within a single lava.

The most serious petrological implications connected with these zones of oxidation is the problem of representative sample collection. Highly oxidized rocks are frequently rejected in geochemical studies, but transitional states of oxidation are more difficult to recognise and so these may frequently be included. It is well known, and it is also common practice, that normative calculations are " arbitrarily adjusted" to account for the effect of oxidation. This is all very well but the oxidation norm is usually taken from a regional study which in itself may be biased by the position of sample collection within a single unit. MacDONALD (1967), in his discussion of the chemical effect of oxidation in a single Soottish Carboniferous hawaiite, points out that there is a strong correlation between high oxygen content and normative hypersthene, and low oxygen content and normative nepheline. KUNO (1965) has stressed that the choice of sample material, for his study of fractionation trends in basalt magmas, was restricted to unoxidized specimens which were finally selected from polished section examination. The present study has also shown that thin section examination of the silicates is inadequate to detect the more subtle stages of oxidation which are manifest in the Fe-Ti oxides. KUNO's

specimens correspond, in terms of the optical classification, to oxidation index I.

Apart from obvious differentiation, oxidation is also considered to effect some control on the stability and mobility of both minor and major elements; iron is the classic example. Another example is the effect of oxidation on uranium and thorium. These latter elements have become increasingly more important in recent studies of upper mantle petrogenesis. The results may be misleading if the elements are sensitive to oxidation gradients, particularly if it is assumed that single samples are representative of the entire body. Thorium and Uranium concentrations have been determined on lava No.S. The determinations were carried by DR. C.W. HOLMES and the results have been reported by WATKINS, HOLMES and HAGGERTY (1966). Figures 18.2 and 18.3 show the distribution of the elements vertically throughout the flow and their relationship to the chemical oxidation index (Fe_2O_3 : FeO). The correlation is relatively good and the position of the maximum Th:U peak is strikingly similar to the optical oxidation index profile for this lava (Figure 15.1).

HEIER and ROGERS (1963) have pointed out the marked correlations that exist betweeen K and Th, and between K and U in oceanic as well as in continental rocks. If this dependance is partly a function of the oxidation state of the

rock it seems reasonable to speculate that radiometric K:Ar age determinations may be in serious error and these need, therefore, to be carefully scrutinized mineralogically before being fully accepted. In an unpublished report to PROFESSOR F.J. TURNER on a selection of dyke samples from southern Brazil, marked variations were found in the state of oxidation towards the centre of a dyke which appeared to correspond to the anomalously high K:Ar ages; in this case the effect was probably due to argon loss. A programme is now underway to date the oxidation zones of some selected Icelandic basalts from this study, to see whether any systematic correlation can be established between age and the state of oxidation.

18.4 Oxidation and Magnetic Polarity Correlations

It has now been firmly established that the geomagnetic polarity has changed at least eleven times during the past 3.5m.y (COX, DOELL and DALRYMPLE, 1967) and perhaps as many as sixty times during the past 20 m.y (DAGLEY et. al 1967). Because of the consistency of the polarity time scale data, it would appear that self reversal mechanisms are not common, at least in rocks younger than 3.5 m.y. unless of course the selection process involved in the isotope dating of basalts has led to the exclusion of such material from analysis. It would appear therefore that the self reversal process, by

which an igneous rock acquires natural remanent magnetism (NRM) antiparallel to the ambient magnetic field during the initial cooling, is extremely rare.

The present study and other studies (VERHOOGEN, 1962; MEITZNER, 1963) suggest that oxidation of the Fe-Ti oxide minerals controls and systematically influences the magnetic properties of rocks, and it has been shown further that there is an apparent link between high states of oxidation and reversed directions of magnetization (see Table 181 for summary of references).

These results are very difficult to explain, in view of the fact that the geomagnetic field has undoubtedly reversed its polarity, and therefore any self-reveral process would appear to be as likely to take place during a period of reversed polarity (to create an apparent normal polarity rock) as during a period of normal polarity (to create an apparent reverse polarity rock). The net result of this is that there should be no observable correlation.

There are at least two explanations for the correlations so far observed: either some unknown process is active only during periods of reversed polarity which enhances oxidation, or the observed correlations are accidental functions of sampling. Neither of these is entirely acceptable.

In the present study all units have a single polarity which is either normal (N) or reversed(R). Those units which have mixed NRM directions (N and R)isanindication that some portions of the unit are magnetically unstable; these superimposed magnetic effects are easily removed by demagnetization and the initial and stable TRM direction is the one which prevails throughout.

Since there are wide variations in the state of oxidation between units and also within the same unit it would suggest that the polarity-oxidation correlations are in serious jeopardy.

In spite of this apparent anticorrelation it was decided that the data should, nevertheless, be analysed, especially since LARSON and STRANGWAY (1967) have shown in their study, that no correlation exists between polarity and the coexisting state of oxidation. A further motive in testing the data is to see whether there are any possible in-built biases, either in the method of regional sampling, in the method of the oxidation classification, or in the method of magnetic analysis, which would account for the observed correlations. The last of these may be neglected since magnetic cleaning is now widely used and so, therefore, the recorded polarity is the polarity of the ambient field

at the time of cooling. The present study is particularly well suited to this type of analysis because a strict procedure of sampling was followed in the field and also because of the large number of samples involved.

All the samples have been classified according to the magnetite-ilmenite oxidation system on a scale of I-VI; intermediate indices such as I/II, II/III etc. are those defined by having approximately 50% of each oxidation assemblage present. This means that here are elevan separate oxidation divisions.

Table 18.1 lists the lava thickness, polarity and the number of samples in each oxidation class for the 15 single lava traverses. In Table 18.2 the normal and the reversed traverses are separated into two groups and the values are expressed in terms of percentages; also included are (a) percentage of each of the oxidation indices which are either normal or reversed, and (b) the percentage of samples in each of the oxidation classes (Figure 18.4b).

In Figure 18.5, the percentage of reversed samples as a function of the oxidation index is shown, and from this plot a strikingly good general correlation emerges. This suggests, in common with previous correlations, that those samples which are more highly oxidized are also reversely

magnetized. The correlation is particularly well defined for the group of specimens classified by subsolidus oxidation (I-III) but is less well defined for the pseudomorphous group (IV-VI). The only anomalous value in the latter trend is index V, and the reason for a decrease at this point is, as yet, not fully understood.

The general correlation does not depend upon the total number of samples in each class of oxidation since there are an almost equal number of specimeous at the two extremes (Class I = 11.1%; Class VI = 10.6%) (Figure 18.4a)

It is possible that the correlation may depend, however, upon the system of classification, but since this has been shown to be a function of the chemical oxidation index (Fe_2O_3 : FeO) the effect we are studying is still fundamentally an oxidation effect.

In order to investigate the possibility that some differences may arise in using different classification systems, the data may be treated to include for example the "low, moderate and high extent of oxidation" defined by LARSON and STRANGWAY (1967).

In the first instance, specimens having intermediate indices of oxidation (i.e. I/II, II/III etc.) may be absorbed into the classification by moving them up or down by one

class of index. Since it is generally agreed that homogeneous titanomagnetite represents the lowest observable state of oxidation in the Fe-Ti oxide group it is an advantage to maintain it as oxidation index I; all intermediate specimens are moved therefore towards a higher index, thus I/II joins II, V/VI joines VI and so on. This system is less desirable because it limits the number of divisions to a six fold classification. The effect of doing this however is that the curve becomes slightly more refined (Figure 18.6a) but more important is the fact that the general trend is still maintained. This process may be continued, progressively, until the system of classification is reduced to three basic types of assemblages:

(a) Homogeneous titanomagnetite

(b) Titanomagnetite containing ilmenite (unspecified)

(c) Highly oxidized titanomagnetite with pseudobrookite, rutile and titanohematite

The trend, in using this highly simplified system of classification, is still maintained (Figure 18.6b), indicating that the observed correlations do not depend on a detailed mode of classification.

Magnetic polarity is obviously independent of lava thickness but it has been pointed out, nevertheless, that thin lavas behave differently from thicker lavas during deuteric

cooling. The effect of this is that the state of oxidation reached by thin flows may be very different from those of thicker flows. In essence it is not the "state" of oxidation that is different but merely the spectrum of oxidation throughout the flow; in thin flows the spectrum is very much more restricted, whereas in thicker flows well defined and systematic zones of oxidation develop during cooling. Although the present data do not suggest a dependence of any one type of oxidation assemblage on lava thickness this aspect should, nevertheless, be considered an important feature in future magnetic-mineralogical correlation studies.

In six (5R and IN) of the 15 traverses, the underlying baked rock has been checked magnetically. In all cases the polarity agrees with the polarity of the baking rock suggesting that a self reversed mechanism has not been operative in the overlying lava. Self reversal may also be excluded because single, stable magnetic polarities are still maintained regardless of mineral assemblage.

The suggestion that high oxidative processes, or processes connected with high oxidation events, during periods of geomagnetic reversals, is untenable because the observed states of oxidation are equally variable in both N and R rocks.

In conclusion the position is that an apparent correlation exists between high states of oxidation in the magnetic minerals and reversed directions of magnetic polarity. This correlation exists in spite of the overwhelming evidence for field reversal and the absence of a self reversal mechanism in the present collection.

It would seem therefore that we are left with the one remaining, but equally unlikely suggestion, that the observed correlation, and those found previously, may fortuitously be a function of sampling. Many authors seem satisfied in accepting that samples from road-cuts or recently exposed surfaces, or even sampling by drilling for that matter, as is now common palaeomagnetic practice, will yield "fresh" unaltered material. These methods may well limit the effects of secondary alteration (e.g. weathering, burial) but obviously this form of sampling will have no effect in minimising processes of primary, deuteric oxidation. Sampling in volcanic regions can be an arduous task and controlled sampling may sometimes be even more difficult. It is our experience that it is the most accessible parts of the outcrop that are generally sampled (usually near the base of a lava) and again if drilling methods are not used, then samples are usually taken from those areas which would provide a good block, and of course these areas are often associated with joint surfaces.

In all previous studies, primary and secondary alteration effects were not recognised and hence were not separated. Neither were sufficient samples collected from within all parts of the same unit to enable an oxidation norm to be established for the entire unit. The position of sampling within a lava, which may vary with thickness, is of outstanding importance in assessing the various oxidation states of the magnetic minerals. Provided that adequate and truly representative sampling is carried out, then the state of oxidation and the magnetic polarity of a body will in most cases be random.

In previous work the presence or lack of a correlation between oxidation state and polarity is believed to be due to inadequate or biased sampling of the widespread mineralogical variations which this study has demonstrated to exist within single lava units. The accumulation of much additional data along these lines is evidently needed to resolve further observed oxidation and polarity correlations.

TABLE 18.1

Rock type and location	Nature of differences between normal and reversed specimens
Basalts in Germany	A difference of petrological texture (VOGELSANG, 1957).
Basalts in Germany	Differences of grain size and texture. Also differences in form of olivine grains (REFAI, 1961)
Metamorphic rocks in the Adirondack mountains, United States	Reversed specimens more highly oxidized than normal specimens. Petrological and chemical analysis (BALSLEY & BUDDINGTON 1958; BUDDINGTON & BALSLEY, 1961; BUDDINGTON et. al. 1963).
Angara basalt traps, Southern Siberia, Soviet Union.	Reversed lavas have 1.36% TiO_2, normal have 0.83%. Also magnetic differences (FAYNBERG et.al. 1960).
Basalt traps of Southern Siberia, Soviet Union	Excess of ilmenite and TiO_2 in reversed specimens. This means a higher oxidation state (FAYNEBERG, 1960; METALLOVA et.al. 1962; METALLOVA 1963.)
Ultrabasic rocks of the Maymecha-Kotuy region, Soviet Union	Chemical and mineralogical differences (unspecified in Geophysical Abstracts 199-241)
Lavas of central Kazakhstan	Reversed specimens more highly oxidized than normal specimens (SMELOV et. al.1962)
Quaternary lavas of Armenia	Fe_2O_3/FeO ratio greater in reversed (4.2) than in normal (1.2). Also seen petrologically. Also excess MgO in reversed lavas (BOLSHAKOV et.al. 1963).
Basalt lavas, Isle of Mull, Scotland.	Reversed specimens more highly oxidized than normal, deduced from several types of petrological observation. Differences in olivine alteration (oxidation) (ADE-HALL 1964; WILSON 1964).
Basalt lavas from Scotland, Japan and Iceland.	Petrological analysis. Reversed specimens more highly oxidized. Icelandic result not statistically significant in itself (WILSON 1965)
Columbia Plateau basalts, United States.	Petrological analysis. Reversed specimens much more highly oxidized than normal. Magnetic differences also exist (WILSON & WATKINS 1967).

TABLE 18.2

				OXIDATION INDEX										
Lava No.	Thickness	No. of specs.	Polarity	I	I/II	II	II/III	III	III/IV	IV	IV/V	V	V/VI	VI
AS	2.5	16	N					3	1			11	1	
BS	5.2	13	N	4	3	3		1		1			1	
CS	4.3	13	N	1	2	6		3			1			
DS	3.6	14	N	4				1	9					
ES	2.6	12	R			1			3	3	5			
FS	8.7	19	R		1			7	6	2	1			2
GS	16.0	38	N	1		5		7	7	5	1	8		4
HS	16.3	31	R		2	1	1	12	4	9				2
IS	11.5	26	R	3		2		11		5	1	4		
JS	14.0	29	R	1		2		5	3	6	2	9		1
KS	14.8	28	N	4	1	7	1	4		4		4		3
LS	14.2	33	N	17	1	4		3		5		2		1
S	11.0	37	R	8		2		8	4	2		4	7	2
MS	11.8	61	R	2	2	10	1	15	5		1	2	4	19
X	11.1	34	R					3	3	6	3	7	3	9
			Total	45	12	43	3	83	45	48	15	51	16	43

Single lava study showing lava thickness, number of specimens sampled, polarity and the number of specimens in each class of oxidation.

TABLE 18.3

	NORMAL							REVERSED							
Ox.Index	AS	BS	CS	DS	GS	KS	LS	ES	FS	HS	IS	JS	S	MS	XS
I		30.9	7.7	28.6	2.6	14.3	51.5				11.5	3.5	21.6	3.3	
I/II		23.0	15.4			3.6	3.0		5.3	6.4				3.3	
II		23.0	46.0		13.2	25.0	12.1	8.3		3.3	7.7	6.9	75.4	16.4	
II/III						3.6				3.3				1.6	
III	18.7	7.7	23.2	7.1	18 4	14.3	9.1		36.6	38.6	42.3	17.2	21.6	24.6	8.8
III/VI	6.3			64.3	18.4			25.0	31.6	12.9		10.3	10.8	8.2	8.8
IV		7.7			13.2	14.3	15.2	25.0	10.6	29.0	19.3	20.7	5.4		17.6
IV/V			7.7		2.6			41.7	5.3		3.8	6.9		1.6	8.8
V	68.7				21.0	14.3	6.1				15.4	31.0	10.8	3.3	20.7
V/VI	6.3	7.7											19.0	6.6	8.8
VI					10.6	10.6	3.0		10.6	6.4		3.5	5.4	31.1	26.5

	%N	%R	Normal Lavas(%)	Reversed Lavas(%)	All Lavas (%)
I	68.9	31.1	20.0	5.6	11.1
I/II	58.5	41.5	4.5	2.0	2.9
II	58.2	41.8	16.1	7.2	10.6
I/III	33.3	66.7	0.6	0.9	0.7
III	26.5	73.5	14.3	24.5	20.6
III/VI	37.8	62.2	11.0	11.3	11.4
IV	31.2	68.8	9.6	13.3	11.9
IV/V	13.3	86.7	1.3	5.2	3.7
V	49.0	51.0	16.1	10.4	12.6
V/VI	12.1	87.9	1.3	5.6	3.9
VI	18.6	81.4	5.2	14.0	10.6

Percentages of samples in each oxidation class for each of the lava traverses.

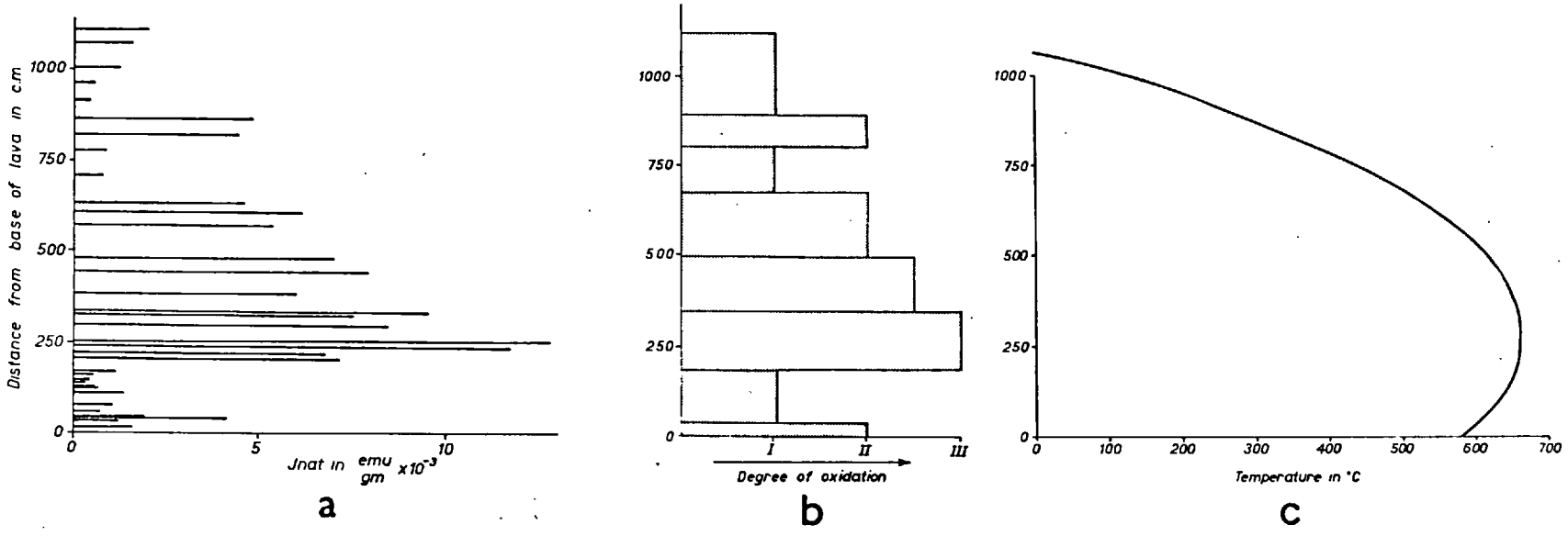
Distance from base of lava in c.m
1000
750
500
250
0
0
5
10
Jnat in emu gm x10⁻³
a
1000
750
500
250
0
I
II
III
Degree of oxidation
b
1000
750
500
250
0
0
100
200
300
400
500
600
700
Temperature in °C
c

Fig 18.1

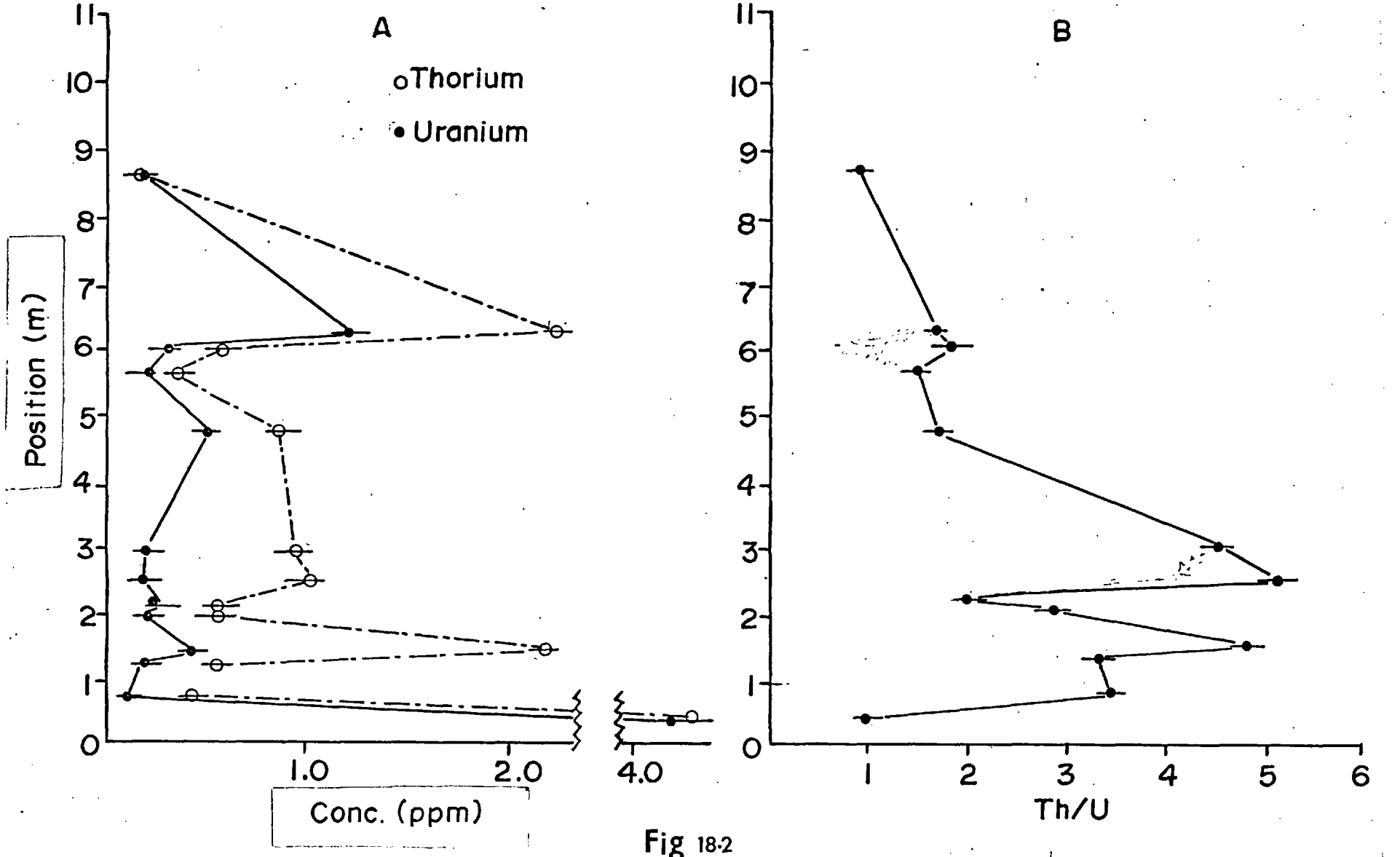
A
B
oThorium
• Uranium
Position (m)
Conc. (ppm)
Th/U
0
1
2
3
4
5
6
7
8
9
10
11
1.0
2.0
4.0

Fig 18.2

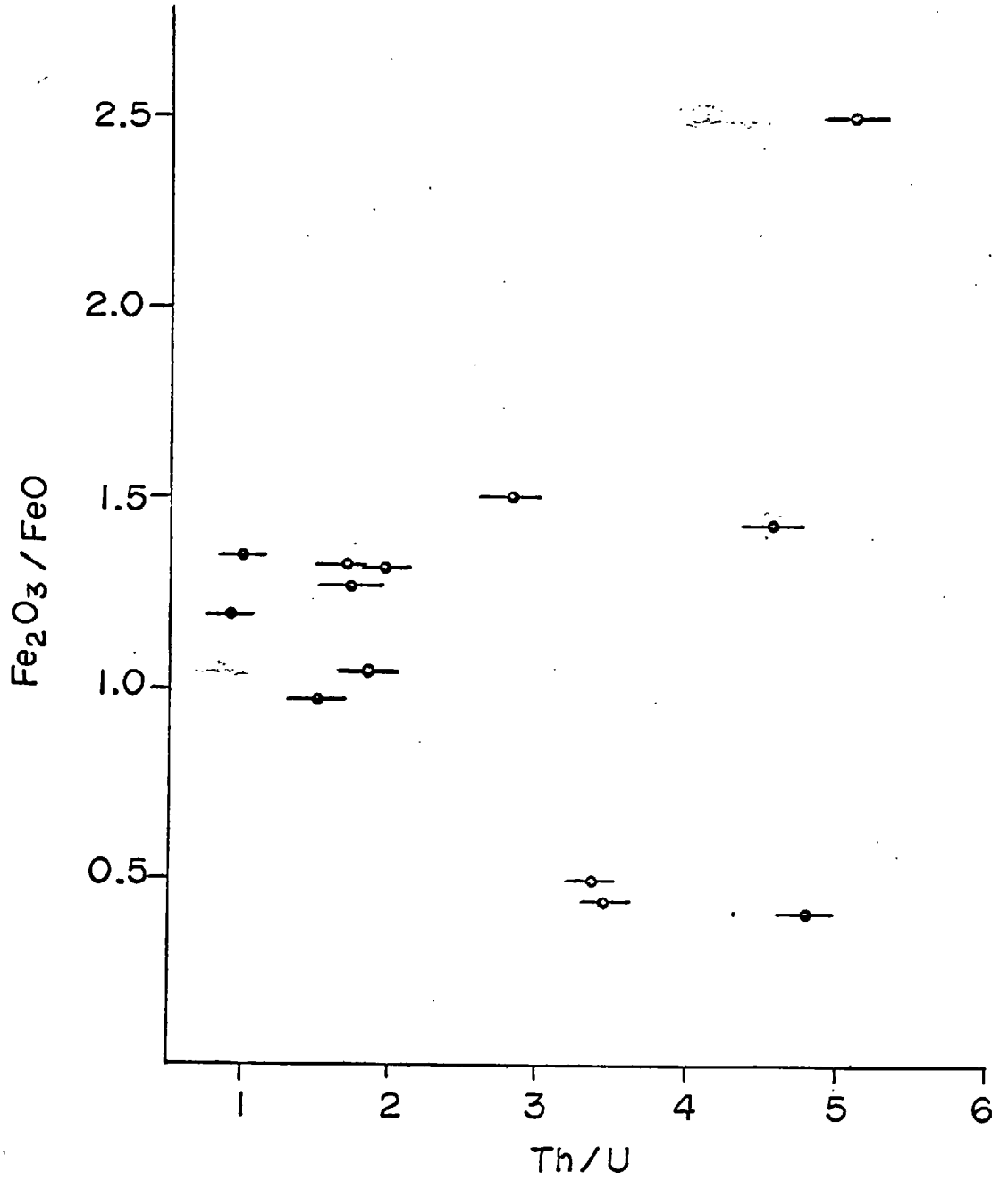

Fig 18·3

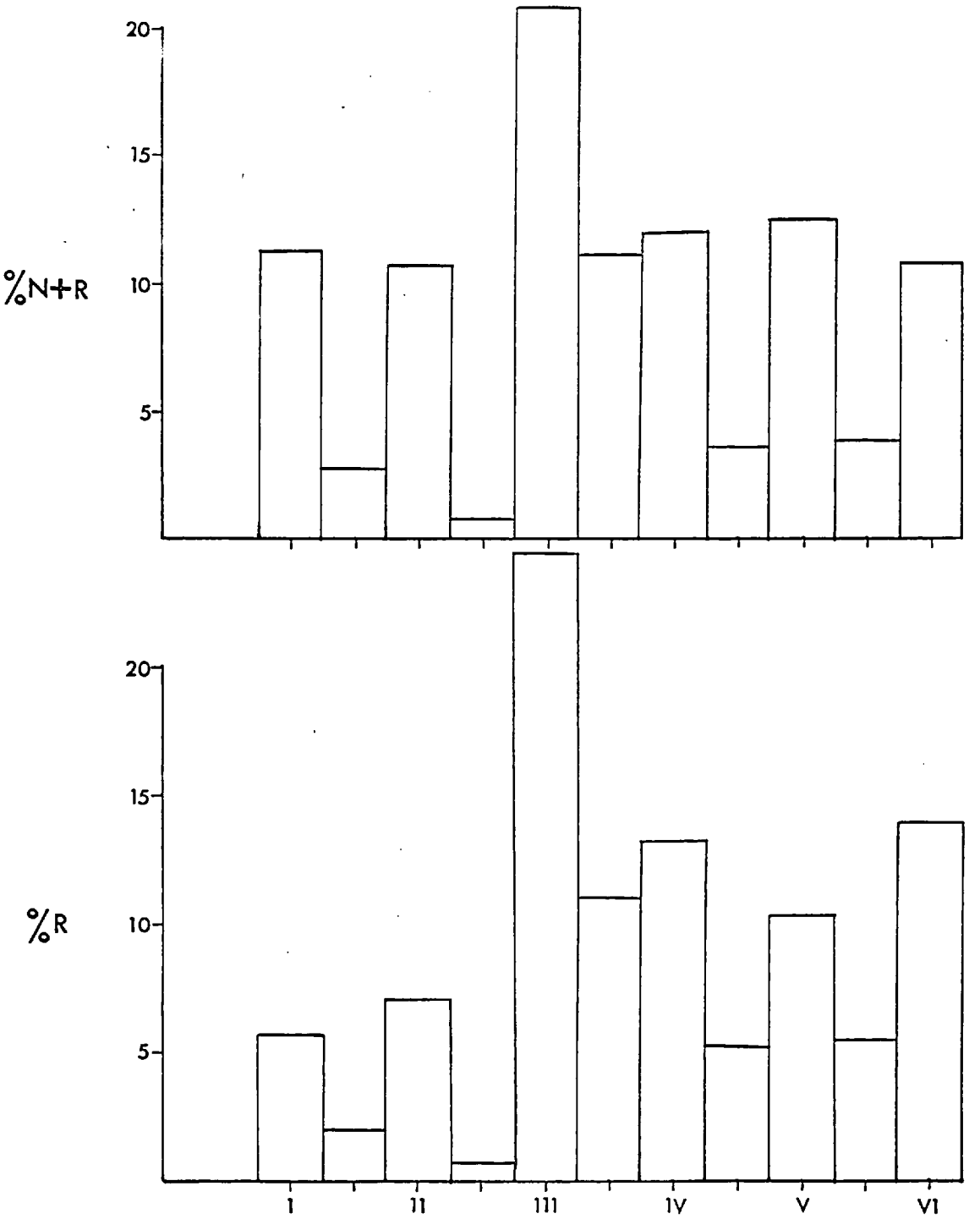

Fig 18·4

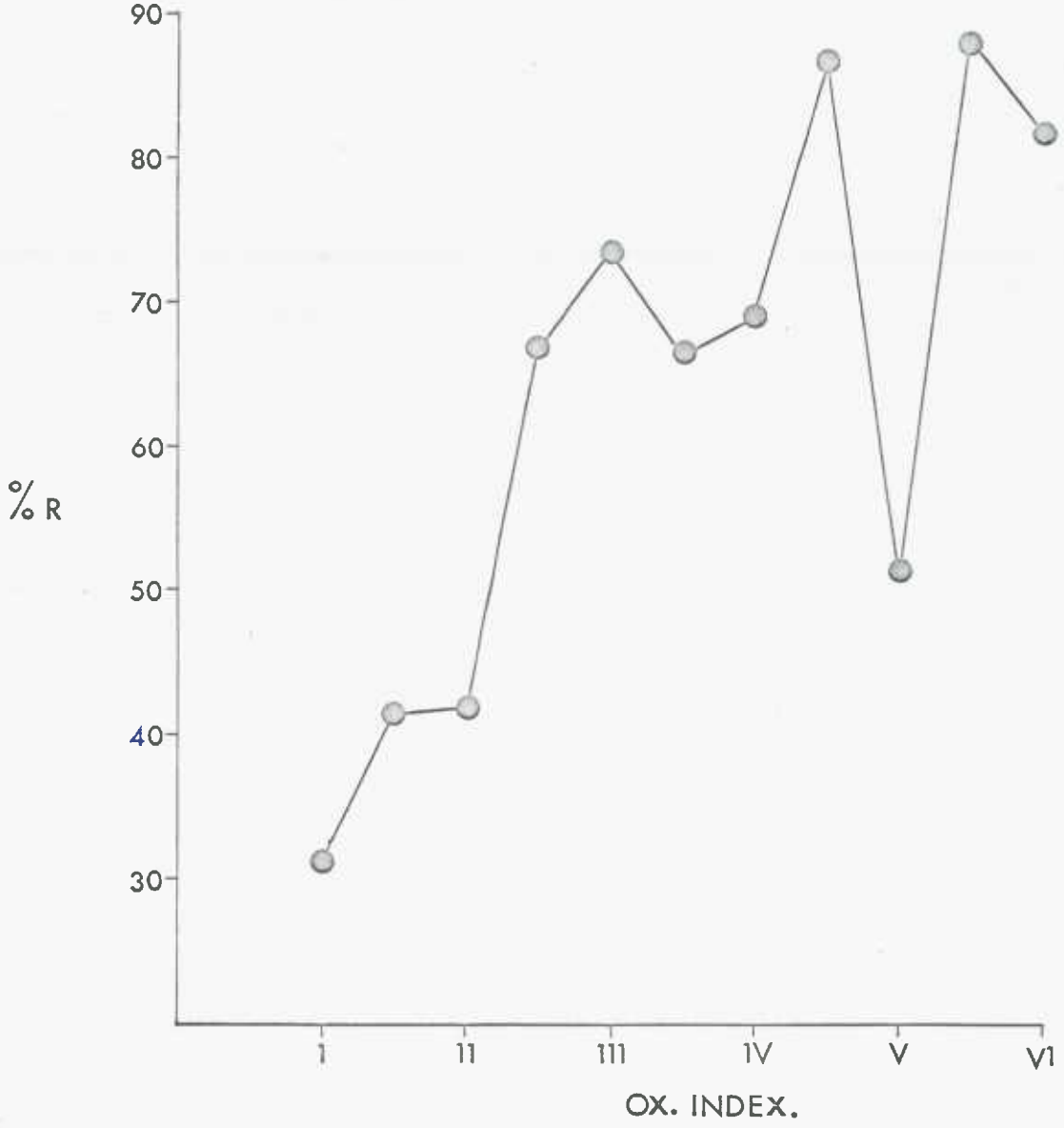

Fig 18.5

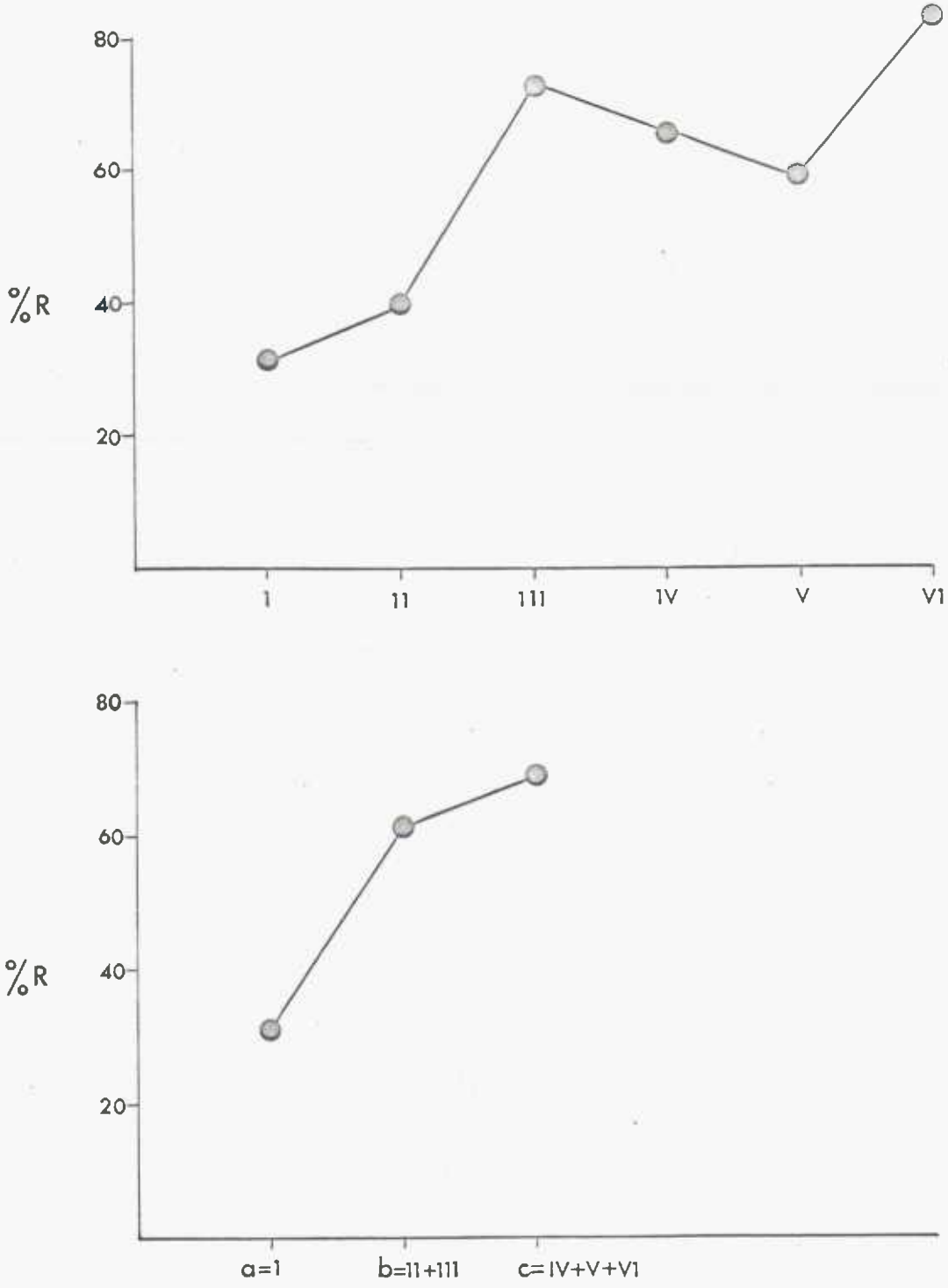

Fig 18·6

APPENDIX I

Nile Delta Black Sand

Samples of a Nile Delta black sand deposit were examined in polished section under the ore microscope. There is a voluminous literature on the alteration of Fe-Ti oxides under conditions of supergene weathering, particularly in beach sands. Examination of the concentrate has permitted a comparson to be made betweenthe alteration trends effected by weathering agencies and the alteration trends formed at high temperatures. One significant feature of this comparison may serve as an example. In the case of ilmenite, the bulk Fe:Ti ratio remains constant during high temperature oxidation, contrasting strongly with the increase in the Ti:Fe ratio of ilmenite under weathering conditions.

Since the concentrated material has originated from a variety of geological environments many different types of Fe-Ti oxide intergrowths were found and these have formed a very useful source of comparison for the Iceland study. Furthermore, the recognition of high temperature assemblages such as those produced in lavas, has now given a clearer understanding of the mineral assemblages which may be attributed to alteration within the parent rock and assemblages which are due to post deuteric effects. Most authors have not previously considered the effects of primary oxidation, or the effects of superimposed alteration on ilmenite, and as a result many conflicting reports are to be found in the literature.

A.1.1 Reflection Microscopy

Grains in the concentrate are generally rounded and well sorted, averaging 100u in diameter. Magnetite (titanomagnetite), ilmenite and hematite exist as discrete homogeneous phases. Oxidation-exsolution lamellae of ilmenite occur in titanomagnetite grains. Ilmenite-hematite, ilmenite hematite-rutile and hematite-rutile exhibit exsolution intergrowths. Typical high temperature deuteric oxidation phases such as pseudobrookite, rutile and hematite as well as secondary supergene minerals (goethite, amorphous Fe-Ti oxide, "leucoxene") have been found to replace the primary assemblage. The variation of intergrowths and the diverse oxidation states encountered suggest that the minerals are derived from a wide variety of rock types.

A.1.2 Ilmenite-Hematite-Rutile

Homogenous ilmenite forms approximately 50% of the concentrate examined. Extensive exsolution, resulting from the progressive "unmixing" of titanohematite and ferri-ilmenite from a member of the Fe_2O_3-$FeTiO_3$ solid solution series, is shown in Plate A.1. The titanohematite (Plate A.1a) bodies are elongated with their long axes parallel to one another and to the (0001) parting planes of the host ilmenite. Titanohematite occurs in large lenses and as a finer phase in parallel rows between the larger bodies. There is a general decrease in size and abundance of the finer phase towards the larger bodies, (seriate distribution). It has been suggested that since the exsolution bodies grow by diffusion, the earlier formed ones are comparatively large, while the smaller bodies are produced during the low temperature stages of exsolution. The exsolved titanohematite exsolves a second phase of ferri-ilmenite. This fine phase also shows a seriate distribution at high magnification.

The above remarks apply equally well to Plate A.2 a-b, in which titanohematite is the host phase.

In Plate A.1 c-d, the exsolution of titanohematite is complicated further by the exsolution of rutile. Rutile characteristically exsolves along the less prominent $(01\bar{1}2)$ rhombohedral parting plane in ilmenite or hematite. In some grains a textural interpretation would suggest that rutile is the first phase to exsolve, but in others the reverse seems to be true.

A feature which has not been stressed in the literature and one which is evident in the samples under examination is the fact that rutile does not exsolve directly from ilmenite but tends to segregate out in close association with titanohematite, suggesting a breakdown mechanism rather than exsolution. The tendency for titanohematite to exsolve its excess Ti in the form of ilmenite in some cases and as rutile in others must depend on their critical stability relationships. These have not been determined experimentally. The textural form of rutile differs depending on whether it exsolves from a primary titanohematite or a primary ilmenite. In the former case (Plate a.3) rutile is lamellar in form, but in the latter (Plate A.1) an oleander leaf-like texture is more common. A comparison of this sygmoidol form with Plate A.6c, which is a deuterically oxidized ilmenite suggests this maybe the result of an oxidation-exsolution process similar to that relating titanomagnetite with ilmenite. Note that the

density of exsolved rutile is particularly variable in the discrete titanohematite grains (Plate A.3).

A.1.3 Ilmenite Alteration

(a) Supergene Alteration

BAILEY et.al (1956) optically define the progressive alteration stages in black sand ilmenite as

i) patchy ilmenite
ii) amorphous Fe-Ti oxide
iii) "leucoxene"

It is stressed that "leucoxene" is not a specific mineral species and is used only as a general term for amorphous and usually hydrous, cryptocrystalline alteration products of ilmenite. LYND et.al (1954) examined several altered ilmenites and assigned all the X-ray lines to either ilmenite, hematite or rutile. At the same time however he observed that in the case of the least magnetic (more altered) fractions, principle lines of hematite and rutile were not apparent although other spacings were present. FLINTER (1959) in studying altered ilmenite from Malaya reported ilmenite and "diffuse rutile". KARKHANAVALA et.al (1959) studied commercial Quilon "leucoxene" and concluded that the concentrate included the minerals rutile, pseudobrookite, anatase and hematite; however a study of individual white "leucoxene" grains indicated that most of these consisted of rutile, and a small number of rutile plus anatase; the brown and black grains contained pseudobrookite. A mineral assemblage such as this could not possibly have originated in the same environment and under the same conditions of temperature and pressure. In a subsequent paper KARKHANAVALA and MOMIN (1959) demonstrated that ilmenite oxidized to hematite, pseudobrookite and rutile in an approximate 1:5:7 molar ratio. This experiment was carried out at 850°C; at 650°C only hematite and rutile were formed. In spite of the fact that the high temperature nature of pseudobrookite had been determined, these authors nevertheless concluded that the 1:5:7 'product is almost identical with naturally occuring "brown leucoxene", a naturally occuring alteration(weathering) product of ilmenite'.

BAILEY and CAMERON (1957) have recorded both anatase and brookite from the black sands of Mozambique. ALLEN (1956) has pointed out that "leucoxene" may consist of an amorphous

Fe-Ti oxide or a cryptocrystalline mixture of anatase, rutile, brookite and sphene. Both anatase and brookite are reported from bauxite and clay, with rutile apparently the predominant species in bauxite, and anatase in clay (HARTMAN 1959).

In all these reports not a single mineral phase was optically identified. The photomicrographs, of BAILEY et.al, LYND et.al, and TEMPLE (1966), showing altered grains of ilmenite, appear optically murky and without textural character. A wide variety of Fe-Ti oxides are common in ilmenite concentrates and a range of alteration states may also exist. It is not surprising therefore that so many phases have been detected in these concentrates, when accurate sampling techniques have not been employed. In addition, no previous attention has been paid to the oxidation effects which may take place at high temperatures in the parent rock, and as a result all the alteration products, of ilmenite, have been ascribed to minerals of supergene origin (see for example KARKHANAVALA and MOMIN 1959).

Plate A.4 shows the patchy ilmenite; amorphous Fe-Ti oxide; "leucoxene" trend of BAILEY et.al. Plate A.4b is similar to the amorphous Fe-Ti oxide stage, and in fact although an X-ray powder photograph was diffuse only ilmenite was detected. A grain similar to that shown in Plate A.4d, which would normally be described as "leucoxene", gave a good anatase pattern.

Previous investigators agree that the Ti:Fe ratio increases during the supergene alteration process, indicating the high mobility of iron under these conditions. This results in a product essentially TiO_2. During the course of this alteration, it is evident that ilmenite assumes a sponge-like appearance, as iron is gradually leached from the structure. This loss of iron has been chemically demonstrated by BAILEY et.al (1956) and TEMPLE (1966).

In order to supplement this study, a large number of ilmenite concentrates were obtained from the Rhodesian Selection Trust Company.

In one collection of Kimberlitic ilmenite nodules, from the Mali Republic, coarsely crystalline anatase is the most abundant and common alteration mineral. Accessory hematite (titanohematite) is also present. Many samples contain finely dispersed and characteristic "leucoxenic"

haloes (anatase) but owing to the large grain size (1-1.5 cm) of the ilmenites the cores are generally unaffected. The sequence of alteration may therefore be followed along a traverse from the centre of a grain to the grain boundary. It is evident that the formation of microcrystalline anatase and a simultaneous leaching of iron may take place as a single event (Plate A.5d). On the other hand, the alteration of ilmenite along parting planes to an amorphous Fe-Ti oxide phase, may develop as an intermediate stage (Plate A.5b). As the process progresses, and the iron is removed, the grainsize of the TiO_2 phase increases and results finally in an interlocking framework of large, euhedral anatase crystals (Plate A.5c). In Plate A.5d most of the iron has been removed, but remnants of attached hematite may still be seen. The percentage of hematite in supergene altered ilmenite is generally very small even at the oxidation front. Grains of primary titanohematite (containing exsolution bodies of ferri-ilmenite from the same Kimberlitic environment) are not affected by the alteration process; active breakdown is selectively confined to the more susceptible ilmenite. As the titanohematite is not affected it suggests that the mechanism of ilmenite alteration results in the active solution of iron, during the inversion process, and does not result in the formation of hematite as a major intermediate phase, which is then subsequently removed as a leached product. The higher mobility of ferrous iron is well known.

Ilmenite, hematite and anatase have all been confirmed by X-ray powder photography on samples extracted from the surfaces of polished specimens. The unit cell parameters for anatase were found to be $a = 3.789 \pm .001$; $c = 9.526 \pm .007$; these values are comparable to the ASTM index values.

(b) Deuteric Oxidation

Within the same sample of Nile black sand a large number of ilmenite grains were found to show progressive oxidation features similar to the trends that have been decribed for the Icelandic lavas (Chapter 5.2). Photomicrographs in Plate A.6 - illustrate this transformation. In the first stage fine oriented filaments of ferri-rutile develop along the rhombohedral parting planes in ilmenite. With progressive breakdown of the host ilmenite the Ti content of the rutile increases with the simultaneous development of titanohematite. Plate A.6b shows an intergrowth of rutile and ferri-rutile in a web-like host of titanohematite and ilmenite. This complex assemblage may be

described as "metailmenite". Plate A.6c shows the stage at which the Ti and Fe have segregated completely into bladed rutile and hematite. With increasing oxidation, pseudobrookite develops along the grain bounderies of the Fe_2O_3-TiO_2 intergrowth (Plate A.6d). The end product in this high temperature oxidation sequence is pseudobrookite, pseudomorphous after original ilmenite, containing a small percentage of fine subgraphic hematite and rutile.

Plate A.7 shows the alteration products, Fe_2O_3, TiO_2 and pseudobrookite. In all cases the oxidation is selectively confined to the ilmenite areas.

A.1.4 Magnetite

Homogeneous magnetite (titanomagnetite) is a fairly common constituent in the concentrate. A few grains show oxidation-exsolution lamellae of ilmenite along (111) parting planes (Plate A.8). The successive high temperature deuteric oxidation trend described for discrete ilmenite applies equally to intergrowths of titanomagnetite and ilmenite. The stages involve a breakdown of the ilmenite and the titanomagnetite into rutile plus titanohematite. The rutile: titanohematite ratio is higher in the replaced ilmenite lamellae (Plate A.8b). With increasing oxidation pseudobrookite forms from the rutile-titanohematite intergrowth and tends, as is seen in Plate A.8c, to completely pseudomorph the original ilmenite. The (111) relic structure is well preserved. The textural development of inter-lamellar pseudobrookite on the other hand, tends to be rather irregular. Plate A.8d shows far less crystallographic control of the pseudobrookite in titanohematite, suggesting that the oxidation stems directly from a homogeneous titanomagnetite grain.

A.1.5 Accessory Minerals

(a) Spinels. Primary aluminous spinels (Mg, Fe) O.$(Cr, Al)_2O_3$ are common in crystal accumulates of differentiated igneous bodies. They occur as accessory minerals in ferromagnesian rich basalts and form a minor constituent of olivine nodules. Plate A.9 shows respectively an unzoned spinel incipiently oxidized, a spinel rimmed by titanomagnetite and finally a zoned spinel which is highly oxidized.

(b) Sphene. Plate A.10a shows sphene rimming a homogeneous ilmenite grain. In Plate A.10b, sphene distinctly embays both the titanohematite-ilmenite intergrowth as well as the ilmenite-titanohematite intergrowth It has been

that sphene may replace ilmenite during the late stages of crystallization or during metamorphism.

A.1.6 Ilmenite from the Abu-Ghalagar Metagabbro

The Abu-Ghalagar samples contain large (200-300u) equant grains of ilmenite, ferromagnesian silicate minerals and disseminated pyrrhotite and pyrite-marcasite inversion products after pyrrhotite. Traces of chalcopyrite, covellite, bornite, magnetite, hematite and goethite are also present. All the ilmenite grains are crowded with exsolution spindles of titanohematite, aligned parallel to the (0001) basal parting plane. Some exsolution segregation to grain boundaries has also taken place. The occasionally large anhedral grains of pyrrhotite which occur interstitially to the ilmenite (Plate 14.11a) appears to have either inhibited the exsolution of titanohematite, or as seems more likely, has homogenised the oxide intergrowth in a narrow concentric rim around the sulphide grains (Plate 14.11c).

A.2 Reduction Experiments in Hydrogen

A.2.1 Introduction

Reduction experiments were carried out, on samples of basalt, on the Nile Delta black sand, and on the Abu-Ghalagar ilmenite, in a flow of hydrogen at 800° and 1000°C. Although reducing conditions as drastic as these experiments are unlikely to occur in nature, the importance of these experimental runs is that members of the pseudobrookite series and a modified form of rutile develop as major reduction products of ilmenite and titanomagnetite. The widespread association of pseudobrookite and rutile with highly oxidizing environments has already been stressed in previous chapters. The considerable advance that has been made in the field of extractive metallurgy on the thermal decomposition of ilmenite by reduction, further warrents the closer examination and comparison of reduction assemblages with their oxidized counterparts. It is unfortunate however that the nature of the textural intergrowths as seen in reflected light under the ore microscope has not received the attention it deserves.

Plate A.12 illustrates the similarity in textural form of oxidized and reduced titanomagnetite-ilmenite grains from basalts; the oxidized grains, (a) and (b), contain titanohematite, rutile and pseudobrookite whereas the reduced grains, (c) and (d) contain metallic iron, a pseudobrookitic phase ($FeTi_2O_5$) and rutile.

The usual reason for reducing ilmenite beach sands on a commercial scale is to up-grade the TiO_2 content of the concentrate by separation of the iron in a metallic form.

The selective reduction of iron in ilmenite by hydrogen takes place according to the following reaction:

$$FeTiO_3 + H_2 = Fe + TiO_2 + H_2O$$

This equilibrium has been studied over the temperature range 950°-1000°C by various workers with good agreement (SHOMATE et.al, 1964; MICHAUD and PIDGEON 1954).

The activity and pressure of the water formed during the reaction determines the state of oxidation of the rutile phase (TiO_{2-x}).

The stable anionic forms of rutile (TiO_{2-x}) which have been described by EHRLIEN (1938) are as follows;-

α form	$TiO_2 - TiO_{1.90}$	tetragonal
β form	$TiO_{1.80} - TiO_{1.65}$	(?)tetragonal
γ from	$TiO_{1.56} - TiO_{.146}$	trigonal
δ from	$TiO_{1.25} - TiO_{0.60}$	cubic

Previous work in controlled partial pressure experiments at 1200°C indicates that ilmenite may be reduced to a member of the pseudobrookite solid-solution series with partial reduction of the Fe to the metallic state. (WEBSTER and BRIGHT, 1961). This result has been confirmed in the Abu-Ghalagar experiments in which the available water from the selective reduction of Fe in ilmenite has effectively oxidized the titanium at very low oxygen partial pressures to a pseudobrookitic phase and rutile.

In reduction experiments of <u>rutile</u>, MICHAUD and PIDGEON (1954) have shown that the end point of the reduction in dry hydrogen is Ti_3O_5 (Anosovite); in one case Ti_2O_3 was reported as the end product (NASU, 1936).

In all cases a selective reduction of iron has been reported but a degree of uncertainty has arisen as to the precise nature of the minor Ti or Fe-Ti phases formed during the experiment. This is not surprising as a notable feature of Ti is the multiplicity of apparently stable, non-stoichiometric compounds which it may form with oxygen.

In a recent review of the system Ti-O, DEVRIES and ROY (1954) noted that ten phases were possible above 800°C; even more recently a further eight synthetic metastable compounds have been reported (ANDERSON et.al; 1957).

A.2.2 Experimental Conditions

(a) Abu Ghalagar Ilmenite

Cubes (2.5cm) of the material were heated in atmospheres of hydrogen and nitrogen at the following temperatures and for the following periods of time;

Hydrogen	800°C for 3 hrs.
	1000°C for 3 hrs.
Nitrogen	800°C for 3 hrs.
	Nitrogen for 3 hours followed by hydrogen for 3 hours at 800°C in each case.

The cubes were cut in half and a polished section was made from one of the halves, so that a cross-section of the heating surface was obtained.

(b) Nile Delta Black Sand

Hydrogen	700°C for 7hrs.
	800°C for 7hrs.

SHOMATE and his co-workers (1946) have shown that hydrogen is not a practical reagent for the reduction of ilmenite, as the theoretical maximum utilization is only 20% at temperatures below the melting point of ilmenite (1450°C). At 1000°C utilization is only 10%. Likewise the maximum utilization of CO is only 8.5% at 1400°C.

As a comparison, the maximum H_2 utilization in reducing iron in chromite at 1000°C is 2.8%. The marked difference is the result of the "free energy of binding" of FeO and TiO_2 in ilmenite.

Carbon is considered by some investigators to be the most effective reducing agent in ilmenite ores.

A.2.3 Results of the Abu-Ghalagar sample reduction experiments

Equilibrium conditions were not reached in the samples after three hours. This has allowed the progressive change

from the edge of the cube to the centre to be studied in each of the homogenization and reduction experiments. Reflection microscopy and X-ray powder photographs have been used in identifying the chief mineral phases. It is emphasised that anionic-deficient rutile (TiO_{2-x}) is used in accordance with previous work and that pseudobrookite is used in terms of the solid solution series (Fe_2TiO_5 - $FeTi_2O_5$).

A.2.4 Reduction at 800°C in Hydrogen

(a) Centre of sample (Plate 14.13a)

Exsolved titanohematite is readily reduced to free iron. The host ilmenite darkens and becomes distinctly less pleochroic than its untreated counterpart. The ilmenite is probably non-stoichiometrically deficient in oxygen but the temperature and activity of hydrogen has not been sufficient to effect a detectable change in the X-ray pattern (Column 1 - Table A.1).

(b) Between Centre and Edge of Sample (Plate A.13b).

Within the darkened ilmenite and between the large lenses of metallic iron, fine blades of rutile (TiO_{2-x}) develop at an angle to the basal exsolution plane. The development of rutile (TiO_{2-x}) along the $(01\bar{1}2)$ parting plane is accompanied by a gradual thickening of the iron laths. The metallic bodies act as foci for the migration of the iron which is selectively reduced from the ilmenite.

(c) Edge of Sample (Plate A.13c)

Complete equilibrium conditions have not been reached at the edge of the section.

$$(\text{i.e. } FeTiO_3 + H_2 = Fe + TiO_2 \text{ (Rutile)} + H_2O)$$

The interlocking groundmass between the iron globules consists of the oxygen deficient ilmenite phase($FeTiO_{3-x}$); an increasingly large percentage of rutile (TiO_{2-x}) is evident towards the edge of the section. The bladed form of rutile is gradually lost as the metal:oxide ratio increases. The interstitial sulphide phases are reduced to free iron with a large volumetric reduction in grain-size.

A.2.5 Reduction at 1000°C in Hydrogen (Plate A.13d).

(a) The rate of solid state diffusion and the increased activity of the hydrogen has been greater at the higher temperature. The sample consists of globular metallic iron, concentrated along (0001) relic basal parting planes, in an interlocking groundmass of rutile (TiO_{2-x}) and a pseudobrookitic phase. Relic zones of anionic-deficient ilmenite are present in some parts of the sample.

At 1000°C the reduction appears to be more complex than has been indicated in the above chemical reaction. X-ray powder data presented in Table A.1 indicate the presence of pseudobrookite. This phase has also been reported as a reduction phase by WEBSTER and BRIGHT (1961).

Besides the obvious increase in the metal:oxide ration, a feature of the 1000°C sample is the formation of microspherulitic blebs of metallic iron in the dark pseudobrookitic areas. It appears that between 800° and 1000°C the sample has passed through a field in which ($Fe + Fe_2TiO_5$-$FeTi_2O_5 + TiO_2$) is the stable assemblage. On slow cooling, however, the pseudobrookitic phase breaks down into rutile plus metallic iron giving the assemblage reported by MICHAUD and PIDGEON (1954). (Data in Table A.1).

A phase which is conspicuously absent in the reduction experiments in Wustite ($Fe_{1-x}O$). The reasons for this are apparent in terms of the reaction:

$$FeO + H_2 = Fe + H_2O$$

A.2.6 Homogenising Experiments - Abu-Ghalagar Ilmenite

Ilmenite and hematite form a continuous solid-solution series above 950°C. In order to completely homogenise Fe_2O_3 - $FeTiO_3$ exsolution intergrowth this temperature would need to be attained. In the experiment samples were heated in a neutral atmosphere of nitrogen at 800°C for three hours. The degree of homogenisation varies within the cube section. It is very nearly complete at the edge of the samples (Plate A.14b but towards the centre (Plate A.14a) the slow diffusion rate has prevented the migration of titanohematite into the ilmenite lattice. During the course of homogenisation an auto-oxidation process was also active. The Fe-Ti oxides are extremely sensitive to oxidation and reduction conditions. The

small amount of oxygen liberated from the silicates during heating has been sufficient to produce fine ferri-rutile filaments in the ilmenite; these develop at an angle to the basal exsolution plane (A.14c). In the more extreme cases ilmenite has been oxidized to pseudo-brookite along cracks and grain boundaries (Plate A.14d).

A.2.7 Abu Ghalager Sample heated in (a) Nitrogen
(b) Hydrogen

The reducing effect on the samples, previously heated in nitrogen, is varied and has been found to depend on the degree of homogenisation. The titanohematite of the grains showing only partial remixing readily inverts to metallic iron (c.f. A.13a). The energy required to reduce a fully homogenised (Fe_2O_3 - $FeTiO_3$) grain is very much greater than one containing an exsolved phase. In fact, the very presence of an exsolved ferric phase appears to trigger off the reduction reaction in the host ilmenite. Plate A.15 shows the limited reduction that has taken place within the Fe-rich areas. The fine cross-cutting structure is a relic of the ferri-rutile phase formed during the auto-oxidation of the ilmenite when heated in nitrogen. These conditions correspond to low oxygen partial pressures.

Hydrogen reduction has produced an oxygen deficient ilmenite as the main phase. The iron zones contain finely dispersed particles of the metallic phase. Minor rutile occurs in the adjacent titanium-rich areas.

A.2.8 X-ray Results

Table A.1 lists the d values (Å) against their visual intensities (I) and notes the phase (phases) represented by each of the reflections. Table A.2 compares the A.S.T.M. index values with the d values of the six strongest lines for each of the phases encountered, with the corresponding values abstracted from Table A.1. These data demonstrate that multi-mineral Fe-Ti oxide assemblages may be adequately separated into their respective components with some confidence.

The Abu-Ghalagar results refer to representative samples of material. These samples were carefully selected, under the ore microscope, and extracted from a particular area on the surface of a polished section, using the microsampling technique. The R.S.M. material, on the other hand, refers to an ilmenite concentrate (from the Ilmen mountains) which

was heated in a different series of experimental runs. The starting material in the latter experiments was crushed to pass a -120 mesh screen (0.01 mm). The R.S.M. powdered samples may be regarded as equilibrim runs whereas the 2.5 cm. Abu-Ghalagar cubes may be regarded as non-equilibrium runs. An 800°C oxidizing run is also quoted here in order to compare the d values of the oxidized phases, pseudobrookite and rutile, with their reduced counterparts.

Ilmenite, in the 800°C reduction run and towards the relatively non-reactive centre of the cube sample, becomes darker in colour and distinctly less anisotropic, but surprisingly enough there are no significant changes in the unit cell parameters.

Metallic iron, readily identifiable in reflected light by its high reflectivity, has an average (4 values) unit cell parameter, a = 2.866 ± .001. This value is .01Å lower than the theoretical value of iron and is well within experimental limits.

The unit cell parameters listed in Table A.3 demonstrate that no appreciable distinction may be drawn between stoichiometric and anionic deficient rutile on the basis of simple X-ray powder photography. The tetragonal lattice however does indicate that we are probably dealing with either the α or β form of rutile (TiO_2-$TiO_{1.65}$).

Stoichiometric TiO_2	a=4.590 c = 2.960	Vol = 62.35
Anionic deficient TiO_{2-x} (average of 5 values)	a=4.497 ±.020c = 2.958 ± .020	Vol = 62.52

Further, as one may expect, no significant differences were found in the unit cell parameters of rutile from either the equilibrium or the non-equilibrium runs.

As far as the pseudobrookitic phases are concerned individual reflections were found to correspond fairly well with the A.S.T.M. index for pseudobrookite. The pseudobrookite solid solution series between Fe_2TiO_5 and $FeTi_2O_5$ is orthorhombic and the series is complete above 1150°C (AKIMOTO et.al 1957). There is a small but systematic increase in the crystal parameters from Fe_2TiO_5 to $FeTi_2O_5$. The volume of the unit cell is the significent parameter (AKIMOTO et.al 1957) and varies as follows:

$FeTi_2O_5$ (Mol.per cent)	Vol.of Unit Cell ($Å^3$)
0.0	361.1
99.9	368.0

The 1000°C Abu-Ghalagar run gives a unit cell volume for the pseudobrookitic phase of 368.226 ± .775 $\AA^3$, indicating that the composition is well towards, and perhaps beyond, the $FeTi_2O_5$ end of the solid solution join; this is entirely acceptable in terms of the FeO-Fe_2O_3-TiO_2 ternary phase diagram. By contrast, the pseudobrookitic phase of the 800°C oxidation run gives a unit cell volume of 364.383 ± 0.452 $\AA^3$ which is equivalent to approximately 35 mol.per cent $FeTi_2O_5$.

The formation of $FeTi_2O_5$, rather than pseudobrookite, is highly significant. LINDSLEY[5](1965) has established, in a series of quenching experiments in sealed evacuated tubes, that $FeTi_2O_5$ decomposes to ilmenite + rutile below 1140°C ± 10°C. It has been shown, on textural evidence alone, that in the highly reactive 1000°C run, that the pseudobrookitic phase breaks down to rutile + metallic iron (Plate A.13d). The reduction trend is now clear in terms of LINDSLEY'S work; the rutile which forms, evidently becomes anionically deficient, and the new generation of ilmenite, resulting from the decomposition of $FeTi_2O_5$, will breakdown in accordance with:

$$FeTiO_3 + H_2 = Fe + TiO_2 + H_2O$$

In summary, metallic iron and anionic deficient rutile are the end products of ilmenite on reduction; $FeTi_2O_5$ may form as an intermediate phase during the course of reduction, at temperatures between 800°C and 1000°C.

A.3 Nile Delta Beach Sand Reduction Experiment (7 hrs. at 700°C in Hydrogen)

The reduction effect, on the variety of minerals and phase intergrowths, in the beach sand has proved to be of great interest.

A.3.1 Ilmenite

(a) Homogeneous Ilmenite

In the reduction experiments carried out by MICHAUD and PIDGEON (1954), ilmenite was reported to breakdown (after 38 hrs.) to metallic iron plus rutile (TiO_{2-x}). Pseudobrookite was also reported by WEBSTER and BRIGHT (1961). Equilibrium conditions after 7 hours have fortunately not been reached in the Nile delta black sand reduction experiments. Reduction has been confined to the grain bounderies and to cracks within the grains. Globules of metallic iron are concentrated

towards the edge of the grain and occur in a groundmass of rutile. Plate 14.16 shows clearly that a reaction zone of "anionic deficient ilmenite" separates the rutile-iron assemblage from the unaltered ilmenite. This zonation is not apparent to the same extent in ilmenite grains containing exsolved titanohematite.

(b) Exsolution in the Fe_2O_3-$FeTiO_3$ Solid Solution Series

The reduction of ferri-ilmenite grains containing exsolved titanohematite compares favourably with the Abu-Ghalagar samples, in which a dark rutile-ilmenite (Fe_2TiO_{3-x}) host contains oriented bodies of metallic iron (Plate A.17a). Plate A.17 d shows the reverse relationship in which titanohematite was the original host phase. The grain in Plate A.17c contained almost equal proportions of ferri-ilmenite and titanohematite. Note the mutual exsolution relationships of one phase within the other.

(c) Titanohematite-Rutile-Ilmenite Intergrowths

Minerals containing exsolution phases show more advanced states of oxidation than their homogeneous counterparts. Chemical activity is not confined to grain boundaries or cracks (Plate A.18) but is given further access along sub-capillary exsolution parting planes. This feature is particularly evident in Plate A.18a where the original titanohematite host has been entirely replaced by free iron. The large blades of rutile are darkened (TiO_{2-x}) but have retained their original sharp outline. The nature of the minor exsolved ilmenite phase follows the trend previously described.

(d) Supergene Oxidized Ilmenite

A notable feature of the reduced ilmenite grains, which have previously suffered supergene alteration, is the finely dispersed nature of the metallic iron throughout, indicating a high grain porosity. The photomicrographs in Plate A.19 show the progressive low temperature oxidation trends of LYND (1954) and BAILEY (1956). The least oxidized state (Plate A.19a) contains irregular areas of unaltered ilmenite, successively zoned during reduction, by anionic deficient ilmenite, rutile and metallic iron (c.f. Plate A.4a). No mineral phases, other than free iron, have been observed within the amorphous Fe-Ti oxide hosts. With increasing alteration

(i.e. increasing transparency-"leucoxinization") the modal percentage of free Fe decreases. Compare Plate A.19a and A.19d. This appears to confirm the finding that the Ti-Fe ratio increases with increasing alteration.

A.3.2 Magnetite (Titanomagnetite)

Plate A.20a-b shows the reduction of magnetite to metallic iron at 700°C and 800°C respectively. Unlike the globular form of iron after ilmenite, in these cases the texture is rather skeletal or feathery. A fine (111) relic structure is preserved in Plate A.20c, suggesting an original titanomagnetite-ilmenite intergrowth. The same texture is apparent in Plate A.20d which shows a clear inter-lamellar concentration of the metallic phase after original titanomagnetite. The (111) ilmenite laths are reduced to micrometallic blebs of iron in a host of $FeTiO_{3-x}$ and rutile (TiO_{2-x}).

A.3.3 Accessory Minerals

Optically the alumino-spinels and the sphene appear to be unaffected by the reduction in hydrogen. The experimental results of McLEAN and WARD (1966) indicate that the reduction of hercynite ($FeAl_2O_4$) to $FeO + Al_2O_3$ takes place well above 1000°C at atmospheric pressure.

TABLE A.2

A.S.T.M. index					Abu Ghalager, U.A.R.		R.S.M. Ilmenite Material	
II	He	Ru	PR	Fe	Hydrogen 800°	Hydrogen 1000°C	Hydrogen 800°C	Air 800°C
			4.96			4.91		4.90
3.73					3.72			
	3.67							3.68
			3.48			3.51		3.49
		3.25				3.24	3.24	3.25
2.74			2.74		2.74	2.76		2.75
	2.69							2.70
2.54					2.54			
	2.51							2.51
		2.50					2.48	2.48
2.23					2.23			
	2.20	2.20				2.09	2.19	2.18
				2.02	2.03	2.02	2.02	
			1.97			1.970		1.970
1.86			1.86		1.866	1.884		1.884
	1.833							1.835
1.72					1.722			
	1.688	1.687					1.684	1.688
		1.624					1.623	1.621
			1.54			1.539		1.540
				1.433	1.431	1.431	1.430	
				1.170	1.171	1.170	1.169	
				1.013	1.014	1.013	1.012	
				0.906	0.907	0.907		

Summary - comparison of A.S.T.M. Index of d values, in Å, for six strongest lines for each of the phases produced by heating experiments; values extracted for Table 1.

TABLE A.1

Abu Ghalager Bulk Samples (2.5cm)	R.S.M. Powdered Samples (>0.01m.m.)
Starting Material: Ferri-Ilmenite + Titanohematite.	Starting Material: Homogeneous Ilmenite

HYDROGEN						HYDROGEN			AIR		
1. 800°C			2. 1000°C			3. 800°C			4. 800°C		
I	d(Å)	Phase	I	d(Å)	Phase	I	d(Å)	Phase	I	d(Å)	Phase
5	3.72	II	3	4.91	PB	8	3.24	Ru	7	4.70	PB
10	2.74	II	3	4.10		3	2.96	Fe	½	3.68	He
7	2.54	II	6	3.51	PB	3	2.86		10	3.49	PB
4	2.23	II	2	3.38		3	2.69	Fe	5	3.25	Ru
5.	2.03	Fe	1	3.24	Ru	5	2.52	Fe	9	2.75	PB
4	1.866	II	1	3.11		5	2.48	Ru	4	2.70	He
8.	1.722	II	1	2.96	Fe	4	2.19	Ru	1	2.51	He
4	1.632		5	2.76	PB	2	2.09	Ru	1	2.48	Ru
½	1.621	II	½	2.47	PB	½	2.05	Ru	4	2.45	PB
5	1.504	II	½	2.41	PB	10	2.02	Fe	4	2.41	PB
5	1.467	II	1	2.21	PB, Ru	5	1.684	Ru	½	2.28	Ru
2	1.431	Fe	½	2.09	Ru	3	1.624	Ru	4	2.22	PB
½	1.374	II	10	2.02	Fe	2	1.617	Ru	4	2.195	He
4	1.340	II	4	1.970	PB	3	1.481	Ru	½	2.051	Ru
½	1.333		4	1.884	PB	2	1.454	Ru	7	1.970	PB
2	1.271	II	3	1.846	Fe	3	1.430	Fe	7	1.864	PB
½	1.247	II	3	1.757	PB	1	1.360	Ru	2	1.845	He
½	1.187	II	2	1.705	PB	2	1.169	Fe, Ru	2	1.749	PB
1.	1.171	Fe	2	1.672	Ru	4	1.093	Ru	6	1.688	He,Ru
½	1.155	II	1	1.664	PB	5	1.012	Fe	2	1.662	PB
1	1.119		2	1.638	PB				2	1.635	PB
1	1.075	II	1	1.610	Ru				½	1.621	Ru
1	1.051	II	2	1.552					½	1.609	He
1	1.014	Fe	2	1.539	PB				5	1.540	PB
1	1.003	II	½	1.500	PB				2	1.501	PB
1	0.907	Fe	5	1.431	Fe				2	1.483	Ru,He
			½	1.362	Ru, PB				2	1.454	Ru,PB
			½	1.320	PB				2	1.422	PB
			½	1.298	PB				1	1.377	PB
			½	1.266	PB				5	1.355	PB
			½	1.247	PB				1	1.321	He
			6	1.170	Fe, Ru				2	1.299	He
			5	1.013	Fe				2	1.265	He,PB
			3	0.907	Fe				2	1.242	Ru,PB
									½	1.232	He
									½	1.218	He
									½	1.202	He
									½	1.188	He
									2	1.094	Ru

Ilmenite	-	Il
Hematite	-	He
Pseudobrookite	-	PB
Rutile	-	Ru
Iron	-	Fe

TABLE A.3

Summary of Table A.2 in Terms of Phases Present & Unit Cell Parameters

Abu Ghalager (Hydrogen)

800°C

Ilmenite	+	Iron
a = 5.090 ± .013 b = 14.122 ± .102		a = 2.867 ± .001

1000°C

Pseudobrookite	+	Rutile	+	Iron
a = 9.814 ± .017 b = 9.952 ± .016 c = 3.770 ± .006		a = 4.593 ± .018 c = 2.951 ± .037		a = 2.864 ± .001

RSM Ilmenite Sample (0.01 mm.)

Hydrogen (800°C)

Rutile	+	Iron
a = 4.601 ± .020 c = 2.965 ± .020		a = 2.862 ± .001

Air (800°C)

Pseudobrookite	+	Hematite	+	Rutile
a = 9.806 ± .010 b = 9.983 ± .013 c = 3.727 ± .004		a = 5.063 ± .007 c = 13.647 ± .049		a = 4.588 ± .004 c = 2.960 ± .011

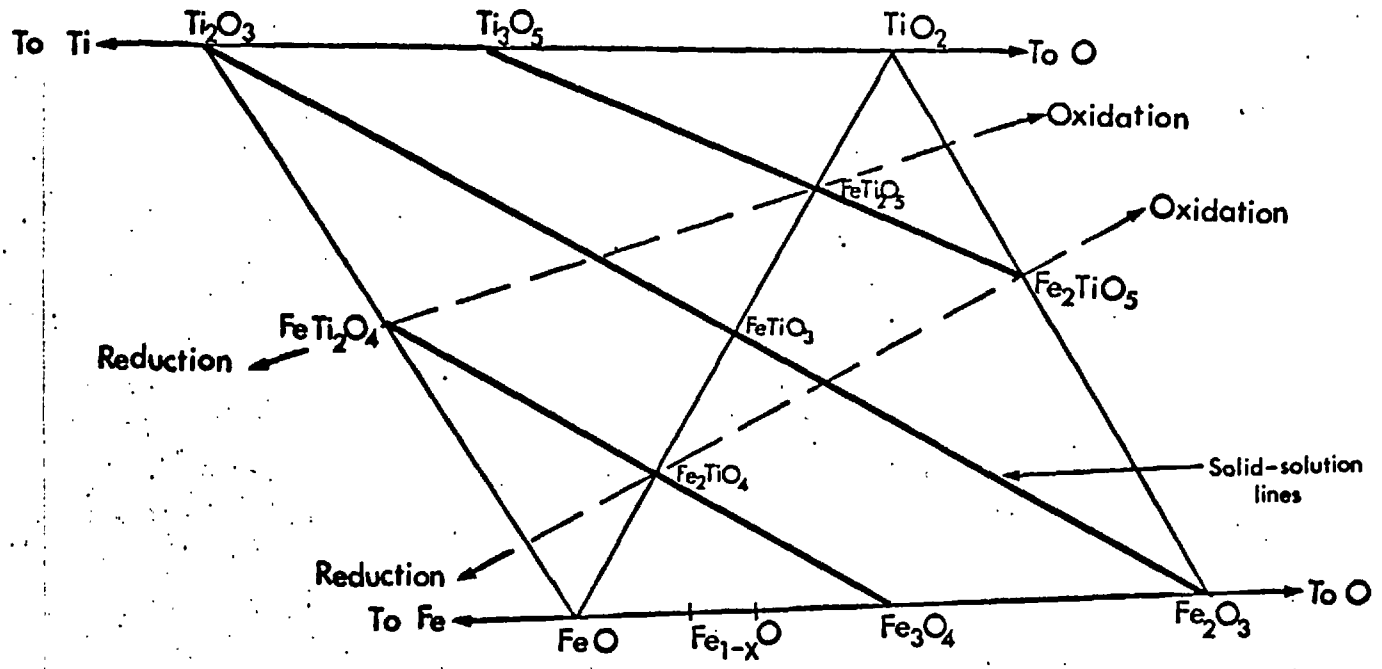

Part of the Fe-Ti-O ternary diagram, embracing the FeO-Fe_2O_3-TiO_2 phase region. The dashed lines indicate the directional changes which may be brought about by simple oxidation or reduction when the Fe:Ti ratio is kept constant. For example; reduction of hematite will produce Fe_3O_4, $Fe_{1-x}O$, FeO and finally free iron in successive stages. Note the reduction trend of rutile to Ti_3O_5 (anosovite) and Ti_2O_3. Fe-Ti compounds reduced in hydrogen follow both trends. The iron is selectively reduced to the metallic state and the Ti-phase is oxidised by the liberated H_2O from the reaction.

Fig A.1

REFERENCES

Ade-Hall, J.M., (1964) Geophys. J. 8 403

Ahearn, P.J., and Quigley, F.C., (1966) Jour. Iron and Steel Iust. 204 16

Akimoto, S., and Katsura, T., (1959) Jour. Geomag. Geoelec. 10 69

Akomoto, S., Katsura, T., and Yoshida, (1957) Jour Geomag. Geoelec. 9 165

Akomoto, S., Nagata, T., and Katsura, T., (1957) Nature 179 37

Allen, V.T., (1956) Econ. Geol. 51 830

Andersson, S., Collen B., Kuylenstierna, U., Magneli, A., (1957) Acta. Chem. Scand. 2 1941

Babkine, J., (1965) Bull. Soc. Franc. Miner. Crist. 88 306

Babkine, J., Conquere, F., Vilminot, J.C., Phan, K.D., (1965) Bull. Soc. Franc. Miner. Crist 88 447

Bailey, S.W., Cameron, E.N., (1957) Econ. Geol., 52 716

Bailey, S.W., Cameron, E.N., Spedden, H.R., and Weege, R.J., (1956) Econ. Geol. 51 263

Baker, I., and Haggerty, S.E. (1967) Contrib. Min. and Pet. 16 258

Barager, W.R.A., (1960) Geol. Soc. Amer. Bull., 71 1589

Barth, T.F.W., and Posnjak, E.,(1932) Z.Krist A, 82 325

Basta, E.Z., (1959) Econ. Geol. 54 698

Basta, E.Z., (1960) N. Jb. Min. Abh. 94 1017

Berry, L.G., and Thompson, R.M., (1962) Geol. Soc. Amer. Men. 85

Bernal, J.D., Dasgupta, D.R., and MacKay, A.L., (1957) Nature 180 645

Bernal, J.D., and MacKay, A.L., (1959) Clay. Min. Bull 4 15

Bhimasankaram, V.L.S., (1964) Nature 202 478

Bolshakov, A.S., Soldovnikov, G.M., and Skvorodkin, V.P., (1964) Bull. Acad. Sci. U.S.S.R. Geophys. Ser. 4 313

Balsley, J.R., and Buddington, A.F., (1958) Econ. Geol. 53 777

Brett, R., (1964) Econ. Geol. 59 7

Buddington, A.F., Fahey, J., and Vlisidis, A., (1963) Jour. Pet. 4 138

Buddington, A.F., and Balsley, J.R., (1961) Mahadavan Vol. U.S. Geol. Surv.

Buddington, A.F., and Lindsley, D.L., (1964) Jour. Pet. 5 310

Carmichael, C.M., (1961) Proc. Roy. Soc.(London) Ser. A 263 508

Carmichael, I.S.E., (1967) Contrib to Min. and Pet. 14 36

Chamberlaine, J.A., McLeod, C.R., Traill, R.J., and Lanchance, G.R., (1965) Can. Jour. Earth Sci. 2 188

Colombo, U., Fagherazzi, G., Gazzarrini, F., Lanzavechia, G., and Sironi, G., (1965) Science 147 1033

Cornwall, H.R., (1951) Econ. Geol. 46 51

Cox, A., Doell, R., and Dalrymple, G.B., (1967) J.Geophys. Res., 72 2603

Dagley, P., Wilson, R.L., Walker, G.P.L., Watkins, N.D., Sigurgersson, I., Haggerty, S.E., Smith, P., Ade-Hall, J.M., (1967) Nature 216 25

Darken, L.S., and Gurry, R.W., (1945) Jour Am.Chem. Soc. 67 1398

Darken, L.S., and Gurry, R.W., (1946) Jour Am. Chem. Soc. 68 798

Deer, W.A., Howie, R.A., and Zussman, J., (1962) Rock forming minerals. Longmans.

De Menezes, I., and Stubican, V.S.,(1966) Jour. Amer. Cer. Soc. 49 535

Desborough, H., (1963) Econ. Geol. 58 332

De Vries, R.C., and Roy, R., (1954) Am. Cer. Bull. 33 370

Ernst, T., (1943) Z. Ang. Min. 4 394

Eugster, H.P., (1959) Researches in Geochemistry. Wiley.

Eugster, H.P., and Wones, D.R., (1962) Jour. Pet 3 82

Everitt, C.W.F., (1962) Phil. Mag. 7 831

Fawcett, J.J., (1965) Min. Mag. 35 55

Faynberg, F.S., (1960) Dokl. Akad. Nauk. S.S.S.R. 9 81

Faynberg, F.S., and Dashkevich, N.N., ibid 6 116

Fleischer, M., (1967) Am. Min. 52 1

Flinter, B.H., (1959) Econ. Geol. 54 720

Foslie, S., (1928) Fennia. 50 nr.26 15

Gheith, M.A., (1952) Amer. Jour Sci. 250 677

Chisler, M., and Windley, B.F., (1967) Grønlands. Geol. Und. Rp. 12.

Goldschmidt, V.M., (1926) Skrifter. Norske. Vids. Akad. Oslo 82

Gorter, E.W., (1957) Adv. in Phys. 6 336

Graham, L.D., and Kraft, R.W., (1966) Trans. Met. Soc. AIME. 236 94

Gruner, J.W., (1959) Econ. Geol. 54 1315

Hartman, J.A., (1959) Econ. Geol. 54 1380

Heier, K.S., Rodgers (1963) Geochim. Cosmoch. Acta. 29 53

Henriques, A., (1963) Arkiv for Min. och Geol. 3 385

Hunt, J.D., (1966) J. Inst. of Metals. 94 125

Irvine, T.N., (1965) Can. Jour. Earth Sci. 2 648

Irvine, T.N., (1967) Ibid 4 71

Irving, E., (1966) Palaeomagnetism and its application to geological and geophysical problems. Wiley.

Jaeger, J.C., (1962) Am. Jour. Sci. 259 721

Jensen, A., (1966) Saer.af. Medd. fra Dansk. Geol. Foer. 16

Karkhanavala, M.D., (1959) Econ. Geol. 54 1302

Karkhanavala, M.D., and Momin, A.C., (1959)Econ. Geol. 54 1095

Karkhanavala, M.D., and Momin, A.C., (1959) Amer. Jour. Cer. Soc. 42 399

Katsura, T., and Kushiro, I., (1961) Amer. Min. 46 134

Kennedy, G.C., (1948) Amer. Jour. Sci. 246 529

Kennedy, G.C., (1955) Geol. Soc. Amer. Spec. Paper. 62 489

Kullerud, G., and Yoder, H.S., (1964) Carnegie Inst. Wash. Year b. 64 192-193

Kullerud, G., and Donnay, G., (1965) Ibid 65 356-357

Kushiro, I., and Yoder, H.S., (1966) Jour.Pet. 7 337

Kuno, H., (1965) Jour. Pet. 6 315

Larson, E.E., Ozima, M., Azima, M., Nagata T., Strangway, D.W., (1966) Trans.Amer. Geophy. Union Meet. Abs 47 1

Larson, E.E., and Strangway, D.W., (1966) Nature 212 750

Legg, C., (1967) Unpublished M.Sc. Thesis Univ. of London

Lepp, H., (1957) Amer. Min. 42 679

Lindsley, D.H., (1962) Cornegie Inst. Wash. Year b. 61 100-106

Lindsley, D.H., (1963) Ibid. 62 60-66

Lindsley, D.H., (1965) Ibid. 64 144-148

Lindsley, D.H., (1965) G.S.A. Meeting. Kansas City.Abs. 96

Lynd, L.E., (1960) Econ. Geol. 55 1064

Lynd, L.E., Sigurdson, H., North, C.H., Anderson, W.W., (1954) Min. Eng. AIME 6 817

MacDonald, J.G., (1967) Scott. Jour. Geol. 3. 34

MacGregor, I.D., (1964) Carnegie Inst. Year b. 63 157

McChesney, J.B., and Muan, A., (1959) Amer. Min. 44 926

McChesney, J.B., and Muan, A., (1961) Ibid. 46 572

McCollister, H., and Van Vlack, L.H., (1965) Amer. Cer.Soc. Bull. 44 915

McLean A., and Ward, R.G., (1966) Jour. Iron and Stell Inst. 204 8

Meitzner, W., (1963) Contrib. Min and Pet. 9 320

Melson, W.G., and Switzer, G., (1966) Amer. Min. 51 664

Metallova, V.V., Faynberg, F.S., (1963) Vest. lening. gos. Univ. Geol. Geogn. 18 46

Mitchell, R.S., (1964) Amer. Min. 49 1136

Morgensen, F., (1946) Geol. Foren. i Stock. Förh. 68 578

Muan, A., (1958) Amer. Jour. Sci. 256 171

Muan, A., and Osborn, E.F., (1956) Jour. Amer. Cer.Soc. 39 121

Muan, A., and Somiya, S., (1960) Jour. Amer.Cer. Soc. 43 204

Mueller, R.F., (1961) Amer. Jour. Sci. 259 460

Nasu, N., (1936) Sci. Report Tohoku Univ. 1 25

Nagata, T., (1962) Rock Magnetism. Maruzen

Nagata, T., Ozima, M., Yama-ai, M., (1963) Nature 198 118

Neel, L., (1951) Adv. in Phys. 4 191

Nicholls, C.D., (1955) Adv. in Phys. 4 113

Nickel, E.H., (1958) Can. Min. 6 191

Opdyke, N.D., Glass, B., Hays, J.D., and Foster J., (1966) Science 154 349

O'Reilly, W., and Barnerjee, S.K., (1967) Min. Mag. 36 29

Osborn, E.F., (1959) Amer. Jour. Sci. 257 609

Ottaman, J., and Frenzel, G., (1966) Schweiz Min. Petr. Mitt., 45 819

Palache, C., Berman, I.H., and Frondel, C., (1946) Dana's System of Mineralogy. Wiley.

Panagos, J., and Ottaman, G., (1966)

Pankey, A., and Seftle, L., (1959) Amer. Min. 44 1307

Peck, D.L., Wright, T.L., and Moore, J.G., (1966) Bull. Volcan. 25 1

Phillips, B., and Muan, A., (1962) Jour. Amer. Cer. Soc. 37 161

Rafai, E., (1961) Geophys., 27 175

Ramdohr, P., (1926) N. Jb. Min 54A 320

Ramdohr, P., (1939) Abh. Preuss Akad. Wiss Mat. Nat. Klasse 14

Ramdohr, P., (1953) Econ. Geol. 48 677

Ramdohr, P., (1956) Bull. Comm. Geol. Finlande, 28 173

Richter, D.H., and Moore, J.G., (1966) U.S. Geol. Surv. Prof. Paper 537-B

Roy, S., (1954) Nat. Inst. Sci. India Proc. 20 691

Sato, M., and Wright, T.L., (1966) Science 153 1103

Schmahl, N.G, and Meyer, G., (1959) Metall 13 1114

Schmidt, E.R., and Vermaas, F.H.S., (1955) Amer. Min. 40 422

Schwartz, G. M., (1929) Econ. Geol. 24 592

Sederholm, J.J., (1929) Econ. Geol. 24 869

Shand, S.J., (1945) Bull. Geol. Soc. Amer 56 247

Shomate, C.H., Naylor, B.F., Boerike, F.S., (1946) U.S. Bureau of Mines R.I. 3864

Smelov, A.A., Zhegolev, L.P., and Khabibullina, R.T., (1962) Zap. lenning gos. Univ, Vospros. Geofiz. 303 245

Smith, D.G.W., (1965) Amer. Min. 50 1982

Smith, P.J. (1966) Unpublished PH.D. Thesis. Univ. of London

Stevens, R.E., (1944) Amer. Min. 29 1

Taylor, R.W., (1963) Jour. Amer. Cer. Soc. 46 276

Taylor, R.W., (1964) Amer. Min. 49 1016

Temple, A.K., (1966) Econ. Geol. 61 695

Teufer, G., and Temple, A.K., (1966) Nature 211 179

Tex, E.den, (1959) Amer. Min. 40 355

Tsventokov, A.I., Myasnikov, V.S., Schepochkina, N.I., Matveyeva, N.A., (1966) Int. Geol. Rev. 8 676

Turnock, A.C., (1959) Carnegie Inst. Wash. Year b. 58 134

Turnock , A.C., and Eugster, H., (1962) Jour. Pet. 3 533

Tunnell, G., and Posnjak, E., (1931) Econ. Geol. 26 337

Uyeda, S., (1958) Jap. Jour. Geophys. 2 1

Vaasjoki, O., and Heikkinen, A., (1961) Comm.Geol. Finlande, Ball 194 1

Verhoogen, J., (1962a) J. Geol. 70 168

Verhoogen, J., (1962b) Amer. Jour. Sci. 260 211

Vincent,E.A.,(1960) Neus. Joh. Min. Abh. 94 993

Vincent, E.A., and Phillips, R., (1954) Geocham. Cosmoch. Acta. 6 1

Vincent, E.A., Wright, J.B., Chevallier, R., and Mathieu, S., (1957) Min.Mag. 31 624

Vogelsand, D., (1957) Notizble. hess. Landesamt. Bodenforsch., Weisbaden, 85 390

Van Knorring, O., and Cox., K.G., (1961) Min. Mag. 32 676

Wahlbeck, P.G., and Gillies, P.W., (1966) Jour. Amer. Cer. Soc. 49 180

Walker, G.P.L. (1959) Quart. Jour. Geol.Soc. 114 367

Walker, G.P.L. (1960) J. Geol. 68 515

Walker, G.P.L., (1963) Quart. Jour. Geol. Soc. 119 29

Warshaw, I., and Keith, M.L., (1954) Jour. Amer. Cer. Soc. 37 161

Watkins, N.D., and Haggerty, S.E., (1965) Nature 206 797

Watkins, N.D., and Haggerty, S.E., (1967) Contrib. Min. Pet. 15 251

Watkins, N.D., and Goodell, H.D., (1967) Science 156 1083

Watkins, N.D., Holmes, C.W., and Haggerty, S.E., (1967) Science 155 579

Webster, A.H., and Bright, N.F.H., (1961) Jour. Amer. Cor. Soc. 44 110

Wilson, R.L., (1963) Geophys. Jour. 8 235

Wilson, R.L., (1964) Geophys. Jour. 8 403

Wilson, R.L., (1966) Earth Sci. Rev. 1 175

Wilson, R.L., and Watkins, N.D., (1967) Geophys. Jour. 12 405

Wilson, R.L., Haggerty, S.E., and Watkins, N.D., (1968) Geophys. Jour. (in the press)

Wittke, J.P., (1967) Jour. Amer. Cer. Soc. 50 586

Wright, J.B., (1959) Min. Mag. 32 32

Wright, J.B., (1964) N.Z. Jour. Geol. Geophys. 7 424

Wright, J.B., and Lovering, J.F., (1965) 35 604